Gut microbial regulation of organismal health through *Tachykinin* in *Drosophila*

Diana Elena Marcu

Supervisor: Dr Adam Dobson

Submitted in fulfilment for the degree of Doctor of Philosophy in Molecular Genetics

School of Molecular Biosciences

College of Medical, Veterinary and Life Sciences

University of Glasgow

April 2024

Abstract

The complex relationship between the gut microbiota and host physiology is a multifaceted area of investigation with profound implications for systemic health and ageing. Despite residing predominantly in the gut, the microbiota holds the potential to systemically impact overall host health, including complex processes like ageing. This prompts the question, by what mechanisms does the gut microbiota systematically influence the host? Host-derived hormones, particularly gut peptides secreted by enteroendocrine cells, emerge as potential mediators for conveying the microbiota's influence on lifespan and metabolism. However, the exact molecular mechanisms through which microbiota regulate host enteroendocrine signalling, and the relevance of this in systemic host health, is unknown.

Drosophila melanogaster was used as an *in vivo* model to study the impact of microbiota on host via enteroendocrine signalling. To address this, I used a unique approach, integrating germ-free and gnotobiotic conditions with targeted genetic manipulations. This strategy provided a platform to unravel the specific roles of enteroendocrine peptides in the context of microbial influence. RNAseq analysis and fluorescence staining showed that the microbiota shapes the expression levels of gut peptides, and the number EE cells present in the gut. In particular, the differentially expressed host derived gut peptide, *tachykinin* (*TK*), proved to be a strong candidate to mediate the influence of microbiota on host health. Germ-free and conventional flies were used to determine if *TK* responds to microbial cues to regulate complex host phenotypes such lipid metabolism, lifespan, starvation resistance, feeding behaviour and fecundity. The focus was specifically on two phenotypes: lifespan and lipid metabolism. In the presence of microbiota, ubiquitous RNAi against *TK* extended lifespan, but eliminating the microbiota had no additive effect. *TK* knockdown also increased lipid levels in conventional flies, but this effect was reversed in germ-free flies, demonstrating that the microbiota regulates complex host traits through a *TK* mediary. To refine which members of the microbiota interact through *TK*, gnotobiotic flies mono-colonised by either the gut symbiont *Acetobacter pomorum*, or *Lactobacillus brevis* were used. *A. pomoru*m was found to strongly modulate lifespan and lipid levels via *TK,* while *L. brevis* had a marginal impact.

It was further determined that in order to achieve lifespan modulation, *A. pomorum* regulated *TK* expression in the gut, which then targets its receptor *TKR99D* in the brain. In terms of potential mechanisms mediating the impact of the interaction between *A. pomorum* and *TK* - feeding and egg laying assays suggest that nutrient restriction and reduced reproduction can be excluded but impacts on *4E-BP and* Akt expression suggest roles for the IIS/TOR signalling network. In support of this, ablation of insulin producing cells phenocopies the *TK* knockdown lifespan phenotype. However, knockdown of *TK* in null-*dFOXO* mutants showed that, while *dFOXO* is required for *TK* to modulate lifespan, it is not required for microbial lifespan regulation, suggesting that other interacting mechanisms are likely to be involved.

In conclusion, this thesis implicates *TK* as a pivotal mediator of the effect of microbiota on host lifespan, setting the stage for innovative approaches to delay ageing and improve healthspan.

Table of contents

List of tables

List of figures

Acknowledgments

I would like to thank in the first place my supervisor Dr Adam Dobson, who's support has been the backbone of this thesis. Thank you for all the advice, guidance, moral support and patience which allowed me to move forward and navigate this journey. The countless discussions we had not only contributed to the academic growth of this thesis but also allowed me to grow as a person. I have learned so much during this time.

Special thanks to my lab colleagues and friends, Dr David Sannino and Rita Ibrahim, whose support and friendship made my time in the lab both enjoyable and memorable. Thank you, Dave for guiding me through lab work, troubleshooting experiments, discussing ideas and always making me laugh. Thank you, Rita for your kindness, positivity and heartfelt advice. I am grateful that I have shared the lab with both of you.

I would like to thank Dr Anthony Dornan for your advice and for all the help in the lab. I would like to thank Dr Nathan Woodling for the advice, support and help with experiments. I would like to thank Miriam Wood for all her hard work in the lab. I would also like to thank Dr Andre Medina and the Cordero lab for the advice, support and for always welcoming me in their lab. Also, thanks to all the members of the Sanz lab, and special thanks to Ignacio Fernandez Gurrero for helping with the RNAseq analysis. Many thanks to my secondary supervisor Professor Dr Julia Cordero for her valuable advice. I would also like to thank Professor Dr Colin Selman for being my mentor and for all the advice and support over the years.

Lastly, I would like to thank my family: Va iubesc si va multumesc pentru tot!

List of abbreviations

5-HT	5-hydroxytryptamine
AHR	aryl hydrocarbon receptor
AKH	adipokinetic hormone
AMPs	antimicrobial peptides
AP	acetobacter pomorum
AstA	allatostatin A
AstB	allatostatin B
AstC	allatostatin C
ATP	adenosine triphosphate
AX	axenic
Burs	bursicon
CAFE	CApillary FEeder assay
CCAP	crustacean cardioactive peptide
CCHa1	CCHamide-1
CCHa2	CCHamide-2
CCK	cholecystokinin
ChAT	choline acetyltransferase
CNS	central nervous system
Cp15	chorion protein 15
CV	conventional
DaGS	Daughterless Gene Switch
DAPI	4′,6-diamidino-2-phenylindole
DH31	diuretic hormone 31
DTKR	*Drosophila* tyrosine kinase related
EB	enterocytes
EB	enteroblast
EE	enteroendocrine
EEC	enteroendocrine cells
EEP	enteroendocrine progenitor
EMMs	estimated marginal means
FLIC	Fly Liquid-Food Interaction Counter
flyPAD	Proboscis and Activity Detector
FOXO	Forkhead box-O transcription factor
GF	germ-free
GFP	green fluorescent protein
GI	gastrointestinal
GIP	gastric inhibitory peptide
GLP-1	glucagon-like peptide-1
GLP-2	Glucagon-like peptide-2
GN	gnotobiotic
Gpb5	glycoprotein hormone beta 5
GPCRs	G protein-coupled receptors
GWA	genome-wide association
H2S	hydrogen sulphide

HMP	Human Microbiome Project
HPA	Hypothalamic-pituitary-adrenal
HSP	heat shock protein
IBD	Intestinal bowel disease
IIS	Insulin/IGF-1 signalling
IL	interleukin
Ilps	insulin like peptides
IMD	Immune deficiency
INSL5	Insulin-like peptide-5
IP	intercerebralis
IPA	Indole-3-propionic acid
IPCs	insulin producing cells
IR	insulin receptor
ISCs	intestinal stem cells
ITP	ion transport peptide
JAK-STAT	Janus kinase–signal transducers and activators of transcription
LB	Lactobacillus brevis
LPS	lipopolysaccharide
mAMPs	microbial associated patterns
MetaHIT	Metagenomics of the Human Intestinal Tract
NF-κB	nuclear factor–kappa B
NGS	next generation sequencing
NKD	neurokinin receptor from Drosophila
Nlaz	Neuronal Lazarillo
NLRs	NOD-like receptors
NPF	Neuropeptide F
Nplp2	Neuropeptide-like precursor 2
NPY	Neuropeptide y
Ork-B	Orcokinin B
PCA	principal component analysis
PER	Proboscis extension response
PGRP	Peptidoglycan recognition protein
PQQ-ADH	pyrroloquinoline quinone–dependent alcohol dehydrogenase
PRR	pattern-recognition receptors
PYY	Peptide Y
QTL	quantitative trait loci
RLRs	RIG-1-like receptors
rRNA	16S ribosomal RNA
SCFA	short-chain fatty acid
SIFR	SIFamide receptor
sNPF	short neuropeptide F
SP	substance P
SREBP	sterol regulatory element binding proteins
SST	somatostatin
T2D	Type 2 Diabetes

TAG	triglyceride
TF	transcription factor
TK	Tachykinin
TLRs	Toll-like receptors
TNF	tumor necrosis factor
TOR	target-of-rapamycin
WD	White Dahomey

Author’s Declaration

I declare that the content presented in this thesis is entirely my own, except where specific acknowledgment is given to the contributions of others. No part of this work has been previously submitted for any other degree at any institution.

Diana Elena Marcu

Chapter 1 General introduction

1.1 Unveiling the hidden universe within: A journey into the microbiome

1.1.1 Introduction to the human gut microbiota

Until the advent of next-generation sequencing (NGS), knowledge of the adult human gut microbiota relied on labour-intensive culture-based methods (Moore and Holdeman, 1974). Advances in culture-independent techniques, such as high-throughput sequencing, have greatly enhanced our ability to explore the microbiota. Targeting the 16S ribosomal RNA (rRNA) gene, which is universal in bacteria and archaea, has become popular, allowing easy species distinction (Mizrahi-Man et al., 2013; Poretsky et al., 2014). Previously, sequencing efforts primarily targeted the entire 16S rRNA gene. An early study using this method underscored the insensitivity and bias of culturing techniques, revealing that 76% of rRNA gene sequences from an adult male faecal sample belonged to novel, uncharacterised species (Suau et al., 1999). Recently, there has been a shift in focus to analyse shorter subregions of the 16S rRNA gene more thoroughly (Mizrahi-Man et al., 2013). However, the use of shorter read lengths in this approach can introduce errors (Poretsky et al., 2014). For enhanced reliability in estimating microbiota composition and diversity, whole-genome shotgun metagenomics is now preferred due to its higher resolution and sensitivity (Poretsky et al., 2014).

Two large-scale research initiatives were undertaken with the primary purpose of comprehensively characterising the microbial communities associated with the human body, particularly focusing on the gut microbiota, to better understand its function in health and disease (Hugon et al., 2015; Li et al., 2014). Launched in 2007, the Human Microbiome Project (HMP) analysed the microbiota associated with various human body sites, including the skin, oral cavity, nasal passages, urogenital tract, and the gastrointestinal (GI) tract (Creasy et al., 2021; Hugon et al., 2015; Proctor, 2016). The HMP employed a multi-omics approach, combining metagenomics, metatranscriptomics,

metaproteomics, and metabolomics, to analyse the microbial communities and their functional activities. The HMP aimed to establish a reference catalogue of microbial communities in healthy individuals, facilitating the identification of normal microbial variations and aiding in the exploration of how changes in the microbiome may relate to various diseases (Hugon et al., 2015). The Metagenomics of the Human Intestinal Tract (MetaHit) project, launched in 2008, aimed to decipher the genetic makeup of the human intestinal microbiota using metagenomic approaches (Li et al., 2014; Qin et al., 2010). MetaHit employed whole-genome shotgun metagenomics, to analyse the collective genetic material of microbial communities without the need for culturing individual species (Dusko Ehrlich and MetaHIT consortium, 2010).

The combined data from the HMP and MetaHit offer the most comprehensive insight into the microbial communities associated with humans to date (Hugon et al., 2015; Li et al., 2014). These initiatives have laid the groundwork for subsequent studies exploring the functional and compositional aspects of the microbiome and their implications for various diseases and conditions. A synthesis of the data from these investigations revealed the isolation of 2172 species from human subjects, categorized into 12 distinct phyla. Notably, 93.5% of these species were affiliated with members of four phyla: Pseudomonadota (Proteobacteria), Bacillota (Firmicutes), Actinomycetota (Actinobacteria), and Bacteroidota (Bacteroidetes). Interestingly, three out of the identified phyla featured only one species each, including the intestinal species *Akkermansia muciniphila*, which stands as the sole representative of the Verrucomicrobiota phylum. Among the identified species in humans, 386 are strictly anaerobic and are predominantly localised in mucosal regions, such as the oral cavity and the GI tract (Hugon et al., 2015).

1.1.2 Bacterial gut microbiota composition throughout development

It has been well established that the human gut is colonised by microorganisms shortly after birth (Thursby and Juge, 2017). However, several studies suggest the possibility of a prenatal in-utero origin as bacteria have been detected in the

placenta, amniotic cavity, umbilical cord, and meconium (Aagaard et al., 2014; Collado et al., 2016; Jiménez et al., 2005). Regardless, the foundational configuration of the infant's microbiota undergoes substantial fluctuations, particularly within the first three years, before stabilising into a structure resembling that of the adult microbiota (Pellanda et al., 2021). Various factors, including delivery mode, feeding method, antibiotic exposure, maternal diet and microbiota, and surrounding environment, influence the composition of this early intestinal microbiota (Nagpal et al., 2018). Previous studies indicate that infants delivered vaginally experience an early and heightened presence of *Lactobacilli*, *Bacteroides*, and *Prevotella*, primarily acquired from the maternal vaginal and faecal microbiota. In contrast, caesarean-born infants tend to exhibit delayed or reduced levels of *Bacteroides*, *Bifidobacteria*, and *Lactobacilli*, with an enriched colonization of *Clostridium difficile, C. perfringens, and Escherichia coli* (Nagpal et al., 2017, 2016). Furthermore, infants subjected to antibiotic treatment exhibit reduced levels of *Lactobacilli, Bifidobacteria*, and *Enterococci* (Bokulich et al., 2016). Following birth, the method of feeding becomes a crucial factor influencing the development of the gut microbiota. Breast-fed infants demonstrate increased levels of *Bifidobacteria*, *Lactobacilli*, *Staphylococci*, and *Streptococci*, whereas formula-fed infants exhibit heightened colonisation of *Bacteroides*, Clostridia, and Pseudomonadota. However, these distinctions gradually wane, and the overall composition of the gut microbiota begins to stabilize, particularly upon the introduction of solid foods during weaning (Bäckhed et al., 2015; Favier et al., 2002; Tsuji et al., 2012). Subsequently, from this stage onward, diet emerges as the predominant factor strongly influencing the subsequent maturation and maintenance of the gut microbiota configuration throughout the lifespan (David et al., 2014b; De Filippo et al., 2010).

1.2 Factors shaping the gut microbiota

The composition and dynamics of the gut microbiota are influenced by a myriad of factors that collectively shape the microbial communities residing in the GI tract. Diet, host genetics, age, lifestyle, and environmental exposures are among the key determinants influencing the abundance and diversity of gut microbes. Dietary habits significantly impact the gut microbiota, with variations

in macronutrient intake and fibre consumption demonstrating distinct microbial signatures (Donaldson et al., 2016). Host genetics play a pivotal role in shaping the baseline microbial profile, as evidenced by studies highlighting familial similarities in microbiota composition (Goodrich et al., 2014). Age-related shifts in the gut microbiota have been observed, reflecting the dynamic nature of microbial communities throughout the lifespan (Ghosh et al., 2022). Lifestyle factors, including physical activity and stress, can also impact the gut bacterial composition (Benson et al., 2010). Environmental exposures such as antibiotic usage and geographical location further contribute to microbial variability (Benson et al., 2010). These factors collectively underscore the intricate interplay between host and microbial elements in the gut ecosystem, emphasising the need for a holistic understanding of the multifaceted influences on gut microbiota composition.

Nevertheless, it is important to highlight that microbiotas with distinct compositions may possess a degree of functional redundancy, resulting in comparable protein or metabolite profiles (Moya and Ferrer, 2016). This insight is vital for the development of therapeutic interventions aimed at altering and influencing microbial communities in the context of disease and general health and well-being.

1.2.1 Diet

Diet plays a vital role as a modifiable factor that significantly affects the composition of gut microbial composition (Donaldson et al., 2016). More than half of the variations in microbiota can be traced back to changes in dietary patterns (Oriach et al., 2016; Zhang et al., 2010). Meta-transcriptomic studies have unveiled that the composition of gut microbiota is influenced by the ability of commensals to metabolise simple sugars, indicating the microbiota's adaptation to nutrient availability in the GI tract (Zoetendal et al., 2012). The configuration of the gut microbiota is contingent upon the presence of microbiota-accessible carbohydrates, primarily found in dietary fibre. The influence of fibre was demonstrated in a crossover study showing that otherwise matched diets high in resistant starch or in non-starch polysaccharide fibre (wheat bran) led to significant and consistent enrichment of different bacterial species in the human gut (Walker et al., 2011). Moreover, fibres can act as

‘prebiotics’, functioning as substrates for beneficial gut bacteria and contributing to a well-balanced and diverse microbiota. A consensus definition identifies prebiotics as fermentable dietary compounds that, upon consumption, specifically stimulate the growth and/or activity of beneficial gut bacteria, as outlined by Gibson et al. (2017). Prebiotics, such as fructans and galactans, undergo fermentation by bacteria like *Bifidobacteria* and *Lactobacilli*, thereby promoting their proliferation (Gibson et al., 2017). This fermentation process results in the production of short-chain fatty acids (SCFAs), recognised for their role in sustaining gut and microbiome health as well as systemic well-being.

Human studies have shown that extreme adherence to 'animal-based' or 'plant-based' diets leads to substantial modifications in the gut microbiota (David et al., 2014b). Generally, a more diverse diet has been demonstrated to offer a broader spectrum of nutrients for the gut microbiota, therefore facilitating a wider range of microbes to inhabit the gut (Johnson et al., 2019). Simultaneously, a varied diet is correlated with a more stable and resilient gut microbiota (Sommer et al., 2017). The gut microbial ecosystem demonstrates resilience to short-term individual changes, such as alterations in diet (David et al., 2014a). While short-term dietary interventions may induce temporary shifts in the composition of the gut microbiota, these changes tend to resolve within a few days (David et al., 2014a). Notably, an individual's distinctive gut microbiota composition appears to be more closely linked to long-term dietary patterns, emphasising the need for consistent daily dietary choices to shape and maintain a specific gut microbial ecosystem (Wu et al., 2011).

1.2.2 Host genetics

Host genetic factors contribute significantly to individual variations in the gut microbiota. Studies, such as those by Goodrich et al., have demonstrated heritability patterns influencing microbial composition (Goodrich et al., 2014). For decades, the use of twins has been pivotal in exploring the correlation between host genetic variation and the microbiome (Goodrich et al., 2016). Identical twins, sharing 100% of their genes, and fraternal twins, sharing an average of 50%, have been integral to twin heritability studies based on the assumption that co-raised twins experience similar environments. This has been

particularly relevant for quantitative traits like bacterial relative abundances, where the greater similarity observed in identical twins can be attributed to shared genes, indicating heritability.

For robust genetic assessments, larger sample sizes are crucial. Using a sample size of 416 twin pairs, Goodrich et al. demonstrated that identical twin microbiomes were overall more similar than those of fraternal twins (Goodrich et al., 2014). Notably, this larger sample also allowed heritability estimates for individual taxa. The bacterial family with the highest heritability was Christensenellaceae, known for co-occurring with other heritable taxa, including the gut methanogen *Methanobrevibacter smithii*. Previous work in humans has associated methanogens and species richness with leanness (Le Chatelier et al., 2013a) and Christensenellaceae with low serum triglyceride levels (Fu et al., 2015). Moreover, in one study faeces from an obese human donor lacking this consortium were transferred to GF mice, both with and without the addition of *Christensenella minuta* (Goodrich et al., 2014). The introduction of *Christensenella minuta* led to a decrease in adiposity in the recipient mice, implying that host genes might impact phenotype by regulating microbiome components.

Previous human studies, including human genome-wide association (GWA) studies - e.g., UK Twins (Goodrich et al., 2014), HMP subjects (Blekhman et al., 2015) and Hutterites (Davenport et al., 2015), as well as mice studies, such as quantitative trait loci (QTL) studies - e.g., advanced intercross lines (Benson et al., 2010; Leamy et al., 2014), Hybrid Mouse Diversity Panel (Org et al., 2015), collaborative cross/diversity outbred mapping panels (O'Connor et al., 2014) and recombinant inbred strains (McKnite et al., 2012) have identified several taxa as heritable or linked to host genes. Predominantly, these heritable taxa belong to the Bacillota, whereas Bacteroidota are generally not heritable. Technical constraints hinder direct comparisons for some taxa, such as the absence of Christensenellaceae in all taxonomies. Although heritability estimates tend to be higher on average for mice due to controlled environmental variability, certain taxa consistently emerge across various studies.

Studies in *Drosophila melanogaster* have also provided valuable insights into the influence of host genetics on gut microbiota composition. The taxonomic

composition of *Drosophila* microbiota was shown to influence the gene expression profile of the gut (Broderick et al., 2014; Newell and Douglas, 2014). Further analysis also showed that gene-bacterial interactions shape the nutritional status of the fly, emphasising the crucial role of host genotype in shaping the impact of microbiota on animal nutrition (Chaston et al., 2016; Dobson et al., 2015). Overall, findings across studies conducted in flies, mice, and humans exhibit a striking similarity, underscoring the intricate dynamics of host-microbiota interactions and emphasising the pivotal role of host genetics in shaping microbial communities.

1.2.3 Age

While gut microbes themselves do not undergo ageing, the prevalence of comorbidities linked to gut microbiota tends to rise with the host's advancing age (Ghosh et al., 2022). However, it remains uncertain whether changes in microbiota are a cause or a consequence of ageing (Bartosch et al., 2004; Han et al., 2017). This uncertainty is attributed to the fact that age-related alterations in the microbiota are highly variable, influenced by both individual factors and external environmental conditions. For instance, the gut microbiota undergoes predictable changes associated with the progressive decline in alimentary tract physiology, such as increased age-related inflammation, genomic instability, dysfunction in cellular and mitochondrial processes, compromised proteostasis, and epigenetic dysregulation. Consequently, these alterations contribute to the emergence of chronic diseases, metabolic disorders, and disruptions in gut–brain communication (Cryan et al., 2019; Pellanda et al., 2021). Moreover, age-related lifestyle changes, including increased frailty, medication use, surgical interventions, diminished physical activity, and a decline in dietary quality, can further amplify the effects on the gut microbiota (Ghosh et al., 2022; O'Toole and Jeffery, 2015). Additionally, lifelong personal habits, particularly dietary choices, play a crucial role in shaping the composition and functionality of the microbiome in older individuals (Ghosh et al., 2022). Recognising these influences presents opportunities for promoting positive behavioural changes conducive to healthy ageing.

Studies investigating the link between gut microbiota and ageing primarily rely on age-associated shifts in taxonomic composition, thus focusing on correlation

rather than establishing direct causation (Le Chatelier et al., 2013b; Nagpal et al., 2018). These investigations often utilise sequencing technologies to analyse microbial communities in relation to age-related parameters, employing correlation analyses to identify patterns or relationships. Due to ethical considerations and the complex nature of the microbiota-host interaction, interventional studies in humans are limited, making correlation designs a predominant approach in this field.

Studies examining the interplay between gut microbiota and age can be classified into 3 broad categories: (1) studies assessing age-related changes in gut microbiota composition (Iwauchi et al., 2019; Ruiz-Ruiz et al., 2020; Xu et al., 2019; Ghosh et al., 2020; Jackson et al., 2016; Jeffery et al., 2016; Lim et al., 2021), (2) studies examining the microbial signature and adaptations of extremely long-lived individuals (e.g., nonagenarians and centenarians) (Biagi et al., 2016; Collino et al., 2013; Rampelli et al., 2013; Tuikhar et al., 2019) and (3) studies examining changes in the microbiota of older individuals that are linked to specific age-related disorders (Ke et al., 2018; Ruiz-Ruiz et al., 2020).

Collectively, these studies found significant age-associated alterations in microbial diversity. Microbiome diversity is often assessed using two main metrics: alpha diversity and beta diversity (Lozupone et al., 2012). Alpha diversity measures the diversity within a specific microbial community, providing insights into the variety of species present and their abundance (Walters and Martiny, 2020). Higher alpha diversity indicates a more diverse microbial community at a specific site, suggesting a rich array of microbial species. On the other hand, beta diversity assesses the differences in microbial composition between distinct microbial communities, providing a measure of diversity between samples (Walters and Martiny, 2020). Thus, higher beta diversity indicates greater dissimilarity between microbial communities, suggesting distinct compositions at different sites or among different groups. It has been shown that beta diversity distances are significantly different between older adults and younger adults (Biagi et al., 2016; Tuikhar et al., 2019; Wu et al., 2019; Yu et al., 2015). Moreover, centenarians demonstrated higher alpha diversity compared to young-old and younger adults (Kong et al., 2016; Tuikhar et al., 2019), and those with elevated alpha diversity displayed greater temporal

stability in microbiota composition over time (Jeffery et al., 2016). Furthermore, lower alpha diversity was linked to reduced cognition during ageing (Verdi et al., 2018), and correlated with metabolic and inflammatory diseases (Kashtanova et al., 2018). In both centenarians and old adults, a diverse ecosystem was indicative of a resilient and adaptive gut microbiota, potentially serving as a marker of longevity (Allesina and Tang, 2012).

Identifying specific microbial taxa associated with either healthy or unhealthy ageing requires longitudinal studies tracking individuals over an extended period, correlating gut microbiome composition at intermediate points with final physiological or clinical status. Despite the absence of longitudinal studies investigating the age-microbiome connection, a commonly utilised alternative is to use a cross-sectional study design (Ghosh et al., 2022). This design stratifies older populations based on markers of healthy and unhealthy ageing, revealing corresponding taxonomic markers. Frailty, the primary characteristic of ageing, has consistently demonstrated associations with the microbiome in studies such as those conducted on the ELDERMET cohort in Ireland (Ghosh et al., 2022; Jackson et al., 2016; O'Toole and Jeffery, 2015). Furthermore, investigations into various disorders linked to an unhealthy ageing trajectory, such as reduced physical activity, cardiometabolic disorders or cognitive decline have revealed microbiome changes akin to those broadly associated with frailty (Ghosh et al., 2022; Haran et al., 2019; Langsetmo et al., 2019; Verdi et al., 2018).

Overall, these microbiota changes are primarily characterised by loss of commensals that are reduced with ageing in general and proliferation of pathobionts, including *Eggerthella*, *Desulfovibrio*, Enterobacteriaceae members and disease-associated Clostridia (Ghosh et al., 2022). Moreover, other commensals (such as *Akkermansia, Odoribacter, Butyricimonas, Butyrivibrio, Oscillospira, Christensenellaceae* and *Barnesiellaceae*) increase with age, especially in centenarians, but decrease in certain age-associated disorders (Badal et al., 2020).

In conclusion, during ageing, gut microbiota become less diverse, health-promoting bacteria decrease, while opportunistic bacteria or pathobionts increase, especially in unhealthy ageing. Extremely long-lived individuals tend to overcome those changes by increasing healthy ageing-associated microbial taxa

that are otherwise lost when transitioning to a state of physiological decline, as well as maintaining alpha diversity.

1.2.4 Lifestyle and environmental exposure

The composition of the gut microbiota is influenced by several environmental factors, including antibiotic treatment, exercise, geographical location, smoking and sleep. Antibiotic exposure is known to have a significant impact on gut bacterial composition, often disrupting both short and long-term microbial balance, including decreases in the richness and diversity of the community (Dethlefsen et al., 2008). The impact and duration of microbiota recovery after antibiotic administration seems to vary among individuals, likely influenced by the initial inter-individual diversity of the microbiota before treatment (Dethlefsen and Relman, 2011; Jakobsson et al., 2010). One previous human study revealed that the administration of intravenous ampicillin, sulbactam, and cefazolin significantly impacts both microbial ecology and the production of crucial metabolites, such as acetyl phosphate and acetyl-CoA, crucial for major cellular functions (Pérez-Cobas et al., 2013). Additionally, antibiotic-treated mice exhibit increased susceptibility to pathogenic infections, specifically by antibiotic-associated pathogens such as *Salmonella typhimurium* and *C. difficile*, attributed to alterations in mucosal carbohydrate availability that favour their proliferation in the gut (Ng et al., 2013).

Furthermore, regular physical activity has been associated with a more diverse and beneficial gut microbiota (Allen et al., 2018; Clarke et al., 2014). When investigating professional athletes, one study provides insights into the compositional and functional distinctions in the gut microbiota associated with endurance exercise. Athletes were shown to have increased pathways related to amino acid biosynthesis and carbohydrate metabolism as well as higher levels of microbial produced metabolites (i.e. SCFAs) when compared with sedentary control groups (Barton et al., 2018).

Moreover, previous studies have demonstrated significant differences in microbial profiles between individuals from different geographical regions (Yatsunenko et al., 2012). Other studies have indicated that smoking is an environmental factor modulating the composition of human gut microbiota (Biedermann et al., 2013). More exactly, microbial composition changes

following smoking cessation were observed leading to increased levels of Bacillota and Actinomycetota and a lower proportion of Bacteroidota and Pseudomonadota. In addition, smoking cessation led to an increase in microbial diversity (Biedermann et al., 2013). Moreover, one murine study demonstrated that chronic sleep disruptions negatively impact gut microbiota (Poroyko et al., 2016).

In conclusion, understanding the intricate relationships between these lifestyle and environmental factors and the gut microbiota provides valuable insights into potential avenues for modulating microbial communities to promote health and prevent disease.

1.3 Bi-directional relationship between gut microbiota and host: commensal microbes influence host traits

In essence, while the composition of the gut microbiota is influenced by an array of factors, commensal microbes along with their components and by-products heavily influence host physiology. Emerging research has demonstrated that the gut microbiota play a critical role in modulating host immune defence (Belkaid and Hand, 2014), brain function (Rogers et al., 2016), host metabolism (Le Chatelier et al., 2013b; Martin et al., 2019; Turnbaugh et al., 2006; Wong et al., 2016; Zheng et al., 2016), circadian rhythm (Choi et al., 2021), feeding behaviour, food preferences and satiety (Alcock et al., 2014), host gene expression (Nichols and Davenport, 2021), ageing and susceptibility to diseases (de Vos et al., 2022; O'Toole and Jeffery, 2015). Understanding the bidirectional relationship between the gut microbiota and host physiology provides valuable insights into human physiology, health and disease (Figure 1.1). However, the challenges of causation underscore the need for rigorous study designs and continued research to elucidate the specific mechanisms underlying microbiota-host interactions.

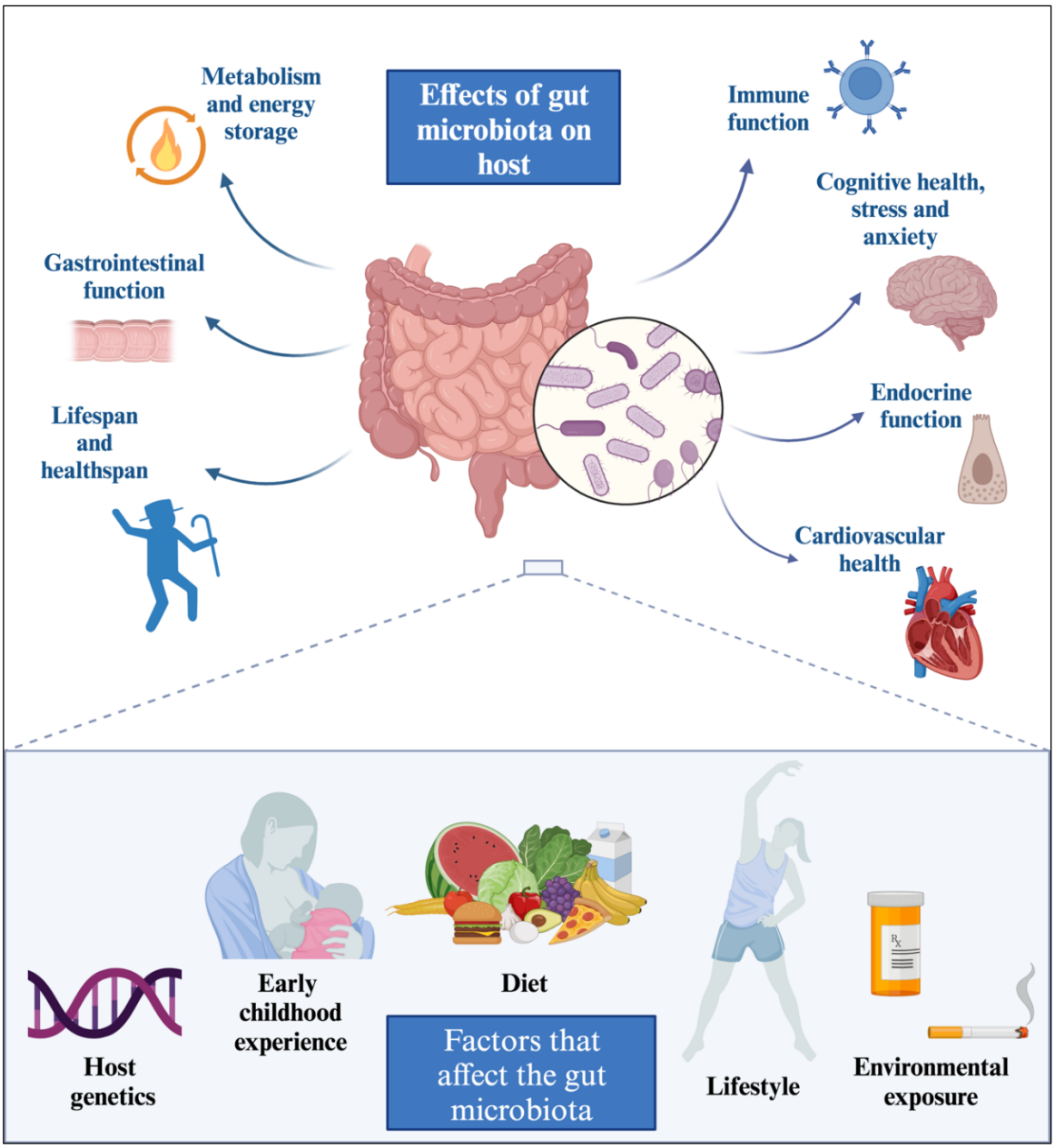

Figure 1.1 The bidirectional nature of the gut-microbiota-host interaction.

Most insights into the impact of gut microbiota on host physiology and health have been derived from experimental studies employing germ-free (axenic) and gnotobiotic animal models (Uzbay, 2019). The designation 'germ-free' (GF) denotes an organism entirely devoid of microbes, including bacteria, viruses, fungi, protozoa, and parasites, for its entire lifespan (Wostmann, 2020). Animals that are GF and subsequently colonised with specific bacterial species are termed gnotobiotic (Wostmann, 2020). These models, allow for meticulous control over the microbial environment, enabling researchers to unravel the molecular intricacies of the host-microbiota interplay, allowing researchers to determine the function of individual species or a consortium of bacteria (Bäckhed et al., 2005). Thus, comparisons of GF mice with conventionally raised

mice have unveiled a multitude of impacts that commensal microbes exert on host biology. The following section elucidates key highlights from studies examining GF rodent models. For a more comprehensive overview of the phenotypes observed in GF rodents, please refer to Table 1.1.

1.3.1 Metabolism and energy storage

Early studies have delineated differences in host physiology between GF and conventional mice, with notable observations such as an enlarged cecum and modified gastrointestinal physiology and function (Bolsega et al., 2023; Donowitz and Binder, 1979; Banasaz et al., 2002; Pull et al., 2005; Savage et al., 1981; Abrams and Bishop, 1967; Manca et al., 2020; Gustafsson et al., 1966; Ridlon et al., 2014; Wostmann, 1973; Uribe et al., 1994). These changes signify an adaptation to the absence of microbes, and the reintroduction of gut microbiota was shown to partially revert these alterations (Gordon and Pesti, 1971), offering valuable insights into the influence of gut microbes on host function. Another essential discovery from studies on rodents raised in GF conditions is that the gut microbiota contributes significantly to host energy harvest, as it converts less accessible nutrient sources like plant polysaccharides and complex carbohydrates into easily absorbable metabolites (Tremaroli and Bäckhed, 2012; Yamanaka et al., 1977).

Furthermore, conventionally raised rodents were shown to have 40% more total body fat than their GF counterparts fed the same polysaccharide-rich diet, even though conventional animals feed less on average per day (Bäckhed et al., 2004). This phenomenon may appear paradoxical initially, but can be clarified by recognising that the gut microbiota facilitates energy extraction from otherwise indigestible dietary polysaccharides (Yamanaka et al., 1977). Faecal transplantation from conventional donors to GF mice was shown to raise body fat content to levels comparable to those of controls (Bäckhed et al., 2004). However, subsequent studies reported the opposite - decreased body fat levels and plasma triglycerides in the presence of gut microbes (Caesar et al., 2016; Le Roy et al., 2019; Vijay-Kumar et al., 2010). This discrepancy has been largely attributed to differences in diets (Le Roy et al., 2019). Overall, in the present consensus, it is acknowledged that biological processes, specifically lipid metabolism, can be influenced by interactions between microbes and nutrients,

rather than being solely determined by microbiota or diet in isolation. Moreover, strain specificity also plays a role, with different mice strains exhibiting inherent genetic variations, immune system responses, physiological characteristics and thus different responses to microbiota depletion.

Additionally, transplantation studies demonstrate that GF mice are resistant to obesity in a Western diet context (Bäckhed et al., 2007). Intriguingly, transferring gut microbiota from obese mice to GF mice significantly increases body weight and fat mass compared to colonisation with a lean microbiota, thus establishing a causal relationship (Turnbaugh et al., 2006). Furthermore, transplanting faecal microbiota from human twin pairs discordant for obesity into GF mice resulted in the acquisition of lean and obese phenotypes according to the donor (Ridaura et al., 2013). However, this phenotype transmission is highly dependent on diet, particularly facilitated by a low-fat diet with increased vegetables and fruits, and consequently enriched in fibre.

1.3.2 Immune system

The gut microbiota plays a crucial role in maintaining the normal function of the mucosal immune system. Toll-like receptors (TLRs) are responsible for recognising microbial associated patterns (mAMPs) in the gut, distinguishing pathogenic bacteria from harmless commensal microorganisms (Akira and Hemmi, 2003). GF animals exhibit decreased or absent expression of TLRs and reduced antibody (IgA) secretion (Abrams et al., 1963; Grenham et al., 2011; Shanahan, 2002; Wostmann et al., 1970). Moreover, the immune response in GF mice is attenuated, characterised by reduced production of the proinflammatory cytokine tumour necrosis factor α after splenocyte stimulation with lipopolysaccharide (Clarke et al., 2013). Interestingly, the colonisation of GF mice restores the function of the mucosal immune system (Umesaki et al., 1995). These findings collectively underscore the necessity of bacterial exposure for mounting a normal immune response.

1.3.3 Endocrine system

Moreover, comparing hormone levels between GF and conventional mice has provided direct evidence of microbial regulation of intestinal hormones. Glucagon-like peptide-1 (GLP-1) is one of the most widely studied gut-derived

peptide hormones and is produced in intestinal enteroendocrine cells (EEC) (Lebrun et al., 2017). Postprandial GLP-1 levels exhibit a nutrient-dependent increase, facilitating insulin release in response to glucose and thereby being a crucial regulator of glucose metabolism (Jørgensen et al., 2013). Given these effects, GLP-1 has emerged as a highly successful therapeutic approach in treating Type 2 Diabetes (T2D) (Buse et al., 2019) and, more recently, obesity (Wilding et al., 2021). Peptide Y (PYY), another peptide hormone co-produced in EECs alongside GLP-1, plays a significant role in regulating intestinal transit and appetite, with both PYY and GLP-1 contributing to these functions (Lafferty et al., 2018).

The concept of microbial modulation of intestinal hormones is not novel, as hormone assays conducted as early as 1989 revealed elevated basal plasma levels of both GLP-1 and PYY in GF mice (Goodlad et al., 1989). Subsequent observations demonstrated that the conventionalisation of GF mice led to a corresponding reduction in GLP-1 levels (Gregor et al., 2009). Another study found increased basal intracellular content of GLP-1 and PYY proteins in the EECs of GF mice compared to those of conventional mice. Moreover, Wichmann and colleagues confirmed higher GLP-1 expression in the colon of both GF and antibiotic-treated mice (Wichmann et al., 2013).

Insulin-like peptide-5 (INSL5) belongs to the relaxin peptide family and is co-expressed with GLP-1 and PYY in the EECs of the distal gut and is released in response to various nutrient or metabolite stimuli (Billing et al., 2018). Significantly, GF mice demonstrate an 80-fold increase in colonic INSL5 expression compared to conventional mice (Lee et al., 2016). This elevated expression returns to normal when GF mice are re-colonised with bacteria or provided with energy in the form of fat, suggesting that INSL5 exhibits energy-sensing properties (Lee et al., 2016).

Serotonin, also known as 5-hydroxytryptamine (5-HT), is produced in the brain and the gut, specifically in enterochromaffin cells, a subtype of EECs (Bellono et al., 2017). In contrast to the higher levels observed for other gut hormones in GF mice, serotonin levels are notably diminished in GF mice when compared to conventional mice (Yano et al., 2015). Moreover, GF mice experiments,

demonstrated that gut-microbiota-derived serotonin plays a role in regulating intestinal motility, platelet function, and neurogenesis in the host (De Vadder et al., 2018; Yano et al., 2015).

In summary, the communication between commensal microbes and intestinal hormones underscores the intricate interplay between gut microbiota and host physiology. Exploring and understanding these interactions can lead to innovative strategies for maintaining or restoring systemic health and developing targeted therapies for a wide range of diseases.

1.3.4 Cognitive health, stress and anxiety

There is now a growing body of literature supporting the role of the gut microbiota in the regulation and development of the stress response system (Collins et al., 2012; Cryan and Dinan, 2012; Foster and McVey Neufeld, 2013; Rhee et al., 2009; Sampson and Mazmanian, 2015). Most of the current knowledge about the impact of the gut microbiota on stress responsivity has emerged from GF rodent studies. Hypothalamic-pituitary-adrenal (HPA) axis responsivity studies in GF mice have unveiled the crucial impact of commensal microbes on the development of the HPA axis. The ground breaking work of Sudo et al. (2004) was the first to reveal that GF mice exhibit an exaggerated release of corticosterone in response to acute restraint stress compared to control mice (Sudo et al., 2004). This hyperactivity is entirely rescued when GF mice are mono-colonised with *Bifidobacterium infantis* during the neonate period (Sudo et al., 2004). On the other hand, mono-colonisation with the enteropathogenic bacteria *Escherichia coli* triggers even higher stress hormone release in GF mice (Sudo et al., 2004). These divergent outcomes highlight the strain-specific effects of bacteria on stress response. Similar findings of increased stress-induced corticosterone release have also been reported in GF rats (Crumeyrolle-Arias et al., 2014).

Given the observation of HPA axis hyperactivity in GF mice, the subsequent question was whether stress-related behaviours were likewise impacted by the gut microbiota. However, unexpectedly, several studies have indicated that GF

mice display a decrease in baseline levels of anxiety-like behaviour (Clarke et al., 2013; Diaz Heijtz et al., 2011; Neufeld et al., 2011). The stress-related behavioural characteristics of germ-free (GF) mice seem responsive to microbial intervention, as the colonisation of GF mice restores normal anxiety-like behaviour (Clarke et al., 2013).

Overall, the conflicting results observed in GF rodent studies, where corticosterone levels are higher, but anxiety-like behaviour is lower, can be attributed to the complex and multifaceted interactions between the gut microbiota and the host's neuroendocrine and behavioural responses. The absence of gut microbiota may trigger compensatory mechanisms in the host, attempting to regulate stress responses and maintain homeostasis. These compensatory mechanisms may manifest as alterations in anxiety-like behaviour despite elevated corticosterone levels.

1.3.5 Lifespan

Furthermore, accumulating evidence suggests a role for the gut microbiota in influencing the ageing process. Notably, mice raised in a GF environment exhibit extended lifespans compared to conventionally colonised control mice (Reyniers and Sacksteder, 1958; Gordon et al., 1966; Tazume et al., 1991). As GF mice are raised in sterile conditions, their longer lifespan is likely in part due to the absence of pathological infections. Another explanation for their long-lived phenotype could be that GF mice often exhibit lower levels of inflammation due to the absence of microbial-induced inflammatory responses in the gut (Honda and Littman, 2016). Moreover, as previously discussed, in humans, microbial diversity and stability decrease with age and are accompanied by physiological decline (O'Toole and Claesson, 2010; Borre et al., 2014). These findings have prompted the idea that interventions aimed at targeting the gut microbiota could be employed to enhance healthspan.

Table 1.1 The impact of gut microbiota on host phenotypes, defined by comparing germ-free (GF) and conventionally raised rodents.

System/Function	*Phenotype*	*References*
GI system	GF mice and rats have enlarged cecum	(Bolsega et al., 2023; Donowitz and Binder, 1979)
	GF mice intestinal villi are thinner	(Banasaz et al., 2002)

	GF mice have slower epithelial renewal rates	(Banasaz et al., 2002; Pull et al., 2005; Savage et al., 1981)
	GF mice have slower gut motility	(Abrams and Bishop, 1967; Manca et al., 2020)
	GF rats have reduced bile acid deconjugation	(Gustafsson et al., 1966)
	GF rats produce more bile acids	(Ridlon et al., 2014; Wostmann, 1973)
	GF rats have fewer enteroendocrine cells	(Uribe et al., 1994)
Central nervous system	GF mice have reduced anxiety behaviour	(Neufeld et al., 2011)
	GF mice have increased HPA stress response	(Sudo et al., 2004)
	GF mice have disrupted neurogenesis	(Scott et al., 2020)
	GF mice have increased blood brain barrier activity	(Braniste et al., 2014)
	GF mice have decreased amyloid-ß pathology	(Harach et al., 2015)
Cardiovascular system	GF mice increased vascular stiffness	(Edwards et al., 2020)
	GF rats have lower cardiac output	(Wostmann et al., 1968)
Endocrine system	GF mice are more insulin sensitive	(Bäckhed et al., 2004; Caricilli and Saad, 2013)
	GF mice have increased GLP-1 and PYY plasma levels	(Wichmann et al., 2013)
	GF mice have increased Insulin like peptide 5 (ILP5) circulating levels	(Lee et al., 2016)
	GF mice have decreased serotonin levels	(De Vadder et al., 2018; Yano et al., 2015)
	GF mice have lower circulating levels of leptin and adiponectin	(Bäckhed et al., 2004)
Metabolism	GF mice are vulnerable to vitamin deficiencies	(Sumi et al., 1977)

	GF rats do not extract as much energy from their diet	(Bäckhed et al., 2004; Gordon and Pesti, 1971)
	GF mice and rats have lower metabolism	Bäckhed et al., 2004)
	GF mice are leaner and have a smaller body size	(Bäckhed et al., 2004)
	GF mice have lower blood glucose and insulin levels and are resistant to obesity induced by a high-fat diet	(Bäckhed et al., 2007)
	GF mice have increased cholesterol, phospholipid and triglyceride levels	(Le Roy et al., 2019)
Immune system	GF mice have reduced B-cells and immunoglobulin secretion	(Horsfall et al., 1978)
	GF mice have reduced TLRs	(Abrams et al., 1963; Grenham et al., 2011; Shanahan, 2002; Wostmann et al., 1970)
	GF mice are resistant to developing inflammatory bowel disease	(Hudcovic et al., 2001; Mizoguchi et al., 2000)
	GF rodents have reduced susceptibility to arthritis	(Hudcovic et al., 2001)
Lifespan	GF rats and mice live longer	(Gordon et al., 1966; Tazume et al., 1991; Wicker et al., 1987)

1.4 Gut microbiota in ageing and disease

In conclusion, germ-free studies played a pivotal role in unravelling the intricate relationship between the gut microbiota and host traits and provided a foundational understanding of how the presence or absence of gut microbiota influences various aspects of host physiology. The ground-breaking insights gained from germ-free studies paved the way for exploring the broader implications of microbiota-host interaction in the context of human health and disease. Subsequent research has focused on elucidating the association between disturbances in the gut microbiota homeostasis (dysbiosis) and a wide

range of diseases, expanding our understanding of the intricate relationship between the microbiota and host health (DeGruttola et al., 2016).

1.4.1 What is a 'healthy' gut microbiota?

A fundamental prerequisite for asserting the disruption of gut microbiota in diseased states is a comprehensive understanding of the composition and function of the gut microbiota in healthy individuals. However, defining a 'healthy' gut microbiota at a detailed taxonomic level remains a challenge. The unique relative distribution of gut microorganisms varies among individuals due to factors such as strain-level diversities, differences in microbial growth rates, structural variations within microbial genes, and the substantial inter-individual variation in environmental exposures and host genetics (Korem et al., 2015; Pedersen et al., 2018; Rothschild et al., 2018; Zeevi et al., 2019).

In general, in healthy conditions, gut microbial communities exhibit high taxa diversity and abundant microbial gene richness (Consortium, 2012). It is crucial to acknowledge, however, that relying solely on high bacterial diversity and richness does not provide an unbiased indication of a healthy intestinal microbiota (Falony et al., 2018). This is due to the influence of intestinal transit time on microbial richness, where prolonged transit times may lead to increased richness without necessarily reflecting a healthy gut microbiota.

Additionally, a 'healthy' gut microbiota exhibits traits of stability, resilience, volatility, and symbiotic relationships with the host (Bastiaanssen et al., 2021; Lozupone et al., 2012). The ability to adapt to stress is a hallmark of health, as health is continuously jeopardised by a variety of stressors (López-Otín and Kroemer, 2021). Consequently, organisms employ a range of strategies, such as resilience, hormesis, repair, and, when possible, regeneration of damaged tissues and organs, to achieve homeostasis (López-Otín and Kroemer, 2021). The gut microbiota ecosystem, which has its own intrinsic homeostasis, typically undergoes transient modifications in response to perturbations, after which it restores its baseline state of homeostasis (Dogra et al., 2020; Sommer et al., 2017). Stability in the context of gut microbiota refers to the ability of the microbial communities to maintain a relatively consistent composition and functionality over time in response to both internal and external perturbations

(Lozupone et al., 2012). While stability focuses on maintaining a baseline state, resilience refers to the capacity to return to homeostasis after a disturbance (Lozupone et al., 2012). Stability and resilience are interconnected, as a stable microbiota is better equipped to exhibit resilience. Moreover, volatility refers to the stress-induced fluctuations in the composition of the gut microbiota over time (Bastiaanssen et al., 2021). High volatility indicates substantial variability in the microbiota, potentially reflecting instability or dysbiosis. In conclusion, diversity, richness, stability, resilience, volatility, and the nuanced interplay between them can be used as parameters to distinguish between healthy and dysbiotic states of gut microbiota.

1.4.2 Communication between gut microbiota and host

When investigating the complex interplay between the gut microbiota and the host, bridging the understanding of 'healthy' gut microbiota and the concept of dysbiosis, a crucial gateway emerges — the communication mechanisms that underscore the profound influence of gut microbes on host physiology. To unravel the nuanced ways in which gut microbiota affect the host, it is necessary to understand the molecular communication they employ. Commensal microbes and their host live in symbiosis, where the host provides the microbes with nourishment and a secure environment, and in return, the microbes assist the host in extracting energy from poorly digested food and producing metabolites and signalling molecules (Neu et al., 2007). At times, this symbiotic relationship can backfire, potentially contributing to the development or advancement of diseases, particularly chronic inflammatory diseases, but also cancer, mental and neurodegenerative disorders (Hou et al., 2022a; Zhang et al., 2023). The crosstalk between microbial and host cells is mediated by microbiota's ability to produce and regulate signals. These signals may consist of either structural components of the bacterial cell or metabolites generated by the microbiota, capable of influencing distant organs directly or through signalling pathways involving nerves or hormones from the gut (Schroeder and Bäckhed, 2016).

Structural components, sometimes referred to as mAMPs, including lipopolysaccharide (LPS) from Gram negative bacteria, teichoic acids from Gram positive bacteria, peptidoglycan and flagellins are detected by pattern-

recognition receptors (PRR), TLRs, NOD-like receptors (NLRs) or RIG-1-like receptors (RLRs), on epithelial and immune cells (Schroeder and Bäckhed, 2016). Generally, the translocation of structural components across the epithelial barrier is inhibited. However, minimal amounts of LPS were reported to reach the lymph and circulation through paracellular diffusion, transcellular transport, or co-transport with chylomicrons (Bäckhed et al., 2003; De Vadder et al., 2018; Ghoshal et al., 2009). Yet, the majority of microbial signalling relies on metabolites, with only a minor portion attributed to structural components. Metabolites generated by gut microbiota can be broadly grouped into three categories: those derived from externally ingested materials, those produced by the host and subsequently modified by gut microbes, and those synthesised *de novo* by gut microbes (Postler and Ghosh, 2017). Approximately 10% of metabolites in mammalian blood are estimated to originate from the gut microbiota, exerting diverse effects on host physiology and homeostasis by binding to host receptors and thus activating downstream signalling pathways (Wikoff et al., 2009).

Belonging to the first category, short-chain fatty acids (SCFAs), such as acetate, propionate and butyrate, produced by microorganisms like Bacteriodota and Bacillota during fermentation of dietary fibres are the most common microbial-produced metabolites (Cheng et al., 2022; Wrzosek et al., 2013). SCFAs modify the intestinal environment by reducing pH, thus preventing the overgrowth of pH-sensitive pathogenic bacteria (Gibson and Roberfroid, 1995; Nie et al., 2019; Canani et al., 2011). SCFAs also contribute to the integrity of the intestinal barrier by synthesising mucus and antimicrobial peptides (AMPs) (Cobo et al., 2017). Additionally, SCFAs, particularly butyrates, help reduce epithelial permeability by targeting the integrity of tight junction complexes (Wang et al., 2012). Moreover, interventional studies have shown that administration of the SCFA butyrate benefits pathological conditions of intestinal inflammation (Blaak et al., 2020; Canani et al., 2011; Jain et al., 2004).

Furthermore, they have been shown to bind G protein-coupled receptors (GPCRs) on EECs and induce expression of intestinal hormones, such as PYY and GLP-1, and thus act as signalling molecules at different body sites (Schroeder and Bäckhed, 2016). Previous studies illustrate that propionate acts as a

precursor for intestinal gluconeogenesis, and both propionate and butyrate induce gluconeogenic enzyme expression, thus controlling metabolic homeostasis (De Vadder et al., 2014). Acetate has been suggested to suppress appetite (Frost et al., 2014); however, a study found that acetate increased the hunger hormone 'gherlin', thus increasing food intake and promoting obesity in rodents fed a high-fat diet (Frost et al., 2014). Moreover, acetate, can trigger insulin secretion from pancreatic Beta cells through vagus nerve stimulation (Frost et al., 2014). Moreover, acetate is used to acetylate coenzyme A, producing acetyl-CoA which can then trigger hepatic *de novo* lipogenesis (Zhao et al., 2020). Acetate was also shown to induce chromatin remodelling within EECs, regulating host metabolism and intestinal innate immunity via a Tip60-steroid hormone axis (Jugder et al., 2021). Additionally, microbiota-derived lactate has been shown to confer broad spectrums of health benefits, such as activation of mucosal and systemic immunity and resistance to infectious illnesses (Schiffrin et al., 1995; Wells and Mercenier, 2008), supporting intestinal stem-cell-mediated epithelial development (Lee et al., 2018) and promoting hematopoiesis and erythropoiesis (Lee et al., 2021).

However, the significance of these mechanisms in humans and whether other microbial metabolites induce similar pathways remain unclear. Overall, in addition to influencing GI health, SCFAs may impact body weight control by affecting appetite and insulin sensitivity, thus contributing to the pathophysiology of obesity and related conditions including T2D (Canfora et al., 2017; Chambers et al., 2015; Ríos-Covián et al., 2016).

Moreover, tryptophan can be catabolised by gut bacteria into several derivatives, such as indole, indole derivatives, and serotonin (Agus et al., 2018). These metabolites have neuroactive potential and play crucial roles in gut health and host physiology. Specifically, indole emerges as a pivotal signalling molecule in colon cancer. It binds and activates the aryl hydrocarbon receptor (AHR) in the GI, which subsequently leads to leads to heightened interleukin (IL)-6 expression in human colon adenocarcinoma cells, thereby amplifying inflammatory responses within the tumour (Hubbard et al., 2015). Other indole-derivates, such as oxindole and isatin, were shown to have neurodepressive properties (Abel, 1995; Bhattacharya et al., 1991; Rothhammer et al., 2016),

while Indole-3-propionic acid (IPA), have been shown to modulate microglia, and thus reduce brain inflammation (Rothhammer et al., 2018).

Secondly, metabolites produced by the host and subsequently modified by commensal microbes include taurine, polyamines and bile acids. Metabolically modified taurine by commensal gut microbes was shown to increase hydrogen sulphide (H_2S) levels, a gaseous signalling molecule implicated in the modulation of many biological processes including ageing and longevity (Dattilo et al., 2022; Wilkie et al., 2021, 2020). Polyamines, such as spermidine and spermine, are bioactive compounds synthesised within eukaryotic cells (Igarashi and Kashiwagi, 2010). The gut microbiota may indirectly influence spermidine levels through their impact on host metabolism and nutrient availability, but they are not the direct producers of spermidine (Igarashi and Kashiwagi, 2010). Spermidine exhibits antioxidant effects by scavenging free radicals and reducing oxidative stress. Notably, spermidine has been shown to exhibit antioxidant, anti-inflammatory cardio and neuro-protective properties (Eisenberg et al., 2016; Gupta et al., 2013; Igarashi and Kashiwagi, 2010). Moreover, the intracellular concentration of spermidine naturally declines during human ageing and spermidine administration significantly extended the lifespan of yeast, flies, worms and mice (Eisenberg et al., 2009). The beneficial effects of spermidine were shown to stem from its ability to increase autophagy, a cellular process that contributes to the removal of damaged cellular components (Eisenberg et al., 2009). Lastly, the extracellular nucleotide adenosine triphosphate (ATP), synthesised *de novo* by gut microorganisms, has been demonstrated to be involved in immune responses by stimulating cytokine production (Faas et al., 2017).

1.4.2 Dysbiosis-induced pathogenesis of metabolic diseases

Having elucidated the intricate communication between commensal microbes and the host, it becomes imperative to delve into the repercussions of dysbiosis. Accumulating evidence indicates that gut microbiota dysbiosis is pivotal in the onset and progression of metabolic disorders (Jandhyala, 2015; Blumberg and Powrie, 2012; Hou et al., 2022). As discussed in the GF rodent studies section,

one of the first pieces of evidence for a mechanistic involvement of the gut microbiota in the regulation of metabolism was based on the discovery that the gut microbiota governs the host's ability to extract energy from the diet and store energy (Bäckhed et al., 2004). Subsequent epidemiological investigations revealed variations in the gut microbiota between obese and lean individuals. Twin studies highlighted associations between obesity and the abundance of certain species: SCFA producers like *Eubacterium ventriosum* and *Roseburia intestinalis* are linked to obesity(Tims et al., 2013), while butyrate producers like *Oscillospira spp.* and *Methanobrevibacter smithii* are associated with leanness (Gophna et al., 2017; Miller et al., 1982). Metagenome-wide analyses in lean and obese individuals identified reduced levels of *Bacteroides thetaiotaomicron* in obesity, inversely correlated with serum glutamate concentration (Liu et al., 2017). Pathway and gene family analyses indicated decreased unidirectional conjugation capacity and reduced superoxide reductase in obesity, potentially leading to intestinal oxidative stress.

Furthermore, the gut microbiota is implicated in T2D development, evidenced by altered composition in T2D patients. Decreased Bacillota and Clostridia, along with altered ratios of Bacteroidota to Bacillota and Bacteroidota-*Prevotella* group to *C. coccoides-E. rectale* group, were shown to correlate positively with blood glucose levels (Larsen et al., 2010). Furthermore, SCFA-producing bacteria, including *Facalibacterium* and *Roseburia*, are diminished in T2D. Antidiabetic agents were shown to enhance gut microbiota diversity, enriching beneficial bacteria (Almugadam et al., 2020). Considering that T2D is associated with increased inflammation, the underlying molecular mechanisms linking gut microbiota to T2D are thought to involve modulation of inflammation, gut permeability, and glucose metabolism (Gomes et al., 2017). LPS is known to promote low-grade inflammation by activating the NF-κB signalling pathway (Hou et al., 2022), and previous studies have shown that T2D patients have elevated LPS plasma levels which leads to increased levels of inflammatory factors, ultimately inhibiting insulin secretion(Shapiro et al., 2018). SCFAs produced by gut microbiota mediate glucose metabolism and insulin sensitivity by stimulating the release of GLP-1 and PYY, as previously discussed. Furthermore, butyrate protects the intestinal barrier integrity and acts as an anti-inflammatory mediator, potentially limiting autoimmune responses by

promoting regulatory T-cell production (Takahashi et al., 2020). Therefore, the reduced abundance of SCFA-producing bacteria in T2D patients may contribute to disease development.

In conclusion, microbial by-products play a pivotal role in maintaining intestinal health. The mechanistic basis of their beneficial effects includes pH regulation to reduce the overgrowth of pathogenic bacteria, synthesis of mucins and AMPs to fortify the intestinal barrier, and the modulation of epithelial permeability by targeting tight junction complexes. Such local actions contribute significantly to the resilience against pathological conditions, particularly intestinal inflammation. While the local effects are well-documented and understood, the mechanisms governing the systemic consequences remain enigmatic. The potential prevention or induction of chronic metabolic diseases by microbiota metabolites poses a complex puzzle yet to be fully unravelled. Further research is needed to delineate the complex signalling pathways and molecular interactions that govern these systemic effects.

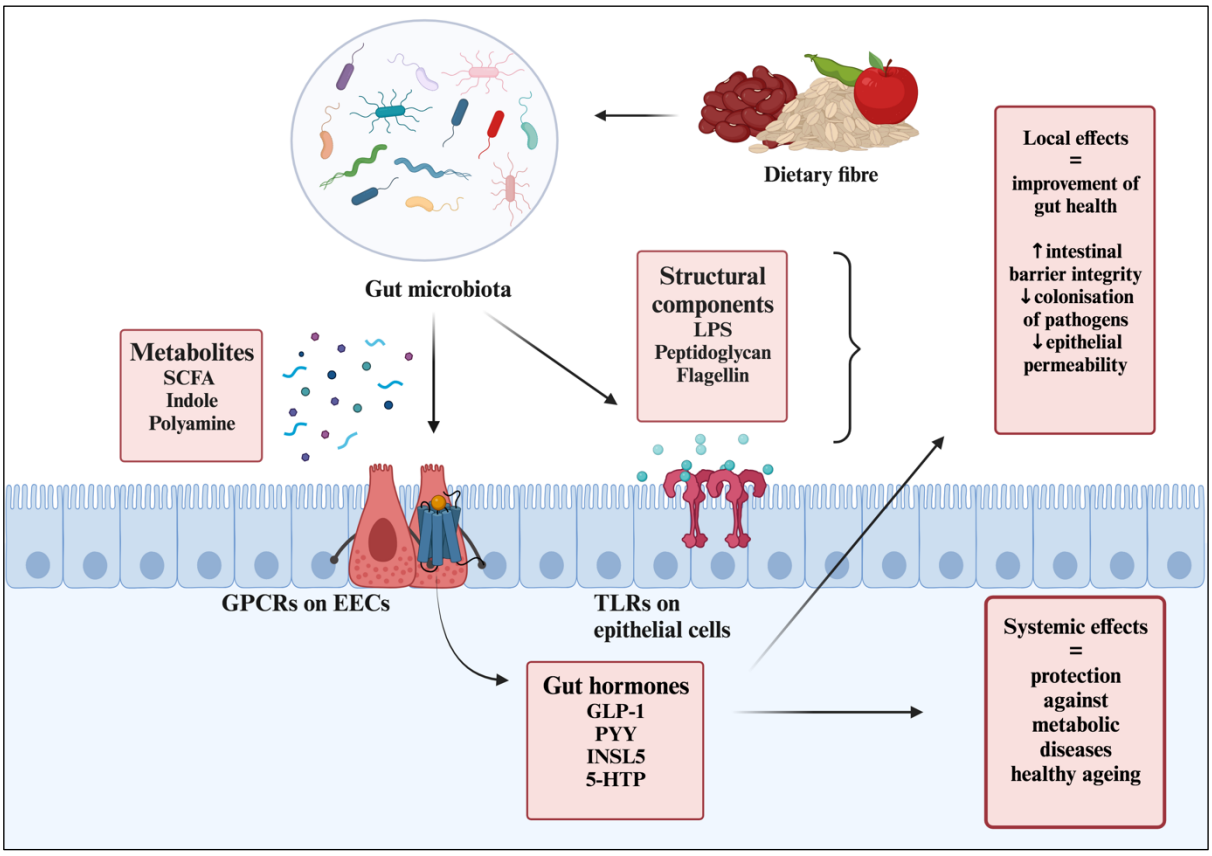

Figure 1.2 Overview of the effects of microbial by-products on host.

Most microbial metabolites are synthesised by gut microbiota from dietary components. They can signal to the host via G protein-coupled receptors

(GPCRs) on enteroendocrine cells (EECs) and induce expression of intestinal hormones and thus act systemically as signalling molecules at different body sites. Structural components are detected by Toll-like receptors (TLRs) on epithelial and immune cells and are generally not translocated across the epithelial barrier.

1.4.3 Dysbiotic changes in the ageing gut

The impact of dysbiosis is not confined to disease states; it extends its influence on the ageing process. The symbiotic relationship between gut microbiota and host physiology undergoes alterations as the host advances in age. These age-related changes in the gut microbiota could be implicated in the ageing-associated decline in physiological functions. However, due to challenges in discerning causation from correlation in microbiota studies and the lack of objective ageing metrics (De Magalhães and Pedro, 2024), verifying or refuting hypotheses regarding the role of microbiota in ageing poses considerable difficulty.

As previously mentioned, studies investigating the link between gut microbiota and ageing rely on age-associated changes in gut microbiota composition (Le Chatelier et al., 2013b; Nagpal et al., 2018). However, insights into the mechanistic regulation of ageing may be gleaned from studying their broader roles in physiology. During ageing, gut dysbiosis increases, disrupting the homeostatic relationship between gut microbiota and host, ultimately affecting whole-organism physiology (Kim and Jazwinski, 2018). Previous studies suggest that age-related microbial dysbiosis induces a proinflammatory environment within the gut (Thevaranjan et al., 2018). Transplantation studies in mice indicated that aged microbiota leads to increased inflammation when grafted in germ-free young mice (Fransen et al., 2017). In ageing flies, eliminating microbiota prevents metabolic deterioration, epithelial dysplasia, and intestinal barrier dysfunction observed when bacteria are present (Biteau et al., 2010).

Other studies demonstrated that ageing induces chronic activation of Janus kinase–signal transducers and activators of transcription (JAK-STAT) signalling

which subsequently leads to intestinal stem cells (ISCs) overproliferation, gut damage, and disorganisation (Buchon et al., 2009). Consistent with this observation, old flies raised without bacteria have reduced JAK–STAT signalling, and gut physiology more similar to that of young flies (Buchon et al., 2009). Moreover, inhibition of JAK-STAT signalling prevents age-related gut disorganisation and extends lifespan (Li et al., 2016). Mechanistically, gut microbes might control ISC activity via uptake of outer membrane vesicles released by gram-negative bacteria. Peptides, DNA and small RNAs contained in these vesicles are thought to modify ISC gene expression (Peck et al., 2017). There is evidence that SCFAs can also alter ISCs – i.e., butyrate was shown to inhibit proliferation of colonic stem cells (Peck et al., 2017). Butyrate is also known to have anti-inflammatory effects by supressing nuclear factor–kappa B (NF-κB) (Qin et al., 2018). Accordingly, centenarians were shown to have increased levels of butyrate-producing bacteria, reinforcing the relationship between gut microbiota, inflammation and longevity (Biagi et al., 2010). Moreover, *A. muciniphila* is known for breaking down mucin and supplying energy to SCFA-producing bacteria. Additionally, it safeguards the integrity of the intestinal epithelium by activating epithelial cells and promoting mucus production, thereby facilitating colonisation of beneficial commensals. Moreover, it has been shown that *A. muciniphila* is reduced in the gut of aged mice and in elderly individuals (Fransen et al., 2017; Ragonnaud and Biragyn, 2021; Xu et al., 2019).

Therefore, age-related dysbiosis leads to local intestinal inflammation which subsequently compromises the integrity of the gut barrier. Intestinal barrier dysfunction was associated with several markers of ageing in *Drosophila*, such as systemic metabolic dysfunction, increased expression of antimicrobial peptides, and reduced spontaneous physical activity (Rera et al., 2012). Another study demonstrated that microbial dysbiosis precede and predict intestinal barrier dysfunction, thus establishing microbiota composition as a predictor of health (Clark et al., 2015). As proposed by Nobel laureate Elie Metchnikoff in 1907, the physiological decline associate with ageing process can be attributed to the accumulation of ‘putrefactive bacterial autotoxins’, leaking from the colon (Metchnikoff, 1907).

Subsequent studies demonstrated that the compromised gut barrier allows for the leakage of microbial products, such as LPS, into the bloodstream. This phenomenon, now referred to as ‘leaky gut’, exposes the systemic circulation to components that are normally restricted to the gut lumen (Camilleri, 2019). For example, studies in mice have demonstrated that increased gut permeability is associated with elevated systemic inflammation, contributing to the development of age-related conditions (Thevaranjan et al., 2017). Consequently, circulating microbial products and inflammatory mediators can trigger systemic inflammation.

In summary, the current understanding of the role of gut microbiota in ageing primarily relies on association studies and investigations into gut permeability (leakiness). Association studies have identified correlations between alterations in the gut microbiota composition and various age-related conditions. However, correlation does not imply causation, and establishing a clear cause-and-effect relationship is challenging. On the other hand, studies on gut leakiness have demonstrated potential links between microbial dysbiosis, chronic inflammation and age-related physiological changes. However, the specific microbial species or metabolites responsible for these effects and the precise mechanisms involved are not fully understood.

While these studies have provided valuable insights, there are significant gaps and the mechanisms underlying the relationship between gut commensal microbes and ageing remain incompletely elucidated. The bidirectional nature of the gut-microbiota-host interaction adds complexity, as ageing-related changes may influence the gut microbiota, and vice versa. Furthermore, the majority of existing research is observational, and mechanistic insights into how gut microbes directly contribute to ageing processes are lacking. Intervention studies and experiments manipulating the gut microbiota in controlled settings are essential to establish causation and identify specific microbial contributions to ageing-related phenotypes. Moreover, the impact of gut microbiota on systemic health and ageing is influenced by individual variations, including genetics, diet, lifestyle, and environmental factors. The heterogeneity in study populations and methodologies across different research studies adds to the complexity of drawing universal conclusions. In conclusion, while existing

research has laid a foundation for understanding the role of gut microbiota in ageing and systemic health, the link between gut microbiota and the ageing process is only partially understood. However, the gut ecosystem shows potential for contributing to systemic health and ageing and understanding the precise role of gut microbiota in regulating host processes remains an evolving area of research.

The subsequent chapters explore these themes using the model system *Drosophila melanogaster* and its microbiota. As many of the effects of the microbiota are fundamental to animal biology, they are conserved from less-complex invertebrates to humans. Due to its low complexity, culturable microbiota, ability to generate complete germ-free flies, its plethora of genetic tools, and its easiness to rear and perform high-throughput life history experiments throughout a lifespan, *Drosophila melanogaster* is the ideal model to understand the role the microbiota plays in host ageing and systemic health.

The primary aim of this thesis is to delineate the mechanisms by which the gut microbiota influences host physiology, with a particular focus on ageing and systemic health, using *Drosophila melanogaster* as a model system. Central to this investigation is the role of gut peptides, with a focus on *tachykinin*, in mediating the microbiota's regulatory functions on host metabolism and longevity. Objectives include assessing the expression patterns of enteroendocrine peptides in response to microbial presence, dissecting the influence of individual microbial species such as *Acetobacter pomorum* and *Lactobacillus brevis* on these processes, and elucidating the signalling pathways involved, particularly the IIS/TOR network and the action of insulin-producing cells. The pursuit of these objectives is intended to provide a deeper understanding of the gut microbiota's systemic impact on host health and ageing, potentially paving the way for innovative strategies to bolster healthspan through microbiota-targeted interventions.

Chapter 2 Materials and methods

2.1 *Drosophila melanogaster*

2.1.1 Fly husbandry – Conventional flies

All flies were kept in temperature-controlled incubators with a 12-12-hour light-dark cycle on standard 5% Sugar, 10% Yeast, and 1.5% Agar (SYA) medium. Fly stocks were kept at 25°C. All crosses for experiments were set up at 25°C. The progeny of all crosses were moved onto fresh SYA food on day 1 and kept for 3 days in the same temperature as parental crosses. All experiments were performed on day 3, unless stated otherwise. Stock flies at 25°C were transferred to fresh medium every two weeks. Only mated female flies were used for experiments.

When the RU486-inducible gene switch system was employed, for every 1mL of food, 2µL of RU486 (Mifepristone; Sigma-Aldrich) was used making a final concentration of 200µM. To induce gene expression, flies were transferred to SYA vials supplemented RU486 on day 3. Control groups were treated similarly, with the exception of RU486 addition. Flies were fed on RU486 supplemented SYA for the whole duration of experiment

Table 2.1 Standard *Drosophila* SYA medium recipe per 1L of ddH_2O. The medium is cooked until it begins to boil and then allowed to cool below 60 °C before adding the preservatives.

Ingredient	*Quantity per litre*	*Percentage*
Agar	15 g	1.5%
Sugar	50 g	5%
Brewer's yeast	100 g	10%
Propionic acid	3 mL	0.3%
Nipagin (Sigma-Aldrich)	30 mL	3%

2.2.2 Fly stocks

Table 2.2 List of *Drosophila* stocks used in this study.

Abbreviation	*Genotype*	*Source*		
		BDSC	**VDRC**	**Other**

	***UAS* lines**			
	UAS-TK-shRNAi		v330743	
	UAS-TK-RNAi	B25800		
	UAS-TK-RNAi		v103662	
	UAS-ITP-RNAi		v330021	
	UAS-DTKR-RNAi		v44369	
	UAS-NKD-RNAi		v107090	
	UAS-Reaper			
	UAS-AkhR-RNAi			
	UAS-MCD8::GFP			
	***Gene Switch* lines**			
DaGS	*Daughterless-GeneSwitch;*			
Dilp-GS	*Dilp2,3-GeneSwitch*			
S106-GS	*S106-GeneSwitch*			
Elav-GS	*Elav-GeneSwitch*			
Mex-GS	*Mex-GeneSwitch*			
	***GAL4* lines**			
	Voila-GAL4			
	Akh-GAL4			
TK-GAL4	*TK-GAL4 (knock-in)*			Rewitz lab
	Gal80 lines			
	Chat-Gal80			
	Auxin-Gal80			
	R57C10-Gal80			Rewitz lab
	Other lines			
wD^{-20}	*White Dahomey-20*			
	FOXO Δ			

2.1.3 Backcrossing

To generate experimental transgenic flies two inbred lines are crossed - one containing the transgene to be activated and the other containing a genetic construct that drives the expression of the first. However, it is extremely important to standardise the genetic background of all lines. Otherwise, the

cross can produce a hybrid genetic effect, also termed heterosis, which can affect different fitness trains, such as lifespan, which is generally increased compared to inbred controls (Pearl, 1921; Mackay et al., 1998). This would lead to confounding results; lifespan extension being solely attributed to heterosis and irrespective of any effect of the transgenes (Burnett et al., 2011). To avoid this, the mutant lines were backcrossed into a standardised wild-type genetic background, white$^{Dahomey-20}$ (w^{D-20}), for six generations (Figure 2.1). There are two commonly used genetic *Drosophila* strains called white^{1118} (w^{1118}) and w^{D}. The *white*^{1118} strain originates from the wild caught Oregon R strain, containing a spontaneous partial deletion in the *white* (*w*) gene discovered by R. Levis (Bingham, 1980; Hazelrigg et al., 1984), producing white eyes instead of red. On the other hand, the w^{D} strain was created in the Partridge Lab by repeatedly backcrossing the mutated w gene from white^{1118} into the outbred wild-type Dahomey strain. The Dahomey strain was originally collected in Dahomey, now Benin (Puijk & de Jong, 1972), and has been maintained since then in large population cages with overlapping generations. Most mutant lines used in this study (Table 2.2) have been backcrossed into w^{D} for 6 generations (Figure 2.1). Exceptions are the *TK-GAL4* (knock-in) and *R57C10-Gal80* lines from Rewitz lab, which were backcrossed into the white^{1118} strain.

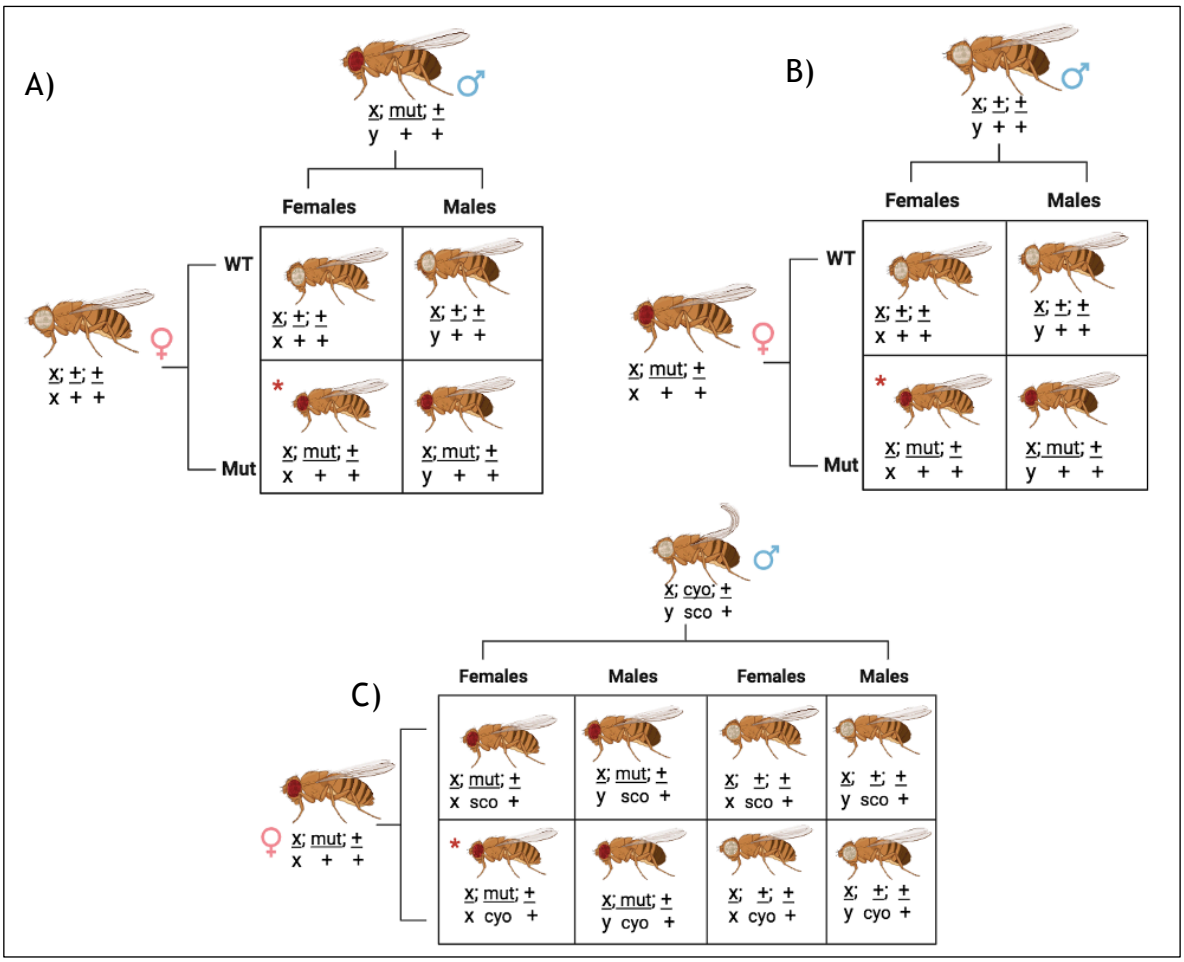

Figure 2.1 Scheme of backcrossing transgenic lines into white^{Dahomey}.

A) In the first cross w^D virgin females were crossed with transgenic males. In this example, the mutation was on the second chromosome and heterozygous. From this cross we selected the females that contained the mutation and thus had red eyes. B) Virgin females containing the mutation selected from cross A were backcrossed with w^D males for 6 generation. C) Virgin females containing the mutation were ultimately crossed with a balancer for the second chromosome (*cyo*/*sco*). The offspring from this last cross will have the mutation balanced with either *cyo* or *sco*. Virgin females and males balanced with the same balancer are crossed and maintained into stocks. In the case of transgenes on the third chromosome, insertions would be balanced using a *TM6B*/*MKRS* stock.

2.1.4 Generating axenic and gnotobiotic flies

Axenic flies were prepared and reared on sterile SYA food (5% sucrose (Fisher Chemical), 10% lyophilised yeast (Sigma-Aldrich), 1.5% agar (Sigma-Aldrich)). Food was prepared in an Integra Mediaclave and dispensed in a laminar flow cabinet using sterile technique. To generate axenic flies, eggs were collected on

juice agar plates within 18h of egg deposit. To sterilise the eggs, they were washed 2x in alternating 10% bleach for 3 min and sterile ddH2O for 1 min. Subsequently, the eggs were transferred into sterile food bottles containing 50mL of food. Food bottles were then incubated at 25°C.

To generate gnotobiotic flies, *Acetobacter pomorum* was streaked and grown on M9+lactate agar (1.5%), before growing single colonies in liquid M9 medium + + lactate at 30°C with shaking at 225 rpm for 2 days. *Lactobacillus brevis* was streaked on Yeast Peptone Dextrose (YPD) agar (1.5%), then grown in YPD media for two days at 30C in static culture. Cultures were pelleted, washed with 1xPBS, then resuspended in 1xPBS at an OD_{600} of 0.2. 200 µL of bacterial suspensions were added to their respective food bottles containing axenic eggs. Food bottles were then incubated at 25°C. Flies were incubated until emergence to adulthood (day 10) before transfer to fresh medium. Flies were allowed to make three days before males were removed by gentle anaesthesia on CO_2 followed by sorting on ice in a sterile petri dish.

2.2 Bacterial strains and media

- *Lactobacillus brevis DmCS003* (*Lb*) was grown and maintained in Yeast Peptone Dextrose (YPD) medium at 30°C without shaking.
- *Acetobacter pomorum DmCS004* (*Ap*) was grown and maintained in M9 medium with 0.5% DL-lactic acid at 30°C with shaking at 250 rpm.

Table 2.3 Standard YPD medium recipe per 1L.

Reagents	*Quantity per litre*
Yeast	10 g
Peptone	20 g
Dextrose	20 g

Table 2.4 Standard M9 medium recipe per 1L.

Reagents	*Quantity per litre*
5x M9 salts	200 mL
1M $MgSO_4$	2 mL

1M $CaCl_2$	1 mL
20% (v/v) Lactate	25 mL
ddH_2O	772 mL

2.3 Phenotyping

2.3.1 TAG assay

Female flies were collected and divided into groups of 5, 3 days post eclosion. Each group was weighed on a Thermo microbalance to an accuracy of .01 mg. Weighed females were added to a sterile 2mL screw-cap tube containing sterile 1.4mm ceramic beads and 125 µL of TET buffer (10mM Tris, 1mM EDTA, pH 8.0, 0.1% (v/v) Triton-X-100). Samples were homogenised for 30s at max speed. After homogenisation, samples were incubated at 72°C for 15 min in a dry bath to inactivate lipases and other enzymes. Then samples were centrifuged at max speed for 5 min at 4°C. From each sample 3 µL of the supernatant was added to a clear, flat bottom 96 well plate. Standard curves were generated using a glycerol stock ranging from 1-0 ug/ul.

Experiments in chapter 3 and 4 were done using the Infinity Triglycerides (Fisher Scientific) reagent. 300 µL of Infinity Triglycerides reagent was added to each well containing either standard or sample. The plate incubated at 37ºC for 20 minutes in the dark. After incubation, absorbance reading was taken on the multiscan plate reader at 540 nm. Values were then normalised to the body weight of the 5 females.

Experiments in chapter 5 and 6 were done using the Sigma Triglycerides reagent. 5 µl of sample or standard was added to the plate, using the same layout as previously described. 200 µl of pre-warmed Sigma glycerol reagent was added, the plate covered with foil and incubated for 10m at 37ºC. The absorbance reading for glycerol was taken on the multiscan plate reader at 540 nm. Next, 50 µl of triglyceride reagent was added, the plate covered with foil and incubated at 10m for 37ºC. After incubation, the absorbance reading was taken on the multiscan plate reader at 540 nm. The glycerol values were then subtracted from the triglyceride reading. Values were then normalised to the body weight of the 5 females.

2.3.2 Lifespan

Parental flies were crossed in cages containing juice agar plates with a smear of yeast. After 24h, the juice agar plate containing the eggs was disposed and replaced with a fresh one. After 18h of egg deposit eggs were collected and placed on SYA food and incubated at 25ºC. 3 days post-eclosion, female progeny with the desired genotype were collected and divided into groups of 15. Flies were transferred to fresh food every 2–3 days. For each transfer, deaths and censors were scored until all flies were dead. For axenic and gnotobiotic lifespans, the axenic protocol was followed, the sorting and tipping was done in a sterile laminar flow hood and the food was sterile in sterile glass vials.

2.3.3 Starvation resistance

Parental flies were crossed in cages containing juice agar plates with a smear of yeast. After 24h, the juice agar plate containing the eggs is disposed and replaced with a fresh one. After 18h of egg deposit eggs were collected and placed on SYA food and incubated at 25ºC. 3 days post-eclosion, female progeny with the desired genotype were collected and divided into groups of 15. Flies were then transferred to vials containing 1% agar and kept at 25ºC. Dead flies were counted once a day, until all flies were dead. For axenic and gnotobiotic starvation resistance experiments, the axenic protocol was followed, the sorting and tipping was done in a sterile laminar flow hood and the agar was sterile in sterile glass vials.

2.3.4 Proboscis extension response assay and egg laying

Feeding rate was measured by a behavioural assay, quantifying average proboscis extension rate (PER) over 3-4 hours. After setting up female flies as described above at a density of 5 flies per vial, vials were arranged on a benchtop in a 25ºC room such that the experimenter could see all vials. The night before behavioural observations, vial numbers were recoded to blind the experimenter, and the distribution of conditions among the new code was randomised to indiscriminate the position of conditions on the bench. The following morning, PER was recorded by iteratively counting the instantaneous number of flies feeding per vial for 3-4 hours. The average of these measurements per each given vial was taken as that vial's feeding rate. At the

end of the experiment, flies were disposed, and vials frozen. The next day eggs were counted from the same frozen vials.

2.3.4 Colony formation unit assay

Groups of 5 female flies of the desired genotype were collected sterilely in 500 mL 1x PBS. Flies were then homogenised using a sterile pestle. Flies were then serially diluted 1:10 from 10^0 to 10^3. 50µl from each were plated on YPD media. Plates that had between 20-300 colonies were picked, colonies were counted, and colony formation units (CFU) calculated based on which dilution the plate was from.

2.4 Molecular biology assays

2.4.1 RNA extraction

RNA was extracted from whole flies by the addition of 10 female flies per sample to sterile 2 mL screw cap tubes containing 600 µL of TRIzol (Ambion by Life technologies) per sample and homogenised using the the Ribolyzer and running at 6.5 (max) for 10 seconds. Next, 200 µL chloroform was added to each homogenate, briefly vortexed, and incubated at RT for 3 min. Samples were then centrifuged 12,000rpm for 15m at 4ºC and the supernatant containing the RNA was carefully pipetted to a new RNase free Eppendorf tube. Next, to each sample 250µl of isopropanol was added, the samples briefly vortexed, and incubated at RT for 10 minutes. Samples were then centrifuged at 12,000rpm for 10m at 4ºC. The liquid was removed and discarded, while the pellet containing the RNA was washed with 1mL of 75% ethanol. Samples were centrifuged at 12,000rpm for 10m at 4ºC. The liquid was removed without disturbing the pellet, and the tubes were incubated at RT with their caps opened, allowing the remaining ethanol to evaporate. RNA pellet was reconstituted by adding DEPC water (10µl/fly) and stored at -80ºC.

2.4.2 RT-qPCR

RNA samples were quantified by spectrophotometry using a Nanodrop 1000 UV-Vis spectrophotometer (ThermoScientific). First strand synthesis of cDNA was performed using the SuperScriptTM Reverse Transcriptase (RT) kit (Invitrogen), following the manufacturer's protocol (using 2µg of RNA). The PCR profile was as

follows: 95°C for 2 minutes; 94°C denaturation for 30 seconds, 60°C annealing for 30 seconds, 72°C extension for 30 seconds each for 40 cycles, with a final extension at 72°C for 5 minutes. The amplicon was migrated through a 1% (w/v) agarose gel. To test for relative gene expression levels, RT-qPCR was performed. Each well contained 2 µl cDNA, 1.5 µl 10 mM forward primer, 1.5 µl 10 mM reverse primer, 3 µl water, 10 µl SYBR green PCR master mix, and 2 ul ROX (Qiagen, UK). The following PCR profile was used: 95°C for 5 minutes; 94°C for 30 seconds, 60°C for 30 seconds, 72°C for 30 seconds each for 40 cycles, and a final extension at 72°C for 5 minutes. Mean cycle threshold (Ct) values for duplicates of each of the studied genes were derived by subtracting the combined mean Ct value of constitutively expressed housekeeping gene *alcohol dehydrogenase* (*ADH*) or *tubulin*. To ensure the validity of RT-qPCR experiments, the housekeeping genes were chosen based on their stable expression across axenic and conventional flies, as validated by the differential expression analysis in Chapter 3. This precaution was taken to confirm that the absence of microbiota does not inadvertently influence the expression stability of these reference genes.

Table 2.5 List of primers for RT-qPCR used in this thesis.

Target	*Forward*	*Reverse*
TK	TTCATATGCGCCCTCTGAGCG	ATGAAGCTGGACGTGGGCGC
Bursicon	CGCCACGAGAACAACAAGGT	CATCCAGGATACTGGAGCAC
ADH	GCTAACGAGTACTTGCATCTCTTC	AGACCGGCAACGAAAATCAC
Tubulin	TCGCCGTCACCGGAGTCCAT	TGGGCCCGTCTGGACCACAA
Attacin A	CACAACTGGCGGAACTTTGG	AAACATCCTTCACTCCGGGC
Attacin B	GCAATGGAGCTGGTCTGGAT	CCGATTCCTGGGAAGTTGCT
Attacin C	TGCCCGATTGGACCTAAGC	GCGTATGGGTTTTGGTCAGTTC
Dilp2	ATGGTGTGCGAGGAGTATAATCC	TCGGCACCGGGCATG
Dilp3	AGAGAACTTTGGACCCCGTGAA	TGAACCGAACTATCACTCAACAGTCT
Dilp4	GCGGAGCAGTCGTCTAAGGA	TCATCCGGCTGCTGTAGCTT
Dilp5	GAGGCACCTTGGGCCTATTC	CATGTGGTGAGATTCGGAGCTA
Dilp6	CGATGTATTTCCCAACAGTTTCG	AAATCGGTTACGTTCTGCAAGTC
Dilp7	CAAAAAGAGGACGGGCAATG	GCCATCAGGTTCCGTGGTT
4ebp	CACTCCTGGAGGCACCA	GAGTTCCCCTCAGCAAGCAA

2.4.3 Protein extraction

Protein was extracted from whole flies Sigma RIPA homogenising buffer. 9.9mL of RIPA was mixed with 100µl of Halt protease and 100X phosphatase inhibitor. 20 flies were homogenised in 300µl of RIPA buffer mixed with the inhibitors in a 1.5mL Eppendorf tube. Samples were incubated on ice for 10ms to activate the protease and phosphatase inhibitors. Samples were then centrifuged for 15m at 13,000 rcf at 4ºC. Supernatant containing protein extracts was then collected in a new Eppendorf and the pellet was discarded

2.4.4 Western blotting

Protein concentration was determined by Bradford assay. 25 µg of protein was loaded per well into Mini-PROTEAN TGXTM precast polyacrylamide gels. Precision Plus ProteinTM Dual Xtra Standards protein marker was loaded to the first well on each gel. Proteins were separated by electrophoresis at 90V for 90m and then transferred onto a nitrocellulose membrane at 0.25V for 1 hour. Membranes were blocked with 5% milk in 1xTBST for 50m. The membrane was washed 5 times with 1X TBST for 5min under constant shaking. Primary antibodies were diluted in 5% BSA in 1x TBST and added to the membrane. Primary antibodies were allowed to incubate overnight at 4ºC, under constant shaking. Fluorescently-labelled secondary antibodies were used at a 1:10000 dilution in 5% milk in 1xTBST for all blots. The secondary was allowed to incubate with the membrane for 1h. Blots were protected from light during incubation. The membranes were then washed 5 times with 1X TBST for 5m, under constant shaking. For imaging, Odyssey Infrared Imaging System was used. Protein signals were quantified using Empiria Studio® Software.

Table 2.6 List of antibodies used for western blotting in this thesis.

Antigen	*Species*	*Source*	*Dilution*	
p-Akt	Mouse	Cell Signalling	1:10000	Primary
Total Akt	Rabbit	Cell Signalling	1:10000	Primary
Alexa Fluor 488	Mouse	Invitrogen	1:10000	Secondary
Alexa Fluor 594	Rabbit	Invitrogen	1:10000	Secondary

2.5 Imaging

2.5.1 Staining fluorescent transgenic lines

Whole midguts from 3 days old female flies were dissected in 1X PBS and fixed in a fixative solution (4% formaldehyde in a pH 7.5 solution containing 100 mM glutamic acid, 25 mM KCl, 20 mM $MgSO_4$, 4 mM sodium phosphate dibasic, 1 mM $MgCl_2$) for 45 min. The fixative solution was removed through a fast fluid exchange and replaced by 1X PBS, followed by 3x30 min washes in 0.1% PBS-Triton at RT. Samples were then incubated in DAPI (Vector Laboratories) [1ug/mL] for 2 mins at RT. This was followed by one fast fluid exchange in 1X PBS at RT and one wash in 0.1% PBS-Triton (PBST) for 10 min at RT. Samples were then mounted in Vectashield mounting medium and covered with a coverslip.

2.5.2 Antibody staining

Whole midguts from 3 day old female flies were dissected in 1xPBS and fixed in a fixative solution (4% formaldehyde in a pH 7.5 solution containing 100 mM glutamic acid, 25 mM KCl, 20 mM $MgSO_4$, 4 mM sodium phosphate dibasic, 1 mM $MgCl_2$) for 45 min. The fixative solution was removed through a fast fluid exchange and replaced by 1xPBS, followed by 3x30 min washes in 0.1% PBST at RT. Samples were then blocked in PTN (1x PBS, 2.5% Normal Goat Serum, 0.5% Triton-X, ddH2O) for 1h at 4ºC. Primary antibody was incubated O/N at 4ºC (1:1000 dilution in PTN) and removed through one fast fluid exchange in 1xPBS, 3 X 10 Min 0.1% PBST Washes + 1h longer 0.1% PBST wash. Secondary antibody was incubated O/N (1:600 in PTN) and removed through one fast fluid exchange in 1xPBS, 3 X 10 Min 0.1% PBST washes, and1h longer 0.1% PBST wash. Samples were then incubated in DAPI [1ug/mL] for 2 mins at RT. This was followed by one fast fluid exchange in 1X PBS at RT and one wash in 0.1% PBST for 10 min at RT. Samples were then mounted in Vectashield mounting medium and covered with a coverslip.

For brains and ventral nerve cord (VNC) dissection, fly heads or whole flies were first washed in 70% ethanol for 30 seconds and fixed as described above. Brains and VNC were transferred to 0.1% PBST and dissected. After dissecting, they were washed two times in PBST and blocked with 7% goat serum (in PBST) for 1

hour. Samples were incubated with primary antibodies in PBS for 48 hours at 4°C followed by the steps mentioned above.

Table 2.7. Antibodies used for immunofluorescence assays.

Antigen	*Species*	*Dilution*	*Supplier*	*Type*
anti-LemTRP1	Rabbit	1:1000	Dick Nassel (Nassel, 1999)	Primary
Alexa Fluor 546	Goat	1:600	Invitrogen	Secondary

2.6 Microscopy

2.6.1 Confocal microscopy

Imaging was performed on a Zeiss LSL 880 confocal microscope and processed using ImageJ software 1.53a.

2.6.2 Automated confocal microscopy

Images for quantification were taken with the automated confocal microscope Opera Phenix (Perkin Elmer) using a 5X objective for pre-scan and 20X water objective for re-scan. Images were analysed with Harmony 4.9 (Perkin Elmer) or ImageJ software 1.53a.

2.7 RNA-seq analysis

2.7.1 Re-analysing published data

Transcriptome sequences were analysed from data published by Bost et al 2017. The quality of sequencing samples was checked with FastQC. Transcript level abundances was quantified using Salmon. Subsequent analysis was conducted in R studio version 1.2.1335. The *tximport* package was used to import Salmon's transcript-level quantifications and aggregate them to the gene level for differential expression analysis. Downstream analysis was performed using *DESeq2* package (Love et al., 2021).

2.7.2 Analysing our own samples

RNA was extracted from whole-flies *w/w; DaGS/UAS-TK*^{RNAi} in the presence or absence of RU486 when they were axenic or colonised with *Acetobacter*

pomorum or *Lactobacillus brevis*. Samples were prepared for 3' RNA sequencing by Glasgow PolyOmics using the Lexogen QuanSeq kit. Samples were sequenced on an Illumina NextSeq 2000 in single-end mode (50 bp) to a depth of ~20M reads per library. FastQC files were then aligned using the Spliced Transcripts Alignment to a Reference (STAR) software (Dobin et al., 2013). The core workflow for both normalised expression and differential expression analysis was generated using the Searchlight pipeline (Cole et al., 2021). Downstream analysis was performed using *DESeq2* package (Love et al., 2021).

2.8 Statistical analysis

Statistical analysis was performed in R studio version 1.2.1335. Tests used and statistical significance for each experiment are included in figure legends. Two-way ANOVA, followed by either Tukey post-hoc test or post-hoc joint test (as stated in the figure legend) was used for analysis of TAG assays, colony formation unit assay, egg laying assays, RT-qPCR and Western blotting. RT-qPCR data was analysed using two-way ANOVA, followed by either Tukey post-hoc test or post-hoc joint test, except for datasets in figure 3.4 and figure 3.6 where Wilcoxon tests were employed and dataset in figure 5.1 determined by one-way ANOVA with Tukey post-hoc test. Quantification of imaging experiments was performed using, unpaired two-sample t-test, except for dataset in figure 5.2 which was analysed using one-way ANOVA with Tukey post-hoc test. For lifespans and starvation resistance assays log-rank test was employed for datasets in figure 3.8 and figure 3.9. All the other lifespan and starvation resistance assays were analysed using analysis of deviance (type III tests) for cox proportional-hazards analysis, followed by pairwise comparisons for estimated marginal means.

Chapter 3

3.1 Summary

The gut microbiota impacts host development, metabolism and lifespan. Age-related microbial changes result in deleterious events for the host including increased inflammation, reduced intestinal permeability and stem cell over proliferation. While microbiota are confined to the gut, they have the potential to systemically modulate whole-organism physiology. Host derived hormones,

such as gut peptides secreted by enteroendocrine cells (EECs), are strong candidates to mediate the influence of microbiota on host health. Our results demonstrate that microbiota impact EECs function and that EECs mediate the impact of microbiota on its host. I reanalysed public data, observing that the gut transcriptome varies with the presence or absence of microbiota. Four gut peptides, *TK*, *ITP*, *AstC* and *NPF*, were differentially expressed in axenic flies compared to control flies. Of these peptides, systemic genetic *TK* knockdown extended lifespan in conventional flies. Our results implicate *TK* as a key mediator of the microbe-host crosstalk, with knockdown extending lifespan in conventional flies, while axenic flies are long-lived and do not respond to *TK* knockdown. Also, *TK* knockdown flies had increased TAG levels compared to control flies. However, the effect of *TK* knockdown on TAG was masked when microbiota was depleted. This suggests that microbiota and *TK* interact epistatically, with the outcome of manipulating either contingent on the other. Moreover, *TK*-knockdown extends lifespan, effect dependent on the interaction with microbiota, without trade-offs for reproduction. It was also noticed that knocking down *TK* does not affect feeding rate in conventional flies but rescues reduced feeding in axenic flies. Survival under starvation conditions was also influenced by the microbiota-*TK* interaction, with axenic flies exhibiting greater starvation resistance, but *TK* knockdown rendering flies constitutively more sensitive to starvation, independent of the microbiota. Furthermore, the interaction between *TK* and microbes is bidirectional, microbes increasing *TK* levels and *TK* increasing microbial growth. Altogether the data show that *TK* is genetically required for a normative response to eliminating microbiota, implicating this peptide as an intercellular signal that mediates microbial influences on numerous aspects of host health.

3.2 Introduction

3.2.1 The *Drosophila* versus the mammalian GI tract

The GI tract acts as a crucial mediator between the external environment and the internal body, orchestrating processes such as sensing, digesting, and nutrient absorption, while also providing defence against pathogens (Furness et al., 2013; Miguel-Aliaga et al., 2018). Importantly, the EE signalling of the gut

serves as a means of communicating the nutritional and physiological state to distant organs. Moreover, the presence of the microbiota within the gut contributes significantly to shaping the overall health and fitness of the organism (Schroeder and Bäckhed, 2016). Operating as a central hub for metabolism, immune function and endocrine signalling, the multifaceted responsibilities of the gut are sustained by a protective mucosal layer and a selectively permeable barrier, facilitated by specialised epithelial cells with distinct roles (Ahlman and Nilsson, 2001; Furness et al., 2013; Gribble and Reimann, 2019; Miguel-Aliaga et al., 2018).

The intestinal epithelium serves as the first line of defence against pathogens, utilising innate immune receptors that recognise mAMPs and thus activate of cellular immune signalling pathways (Buchon et al., 2013; Perez-Lopez et al., 2016; Thaiss et al., 2016). Not only infection by pathogens, but also age-related or disease induced dysbiosis can significantly impact the function, stability, and homeostasis of the intestinal epithelium, potentially leading to severe pathologies, as discussed in chapter 1 (Buchon et al., 2013; Resnik-Docampo et al., 2018; Watnick and Jugder, 2020). Overall, these attributes are conserved across various metazoans, including both *Drosophila* and mammalian GI systems (Capo et al., 2019).

The adult *Drosophila* gut consists of a pseudo-stratified epithelium surrounded by visceral muscles, nerves, and trachea (Miguel-Aliaga et al., 2018). This epithelium is divided into foregut, midgut, and hindgut. The midgut is further segmented into six regions (R0 to R5) with distinct metabolic functions (Buchon and Osman, 2015). The structural and functional resemblance of the *Drosophila* gut to the human intestine is highlighted by the posterior midgut's metabolic activity and immune responsiveness, reminiscent of the human small intestine, while the hindgut aligns with the human colon (Micchelli and Perrimon, 2006). Notably, the posterior midgut lacks the anatomical crypt-like niche structure found in mammalian counterparts (Bonfini et al., 2016). Unlike mammalian digestion, which occurs in acidic conditions, *Drosophila* digestion takes place under predominantly neutral or basic pH conditions (Miguel-Aliaga et al., 2018). While the *Drosophila* gut is generally neutral or mildly alkaline, specific regions, such as the R3 midgut region and the hindgut, exhibit strong acidity (Overend et

al., 2016; Shanbhag and Tripathi, 2009). These physiochemical properties play a crucial role in shaping the distribution, composition, and density of microbes along the gut (Sommer and Bäckhed, 2016). The differences in commensal gut microbial communities between mammals and flies are further discussed in chapter 4.

In mammals, Lgr5+ stem cells differentiate into either absorptive or secretory progenitors, as dictated by Notch signalling (Barker et al., 2007). Absorptive progenitors further differentiate into enterocytes (ECs), while secretory progenitors differentiate into EECs, Paneth and Goblet cells (Chen et al., 2019; Gehart et al., 2019). On the other hand, the fly gut epithelium is maintained and regenerated by resident ISCs which give rise to two types of lineage-committed progenitor cells: the secretory enteroendocrine progenitor (EEP) and absorptive enteroblast (EB) (Micchelli and Perrimon, 2006; Ohlstein and Spradling, 2006). The expression of the TF prospero encourages the commitment and maturation of EEC fate, while Notch activation-induced E(spl) factors promote EC differentiation (Chen et al., 2018).

In both flies and mammals, ECs secrete digestive enzymes and transport nutrients, whereas EECs release hormones and peptides in response to luminal stimuli (Capo et al., 2019). By secreting signalling molecules, EECs regulate inter-organ communication, thus conveying the organism's nutritional status and modulating behaviour and physiology in response to nutrient availability, analogous to their mammalian counterparts (Drucker, 2016; Gribble and Reimann, 2019; Reiher et al., 2011).

3.2.2 Enteroendocrine signalling in *Drosophila* vs mammals

EECs in mammals have been classified using letters, based on the specific hormone they secrete or structural characteristics (Guo et al., 2022). Following this nomenclature, at least 12 EEC subtypes have been recognised, including D cells, enterochromaffin cells, enterochromaffin-like cells, G cells, I cells, K cells, L cells, M cells, N cells, S cells, and X/A cells (P/D1 cells in humans). Collectively, these cells secrete more than 20 types of hormones. The spatial distribution of each subtype is correlated to specific physiological functions (Guo et al., 2022) (Figure 3.1). For instance, G and X/A cells are situated in the

stomach, where they secrete gastrin and ghrelin, regulating the secretion of gastric acid from ECs (Kopin et al., 1992; Masuda et al., 2000; Tack et al., 2006). I, K, and L cells are predominantly found in the small intestine, the primary site for food digestion and absorption, where they release cholecystokinin (CCK), gastric inhibitory peptide (GIP), and PYY/GLP-1, contributing to the coordinated regulation of gut motility, metabolic homeostasis and satiety (Martin et al., 2019; Yu et al., 2020).

In *Drosophila* single-cell RNA sequencing (scRNA-seq) analysis of intestinal cells classified EECs into 10 subtypes (Guo et al., 2019). These EECs collectively express genes encoding at least 15 different peptide hormones, including *Allatostatins (AstA, AstB/Mip, AstC), Tachykinin (TK), neuropeptide F (NPF), short neuropeptide F (sNPF), diuretic hormone 31 (DH31), CCHamide-1 (CCHa1), CCHamide-2 (CCHa2), Neuropeptide-like precursor 2 (Nplp2), glycoprotein hormone beta 5 (Gpb5), ion transport peptide (ITP), crustacean cardioactive peptide (CCAP)*, and *Orcokinin B (Ork-B)* (Guo et al., 2019). *Bursicon (Burs)* expression is documented in certain EECs within the posterior midgut following starvation, despite its absence in both in situ hybridization and scRNA-seq data under normal conditions (Chen et al., 2016; Guo et al., 2019; Scopelliti et al., 2019). The evolutionary conservation of peptide hormones between *Drosophila* and mammals is shown in table 3.1 and table 3.2.

In conclusion, *Drosophila* emerges as a robust model system for investigating EE signalling due to several key factors. Both mammalian and *Drosophila* GI tracts exhibit regional specificity in EEC subtypes (Guo et al., 2022) (Figure 3.1). Additionally, each EEC subtype in both systems expresses 2–5 peptide hormone genes, emphasising shared features (Guo et al., 2022). The compact dimensions of the *Drosophila* midgut allow for a more targeted examination of regional identities. Consequently, *Drosophila* may offer valuable insights into enhancing our understanding of the EECs, the hormones they secrete and their systemic effects.

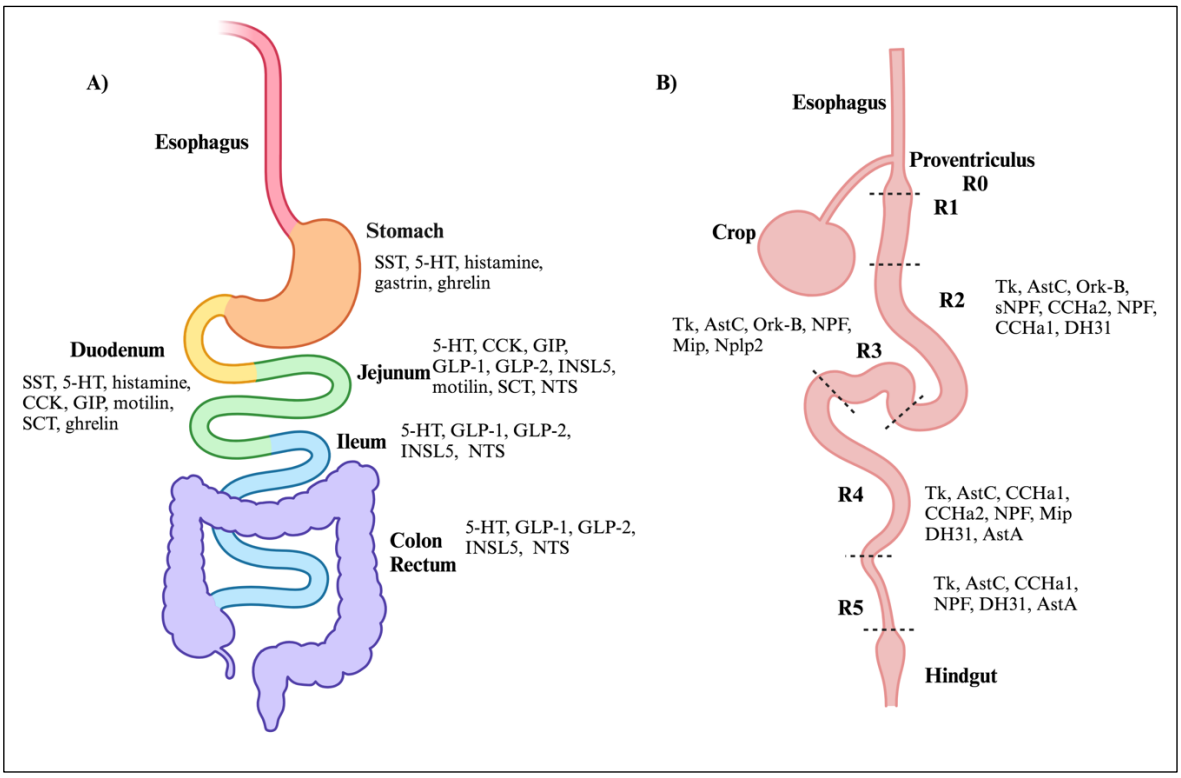

Figure 3.1 Distribution of EEC produced hormones in mammalian a) and b) *Drosophila* GI tract.

Table 3.1 Mammalian homologs of *Drosophila* EEC produced hormones.

Produced in Drosophila	*Mammalian homologue*
TK	Tac1(Song et al., 2014; Thomas et al., 2015)
NPF	NPY (Chung et al., 2017)
DH31	CGRP (Benguettat et al., 2018)
AstC	SST (Zhang et al., 2021)
AstA	Galanin (Mirabeau and Joly, 2013)
CCHa1	N.D.
CCHa2	N.D.
Orcokinin	N.D.
AstB	N.D.
Nplp2	N.D.
Gpb5	Gphb5 (Park et al., 2005)
ITP	N.D.
sNPF	N.D.
CCAP	N.D.

Table 3.2 *Drosophila* homologs of mammalian EEC produced hormones.

Produced in mammals	*Drosophila homologue*
Tac1	Tac1 (Song et al., 2014; Thomas et al., 2015)
Somatostatin (SST)	AstC (Zhang et al., 2021)
5-HT	5-HT
Histamine	Histamine
Gastrin	N.D.
CCK	Dsk (Nässel and Williams, 2014; Rehfeld, 2017)
GIP	N.D.
PYY	N.D.
GLP-1	N.D.
GLP-2	N.D.
Motilin	N.D.
Neurotensin	N.D.
Secretin	N.D.
Ghrelin	N.D.
Oxyntomodulin	N.D.
INSL5	N.D.

3.2.3 Gut microbiome as a signalling organ in ageing and systemic health

Microbial derived SCFAs bind and activate specific receptors on EE cells which are scattered throughout the gut epithelium (Rastelli, Cani and Knauf, 2019). In mice, SCFAs were shown to activate GPCRs that trigger the secretion of gut peptides known to regulate pancreatic function, insulin release, appetite, and energy harvesting (Rastelli, Cani and Knauf, 2019). Furthermore, old mice have increased gut peptide levels in comparison to younger (Johnson et al. 2012), suggesting that microbial signals can influence host endocrine signalling, and this may have consequences in ageing. Thus, EE cells may act as a relay between microbiota and distal host tissues, modifying release of hormones into circulation in response to cues from the gut lumen. However, the functional significance of this behaviour to ageing or to broader physiology is unknown.

Moreover, knowledge of the functions of those neuropeptides is fragmentary. Previous research in flies suggests that *TK* inhibits lipogenesis in enterocytes (EC), playing a key role in intestinal lipid production and homeostasis (Song et al., 2014). Burs was shown to regulate energy metabolism through a neuronal relay leading to the suppression of glucagon-like, adipokinetic hormone (AKH) and subsequent modulation of AKH receptor signalling within the adipose tissue (fat body). Inability of EECs to secrete Burs exacerbates glucose oxidation and depletion of energy stores (Song et al., 2014). Overall, EECs and the peptides they secrete are crucial mediators of metabolism. Intestinal microbiota has the capacity to control and modify gut peptide expression. However, the exact molecular mechanisms through which microbiota regulate host EE signalling, and the relevance of this in host health, is still elusive.

3.2.3 *Drosophila* as a model to study the influence of microbiota on host metabolism and ageing via enteroendocrine signalling

Historically, research using *Drosophila melanogaster* as a model organism has been instrumental in uncovering key insights in molecular biology and genetics (Morgan, 1910, Jennings, 2011). These discoveries range from understanding the chromosomal principles of heredity to unravelling the molecular mechanisms underlying embryogenesis, learning, immunity, ageing and circadian rhythm (Neckameyer and Argue, 2013, Ugur et al., 2016, Droujinine and Perrimon, 2016). Over the years, diverse studies have explored the interactions between *Drosophila* and commensal microorganisms, contributing to the recent surge in research enthusiasm for using *Drosophila* as a model in microbiome research (Broderick and Lemaitre, 2012).

The use of *Drosophila* in microbiome research benefits from powerful genetic and genomic tools available to study the molecular mechanisms of microbe-host interactions. For example, genes of interest can be easily manipulated in specific fly tissues, e.g. by RNAi or overexpression. On the bacterial side, microbiota can be easily manipulated by production of GF (axenic) or gnotobiotic flies. Axenic flies can be generated and maintained, with standard

protocols that are not technically demanding or costly. Moreover, several GF rodent phenotypes (chapter 1) are conserved in flies. In particular, similar to GF rodents, axenic flies live longer (Lee et al., 2019). *Drosophila* is also a valuable model for studying ageing due to its relatively short lifespan, rapid development, convenient husbandry and facile genetics, thus facilitating the discovery of longevity-regulating genetic systems and mechanisms (Douglas, 2018, Piper and Partridge, 2018).

In terms of metabolism, while GF rodents exhibit conflicting metabolic phenotypes, axenic flies consistently show increased fat levels (Smith et al., 2007). However, the metabolic characteristics of axenic flies (i.e. increased lipid, glycogen, glucose and trehalose) resemble the pro-obesogenic effects associated with microbiome perturbation induced by antibiotic treatment in mice (Cox and Blaser, 2015). Moreover, the fly microbiota are simple (few species) and culturable, but fulfil the same functional niche as more complex microbiotas, e.g. as found in mammals (Chandler et al., 2011; Wong et al., 2011). However, in contrast to mammalian microbiota, the fly microbiota are genetically tractable, allowing experimenters to evaluate the function of bacterial genes for host function experimentally (Newell et al., 2022; Shin et al., 2011). This is a powerful feature of the fly system, enabling unprecedented insight into the importance of bacteria for host health. Overall, *Drosophila* is an ideal model organism to study microbiota–host interactions as it allows manipulation of long-distance signals and simultaneously a precisely controlled microbiota and diet, which can be extended to large-scale studies where multiple targets and conditions are analysed (Douglas, 2018).

3.3 Aims

Ageing is a systemic process that dysregulates multiple organ systems (Fabbri et al., 2015), However, despite being confined to the gut, the microbiota has the potential to modulate ageing. Therefore, there must be a mechanism through which gut microbiota systemically affects the body. Host derived hormones, such as gut peptides secreted by EEs, are strong candidates to mediate the influence of microbiota on lifespan and metabolism. Considering that axenic flies are long-lived (Clark et al., 2015) and have increased adiposity (Dobson et al., 2015),

here I will test whether microbe-gut-to-host tissues communication mediates this phenotype.

The main aims of the work presented in this chapter are:
1) To find candidate EEC peptide hormones that mediate the gut microbiota-host crosstalk.
2) To test the influence of those candidates on the host phenotypic response to microbiota.

3.4 Results

3.4.1 Gut transcriptome changes with the presence of microbiota

To investigate how the microbiota impact the gut transcriptome, I analysed published RNA-seq data looking at the gut transcriptome of axenic versus gnotobiotic flies (Bost et al., 2017). In this study, conventionalised gnotobiotic flies were colonised with five bacterial strains of the most abundant microbiota species (5-spp. gnotobiotes - *Acetobacter pomorum, Acetobacter tropicalis, Lactobacillus brevis, Lactobacillus fructivorans, Lactobacillus plantarum*) (Newell and Douglas, 2014). Colonising flies with this standardised microbiota ensured that the microbiota content of replicate samples was uniform, avoiding potential for stochastic variation in microbiota composition that can be observed conventional flies(Wong et al., 2013). These conventionalised flies have a very similar metabolism and overall performance as conventional flies (Douglas, 2019).

I was interested to mine these data to identify putative secreted factors, and especially enteroendocrine peptides, whose expression responds to the presence or absence of microbiota. However, expression of only approx. 5,000 genes was quantified, but the fly genome encodes approximately 17,000 genes, suggesting that a more rigorous analysis may increase the insight that can be mined from these data. I therefore re-analysed the data, by quantifying expression, conducting multivariate analyses, and identifying differential gene expression. Using Salmon, I was able to quantify transcripts from 10,290 genes. To visualise these data, I performed principal component analysis (PCA) of all the expressed

genes (Figure 3.2A). The PCA showed that the expression profile is different between axenic (red) and gnotobiotic flies (blue). To confirm these differences statistically, I performed differential expression analysis (DESeq2), selecting genes with p-value <0.01 and >2-fold change of mean expression level (Figure 3.2B). The chosen cut-offs help to manage the large number of differentially expressed genes by highlighting the most significantly altered expression profiles. I visualised expression of these transcripts in a heatmap (Figure 3.2B).

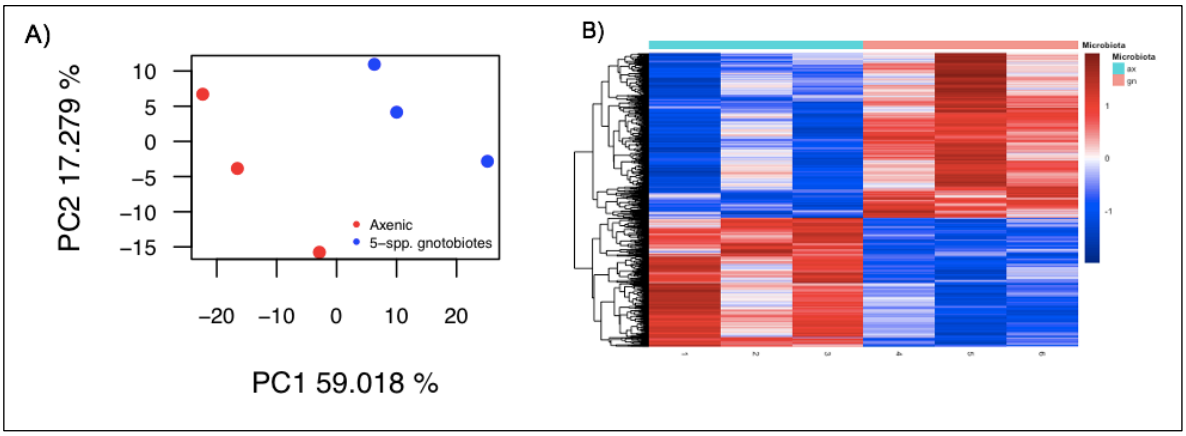

Figure 3.2 The gut transcriptome changes with the presence of microbiota.

The figure presents a reanalysis of public data from Bost et al, 2017. A) Principal component analysis of all 10,290 genes detected in the transcriptome from female axenic fly guts (red) and female conventionalised gnotobiotic fly guts (blue) (30 guts comprising the crop, midgut and hindgut/sample). B) Heatmap of relative expression levels of 470 differentially expressed genes (with a p value < 0.01 and >2-fold difference between mean expression level) between axenic (cyan) and gnotobiotic (pink) flies. The plot shows row Z-scores for read quantifications of the differentially-expressed genes.

To characterise the likely functional outputs of the observed changes in gene expression, I further performed gene ontology enrichment using the TopGO package in R. The results indicated that the differentially-expressed genes were enriched in functions relating to carbohydrate and energy metabolism (Figure 3.3A), have oxidoreductase, catalytic and oxidative phosphorylation functions (Figure 3.3B). Given my goal of identifying putative mechanisms of endocrine signalling, it was encouraging that these genes were also enriched in secreted, extracellular proteins (Figure 3.3C).

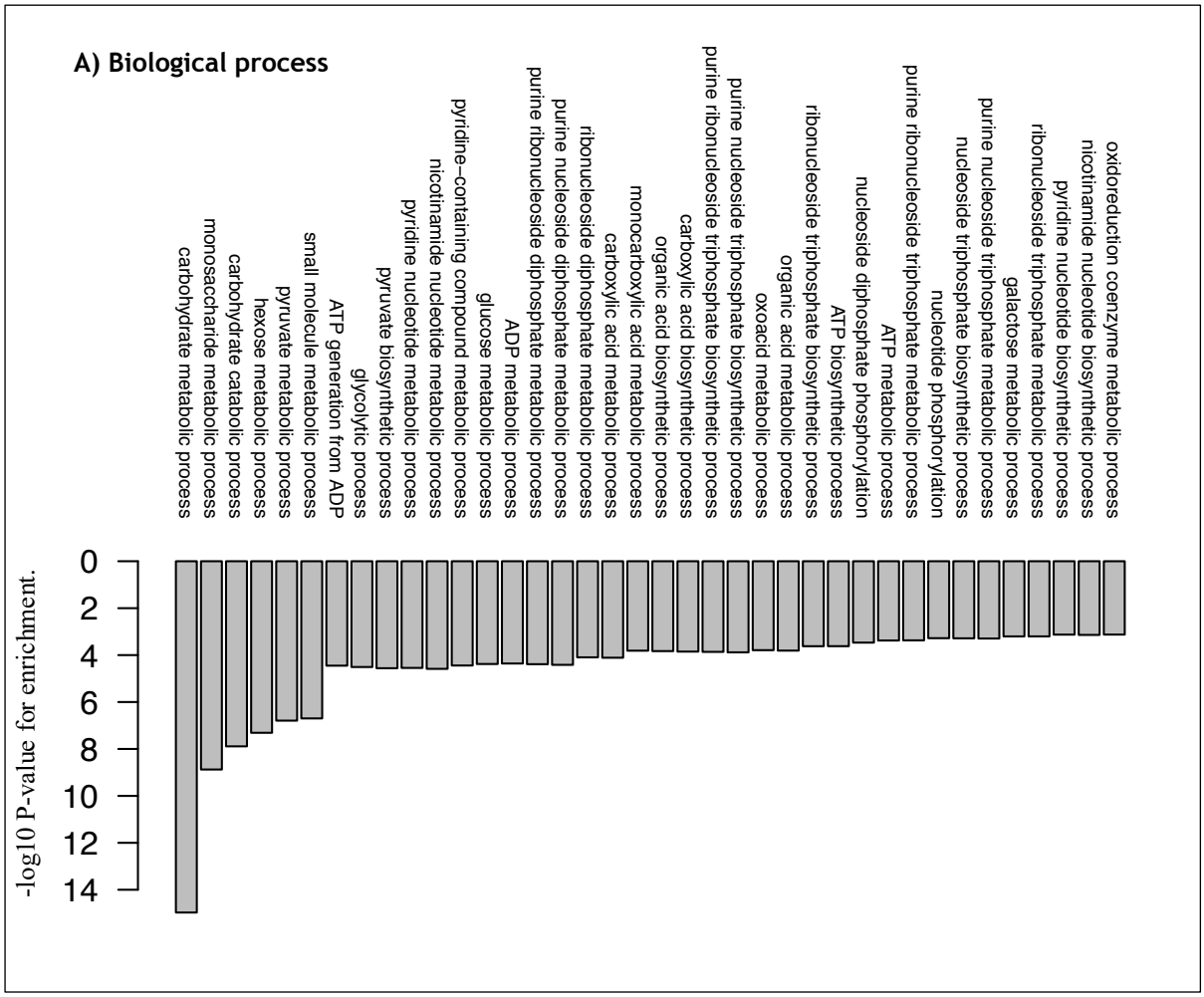
A) Biological process
oxidoreduction coenzyme metabolic process
nicotinamide nucleotide biosynthetic process
pyridine nucleotide biosynthetic process
ribonucleoside triphosphate metabolic process
galactose metabolic process
purine nucleoside triphosphate metabolic process
nucleoside triphosphate biosynthetic process
nucleotide phosphorylation
purine ribonucleoside triphosphate metabolic process
ATP metabolic process
nucleoside diphosphate phosphorylation
ATP biosynthetic process
ribonucleoside triphosphate biosynthetic process
organic acid metabolic process
oxoacid metabolic process
purine nucleoside triphosphate biosynthetic process
purine ribonucleoside triphosphate biosynthetic process
carboxylic acid biosynthetic process
organic acid biosynthetic process
monocarboxylic acid metabolic process
carboxylic acid metabolic process
ribonucleoside diphosphate metabolic process
purine nucleoside diphosphate metabolic process
purine ribonucleoside diphosphate metabolic process
ADP metabolic process
glucose metabolic process
pyridine−containing compound metabolic process
nicotinamide nucleotide metabolic process
pyridine nucleotide metabolic process
pyruvate biosynthetic process
glycolytic process
ATP generation from ADP
small molecule metabolic process
pyruvate metabolic process
hexose metabolic process
carbohydrate catabolic process
monosaccharide metabolic process
carbohydrate metabolic process
-log10 P-value for enrichment.
0
2
4
6
8
10
12
14

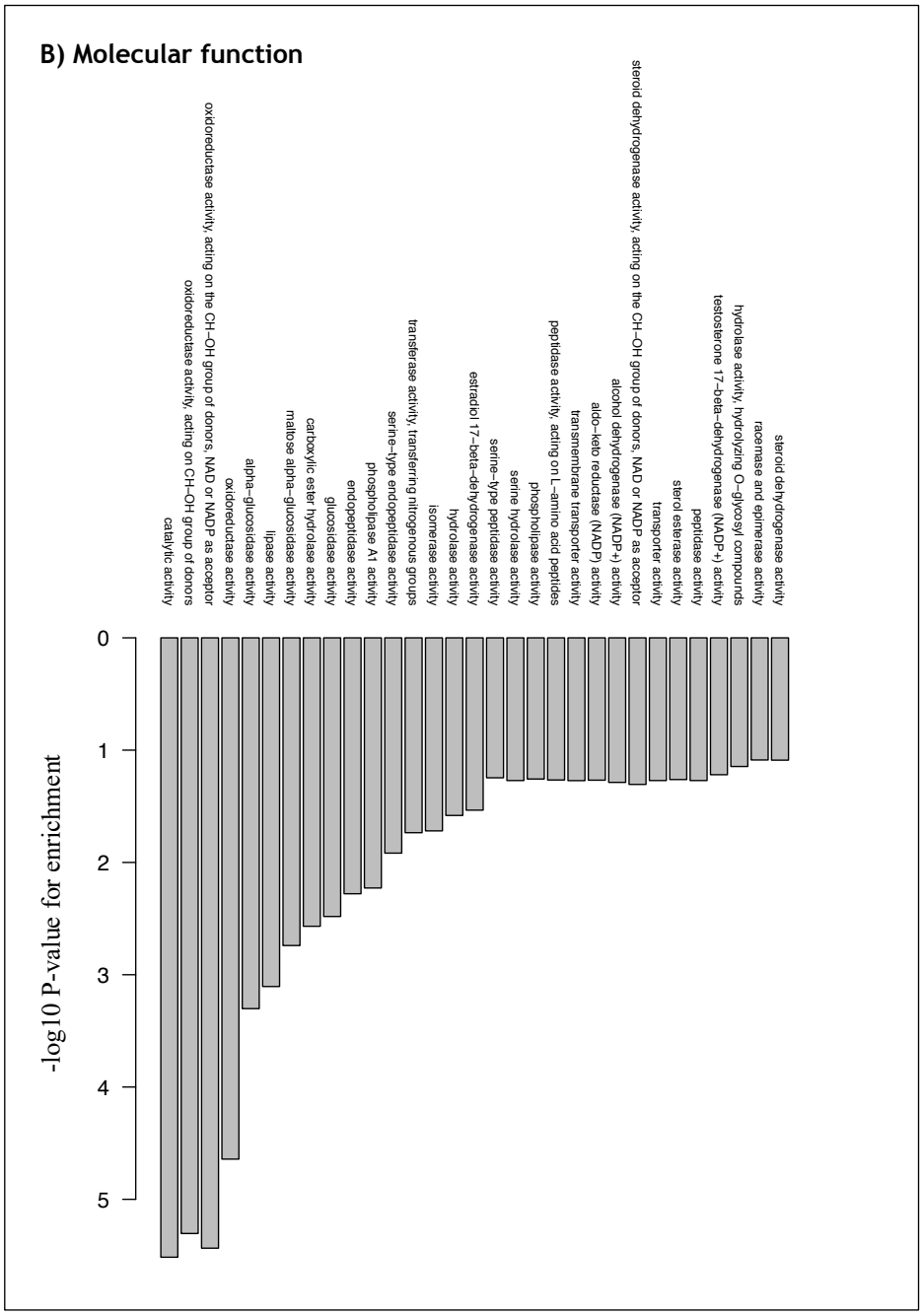
B) Molecular function
-log10 P-value for enrichment
0
1
2
3
4
5
catalytic activity
oxidoreductase activity, acting on CH-OH group of donors
oxidoreductase activity, acting on the CH-OH group of donors, NAD or NADP as acceptor
oxidoreductase activity
alpha-glucosidase activity
lipase activity
maltose alpha-glucosidase activity
carboxylic ester hydrolase activity
glucosidase activity
endopeptidase activity
phospholipase A1 activity
serine-type endopeptidase activity
transferase activity, transferring nitrogenous groups
isomerase activity
hydrolase activity
estradiol 17-beta-dehydrogenase activity
serine-type peptidase activity
serine hydrolase activity
phospholipase activity
peptidase activity, acting on L-amino acid peptides
transmembrane transporter activity
aldo-keto reductase (NADP) activity
alcohol dehydrogenase (NADP+) activity
steroid dehydrogenase activity, acting on the CH-OH group of donors, NAD or NADP as acceptor
transporter activity
sterol esterase activity
peptidase activity
testosterone 17-beta-dehydrogenase (NADP+) activity
hydrolase activity, hydrolyzing O-glycosyl compounds
racemase and epimerase activity
steroid dehydrogenase activity

C) Cellular component

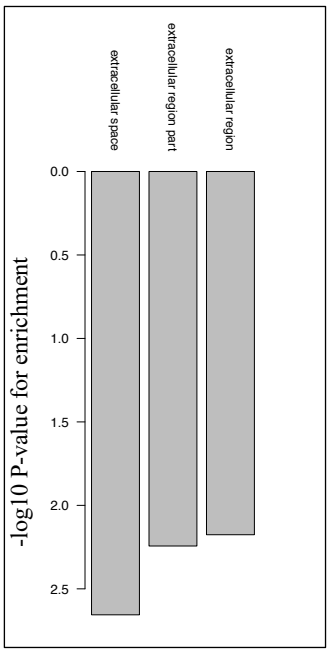

Figure 3.3 Gene ontology enrichment.

A) biological process, B) molecular function and C) cellular composition in the transcriptomes of gnotobiotic and axenic female flies, based on differentially expressed genes with a p value < 0.01 and >2-fold difference between mean expression level.

Having identified transcriptome-wide changes in gene expression, I then asked whether the microbiota modulate expression of peptide hormones. I produced a second heatmap, showing only transcripts from genes encoding the 14 gut peptides secreted by EEC: *Tachykinin (TK), short Neuropeptide F (sNPF), Ion transport peptide (ITP), Orcokinin B (Ork-B), Allatostatin C (AstC), Neuropeptide F (NPF), Allatostatin A (AstA), Myoinhibitory peptide (Mip), Crustacean cardioactive peptide (CCAP), CCHamide 2 (CCHa2), CCHamide 1 (CCHa1), Diuretic Hormone 31 (DH31), Neuropeptide-like precursor 2 (NPLP2), Bursicon (Burs)* (Figure 3.4). The results indicated that *TK*, *ITP*, *AstC* and *NPF* are differentially expressed between axenic and gnotobiotic flies, with *TK* being upregulated by the presence of microbes, with *ITP, AstC* and *NPF* downregulated in gnotobiotic flies. Overall, those findings suggested that microbiota modulate the gut transcriptome, and with specific respect to hormones the analysis identifies *TK*, *ITP, AstC* and *NPF* as candidate mediators of microbiota-host crosstalk (Figure 3.4).

One of the 14 peptide hormones known to be expressed in EECs, *Burs* was not detected in the transcriptome. This is presumably for algorithmic reasons, because *Burs* expression is already conclusively demonstrated in fly gut. Therefore, I quantified *Burs* expression by qRT-PCR in axenic vs conventional guts (Figure 3.5). Although there was a slight increase in *Burs* expression in the presence of microbes, this upregulation was not statistically significant. *Burs* was therefore discounted from further analysis.

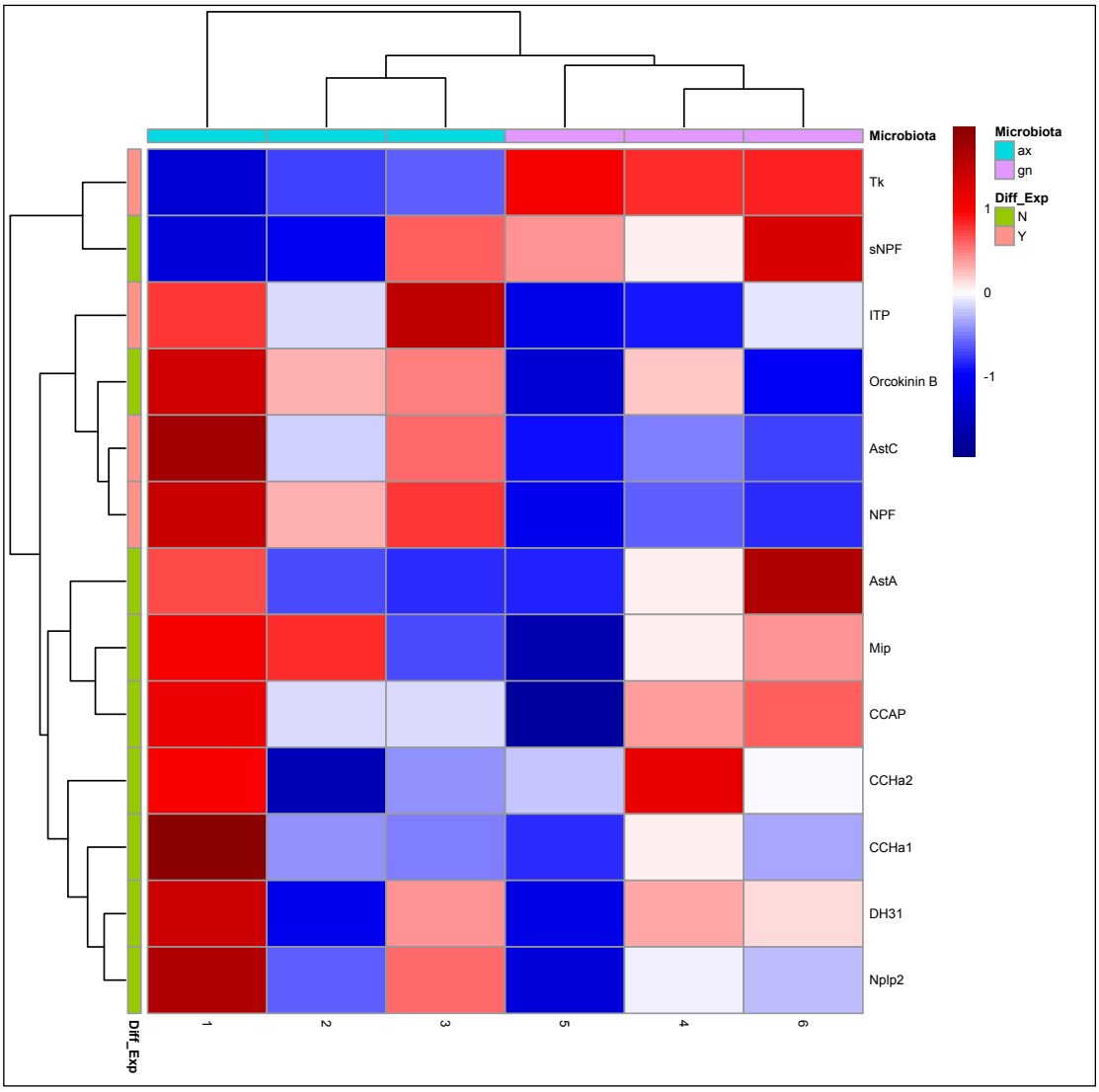

Figure 3.4 Heatmap of expression of genes encoding gut peptides expressed in EECs.

Gut transcriptome from 3 female axenic samples (cyan) compared to gut transcriptome from 3 female conventionalised samples (purple). Differentially expressed genes (p value < 0.01 and >2-fold difference between mean expression level) between axenic and gnotobiotic marked with pink on the left side. *TK* is downregulated in axenic, while *ITP*, *AstC* and *NPF* are upregulated in

axenic compared to gnotobiotic (13/14 EEC produced peptides, *Burs* not detected in transcriptome analysis).

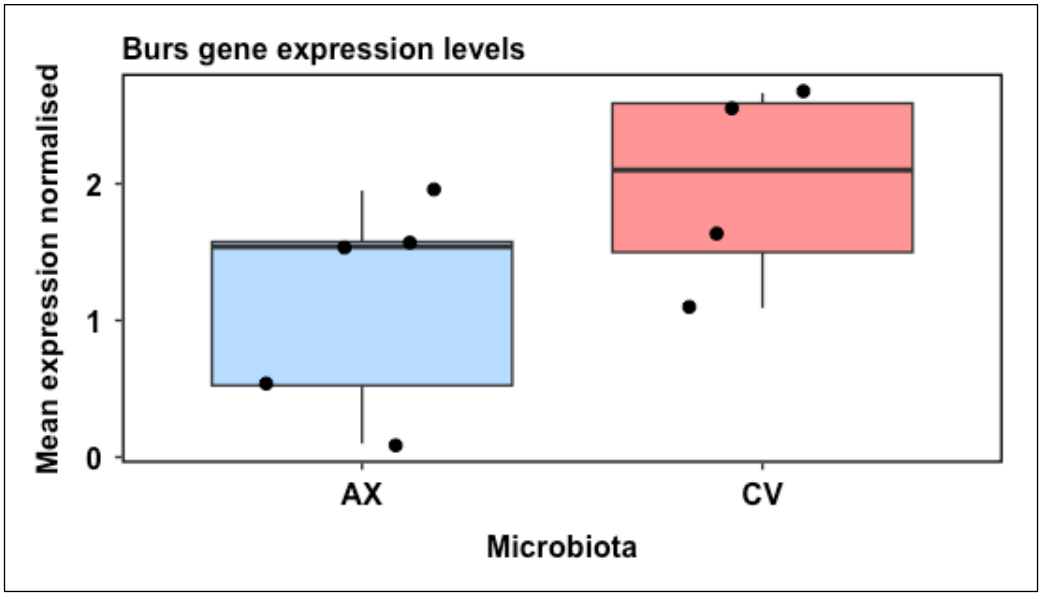

Figure 3.5 Microbiota do not alter intestinal expression of the EE-expressed peptide *Burs*.

The plot shows qRT-PCR from cDNA made from midguts of axenic (blue) and gnotobiotic (red) guts. Difference in expression was tested by Wilcoxon test (p value = 0.1779, n=5 for AX, n=4 CV, each sample containing 10 dissected guts). Relative expression values were derived by subtracting the mean Ct value of the housekeeping gene *Adh* from the mean Ct value for replicates of each sample. *Adh* was used as a housekeeping gene because the preceding RNAseq analysis indicated that commonplace housekeeping genes, e.g. *actin*, *tubulin*; were differentially expressed in axenic versus gnotobiotic flies. However, *Adh* expression was invariant. Boxplots show distribution of the data via Tukey's five numbers, with heavy bar showing median, boxes representing 75th percentile and whiskers showing 95th percentile. Jittered points representing individual data points. AX: Axenic (blue), CV: Conventional (red).

3.4.2 The impact of gut microbiota on enteroendocrine cells

The RNAseq analysis indicated that transcripts of enteroendocrine hormones were differentially expressed upon elimination of the microbiota. This could be mediated by altered numbers of EECs, altered expression per cell, or a combination of the two. To test the first possibility, I quantified EE cells in

axenic versus conventional flies, using a transgenic reporter line (*UAS-mCD8::GFP; Voila-GAL4*) which specifically marks EECs in the gut epithelium, by driving plasma membrane-bound GFP with *GAL4* expressed under control of a fragment of the *prospero* promoter (Figure 3.6). In dissected and fixed guts of adult females, reared either axenically or conventionally, I quantified GFP+ cells in whole gut mounts. The results indicated a significant reduction in numbers of *voila*-positive cells when microbiota were removed. This confirms a connection between the presence of microbiota and EECs, suggesting that microbiota may alter the gut's endocrine capacity.

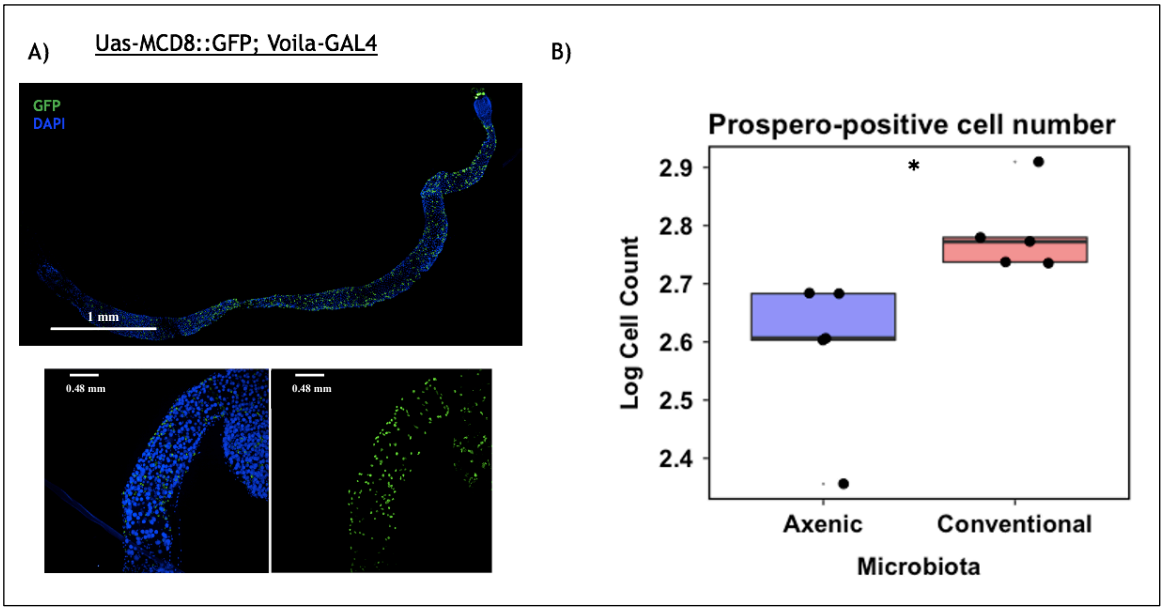

Figure 3.6 Impact of gut microbiota on EE cell quantity.

A) Confocal images showing GFP reporter labelling in midguts of 3 days old transgenic flies (*UAS-mCD8::GFP; Voila-GAL4*) with targeted GFP expression to EE cells (GFP = green, DAPI = blue). B) Quantification of the GFP-positive cells in axenic versus conventional flies. Statistical significance was determined by unpaired two-sample t-test (n=5/Axenic, n=5/Conventional). Boxplots show distribution of the data via Tukey's five numbers, with heavy bar showing median, boxes repesenting 75th percentile and whiskers showing 95th percentile. Jittered points representing individual data points. * indicates $p < 0.05$.

3.4.3 *TK* knockdown extends lifespan

The RNAseq and EEC reporter analysis suggested that EE hormone regulation was indeed responsive to microbiota. I decided to build on the strengths of *Drosophila* as a model system and pursue a genetic strategy to test the role of specific hormones as mediators of the impacts of microbiota on organismal health. I decided to prioritise investigation of *TK*, for two reasons. First, *TK* transcripts showed the strongest response to microbes in the RNAseq analysis. Second, microbiota have a well-established effect of limiting host triglyceride, relative to axenic flies; and *TK* produced by the midgut epithelium has been reported to promote lipolysis in enterocytes: reduced intestinal *TK* activity is therefore expected to phenocopy effects of eliminating the microbiota on host triglyceride (Song et al., 2014, Douglas et al., 2016).

Firstly, I validated the RNA-seq results in our lab flies, because the original RNAseq was conducted in a different lab by different researchers in a different genetic background. I checked the intestinal expression of *TK* in axenic versus conventional flies by qRT-PCR (Figure 3.7). The results were consistent with RNAseq, showing that microbes significantly increase *TK* expression in the gut. Next, I generated flies in which *TK* could be ubiquitously knocked down using the *Daughterless Gene Switch* (*DaGS*) system. The reason for choosing the *DaGS* system was to induce a robust, ubiquitous knockdown and thus gain a holistic view on the role of *TK* in the whole fly. *TK* is expressed in multiple tissues (Figure 3.8), and so I wanted to first ensure that its knockdown somewhere in the fly had physiological effects. Moreover, using GeneSwitch, rather than a constitutively-expressed *GAL4*, allows inducible temporal control of gene expression due to a modified *GAL4* protein that is active only when a synthetic progesterone analogue (RU486) binds to the fused progesterone steroid receptor. In absence of RU486, *GAL4* activity is maintained at a minimum. In this way, the knockdown can be induced in adults only, thus limiting potential impacts of developmental alterations on lifespan.

Using this system, I firstly tested the effect of *TK* knockdown on lifespan in conventional flies, with the expectation that *TK* knockdown would phenocopy impacts of microbiota on lifespan. The results indicate that *TK* knockdown flies

(RU+ CV) had significantly extended lifespan compared to control flies (RU- CV) using two different RNAi lines (Figure 3.9 A and B). Thus, ubiquitous expression of *TK RNAi* does indeed phenocopy the axenic longevity phenotype.

To confirm that the longevity I observed by feeding RU486 to *DaGS/UAS-TK-RNAi* flies was due to transgene expression, and not *GAL4* activation, I conducted a control lifespan experiment to check that the longevity effect observed in *TK* knockdown flies was caused by reduced *TK* levels and not a false positive result of RU486 addition (e.g. sequence non-specific *GAL4* activity). To do this, I have used *DaGS* heterozygote flies with or without RU486 (Figure 3.10). The results indicated that RU486 did not affect lifespan, suggesting that lifespan extension in the presence of *UAS-TK-RNAi* was due to transgene activation.

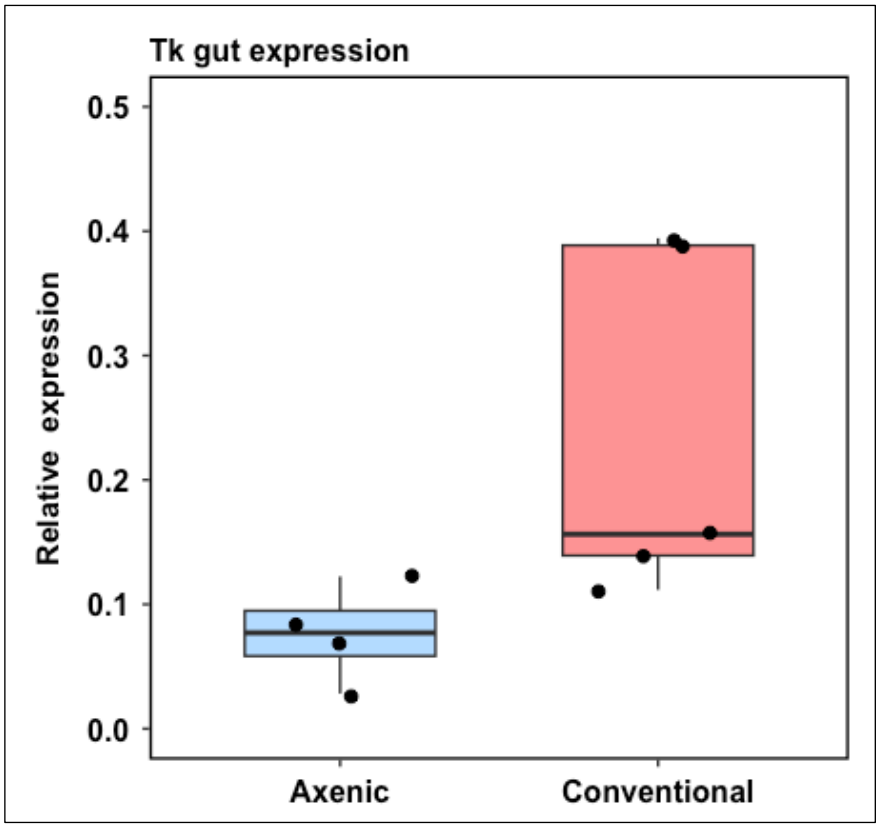

Figure 3.7 Confirmation that microbiota promote *TK* expression in the *Drosophila* midgut.

The plot shows qRT-PCR from cDNA made from midguts of axenic (blue) and gnotobiotic (red) guts. Difference in expression was tested by Wilcoxon test (p value p-value = 0.03734, n=4 for AX, n=5 CV, each sample containing 10 dissected guts). Relative expression values were derived by subtracting the mean Ct value of the housekeeping gene *Adh* from the mean Ct value for replicates of each sample. Boxplots show distribution of the data via Tukey's five

numbers, with heavy bar showing median, boxes repesenting 75th percentile and whiskers showing 95th percentile. Jittered points representing individual data points. Axenic (blue), Conventional (red).

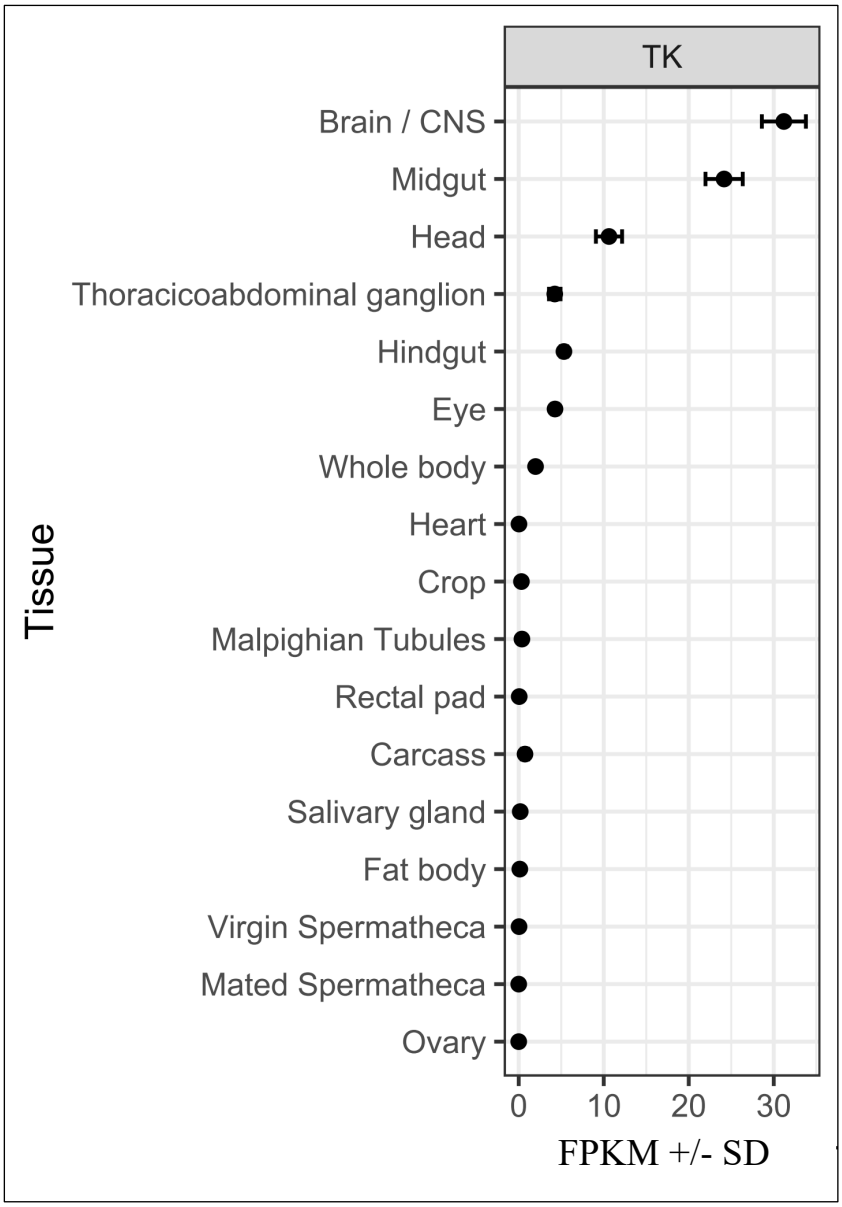

Figure 3.8 Tissues that express *TK* in the adult female fly.

The figure was generated using the database FlyAtlas, showing fragments per kilobase of transcript per million mapped reads (FPKM) +/- standard deviation (SD) for each tissue.

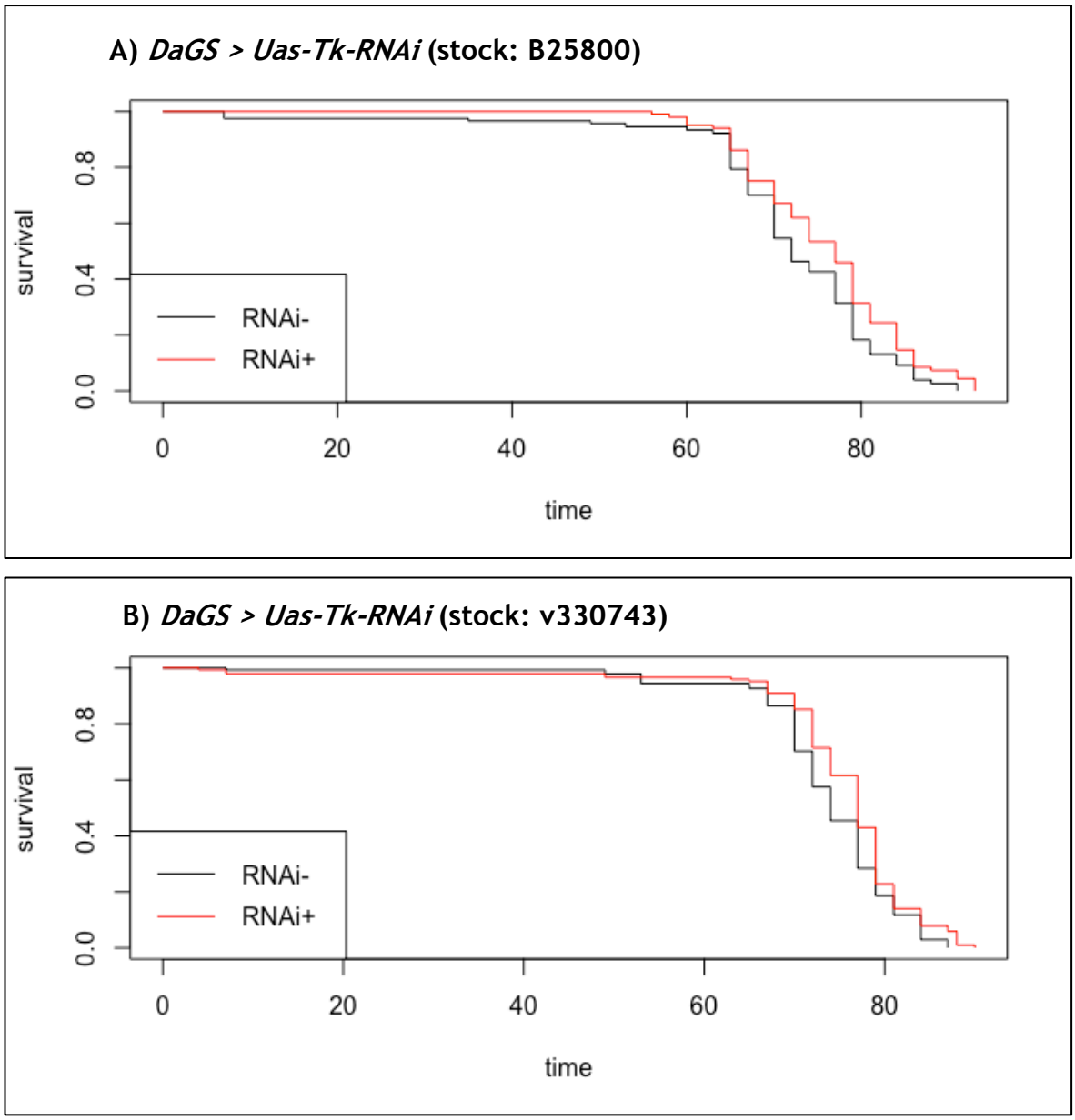

Figure 3.9 Ubiquitous *TK*^{RNAi} increases lifespan, phenocopying elimination of microbiota.

Survival curves in control (*DaGS* > *UAS-TK-RNAi* RU-, black) vs *TK* knock-down flies (*DaGS* > *UAS- TK-RNAi* RU+, blue), using 2 different RNAi lines A) B25800 and B) v330743). Sample size (females): A) RU+, *n* = 150, RU-, n = 150. B) RU+, *n* = 120; RU-, *n* =120; Statistical significance determined by log-rank test on survivorship data A) p value = 0.0089, B) p value = 0.01.

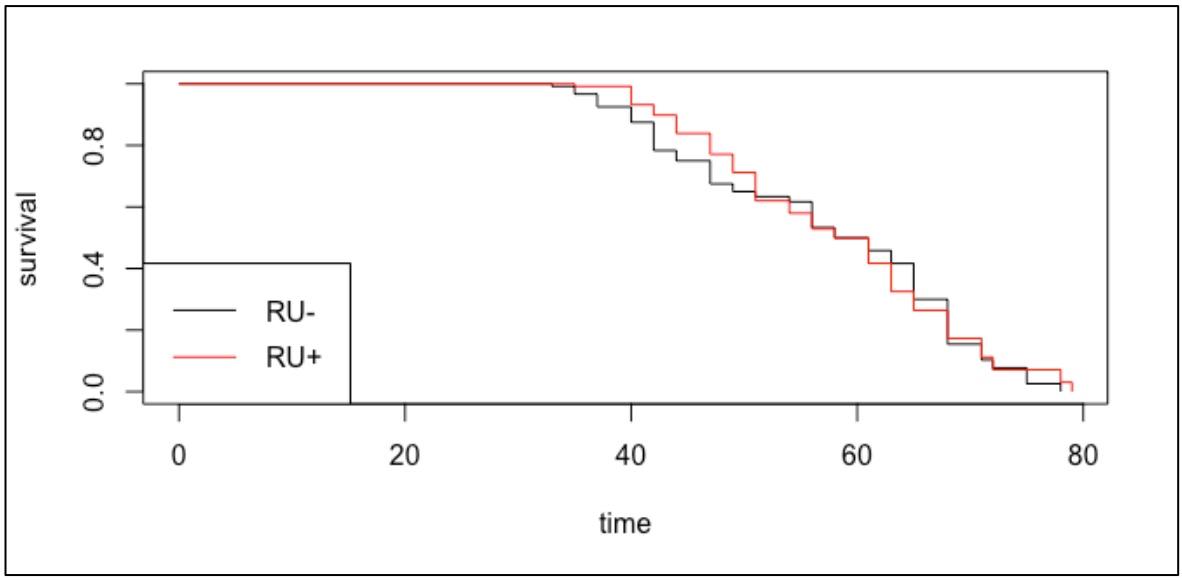

Figure 3.10 RU486 alone does not increase lifespan in *DaGS* flies.

Survival curves in conventional *DaGS* flies with RU486 (red) vs without RU486 (black). Sample size (females): A) RU+, *n* = 120, RU-, n = 120. Log-rank test, p=0.6.

3.4.2 *TK* interacts with commensal microbes to increase lifespan

It was encouraging that ubiquitous *TK-RNAi* expression phenocopied lifespan effects of eliminating the microbiota. I next sought to test whether *TK* and microbiota interact epistatically to determine lifespan. To investigate this interaction, I analysed the lifespan of *DaGS>UAS-TK-RNAi* flies when their microbiota was depleted (axenic) versus unaltered (conventional) (Figure 3.11A). The same genetic system as explained above was used to induce knockdown. The data were analysed by Cox Proportional Hazards analysis in R. *TK* knockdown significantly increased lifespan in the presence of microbes (Conventional *TK-RNAi+* vs Conventional *TK-RNAi+*). Moreover, axenic flies are longer lived than conventional flies (Conventional *TK-RNAi-* vs Axenic *TK-RNAi-*), which is consistent with previous literature and conserved in different model organisms. Thus, both microbes and *TK* knockdown have a significant effect on lifespan (microbes: df=1, p value = 0.01166*, *TK*-RNAi: df = 1, p value = 8.326e-07 ***). However, when flies are depleted by both *TK* and microbes, there was not an additive effect. Thus, *TK* is required for microbiota to modulate lifespan (microbes:*TK*-RNAi: df = 1, p value = 0.04910*). This suggests that microbiota may modulate lifespan by upregulating *TK*.

I conducted additional analysis to visualise quantitatively the interactive effect on lifespan of TK^{RNAi} expression and microbiota. I applied post-hoc analysis using the R package Estimated Marginal Means (EMMs), which provides tools to visualise interactions among factors in experiments. When applied to survival analyses, they provide a helpful statistic, analogous to hazard ratios, which allow us to see differences among conditions and produce interaction plots. The interaction plot for estimated marginal means clearly shows that there is a microbial effect in control flies (-), but no effect in knockdown flies (+) (Figure 3.10B). Associated statistics, showing pairwise differences between conditions, are presented in Table 3.3.

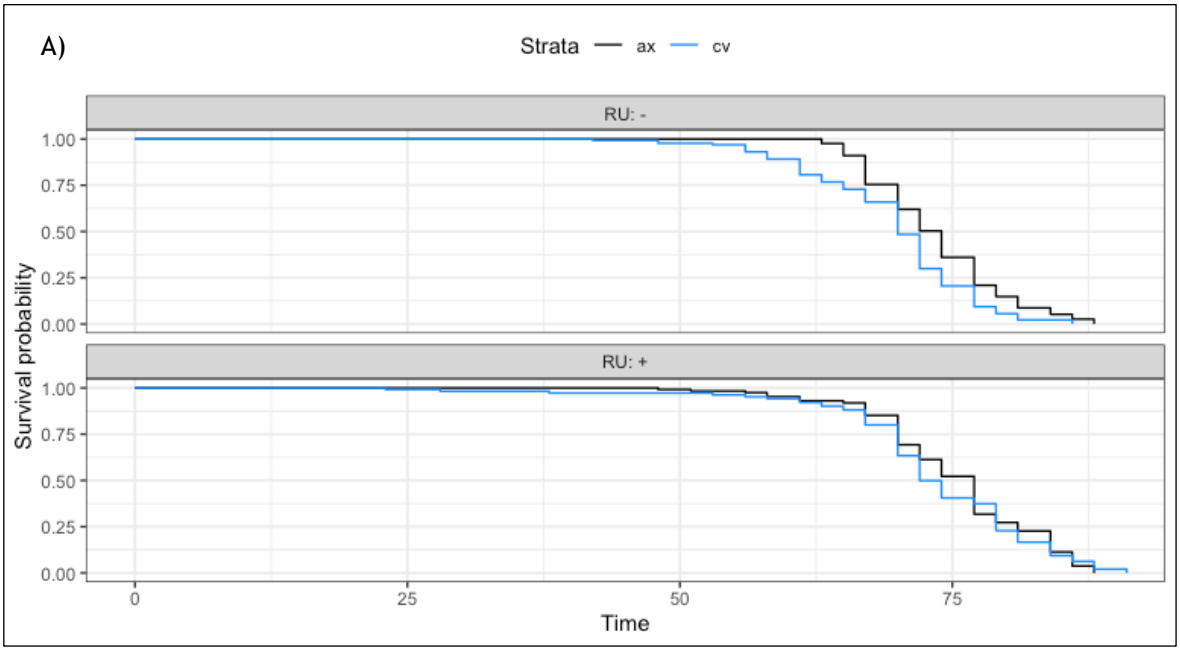

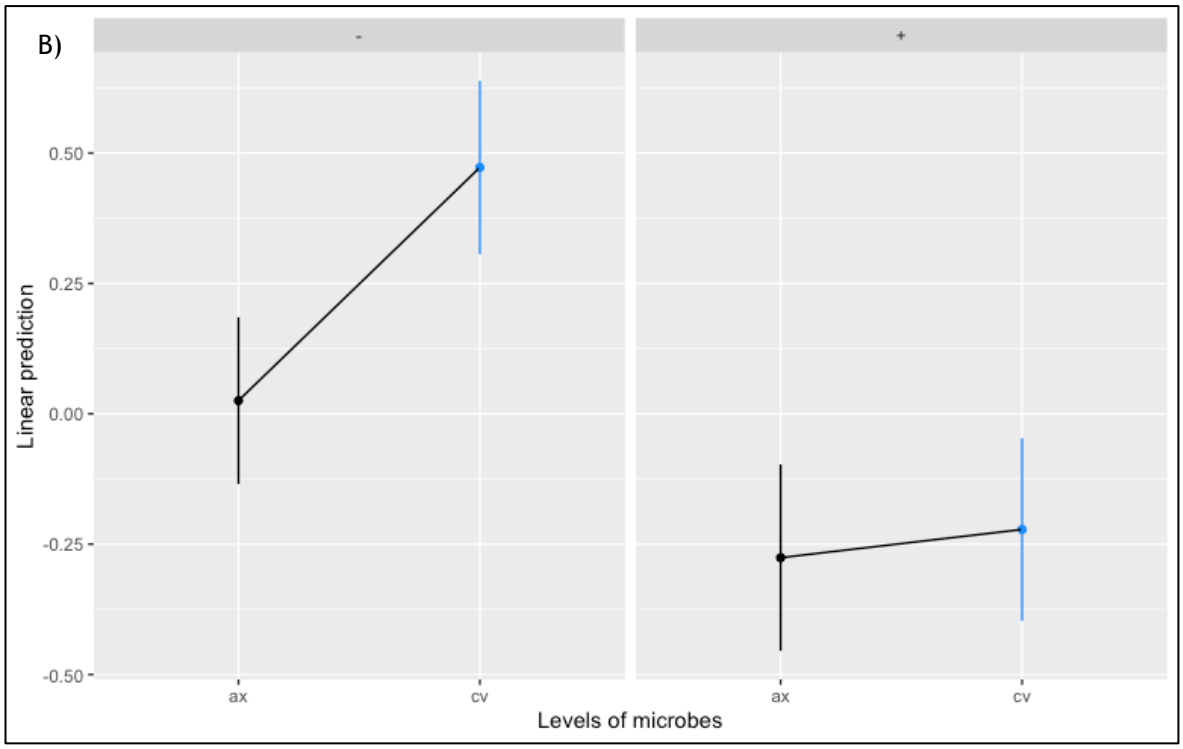

Figure 3.11 The interaction between microbes and tachykinin has an effect on lifespan.

(A) Kaplan-Meier survival curves in *TK* knock-down flies *DaGS>UAS-TK-RNAi* v330743 (lower panel - RU+) versus control flies (upper panel - RU-) when their microbiota is unaltered (conventional, blue) or depleted (axenic, black). Statistical significance determined by analysis of deviance (type III tests) for cox proportional-hazards analysis: microbes: df=1, p value = 0.01166*, *TK*-RNAi: df = 1, p value = 8.326e-07 ***, microbes:*TK-RNAi*: df = 1, p value = 0.04910 *. Sample size (females): n=135. This was followed by pairwise comparisons for estimated marginal means between *TK* knockdown and microbes (values shown in table 3.3). **(B)** Interaction plot for estimated marginal means.

Table 3.3 Pairwise comparisons for estimated marginal means testing the interaction between *TK-RNAi* and microbiota for lifespan data (Figure 3.11).

Control samples are labelled with (-) and knockdown samples labelled with (+). ax = axenic, cv = conventional.

comparison	*estimate*	*SE*	*df*	*z.ratio*	*p.value*
(- ax) - (+ ax)	0.301	0.142	Inf	2.125	0.145
(- ax) - (- cv)	-0.447	0.132	Inf	-3.392	0.0039**
(- ax) - (+ cv)	0.247	0.139	Inf	1.779	0.2835
(+ ax) - (- cv)	-0.748	0.145	Inf	-5.152	<.0001***

(+ ax) - (+ cv)	-0.054	0.149	Inf	-0.362	0.9837

3.4.3 Axenia masks the effect of *TK* knockdown on adiposity

Axenic animals have altered lipid metabolism, displaying elevated levels of storage lipids (Dobson et al., 2015; Vijay-Kumar et al., 2010). Digested lipids are absorbed by ECs, resynthesized into triglyceride (TAG) and packaged into lipoprotein particles that are transported to peripheral tissues for energy supply (Heier and Kühnlein, 2018). Dysregulation of the lipid homeostatic system has been shown to lead to obesity, type 2 diabetes and cardiovascular diseases (Chakaroun et al., 2020; Vallianou et al., 2019). Microbial dysbiosis has been implicated as a disruptor of enteric lipid homeostasis (Jian et al., 2022). On the other hand, *TK* has been shown to regulate intestinal lipid metabolism by controlling lipid synthesis in ECs (Song et al, 2014). Together these results suggest that microbiota may modulate storage lipid levels via *TK*. Thus, I investigated the effect of *TK* knockdown another phenotype with an evolutionarily conserved response to microbiota – TAG storage levels (Figure 3.12).

I generated *TK* knockdown flies using the same genetic system as explained above to ubiquitously drive *TK* knockdown (*DaGS* > *UAS-TK-RNAi*). Because initial results were surprising, I did this experiment twice with two different RNAi vectors V330743 (Figure 3.12A) and V103662 (Figure 3.12B), to confirm that patterns of change were not a genetic artefact. Having knocked down *TK* ubiquitously for one week in adults using *DaGS*, when flies were reared conventionally or axenically, I assayed TAG levels. Published evidence from conventional flies that *TK* knockdown in the gut increases lipid storage via a paracrine effect led me to expect that conventional flies would show elevated TAG levels, but that knockdown in axenics would produce no further increase in TAG. However, with both constructs, knocking down *TK* revealed a remarkable reversal in the response of TAG levels to elimination of the microbiota. While the trends were similar for both RNAi lines, the statistical significance is slightly different (table 3.4). In control flies (RU- blue) axenic flies had significantly higher levels of TAG compared to conventional flies. Moreover, in conventional

flies, *TK* knockdown flies (RU+ CV) had increased TAG levels compared to control flies (RU- CV) – significant for V330743 vector (p value = 0.0005), not significant for V103662 vector (p value = 0.14) (table 3.4 and 3.5 respectively). The discrepancy could be explained by the fact that the V103662 vector is a long hairpin RNAi, while the V330743 vector is a next generation short hairpin RNAi. The latter is capable of integrating into the genomic DNA, allowing longer-term, stable expression and thus improved knockdown potency (Moore et al., 2010). However, the effect of *TK* knockdown on TAG was masked when microbiota was depleted (RU+ AX vs RU+ CV). This suggests that there is an epistatic interaction between microbiota and *TK* for the lipid phenotype.

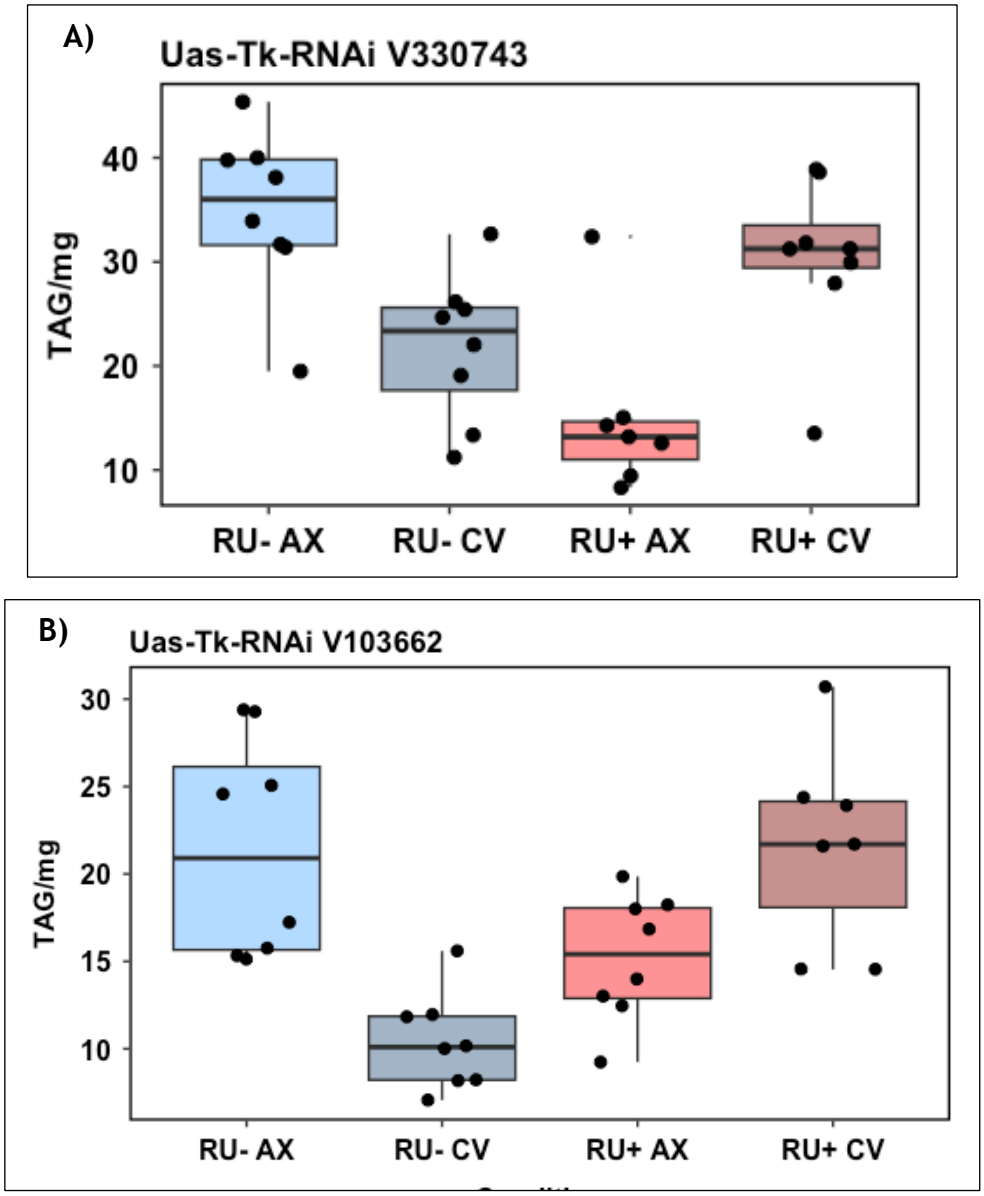

Figure 3.12 Microbiota depletion has an epistatic effect on *TK* knock-down.

A) TAG levels in *TK* knock-down flies using the V330743 RNAi vector (RU+, red) compared to control flies (RU-, blue) when they are axenic (microbiota

removed) or conventional (microbiota unaltered). Statistical significance was determined by two-way ANOVA with interaction between microbes and RNAi (F value = 10.069, p value = 0.0001263 ***) with Tukey post hoc test (table 3.4). Histograms show mean values with error bars representing standard deviation (SD) and jitter plots representing data points. (n=8/RU- AX, n=8/RU- CV, n=8/RU+ AX, n=7/RU+ CV; each sample containing 5 flies). *** p < 0.0001). **B)** TAG levels in *TK* (*TK*) knock-down flies using the V103668 RNAi vector (RU+, red) compared to control flies (RU-, blue) when they are axenic (microbiota removed) or conventional (microbiota unaltered). Statistical significance was determined by two-way ANOVA (F value = 9.985, p value = 0.000134 ***, with Tukey post hoc test (Table 3.5). Histograms show mean values with error bars representing standard deviation (SD) and jitter plots representing data points. (n=8/RU- AX, n=8/RU- CV, n=7/RU+ AX, n=8/RU+ CV; each sample containing 5 flies). *** p < 0.0001., ** p < 0.001., * p < 0.01.

Table 3.4 Tukey post hoc testing multiple comparisons of means for *DaGS > UAS-TK-RNAi* V330743 TAG data (Figure 3.12A).

The contrast column represents the groups to be compared; the values of 'diff' column are the mean difference between two groups; 'lwr' shows the lower end point of the interval; 'upr' shows the upper end point; 'p adj' represents the p-value after adjustment for the multiple comparisons. Control samples are labelled with (-) and knockdown samples labelled with (+). AX = Axenic, CV = Conventional.

contrast	*diff*	*lwr*	*upr*	*p adj*
(-CV) - (-AX)	-11.091522	-17.614052	-4.5689903	0.000426
(+AX) - (-AX)	-6.266983	-12.789514	0.2555486	0.06301
(+CV) - (-AX)	0.159299	-6.5921623	6.9107603	0.999901
(+AX) - (-CV)	4.824539	-1.6979924	11.3470702	0.204253
(+CV) - (-CV)	11.250821	4.4993592	18.0022818	0.000545
(+CV) - (+AX)	6.426282	-0.3251797	13.1777429	0.066385

Table 3.5 Tukey post hoc test multiple comparisons of means for *DaGS > UAS-TK-RNAi* V103668 TAG data (Figure 3.12B).

The contrast column represents the groups to be compared; the values of 'diff' column are the mean difference between two groups; 'lwr' shows the lower end

point of the interval; ‘upr’ shows the upper end point; ‘p adj’ represents the p-value after adjustment for the multiple comparisons. Control samples are labelled with (-) and knockdown samples labelled with (+). AX = Axenic, CV = Conventional.

contrast	*diff*	*lwr*	*upr*	*p adj*
(AX+)-(AX-)	-19.924381	-30.834539	-9.014222	0.000171
(CV-)-(AX-)	-13.137021	-23.677236	-2.596807	0.0104072
(CV+)-(AX-)	-4.564002	-15.104217	5.976212	0.6412956
(CV-)-(AX+)	6.787359	-4.122799	17.697518	0.34204
(CV+)-(AX+)	15.360378	4.45022	26.270537	0.0034392
(CV+)-(CV-)	8.573019	-1.967196	19.113234	0.1418172

3.4.4 *TK* knockdown rescues reduced axenic feeding and egg laying

Generally, any trait that is important in fitness, but requires some limited resource will likely exhibit trade-offs, with a wealth of evidence supporting the existence of energy trade-offs between ageing and reproduction (Maklakov and Chapman, 2019). Considering this, I questioned whether the positive effects that *TK* knockdown has on lifespan come with a trade-off for reproduction. Hence, fly fecundity was tested in axenic and conventional flies +/- *TK* ^{RNAi} by counting the number of eggs laid per fly over a 24h period in axenics and conventionals, following one week of *TK*^{RNAi} induction (Figure 3.13A). The results show that, although *TK* knockdown extends lifespan, this is not concomitant with decreased in fecundity in conventional flies. There was a significant microbiota:RNAi interaction (F=5.5, p=0.02). I then applied post-hoc tests to reveal specific pairwise differences (Table 3.6). When microbiota was depleted in control flies, they laid significantly fewer eggs. Intriguingly, *TK* knockdown rescued those negative effects on reproduction in axenic flies (Figure 3.13B). Therefore, the interactive effects of microbiota and *TK* for lifespan do not appear to be explained by altered egg laying in early life.

I then asked whether the observed differences in lifespan might be caused by different feeding and nutrient intake rates. I quantified feeding behaviour in

axenic and conventional flies, with or without ubiquitous *TK*^{RNAi} expression, using the proboscis extension response assay (Figure 3.13B). There was a significant microbiota:RNAi interaction (F=7.325, p=0.008). I then applied post-hoc tests to reveal specific pairwise differences (Table 3.7). I found that axenic flies ate significantly less than conventional flies. However, when *TK* was knocked down the phenotype induced by the absence of microbes is rescued, mirroring the effect on egg laying. I also tested whether the inducer (RU486) alone affected egg laying (Figure 3.14). To address this, I produced conventional and axenic flies using stock *DaGS* control flies and quantified egg laying when they were exposed to RU486 (+) or not (-). The results demonstrate that RU486 does not change the number of eggs laid in both axenic and conventional flies. Therefore, the interactive effects of microbiota and *TK* for lifespan do not appear to be explained by altered feeding in early life.

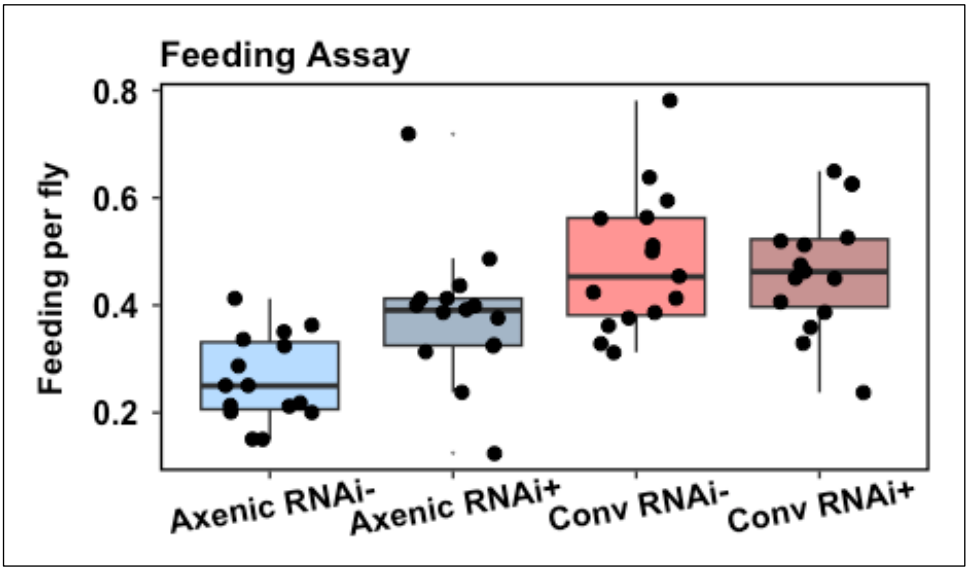

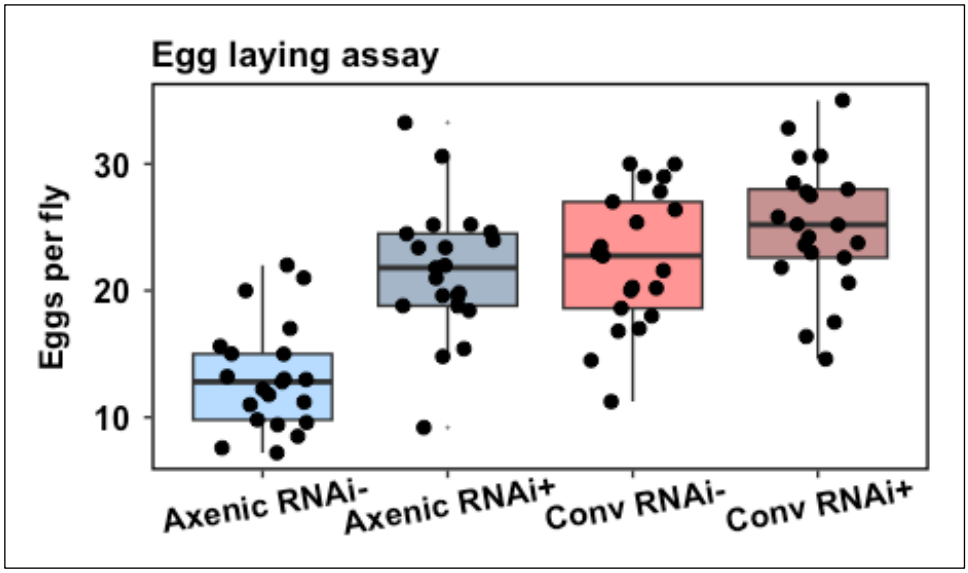

Figure 3.13 Proboscis extension response (PER) assay A) and egg-laying in *TK* knock-down flies.

A) Proboscis extension response (PER) assay to measure behavioural feeding and food preferences in *TK* knock-down flies *DaGS>UAS-TK-RNAi* v330743 (+) compared to control flies (-) when they are axenic (microbiota removed, blue) or conventional (microbiota unaltered, red). Statistical significance determined on logit-transformed data in a linear model, and Type III ANOVA (Microbes: df = 1, F value = 26.0992, p value = 4.052e-06 ***, RU: df = 1, F value = 3.4992, p value = 0.06663, Microbes:RU df = 1, F value = 5.5097, p value = 0.02247 * followed by pairwise comparisons for estimated marginal means. Histograms show mean values with error bars representing standard deviation (SD) and jitter plots representing data points *** p < 0.0005,. *p <0.05. **B)** Number of eggs per fly in *TK* knock-down flies *DaGS>UAS-TK-RNAi* v330743 (+) compared to control flies (-) when they are axenic (microbiota removed, blue) or conventional (microbiota unaltered, red). Statistical significance was determined by two-way ANOVA (Microbes: df = 1, F value = 33.853, p value = 1.18e-07 ***, RU: df = 1, F value = 25.056, p value = 25e-06 ***, Microbes:RU: df = 1, F value = 7.325, p value = 0.00831 **) with Tukey post hoc test (n=21 samples/condition, each sample containing 5 flies). Histograms show mean values with error bars representing standard deviation (SD) and jitter plots representing data points. *** p < 0.0005.

Table 3.6 Pairwise comparisons for estimated marginal means testing the interaction between *TK-RNAi* and microbiota for feeding data (Figure 3.13A).

The contrast column represents the groups to be compared; the values of 'estimate' represent the difference between the two emmeans (estimated marginal means); 'SE' represents standard error; 'df' shows the degrees of freedom; 't ratio' represents the test statistic used to compute the p-value. Control samples are labelled with (-) and knockdown samples labelled with (+). AX = Axenic, CV = Conventional.

contrast	*estimate*	*SE*	*df*	*t.ratio*	*p.value*
(AX -) - (CV -)	-1.004617	0.19054	56	-5.2722	1.31282E-05 ***
(AX -) - (AX +)	-0.568316	0.19054	56	-2.9825	0.021376 *
(AX -) - (CV +)	-0.94039	0.19054	56	-4.9351	4.390996E-05 ***
(CV -) - (AX +)	0.436301	0.19054	56	2.2896	0.112703

(CV -) - (CV +)	0.064225	0.19054	56	0.3370	0.986671
(AX +) - (CV +)	-0.372075	0.19054	56	-1.9526	0.218359

Table 3.7 Pairwise comparisons for estimated marginal means testing the interaction between *TK-RNAi* and microbiota for egg laying data (Figure 3.13B).

The contrast column represents the groups to be compared; the values of 'estimate' represent the difference between the two emmeans; 'SE' represents standard error; 'df' shows the degrees of freedom; 't ratio' represents the test statistic used to compute the p-value. Control samples are labelled with (-) and knockdown samples labelled with (+). AX = Axenic, CV = Conventional.

contrast	*estimate*	*SE*	*df*	*t.ratio*	*p.value*
(Ax RU-) - (Cv RU-)	-9.34047	1.5495	80	-6.0279	2.8874E-07***
(Ax RU-) - (Ax RU+)	-8.45	1.5495	80	-5.4532	3.1692E-06***
(Ax RU-) - (Cv RU+)	-11.8595	1.5495	80	-7.6536	2.2007E-10 ***
(Cv RU-) - (Ax RU+)	0.89047	1.5495	80	0.5746	0.93937
(Cv RU-) - (Cv RU+)	-2.51904	1.5495	80	-1.6256	0.3702
(Ax RU+) - (Cv RU+)	-3.40952	1.5495	80	-2.2003	0.13194

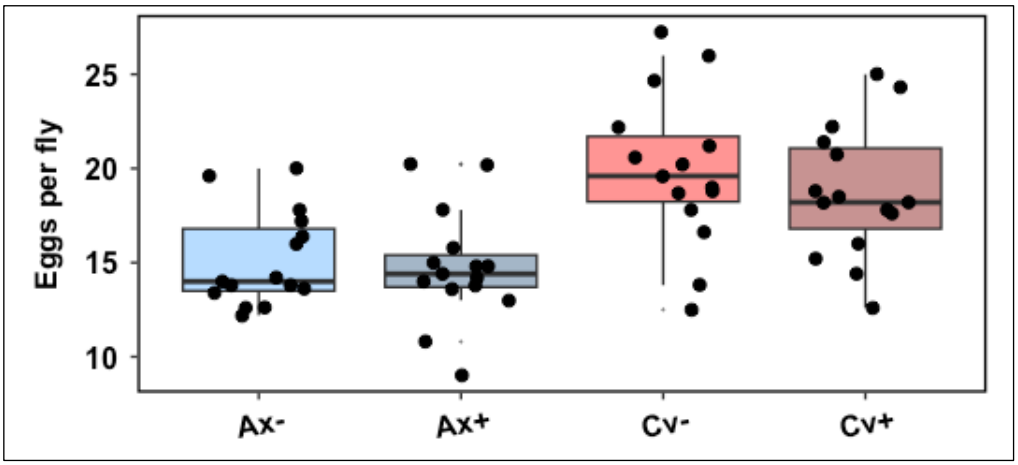

Figure 3.14 RU486 does not affect egg laying in *DaGS* heterozygotes.

Number of eggs per fly in *DaGS*/+ flies in the presence of RU486 (+) vs in the absence of RU486 (-) when they are axenic (microbiota removed, blue) or conventional (microbiota unaltered, red). Statistical significance was determined by two-way ANOVA (F value = 8.9857, p value = 5.941e-05 ***) with Tukey post hoc test. Histograms show mean values with error bars representing standard deviation (SD) and jitter plots representing data points (n=15 samples/condition, each sample containing 5 flies).

Table 3.8 Pairwise comparisons for estimated marginal means testing the interaction between RU486 and microbiota for egg laying data (Figure 3.14).

The contrast column represents the groups to be compared; the values of 'estimate' represent the difference between the two emmeans (estimated marginal means); 'SE' represents standard error; 'df' shows the degrees of freedom; 't ratio' represents the test statistic used to compute the p-value. Control samples are labelled with (-) and knockdown samples labelled with (+). AX = Axenic, CV = Conventional.

contrast	*estimate*	*SE*	*df*	*t.ratio*	*p.value*
(Ax-) - (Ax+)	0.383	1.2155	56	0.3153	0.989
(Ax-) - (Cv-)	-4.778	1.2155	56	-3.931	0.001
(Ax-) - (Cv+)	-3.585	1.2155	56	-2.949	0.023
(Ax+) - (Cv-)	-5.162	1.2155	56	-4.246	0.0004
(Ax+) - (Cv+)	-3.968	1.2155	56	-3.265	0.0098
(Cv-) - (Cv+)	1.193	1.2155	56	0.981	0.7603

3.4.5 Ubiquitous *TK* knockdown reduces starvation resistance

Increased resistance to starvation is associated with increased lifespan and is considered an indicator of healthy lifespan (Bjedov et al., 2010). Indeed, axenic flies are starvation-resistant (Judd et al, 2018). However, starvation resistance may also be influenced by the capacity to mobilise lipid stores when dietary nutrients are absent. Having shown that *TK* knockdown flies are constitutively long-lived, independent of the microbiota, but also that microbial regulation of TAG stores is reversed when *TK* is knocked down, I developed two competing hypotheses for how microbes and TK^{RNAi} expression would modulate starvation resistance. I hypothesised that either (A) the microbial influence on starvation resistance would be controlled by the same physiological processes as lifespan, in which case I predicted *TK* knockdown flies would constitutively display the same elevated starvation resistance as axenic flies, or (B) the microbial influence on starvation resistance would be controlled by the same physiological processes as TAG levels, in which case I predicted *TK* knockdown flies would reverse starvation sensitivity, with axenic flies becoming more starvation-sensitive than conventionals in when TK^{RNAi} was expressed.

I tested the effect of ubiquitous *TK* knockdown (*DaGS>UAS-TK-RNAi*) on starvation stress in conventional vs axenic flies (Figure 3.15). After one week of *TK* knockdown in adult flies, I flipped flies to sterile 1% agarose medium (±RU), and assessed daily survival. I analysed the data with Cox Proportional Hazards. I found a statistically significant interaction of microbiota status and TK^{RNAi} induction (Cox proportional hazards, p<2.2e-16), confirming that *TK* alters the relationship between microbiota and starvation resistance. I applied post-hoc tests to identify differences among conditions (Table 3.9). In the control group, without TK^{RNAi} expression, conventional flies were less resistant to starvation than axenic flies (z=-8.69, p=3.4e-14). However, this relationship was reversed when TK^{RNAi} was expressed, with conventional flies appearing more resistant to starvation than axenic flies (z=2.75, p=0.03). This interaction supports the hypothesis that starvation resistance is modulated by the same physiological processes as TAG levels.

While the interaction of *TK* and microbiota status mirrored TAG regulation, this was not the only informative pattern in the starvation resistance data. I also noticed that *TK* knockdown also had a main effect of making both genotypes less starvation resistant (type-3 ANOVA, main effect of RNAi p<2.2e-16). The microbiota:RNAi interaction was in the context of this main effect. Therefore, at a higher level than microbe-by-gene interactions, wild type *TK* expression levels appear to promote starvation resistance (i.e. independent of microbiota), but shorten lifespan. This might suggest that *TK* activity is selected to enable starvation stress resistance in wild flies, with a trade-off of shortened lifespan.

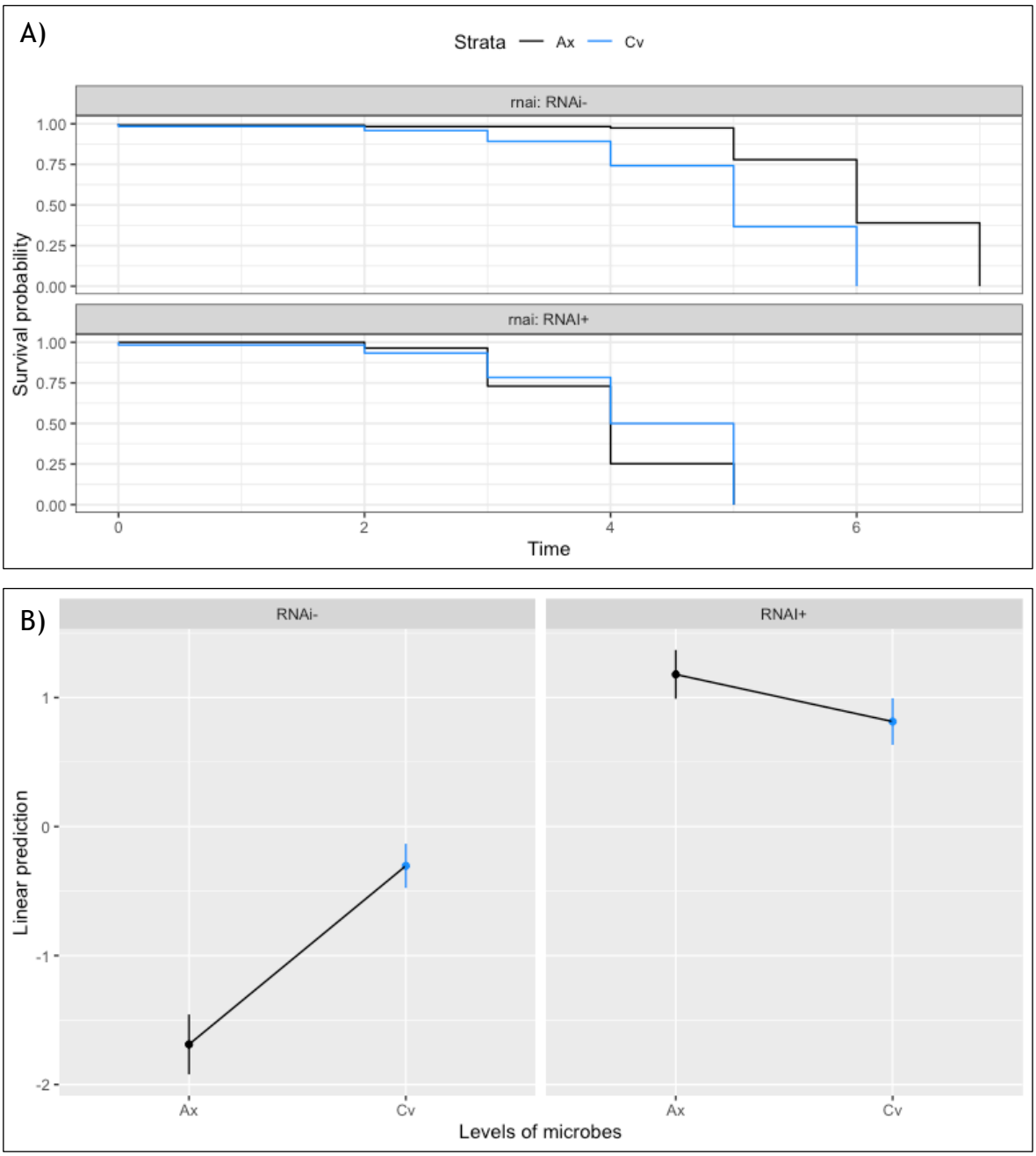

Figure 3.15 *TK* knockdown flies reduces starvation resistance in conventional and axenic flies.

A) Kaplan-Meier survival curves in *TK* knockdown flies *DaGS>UAS-TK-RNAi v330743* (RNAi+) versus control flies (RNAi-) in conventional flies(blue) compared to germ-free flies (black). Statistical significance determined by analysis of deviance (type III tests) for cox proportional-hazards analysis: Microbes: df = 1, p value 652e-09 ***, RNAi: df = 1, p value 2.2e-16 ***, Microbes:RNAi: df = 1, p value 2.2e-16 ***. Sample size (females): n=120. **(B)** Interaction plot for estimated marginal means.

Table 3.9 Pairwise comparisons for estimated marginal means testing the interaction between *TK*-RNAi and microbiota for starvation data (Figure 3.15).

The contrast column represents the groups to be compared; the values of 'estimate' represent the difference between the two emmeans (estimated marginal means); 'SE' represents standard error; 'df' shows the degrees of freedom; 'z ratio' represents the test statistic used to compute the p-value. Control samples are labelled with (-) and knockdown samples labelled with (+). AX = Axenic, CV = Conventional.

contrast	*estimate*	*SE*	*df*	*z.ratio*	*p.value*
(RNAi- Ax) - (RNAi+ Ax)	-2.868	0.189	Inf	-15.1097	0 ***
(RNAi- Ax) - (RNAi- Cv)	-1.384	0.159	Inf	-8.6885	3.3528E-14***
(RNAi- Ax) - (RNAi+ Cv)	-2.503	0.185	Inf	-13.504	0 ***
(RNAi+ Ax) - (RNAi- Cv)	1.484	0.152	Inf	9.7437	4.5075E-14***
(RNAi+ Ax) - (RNAi+ Cv)	0.3655	0.132	Inf	2.7538	0.03 *
(RNAi- Cv) - (RNAi+ Cv)	-1.1184	0.147	Inf	-7.6068	1.9351E-13***

3.4.6 *TK* knockdown inhibits bacterial growth

My initial experiments investigated the requirement for *TK* in microbial regulation of host health. However, symbioses require mutualistic relations to become stable. I therefore speculated that increased *TK* expression might be adaptive for the microbiota, perhaps promoting a more hospitable host environment for the bacteria to inhabit. If so, I would expect that knocking down *TK* expression in conventional flies would reduce bacterial abundance. Indeed, *TK*+ cells in the fly gut epithelium have been reported to be activated by the IMD pathway (Judger et al, 2021), a major regulator of host immunity, hinting at a relationship between *TK* signalling and immune function.

To determine if *TK* knockdown has an effect on bacterial growth, I quantified colony forming units (CFUs) in conventional flies. I manipulated the system using the same genetic system as in previous experiments in this chapter (*DaGS* > *UAS-TK-RNAi*). I also counted CFUs in flies that lacked *UAS-TK-RNAi* (i.e. *DaGS* > +), to control for any possible effects on bacterial growth of feeding the inducer RU486 (Figure 3.16). I tested for differences among conditions with a two-way ANOVA that including terms for genotype (i.e. *UAS-TK-RNAi*) and RU486, on log-

transformed CFU counts, and then applied Tukey post-hoc tests to identify differences among conditions (Table 3.10). Expressing *TK*^{RNAi} reduced CFU counts (t=2.9, p=0.03). However, feeding RU486 to *DaGS* > + flies did not reduce CFU counts (t=1.18, p=0.64), indicating that the observed changes are not an artefactual direct effect of including RU486 in the medium, nor of *GAL4* activation. Overall, this suggests a bidirectional communication between gut microbes and *TK*, with a cost to bacteria of reduced *TK* expression.

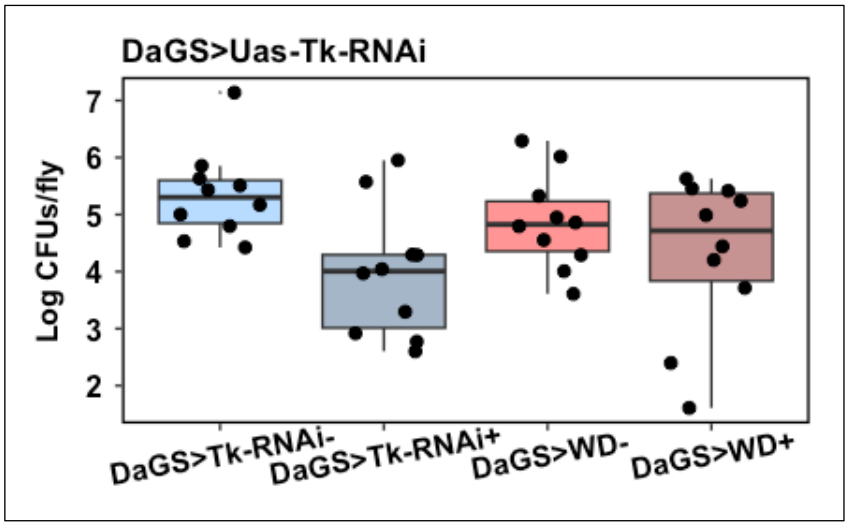

Figure 3.16 Colony forming units (CFUs) assay in *TK* knockdown flies (*DaGS > TK-RNAi+*) compared to control flies (*DaGS >TK-RNAi-*).

The effect of RU486 on bacterial growth was simultaneously tested by crossing *DaGS* flies with wild-type White Dahomey (WD) flies (*DaGS* > *WD*) in the presence or absence of RU486 (+/). Statistical significance was determined by two-way ANOVA (F value = 3.2997, p value = 0.03117 *) with Tukey post-hoc test (n=10 samples/condition, each sample containing 5 flies).

Table 3.10 Pairwise comparisons for estimated marginal means testing the effect of *TK*-RNAi on colony unit formation (Figure 3.16).

The contrast column represents the groups to be compared; the values of 'estimate' represent the difference between the emmeans (estimated marginal means); 'SE' represents standard error; 'df' shows the degrees of freedom; 't ratio' represents the test statistic used to compute the p-value. Control samples are labelled with (-) and knockdown samples labelled with (+). AX = Axenic, CV = Conventional.

contrast	*estimate*	*SE*	*df*	*t.ratio*	*p.value*

(DaGS>TK-RNAi-) - (DaGS>TK-RNAi+)	1.3779	0.4738	36	2.908	0.0301*
(DaGS>TK-RNAi-) - (DaGS>WD-)	0.4789	0.4738	36	1.0108	0.7441
(DaGS>TK-RNAi-) - (DaGS>WD+)	1.0394	0.4738	36	2.1935	0.1443
(DaGS>TK-RNAi+) - (DaGS>WD-)	-0.8989	0.4738	36	-1.897	0.2472
(DaGS>TK-RNAi+) - (DaGS>WD+)	-0.3385	0.4738	36	-0.714	0.8907
(DaGS>WD-) - (DaGS>WD+)	0.5604	0.4738	36	1.1826	0.6414

3.4.7 Screening the interaction between *ITP* and microbes for lifespan

The functional genetic experiments that I present in this chapter reveal a robust role for *TK* in the modulation of lifespan and a panel of related physiological traits in early life. However, enteroendocrine neuropeptides operate in a complex network, and the fly gut expresses 15 of these ligands. My reanalysis of the conventionalised and axenic gut transcriptome (Figure 3.4) suggested that *TK* was one of four neuropeptides regulated at a transcriptional level by the microbiota (*TK, ITP, ASTC, NPF*), and that microbes were shown to increase *TK* levels, but decrease *ITP*, *ASTC* and *NPF* levels. Of these three peptides, NPF and ASTC have recently been shown to modulate physiological responses to elevated dietary sugar and starvation, respectively (Malita et al 2022; Kubrak et al 2022). This suggested a nutrient-responsive network including *TK*, NPF and ASTC. I was therefore interested to ask whether *ITP* may also be involved in this putative network.

I tested whether an interaction between *ITP* and microbes affects lifespan. My previous experiments showed that intestinal *TK* expression was lower in axenic flies than in conventionalised flies, and that recapitulating this difference ectopically with TK^{RNAi} rendered flies constitutively long-lived. By contrast, *ITP* expression was higher in axenic flies, suggesting that blocking this increase may ablate the extension of lifespan in axenics. I tested this prediction in the same framework as I previously tested *TK*, using the *DaGS* driver for a ubiquitous

knockdown to generate a genetic loss of *ITP*. I used the *UAS-ITP-RNAi* vector V330021 to globally knockdown *ITP* in the presence of RU486 (RU+). Again I tested for a microbiota:RNAi interaction using a Cox proportional hazards model and post-hoc tests (Table 3.11). Strikingly, and consistent with my prediction, Kaplan-Meier plots of the data suggested that *ITP* is required for axenia to extend lifespan (Figure 3.17A). There was a significant microbiota:RNAi interaction (p = 5.199e-09), confirming that the impact of microbes was indeed contingent on *ITP* expression levels. In the absence of RU486, the increased lifespan phenotype of axenic control flies, as observed in the *TK*-knockdown experiment was recapitulated (Z=-8.46, p=3.91e-14). This difference between conventionals and axenics was abolished when *ITP* was knocked down (z=-0.57, p=0.94). Intriguingly, ITP^{RNAi} significantly reduced the lifespan of axenic flies (z=-3.37, p=0.004), rendering shorter-lived and more like conventionals. Relative to RU- conventional controls, ITP^{RNAi} modestly increased lifespan of both axenic (z=5.42, p=3.60) and conventional flies (z=5.01, p=3.31). Altogether these results suggest that *ITP* knockdown dramatically reduced longevity in axenic flies, rendering them only modestly longer-lived than conventional controls; but that this difference can be explained by the knockdown itself since conventional flies expressing ITP^{RNAi} are also modestly longer-lived than conventionals without knockdown. This implicates *ITP* as an additional component of the microbiome and nutrient-responsive enteroendocrine network. The rest of this thesis will focus on *TK*, but *ITP* will doubtless prove an interesting subject for future study.

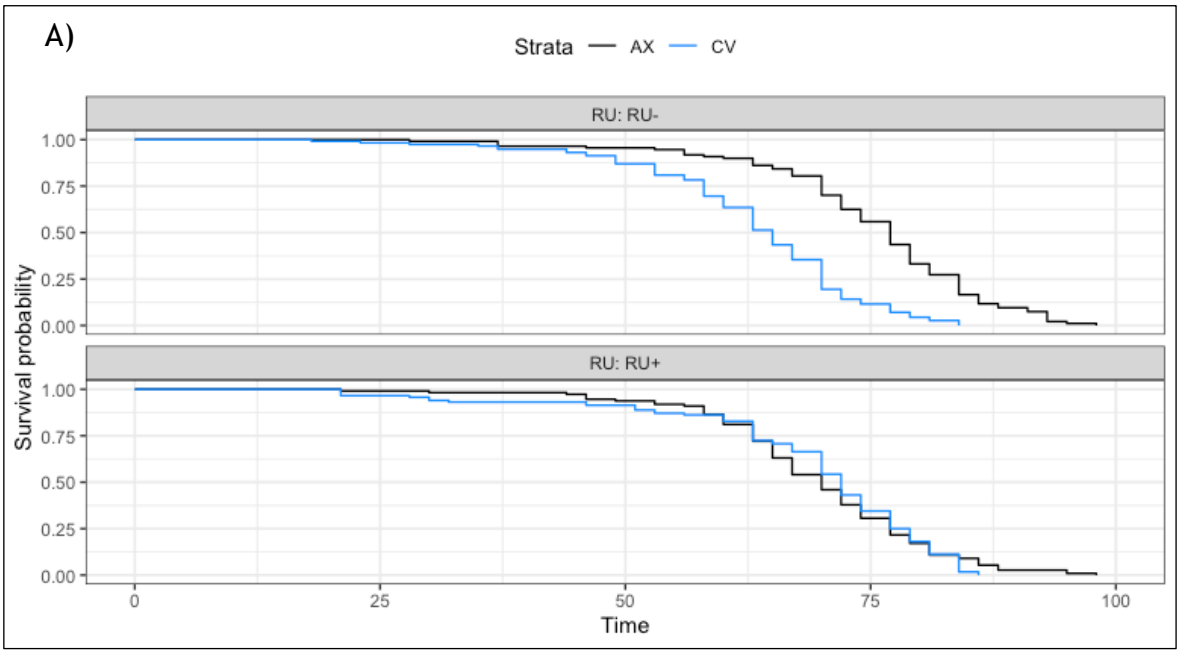

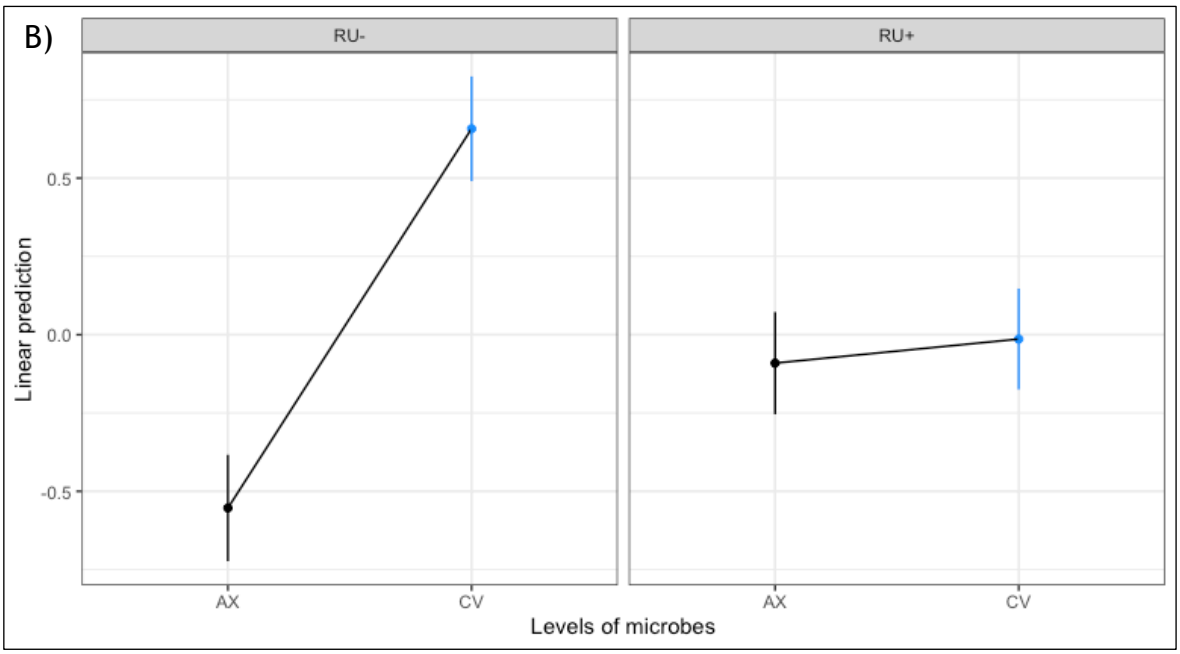

Figure 3.17 *ITP* knockdown shortens lifespan in both axenic and conventional microbiota.

(A) Kaplan-Meier survival curves in *ITP* knock-down flies (lower panel - RU+) versus control flies (upper panel - RU-) when their microbiota is unaltered (conventional, blue) or depleted (axenic, black). Statistical significance determined by analysis of deviance (type III tests) for cox proportional-hazards analysis: microbes: p value = 1.191e-10 ***, *ITP*-RNAi: p value = 0.2735, microbes: *ITP*-RNAi: p value = 5.199e-09 ***. Sample size (females): n=120. This was followed by pairwise comparisons for estimated marginal means between *ITP* knockdown and microbes (values shown in table 3.11). **(B)** Interaction plot for estimated marginal means.

Table 3.11 Pairwise comparisons for estimated marginal means testing the interaction between *ITP-RNAi* and microbiota for lifespan data (Figure 3.17).

The contrast column represents the groups to be compared; the values of 'estimate' represent the difference between the two emmeans (estimated marginal means); 'SE' represents standard error; 'df' shows the degrees of freedom; 'z ratio' represents the test statistic used to compute the p-value. Control samples are labelled with (-) and knockdown samples labelled with (+). AX = Axenic, CV = Conventional.

contrast	*estimate*	*SE*	*df*	*z.ratio*	*p.value*
(AX RU-) - (CV RU-)	-1.2108	0.14311	Inf	-8.4618	3.9079E-14 ***
(AX RU-) - (AX RU+)	-0.4625	0.13726	Inf	-3.3700	0.00418 **
(AX RU-) - (CV RU+)	-0.5394	0.13855	Inf	-3.8936	0.00057 ***
(CV RU-) - (AX RU+)	0.74827	0.13809	Inf	5.41858	3.5956E-07 ***

(CV RU-) - (CV RU+)	0.67140	0.13410	Inf	5.00653	3.3064E-06 ***
(AX RU+) - (CV RU+)	-0.0768	0.13525	Inf	-0.56835	0.941487

3.5 Discussion and conclusions

3.5.1 The impact of commensal microbes on enteroendocrine cells and the peptides they secrete

Previous studies demonstrated that the microbiota of *Drosophila melanogaster* significantly alters gene expression, morphology, tissue architecture, and cellular identity in the gut (Lemaitre et al., 2014, Douglas et al., 2016). Furthermore, Bost et al., 2017 discussed the gut transcriptome as a molecular indicator of microbiota-derived host functional traits. This study also investigated the impact of natural variation in the taxonomic composition of gut microbial communities on host traits, concluding that under natural conditions the influence of microbiota on host may be confounded by both ecological variation and host traits such as genotype, age or physiological conditions and thus microbiota studies using laboratory flies should be extrapolated to field population with great caution. Overall, the focus of the paper was to identify differences in the transcriptome between wild and laboratory flies under different microbial conditions. Using a different approach, I decided to re-analyse this set of transcriptomic data, focusing on the differences between the same strain of laboratory female flies, aiming to identify candidate genes that regulate microbiota effects on host (Figure 3.1).

From the differential expression analysis, I observed two prevailing signals. The first one hints to extracellular proteins which could refer to extracellular signals, therefore confirming our hypothesis that microbiota systemically affect the host through hormone regulation (Figure 3.2 C). The second one refers to genes involved in energy metabolism, oxidative phosphorylation and mitochondrial processes – Figure 3.2 A and B - which is consistent with the fact that microbiota affects host metabolism (Jandhyala, 2015). Moreover, genes encoding the gut peptides, *TK*, *ITP*, *AstC* and *NPF* were differentially expressed between axenic and gnotobiotic flies. Namely, *TK* was downregulated, while *ITP*, *AstC* and *NPF* were upregulated in axenic flies. In mammals, EECs can sense

nutrient and microbial derived metabolites in the intestinal lumen through chemo sensing GPCRs (Hung et al. 2020). Activation of these receptors leads to the release of gut peptides from the basolateral surface of the EECs. While few analogous GPCRs have been characterized in *Drosophila*, they are expressed in these cells and likely function in a similar fashion (Drucker, 2016; Veenstra, 2009). However, to date there are very few studies that discuss the effect of microbes or microbial by-factors on EE peptides. One study published by (Jugder et al., 2021) identified the GPCR Targ required for the EEC response to acetate. This study demonstrates that microbe-derived acetate activates the *Drosophila* immunodeficiency (IMD) pathway in *TK*+ EECs of the anterior midgut. Moreover, it shows that perturbation of the IMD pathway decreases *TK* expression. Overall, this study supports our finding that microbes increase *TK* expression, suggesting that the upstream mechanism is through the acetate-Targ-IMD pathway system.

I then asked whether microbiota directly influence enteroendocrine peptide expression or if this is an indirect consequence of the fact that microbiota impacts EE cells dynamics. Previous research suggests that in young flies intestinal turnover is relatively low and that ISCs reside largely in a quiescent state (Biteau et al., 2010). However, in ageing flies ISCs become hyper-proliferative, due to increased stress signalling linked to commensal dysbiosis and the epithelial inflammatory response (Biteau et al., 2010). Moreover, age-related changes in the composition of the EE progenitor cell population, as well as a significant increase in the proportion of EECs was observed in ageing flies (Jasper et al., 2021). To elucidate the impact of microbiota on EEs I looked at the number of EEs in the presence vs absence of microbes. Our results show that axenic young flies have significantly fewer EE cells than conventional flies, confirming that gut microbes can influence EE cells levels. This suggests that microbiota can increase the proportion of EE cells even under symbiotic conditions in young flies. Future experiments should look at how EE cells dynamics changes during ageing in axenic versus conventional flies. Moreover, other future directions could investigate the molecular mechanism through which microbes act on EE cells. Increased EE cell number in old flies has been linked to polycomb target genes deregulation and increased chromatin accessibility (Jasper et al., 2021). An interesting future experiment would be to check the effect of gut microbes on polycomb target genes.

3.5.2 *TK* – a key mediator of the effects of microbiota on the host

I then focused on the most differentially expressed peptide, *TK*.
Previous research demonstrated that germ-free flies are longer lived (Clark et al., 2015), a phenotype conserved in worms (Cabreiro and Gems, 2013) and mice (Gordon et al., 1966). This has been attributed to the fact that gut dysbiosis increases as an organism ages, disrupting the homeostatic relationship between gut microbiota and host and ultimately affecting whole-organism physiology (Kim and Jazwinski, 2018). However, the molecular mechanisms of this interaction are still poorly understood. Taking into account that *TK* levels are regulated by microbes (Figure 3.3), axenic flies exhibiting lower expression, I tested the effect of *TK* knockdown on the lifespan of conventional flies. Here I demonstrate that downregulating *TK* expression increases lifespan in conventional flies (Figure 3.4). *TK* is highly pleiotropic, regulating gut contractions (Siviter et al., 2000), enteroendocrine homeostasis (Amcheslavsky et al., 2014; Song et al., 2014), stress resistance (Kahsai et al., 2010a; Soderberg et al., 2011), olfaction (Ignell et al., 2009), locomotion (Kahsai et al., 2010b), aggressive behaviors (Asahina et al., 2014), nociception (Gordon et al., 1966), satiety (Qi et al., 2021) and pheromone detection in gustatory neurons (Shankar et al., 2015). However, its function in lifespan has not previously been described.

This also raised the possibility that the beneficial effects of microbiota removal on lifespan could be caused by axenia downregulating *TK* expression. I confirmed this assumption by testing effect of both microbiota depletion and *TK* knockdown on lifespan (Figure 3.4). The axenic vs conventional *TK* knockdown lifespan demonstrates that depleting *TK* increases longevity in the presence of microbes only, without having a significant effect in axenic flies, suggesting either that microbiota and *TK* are co-dependent for their capacity to extend lifespan, or that *TK* signals downstream of microbe sensing apparatus to modulate lifespan. Consequently, I propose a novel function for *TK* as a regulator of ageing, mediating the effect of microbes on lifespan.

In addition, I checked whether *TK* mediates another microbiota-responsive host phenotype – lipid metabolism. Although microbiota depletion has an overall positive impact on host health and ageing, there are also trade-offs, such as

increased adiposity, which is a conserved phenotype in axenic animals (Bäckhed et al. 2007, Dobson et al., 2015, Vijay-Kumar et al., 2010). Furthermore, previous research demonstrates that *TK* acts on ECs to repress TAG synthesis (Song et al., 2014). Consistent with this prior study, my results show that *TK* knockdown leads to increased TAG levels in conventional flies. However, when flies were made axenic, the effect of *TK* knockdown was masked. This suggests that microbiota has an epistatic effect on *TK*. This could mean that microbial factors communicate with *TK* to induce systemic metabolic effects on host. A further step would be to disentangle the signalling pathways through which *TK* exerts its effects and check whether microbes influence other components of those pathways.

3.5.3 *TK*, microbiota, and the trade-offs underlying ageing

Substantial evidence supports the existence of genetic trade-offs between ageing and reproduction, linking increased reproduction with accelerated ageing and vice-versa (Flatt and Partridge., 2018, Luckinbill et al, 1984, Rose 1984). These studies suggest that there are significant costs of reproduction and that organisms can differentially allocate their energy between parental survival, offspring number, and offspring quality. Hence, I tested the effect of *TK* knockdown on egg laying. The results show that although *TK* knockdown extends lifespan this is not concomitant with a decrease in fecundity in conventional flies. More, *TK* knockdown rescued the negative effects on reproduction in axenic flies. These results reject the competitive energy allocation hypothesis, demonstrating that trade-offs between reproduction and survival can be uncoupled. Despite cross-taxonomic support for the energy trade-offs in ageing, plethora of studies also challenge this idea. For example, downregulation of the nutrient-sensing target-of-rapamycin (TOR) signalling pathway in *Drosophila* extends lifespan both in sterile flies and in fertile flies without negative effects on reproduction (Mason et al., 2018). Moreover, downregulation of the Insulin/IGF-1 signalling (IIS) is known to increase lifespan but delay development and reduce reproduction (Maklakov and Chapman, 2019). However, Dillin et al., 2002 showed that the negative effects on reproduction are dependent upon when IIS downregulation occurs. Early-life downregulation results in reduced fecundity. Conversely, downregulating IIS after sexual maturity completely

eliminates the negative effects (Dillin et al., 2002). This could also explain our results, considering that I induce *TK*-knockdown in 3 days old flies.

However, for a more comprehensive understanding of how *TK* regulates the interplay between commensal microbes and reproduction, survival and fitness-related traits of future generations should be examined. Transgenerational effects of the parental commensal microbiota on different aspects of offspring life-history traits, are provided in previous studies (Riberio et al 2017., Ludington et al., 2018, Ponton et al., 2020). Generally, offspring of axenic flies have lower percentage off egg laying, hatching and pupae development as well as a lower bodyweight of both larvae and adults(Nguyen et al., 2020). While the mechanisms are not well understood in *Drosophila*, studies in other insects and nematodes suggests that different microbes on the egg surface regulates hatching and survival (Diehl and Meunier., 2018, Grencis et al., 2010). However, the challenge with those studies is that eggs do not harbour the same microbial community at the beginning of the experiment vs after egg seeding - eggs produced by axenic flies lack vertically transmitted microbes and also bacteria growing in the diet after egg laying might had been different. To our knowledge, there are no studies which investigate the role of *TK* in reproduction in *Drosophila*. Nevertheless, our results clearly demonstrate that *TK* knockdown rescues the negative effects of axenic microbiota on egg laying, suggesting that *TK* could potentially regulate the effects of bacteria on eggs. I will further discuss this in Chapter 4.

Variation in feeding rate determines the level of nutrient intake, which subsequently shapes lifespan and reproduction (Partridge & Gems 2002; Partridge et al. 2005). In order to understand if any of the observed effects of *TK*-knockdown for TAG levels, lifespan and reproduction are caused by differences in nutrient uptake, we examined feeding behaviour in *TK*-knockdown flies. The result indicate that *TK* knockdown does not change feeding in conventional flies, but it rescues the reduced feeding phenotype of axenic. I have chosen the behavioural PER assay as it measures steady state feeding under physiologically relevant conditions. A drawback of this assay is that it does not measure the actual food consumption.

Future experiments should consider measuring feeding through more quantitative approaches. However, despite massive advantages of *Drosophila* as a model organism, measuring food intake remains challenging. An example of a different assay is the fly Proboscis and Activity Detector (flyPAD) which uses an automated, high-resolution behavioural monitoring system, that can detect the physical interaction of individual flies with food (Dickinson and Riberio, 2014). Moreover, Pletcher et al., 2014 developed an assay that detects the electronic signals that occur when a fly makes physical contact with liquid food called Fly Liquid-Food Interaction Counter (FLIC). The software can distinguish the signals arising from different types of behaviours, such as feeding and tasting events (Pletcher et al., 2014). Both flyPAD and FLIC are semi-automated versions of the PER assay used in our experiment, using electric pad (flyPAD) or a combination of electrodes (FLIC) and counted via computer (Dickinson and Riberio., 2014, Pletcher et al., 2014). Furthermore, CApillary FEeder assay (CAFE) is a capillary feeder assay in which flies drink liquid food from a tube and subsequently it measures is how much liquid leaves the tube (Ja et al., 2007). The advantage of this assay is that it directly measures the food uptake, but still holds the problem that the food needs to be liquid, thus changing the physiological conditions of the experiment. Multiple studies have done comparative analysis of feeding methods, emphasising strengths and limitations of each (Ja et al., 2014, Marx 2015). I conclude that the feeding results should be validated with at least one more different assay.

Food shortage represents a primary challenge to survival, and animals have adapted diverse developmental, physiological and behavioural strategies to survive when food becomes unavailable. Our starvation resistance results demonstrate that ubiquitous *TK* knockdown decreases fly resistance to lack of food in both axenic and conventional flies. This is not in accordance with the lifespan phenotype, suggesting that although conventional *TK* knockdown flies live longer, they are substantially less resistant to starvation.

It is known that starvation resistance is influenced by metabolic phenotypes (Yurgel et al., 2014). Moreover, *TK* levels were shown to increase in response to starvation, which subsequently led to inhibition of PKA-SREBP mediated lipogenesis (Song et al., 2014). Starvation is known to reduce lipogenesis and

increase the rate of lipolysis, leading a to net loss of triglycerides from fat cells (Kersten 2001). Taking these into consideration, loss of *TK* will lead to failure of lipogenesis depression in response to starvation, which could lead to a faster loss of lipids, thus explaining their decreased resistance to starvation.

Axenic flies have a higher resistance to starvation than conventional flies. This is consistent with previous results (Giniger 2021). One possible explanation could be that axenic flies have increased fat levels which can be used during starvation (Dobson et al., 2015). Another explanation could be that conventionally raised flies are already using much of their available stress response machinery to protect against the consequences of microbial colonization and therefore have limited capacity remaining to respond to additional, acute stress, whereas axenic flies have less of a chronic load and thus retain that spare capacity.

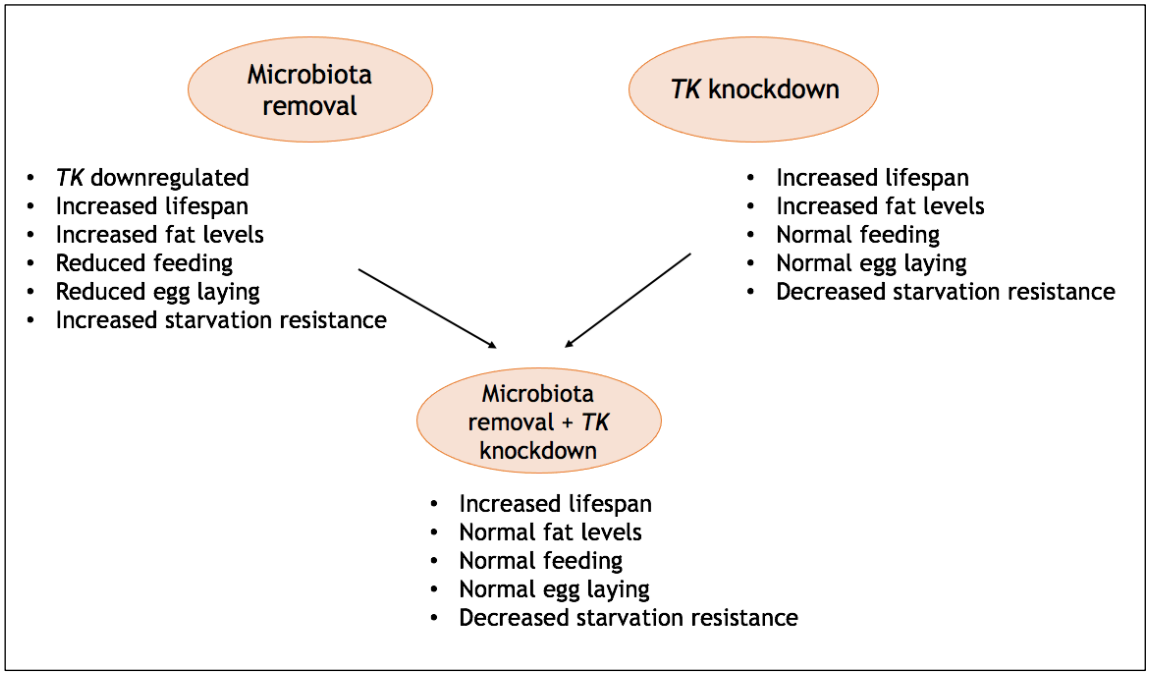

Figure 3.18 Summary of phenotypic outcomes from *TK* knockdown and microbiota removal experiments.

Next, I observed that knocking down *TK* reduces bacterial load (Figure 3.13). Knowing that microbes downregulate *TK*, this suggests that there is a positive feedback between microbiota and *TK*. I have previously discussed that microbial by-products, such as acetate, are transported through EECs by the GPCR Targ, which subsequently activate *TK* via IMD pathway (Judger et al., 2021). However, the mechanistic basis through which *TK* might signal back to commensal

microbes needs to be investigated. While the influence of microbiota on host genetics has been widely studied, there is very little known about how host genes can regulate bacterial load.

Another crucial aspect to consider involves the unique characteristics of fly gut microbiota. Unlike in many other organisms where bacteria colonise the gut, in flies, the gut microbiota is transient (Engel and Moran, 2013). Bacteria proliferate on the food and pass through the gut along with it. Given this, an interesting question arises: could the observed effect of *TK* knockdown on bacterial load be influenced by differences in gut passage time, especially since *TK* affects gut peristalsis (Holzer and Holzer-Petsche, 1997)? This consideration is pivotal because if *TK* signalling modulates gut motility, then its knockdown could lead to changes in the rate at which food and, consequently, bacteria pass through the gut. This might result in observed differences in bacterial load not directly linked to bacterial growth or survival but rather to the kinetics of gut passage. Therefore, the effect of *TK* on microbial load might be mediated, at least in part, by alterations in the physical dynamics of the gut rather than or in addition to direct microbial-host interactions or immune responses.

3.5.4 Are there other differentially expressed peptides that mediate the effect of gut bacteria on lifespan?

From the differential expression analysis, four peptides were significantly different between axenic and conventional samples – *TK, ITP, ASTC, NPF*. While I focused on *TK* as the main mediator of the effects of microbiota on host, I decided to also test the effect of *ITP* knockdown on lifespan in axenic and conventional flies. The long-lived phenotype of axenic control flies is consistent with our *TK* lifespan result and with previous published studies (Clark et al., 2015). *ITP* knockdown had the opposite effect of *TK* knockdown in conventional flies, leading to a significantly decreased lifespan. This could be attributed to the fact that, microbes decrease *ITP* expression, but increase *TK* expression. However, *ITP* knockdown significantly reduced the lifespan of axenic flies, although with a lower magnitude, suggesting that *ITP* regulates lifespan independent of microbes. If axenic flies have higher levels of *ITP* and they live longer, it would be interesting to test the effect of *ITP* overexpression on axenic vs conventional flies. *ITP* was also shown to suppress feeding and energy

balance, therefore the shorter lifespan could be attributed to increased food consumption (Nassel et al., 2018). Nevertheless, future studies should test the impact of *ASTC* and *NPF* on lifespan and other microbiota-responsive host phenotypes.

Chapter 4

4.1 Summary

Gut microbiota impact host lifespan and metabolism across species. The influence of commensal microbes on *Drosophila* physiology relies on intricate interactions that encompass nutrition, metabolism, and the immune system. *TK* responds to microbial cues and this interaction regulates host phenotypes such as, lipid metabolism, lifespan, starvation resistance, feeding behaviour and fecundity. Here we ask how the interaction between *TK* and specific microbes impacts host phenotypes. My results show that, *Acetobacter pomorum*, a predominant gut-symbiont, modulate lifespan and TAG levels via *TK*, whereas *Lactobacillus brevis,* another predominant gut-symbiont, marginally modulates lifespan via *TK*, but has no impact on TAG levels. Moreover, the results indicate that mono-colonisation with specific microbes affects egg laying, but *TK* knockdown does not have a significant effect on egg laying in gnotobiotic flies. Conversely, feeding behaviour is not influenced by *Acetobacter pomorum* or *Lactobacillus brevis,* but is decreased by *TK*, independent of microbiota. Finally, I have also begun to characterise potential mechanisms of the observed phenotypes by looking at differences in the transcriptomes of *TK* knockdown flies when they are axenic or colonised with either *A. pomorum* or *L. brevis*. The increased lifespan phenotype in *A. pomorum* mono-associated flies appears to be mainly attributed to the downregulation of the Imd pathway. In flies colonised with *L. brevis*, the longevity effect might involve a cross-talk with the peptide *CCHamide-2*. Upregulation of heat shock proteins following TK^{RNAi} could also play a role in increasing lifespan in both *A. pomorum* and *L. brevis* gnotobiotic flies. Finally, it appears that *TK* interacts with microbes to control metabolism, and the balance between JNK and IIS/TOR signaling is crucial to ensure the appropriate metabolic response.

4.2 Introduction

4.2.1 Comparison of gut microbiota between mammals and invertebrates

The human microbiome is comprised of microorganisms, such as bacteria, archaea, viruses and eukaryotic microbes inhabiting us (Shreiner et al., 2015). These microbes codevelop with the host from birth and live symbiotically within various habitats of the human body, such as oral cavity, genital organs, respiratory tract, skin and gastrointestinal system (Nicholson et al., 2012). The GI tract accommodates the densest number of microbes, being collectively called the gut microbiota. The human gut microbiota contains approximately 100 trillion bacteria, with the corresponding total number of genes approximately 150 times the number of human genes. Therefore, intestinal bacteria are also known as the 'second genome' of the human body (Hintze et al., 2014). The phylogenetic core is predominantly composed of bacteria from Bacillota *(Firmicutes)* (79.4%), Bacteroidetes (16.9%) Actinobacteria (2.5%), Proteobacteria (1%) and Verrucomicrobia (0.1%) phyla (Tap et al., 2009).

Experimental organisms are the main tools for studying the role of gut microbiota in pathology, pharmacology, metabolism, and pharmacokinetics. Nematodes, *Drosophila melanogaster*, zebrafish, and mice are all model organisms used to study host-gut microbiota interactions, with *Drosophila* having many unique advantages. Firstly, there is a high degree of homology between the sequences of the *Drosophila* and human genomes (Myers et al., 2000). Secondly, 75% of human disease-causing genes have functional homologs in the fly (Pandey and Nichols, 2011). Moreover, the *Drosophila* and mammalian digestive systems are very similar both in terms of genetic control and cellular composition (Wong et al., 2016).

However, compared to humans and rodents, the *Drosophila* gut microbial structure is much simpler with only four to eight bacterial species being associated with a given fly population species. The dominant members are predominated by 2 bacterial families, the Lactobacillaceae and Acetobacteraceae, which are taxonomically distinct. This low complexity contrasts with the abundance and diversity of the mammalian gut microbiota, differing by one to two orders of magnitude (Spor et al., 2011).

Numerous studies on both laboratory raised and wild flies have been conducted in order to identify the commensal bacteria residing in the *Drosophila* gut (Chandler et al., 2011; Corby-Harris et al., 2007; Cox and Gilmore, 2007; Ren et al., 2007; Ridley et al., 2012; Storelli et al., 2011; Wong et al., 2011). Collectively, it has been shown that *Drosophila* gut microbial structure predominantly includes Bacillota (phyla) represented by Lactobacillaceae and Enterococcaceae (families) and mostly the *alpha* and *gamma* classes of *Proteobacteria* (phyla) represented by Acetobacteraceae and *Enterobacteriaceae* (families). Furthermore, the species *Lactobacillus plantarum* and *Acetobacter pomorum* were identified repeatedly in most of the mentioned studies. *Lactobacillus brevis* and *Enterococcus faecalis* were also frequently associated with flies. In conclusion, these four species were defined as the dominant components of the *Drosophila melanogaster* microbiota. All these species are readily cultured, while some can also be genetically manipulated. Furthermore, except for Acetobacteraceae, they are commensals in mammals, including humans.

A contrast between the fly and mammalian gut microbiota is that commensal bacteria from lab-reared flies do not colonise the larval or adult gut, but they proliferate on the food and transit with it through the gut (Blum et al., 2013; Storelli et al., 2018). Therefore, the *Drosophila* microbiota has been defined as transient. However, it has been reported that some commensal microbes from wild-type flies can colonise the crop of adults, thus forming a resident microbiota (Obadia et al., 2017). Nevertheless, both transient and resident microbiota can regulate physiology and thus is a valid model to study the impact of microbes on host health (Ma and Leulier, 2018).

4.2.2 Commensal microbes impact the physiology of *Drosophila Melanogaster*

To explore the relationship between the structure and function of host-associated microbial communities, a powerful approach is provided by gnotobiotic organisms i.e., colonised with a specific set of bacteria. The four bacterial species *(L. plantarum, A. pomorum, L. brevis* and *E. faecalis)* forming

the core fly microbiota have profound effects on the nutritional traits of Drosophila (Newell and Douglas, 2014). One of the main mechanisms through which they do so is by influencing the host's nutritional signalling networks, thereby changing how nutrients are allocated. For instance, it has been shown that acetic acid produced by *A. pomorum* promotes insulin signalling, leading to increased larval growth and development while reducing adult lipid and sugar levels (Shin et al., 2011). Similarly, *L. plantarum* has been associated with the modulation of TOR signalling, which intersects with IIS signalling in the regulation of growth and metabolism (Storelli et al., 2018).Moreover, commensal bacteria can alter the nutritional inputs available to the host by providing extra nutrients and consuming dietary components. This dual role can either be detrimental to the host when essential nutrients are limited or beneficial when there is an excess of certain nutrients.

Moreover, Sannino et al. demonstrated that strains of *Acetobacter* have the ability to supply thiamine (vitamin B1) to *Drosophila* larvae (Sannino et al., 2018). Later, Consuegra et al. systematically removed individual components of the host diet and evaluated whether the decrease in larval growth resulting from each removal could be compensated for by growth-promoting strains of either *Acetobacter pomorum* or *Lactobacillus plantarum* (Consuegra et al., 2020). Their findings revealed that those commensal microbes not only supply specific essential nutrients to *Drosophila* larvae, but also provide precursor compounds or derivatives of the essential nutrients that are missing, rather than the nutrients themselves. In accordance, another study showed that the increased production of N-acetylated amino acids by *Lactobacillus plantarum* enhance larval growth when nutrients are scarce (Martino et al., 2018).

Furthermore, Kamareddine et al. reported that acetate, produced by commensal bacteria belonging to the *Acetobacter* genus, can activate the IMD pathway in a subset of EE cells, which specifically express *TK* (*TK*+ cells) (Kamareddine et al., 2018). The IMD pathway in *TK*+ cells signal via the membrane receptor PGRP-LC, which then triggers the release of lipid reserves in neighbouring enterocytes through *TK* paracrine signalling, ultimately leading to increased growth. Overall, this research demonstrates that local signalling of microbial by-products can have systemic effects on the host's development. In line with this, commensal

microbes have been shown to regulate Drosophila's lifespan. While most studies demonstrate that axenic flies have an increased lifespan (Fast et al., 2018; Iatsenko et al., 2018; Keebaugh et al., 2019; Lee et al., 2019; Obata et al., 2018; Resnik-Docampo et al., 2018), other studies report the opposite (Brummel et al., 2004; Keebaugh et al., 2018). Notably, a previous study revealed that the impact of a commensal yeast, *Issatchenkia orientalis*, on *Drosophila* lifespan is contingent on diet, enhancing lifespan on a low-yeast diet, but diminishes it on a high-yeast (Keebaugh et al., 2019). These findings suggest that the disparities observed in previous studies may be due to differences in the nutritional composition of the diet.

On a low-yeast diet, microbial biomass may serve as a source of nutrients, particularly amino acids, compensating for the diet's low nutrient content and consequently extending lifespan (Brummel et al., 2004; Keebaugh et al., 2018). However, on a high-yeast diet, lifespan reduction was attributed to the overall abundance of microbes in the gut, which increases during ageing (Lee et al., 2019), as well as the composition of the microbiota (Obata et al., 2018). For instance, treatment of larvae with the oxidant tertbutyl hydroperoxide extends lifespan by eliminating *Acetobacter* strains without affecting other microbiota members like *Lactobacilli* (Obata et al., 2018). Furthermore, it has been proposed that the microbe-mediated reduction in lifespan is linked to gut ageing and the associated stem cell over proliferation and hyperplasia (Fan et al., 2018; Iatsenko et al., 2018). For example, *L. plantarum* produces lactate, which can be oxidized to pyruvate in the enterocytes, a process that leads to the generation of reactive oxygen species (ROS), a well-established trigger for the proliferation of ISCs (Jones et al., 2013). In ageing flies, increased levels of *L. plantarum* in the gut result in the over proliferation of ISCs, leading to gut hyperplasia and a shortened lifespan (Min and Tatar, 2018). Overall, the impact of commensal microbes on *Drosophila* physiology is dependent on complex interactions involving nutrition, metabolism, and the immune system.

4.2.3 The interplay between *TK* and commensal gut microbes

As previously discussed in chapter 3, microbial by-products can bind and activate GPCRs on EECs (Rastelli, Cani and Knauf, 2019). These receptors can respond to

SCFAs (Gribble and Reimann, 2019; Nøhr et al., 2013) or bacterial components such as LPS (Lebrun et al., 2017). As further evidence that mammalian EECs respond to microbes, these cells express Toll-like receptors (TLRs) 1, 2, and 4 (Bogunovic et al., 2007). In mice, exposure to LPS triggers the release of the peptide cholecystokinin from EECs and activation of the NF-κB pathway, leading to increased macrophage inhibitory protein 2, tumor necrosis factor (TNF), and transforming growth factor-β levels (Bogunovic et al., 2007; Worthington, 2015). Importantly, Substance P, the mammalian ortholog of insect *TK*, has been shown to be released in response to LPS via TLR4 (Kulka et al., 2009; Mashaghi et al., 2016). Thus, EECs provide an immune endocrine axis with commensal microbes.

The *Drosophila* IMD innate immune signalling pathway, akin to the TNF pathway in mammals, is active in all types of intestinal cells. Instead of Toll-like receptor homologs, the IMD pathway is activated by three peptidoglycan receptors: the cell membrane-associated PGRP-LC, the cytosolic PGRP-LE, and the secreted PGRP-SD (Iatsenko et al., 2018; Leone et al., 2008; Myllymäki et al., 2014). Signalling through these receptors results in the phosphorylation and cleavage of Relish, the *Drosophila* NF-κB homolog, which activates the transcription of numerous genes, including those responsible for encoding antimicrobial peptides (AMPs) (Myllymaki et al., 2014).

TK functions on enterocytes to suppress the synthesis of TAG (Song et al., 2014). *TK*+ EECs coordinate an innate immune response to the intestinal microbiota (Kamareddine et al., 2018). Disruption of the IMD pathway signalling in these cells results in reduced expression of *TK* and AMPs, leading to the accumulation of lipid droplets in enterocytes, depletion of lipid droplets in the fat body, and hyperglycaemia. IMD pathway signalling in *TK*+ EECs is activated by the SCFA acetate (Kamareddine et al., 2018; Shin et al., 2011). Furthermore, acetate was shown to increase acetyl-CoA pools in these cells which will then modulating the activity of Tip60 histone acetylase complex ultimately leading to increased transcription of PGRP-LC (Jugder et al., 2021). In conclusion, previous evidence demonstrates *TK* responds to microbial by-products and that this interaction regulates lipid metabolism and immune signalling.

4.3 Aims

Commensal microbes modulate *Drosophila* physiology in distinct ways depending on their metabolic and immune functions. Previous studies demonstrate that *TK* is regulated by metabolites and bacterial components. Moreover, our results indicate that *TK* expression is increased by the presence of microbes and that the interplay between *TK* and microbes modulates a wide array of phenotypes such as lifespan, lipid metabolism, fecundity and feeding.

The main aims of the work presented in this chapter are to:
1) Test how the interaction between *TK* and specific microbes, such as *A. pomorum* and *L. brevis* impacts host health and lifespan.
2) Understand whether distinct microbial species employ distinct regulation mechanisms.
3) Identify potential mechanisms responsible for the microbial**TK* regulation of lifespan, reproduction and metabolism.

The rationale for choosing *A. pomorum* and *L. brevis* in this study is based on their prominent roles within the *Drosophila* microbiota and their distinct impacts on the host. *L. brevis* is known for recapitulating phenotypes observed in germ-free flies, highlighting its influence on host physiology in the absence of a broader microbial community (Ridley et al., 2012). In contrast, *A. pomorum* mirrors conventional, microbially influenced phenotypes, underscoring its significance in sustaining typical host functions (Wong et al., 2014). This dichotomy offers a compelling basis for their selection in examining the microbial**TK* interaction and its implications for host health, lifespan, and metabolism.

4.4 Results

4.4.1 *TK* knockdown extends lifespan in a bacterial specific manner

Considering that 1) microbe-specific effects have been documented to influence host physiology and nutritional traits and 2) the interaction between *TK* and microbes is required to regulate lifespan, I tested whether specific microbiota

members, namely *A. pomorum* and *L. brevis* regulate lifespan and whether *TK* would regulate these microbe-specific effects on lifespan (Figure 4.1). The results reveal that in the control group (RU-) gnotobiotic flies have a shorter lifespan compared to axenic flies. However, flies colonised with *Acetobacter pomorum* live slightly shorter than those inoculated with *L. brevis*. Furthermore, *TK* knockdown significantly increases lifespan in the presence of *A. pomorum* (p value <0001) and *L. brevis* (p value <0001), with a higher magnitude for A. pomorum (F ratio = 22.816 vs F ratio = 14.789 respectively) (Table 4.1). In the absence of microbes (axenic) *TK* knockdown did not have an effect on lifespan. Moreover, I performed post-hoc analysis to visualise quantitatively the interactive effect on lifespan of TK^{RNAi} expression and microbiota using estimated marginal means. The interaction plot for estimated marginal means clearly shows that each microbial condition has a distinct effect on lifespan in control flies (-), but this contrast is masked in *TK* knockdown flies (+) where the impact of gnotobiotic flies is similar to that of axenic flies (Figure 4.1B).

In addition, I tested the efficiency of *TK* knockdown in the microbial conditions used in this chapter, *A. pomorum* and *L. brevis* gnotobiotic flies and axenic flies, using RT-qPCR (Figure 4.2). The result indicates that both *Ap* and *Lb* colonised flies increased *TK* expression relative to axenic flies. This recapitulates the increased *TK* expression observed in conventional flies, demonstrating that *TK* is not only regulated by a complete set of commensal microbes, but also by individual bacteria. Moreover, flies colonised with *Lb* have lower *TK* levels compared to *Ap* flies. This contrast could explain the difference in the magnitude of the lifespan extension following *TK* knockdown between *Lb* and *Ap* flies. The results also indicate that TK^{RNAi} treatment is successful, significantly depleting *TK* in *Ap* and *Lb* flies. However, *TK* levels were constitutively low in axenic flies, and *TK* knockdown did not have a significant effect on *TK* expression in axenic flies (Figure 4.2).

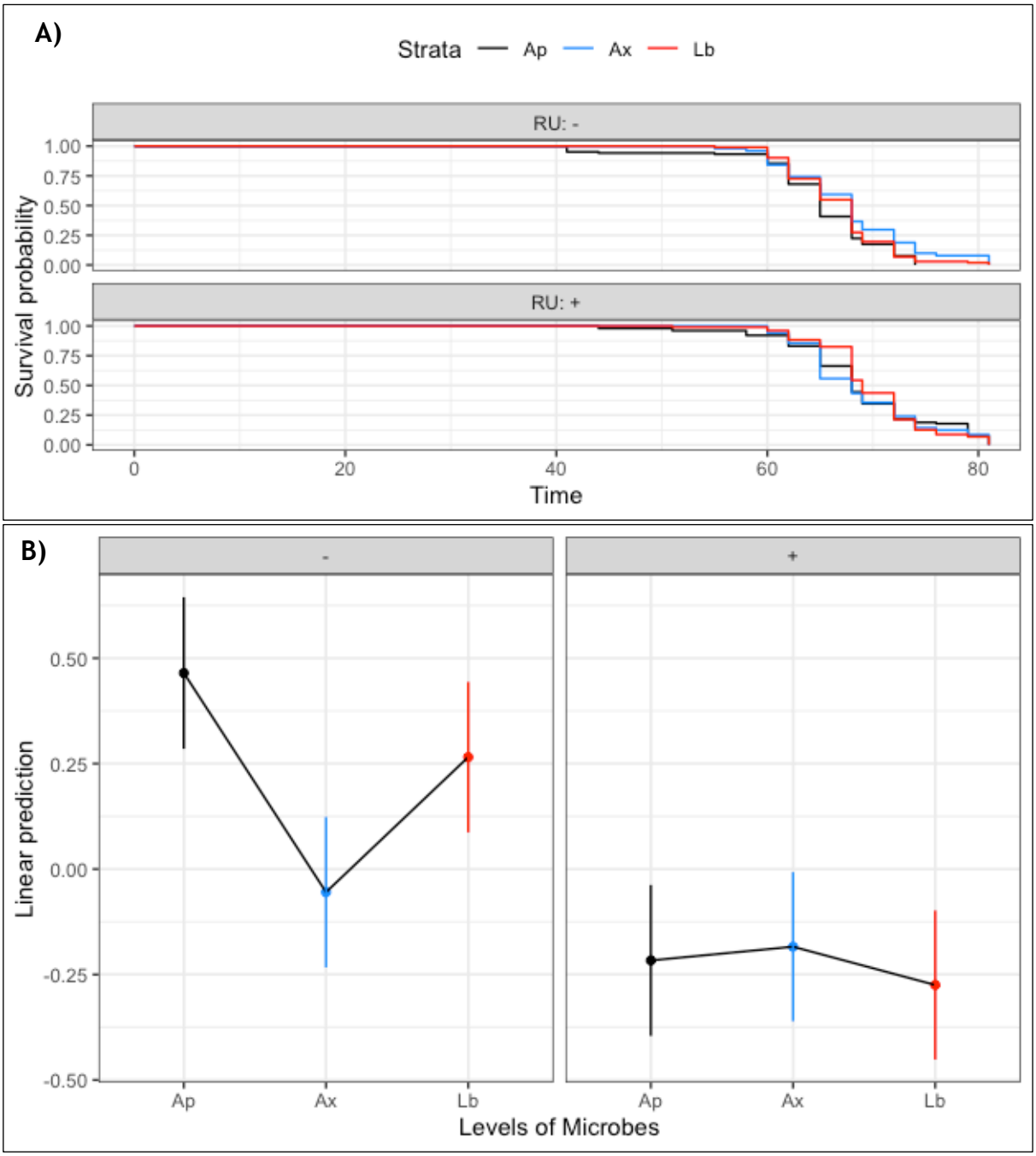

Figure 4.1 *TK* knockdown increases lifespan in a bacteria-specific manner.

(A) Kaplan-Meier survival curves in *TK* knock-down flies *DaGS > UAS-TK-RNAi* V330743 (+, lower panel) versus control flies (-, upper panel) when their microbiota is depleted (Ax, blue), colonised with *Acetobacter pomorum* (Ap, black) or *Lactobacillus brevis* (Lb, red). Statistical significance determined by Cox proportional-hazards analysis: Microbes: p value = 0.001015 **, *TK*-RNAi: p value = 2.092e-06 ***, Microbes * *TK*-RNAi: p value = 0.015853. Sample size (females): n=105. This was followed by followed ANOVA Type III tests (Table 4.1) **(B)** Interaction plot for estimated marginal means from Cox proportional hazards tests.

Table 4.1. Type III test of interactions on the estimated marginal means to determine the effect of *TK*-knockdown by microbes (Ap, Ax, Lb) on lifespan (Figure 4.1A).

model term	*Microbes*	*df1*	*df2*	*F.ratio*	*p.value*
RNAi+/-	Ap	1	Inf	22.816	1.78E-06
RNAi+/-	Ax	1	Inf	0.856	0.35495719
RNAi+/-	Lb	1	Inf	14.789	0.00012023

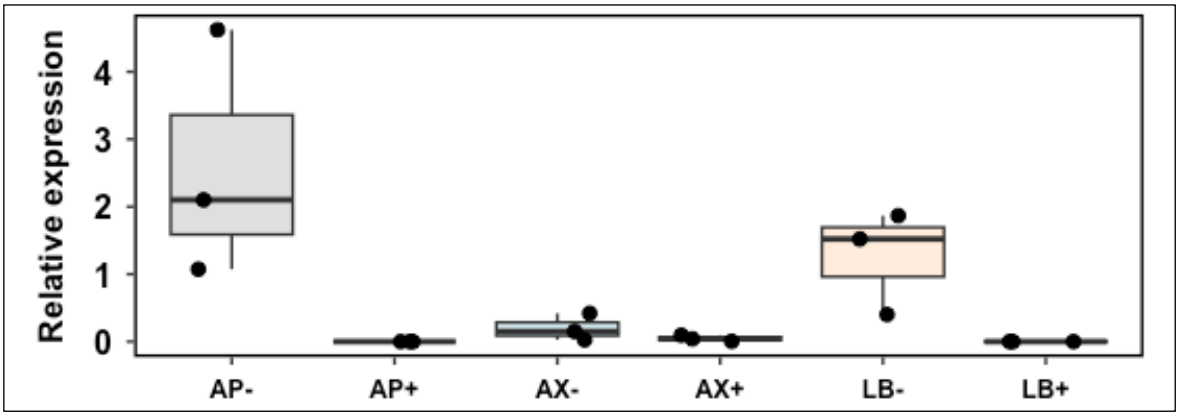

Figure 4.2 Confirmation of *TK* knockdown.

Relative whole-fly gene expression of *TK* normalised to the housekeeping gene *Tubulin* in gnotobiotic flies colonised with *A. pomorum* (Ap) or *L. brevis* (Lb) and axenic flies following *TK* knockdown (+) versus control (-). Statistical significance was determined by two-way ANOVA: Microbes: p value = 0.07877, *TK*-RNAi: p value = 0.00445**, Microbes * *TK*-RNAi: p value 0.06727 (n=3 each containing 10 flies). Box plots show median values, first and third quartiles, and 5th and 95th percentiles. Jitter plots show individual data points. AP: *Acetobacter pomorum*, LB: *Lactobacillus brevis*, AX: Axenic.

4.4.2 Microbiota depletion masks the effect of *TK* knockdown in the presence of *A. pomorum*

In order to better understand how the microbiota composition is coupled to its function(s), i.e., impacts host traits, such as triglyceride levels, the impact of each microbial taxon, and whether the effects are dependent on other microbial taxa, needs to be investigated. Taking into account the fact that 1) *Acetobacter* abundance has been correlated with reductions in host TAG content (Newell and Douglas, 2014), 2) mono-colonisation with *Lactobacillus* had no effect on TAG levels, producing a similar TAG phenotype to axenic flies (Newell and Douglas,

2014), I investigated how *TK* interacts with commensal microbes to regulate lipid metabolism. To address this, I generated *TK* knockdown flies and measured triacyl glyceride levels comparing axenic with gnotobiotic flies colonised with either *A. pomorum* or *L. brevis* (Figure 4.3). The figures refer to *TK*-RNAi+ as RU+ and *TK*-RNAi as RU- based on the genetic system used to induce knockdown (Daughterless Gene Switch system). The results indicated that *TK* knockdown flies colonised with *Ap* (Ap RU+) had significantly increased TAG levels compared to control flies (Ap RU-). In consequence, *A. pomorum* alone recapitulated the TAG phenotype of conventionally-reared flies presented in chapter 3. However, the effect was not observed in flies colonised with *L. brevis*. Furthermore, the impact of *TK* knockdown on TAG in axenic flies was consistent with what we have previously observed, namely axenic control flies have increased TAG levels compared to *Ap* control flies, but the effect was masked when *TK* is knocked down (Table 4.2). Overall, these findings suggested that the interaction between *TK* and *Ap* is sufficient to impact host lipid metabolism.

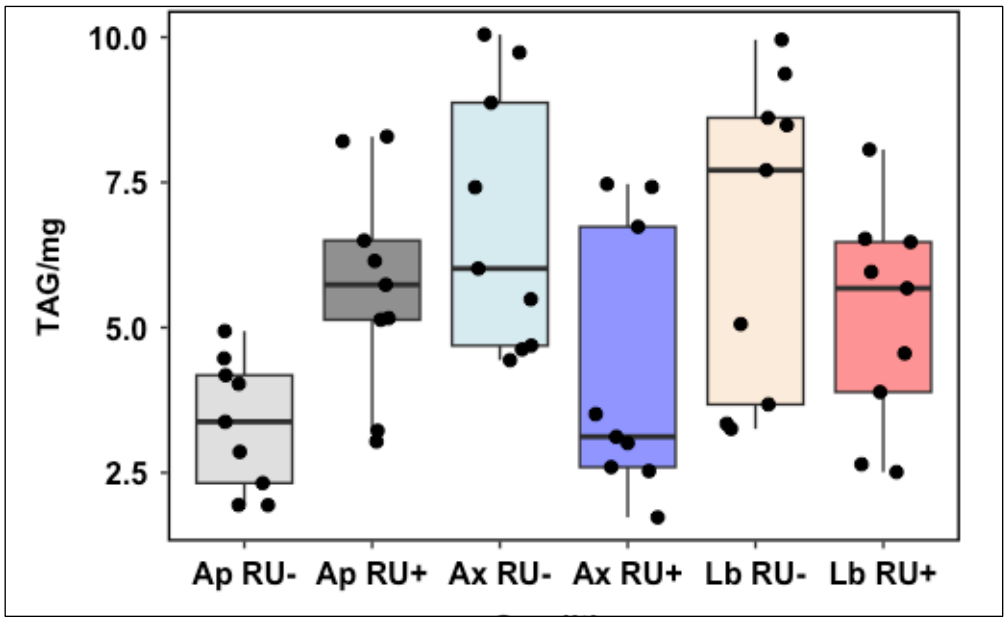

Figure 4.3 Microbiota depletion and ubiquitous *TK* knock-down have epistatic effects on fly TAG levels.

Triglyceride levels in *TK* knock-down flies (*DaGS > UAS-TK-RNAi V330743*) (RU+) compared to control flies (RU-) when they are axenic (blue) or colonised with *A. pomorum* (Ap, grey) or *L. brevis* (red). Statistical significance was determined by two-way ANOVA with an interaction term: Microbes: p value = 0.14427, *TK*-RNAi: p value = 0.33365, Microbes * *TK*-RNAi: p value 0.00222 **. This was followed Type III test of interactions Table 4.2. Box plots show median values, first and

third quartiles, and 5th and 95th percentiles. Each dot is one sample, with sample groups given on the x-axis and TAG levels on the y-axis. (n=9/RU- AX, n=9/RU- Ap, n=9/RU- Lb, n=9/RU+ Ax; n=9/RU+ Ap, n=9/RU+ Lb, each sample containing 5 flies).

Table 4.2 Type III test on the estimated marginal means to determine the effect of *TK*-knockdown in specific microbial conditions (Ap, Ax, Lb) on TAG (Figure 4.2).

model term	*Microbes*	*df1*	*df2*	*F.ratio*	*p.value*
RNAi+/-	**AP**	**1**	**48**	**5.811**	**0.01980423**
RNAi+/-	**AX**	**1**	**48**	**6.848**	**0.01182954**
RNAi+/-	**LB**	**1**	**48**	**2.206**	**0.14401319**

4.4.3 Ubiquitous *TK* knockdown reduces starvation resistance in the presence of *A. pomorum*

According to my previous findings, although global loss of *TK* increased lifespan in conventional flies, it decreased the resistance to stress independent of the presence of bacteria. Therefore, I tested starvation resistance in response to *TK* knockdown in gnotobiotic flies colonised with *Ap* or *Lb* and axenic flies. As previously, the results indicated that knocking down *TK* in the whole fly significantly decreased the resistance to starvation in *Ap* and axenic flies, but not in *Lb* flies (Figure 4.4). Unexpectedly, *Ap* control flies (RNAi-) were more resistant to starvation than both *Lb* and axenic flies. Thus, here, *Ap* mono-associated flies did not recapitulate the conventional phenotype (conventional flies have lower starvation resistance compared to axenics – chapter 3). In conclusion, starvation resistance in gnotobiotic flies is inversely correlated with longevity – *Ap* flies have the highest resistance to starvation, but the shortest lifespan, while axenic flies are less resistant to stress but live longer. Moreover, *TK* knockdown negatively impacts starvation survival in *Ap* and axenic flies, but has no effect in *Lb* flies. Overall, this is a consistent pattern the interaction between *TK* and *Ap* leads to strong phenotypic responses, while the effects of *TK* communicating with *Lb* are milder.

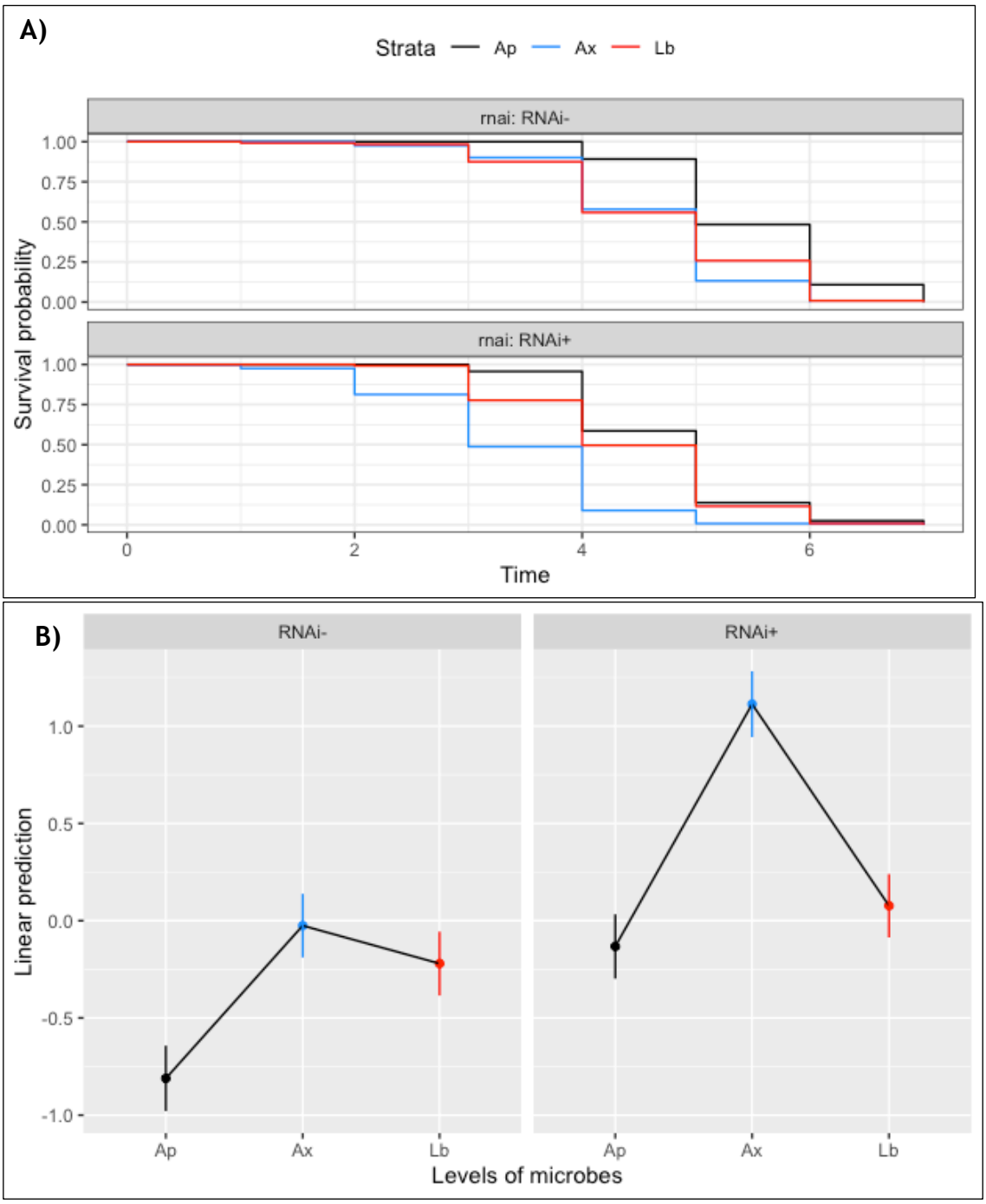

Figure 4.4 *A. pomorum* mono-colonised *TK* knockdown flies have reduced starvation resistance.

A) Kaplan-Meier survival curves in *TK* knock-down flies *DaGS > UAS-TK-RNAi* V330743 (RNAi+) versus control flies (RNAi-) in gnotobiotic flies colonised with *A. pomorum* (black) or *L. brevis (red)* compared to germ-free flies (blue). Statistical significance determined by cox proportional-hazards analysis: Microbes: p value 2.2e-16 ***, RNAi: p value 2.2e-16 ***, Microbes:RNAi: p value 2.793e-05 ***. This was followed Type III test of interactions (Table 4.3.) Sample size (females): n=120. **(B)** Interaction plot for estimated marginal means.

Table 4.3 Type III test of interactions on the estimated marginal means to determine the effect of *TK*-knockdown by microbes (Ap, Ax, Lb) on starvation resistance (Figure 4.3).

contrast	*estimate*	*SE*	*df*	*z.ratio*	*p.value*
(RNAi- Ap) - (RNAi+ Ap)	-0.6781	0.13168	Inf	-5.1497	3.879079E-06
(RNAi- Ap) - (RNAi- Ax)	-0.7852	0.13169	Inf	-5.9622	3.726421E-08
(RNAi- Ap) - (RNAi+ Ax)	-1.9239	0.13505	Inf	-14.245	2.2E-16
(RNAi- Ap) - (RNAi- Lb)	-0.5901	0.13046	Inf	-4.523	8.91121812E-05
(RNAi- Ap) - (RNAi+ Lb)	-0.8874	0.13112	Inf	-6.7683	1.95832E-10
(RNAi+ Ap) - (RNAi- Ax)	-0.107	0.13029	Inf	-0.8214	0.9636
(RNAi+ Ap) - (RNAi+ Ax)	-1.2457	0.13237	Inf	-9.4107	5.5512578E-14
(RNAi+ Ap) - (RNAi- Lb)	0.08805	0.13065	Inf	0.6739	0.9848
(RNAi+ Ap) - (RNAi+ Lb)	-0.2093	0.13008	Inf	-1.60914	0.5924
(RNAi- Ax) - (RNAi+ Ax)	-1.1387	0.1313	Inf	-8.6723	5.0629071E-14
(RNAi- Ax) - (RNAi- Lb)	0.195087	0.12932	Inf	1.508512	0.658788
(RNAi- Ax) - (RNAi+ Lb)	-0.10229	0.12862	Inf	-0.79522	0.968418
(RNAi+ Ax) - (RNAi- Lb)	1.333828	0.13286	Inf	10.0389	7.0166E-14
(RNAi+ Ax) - (RNAi+ Lb)	1.036451	0.13089	Inf	7.91831	1.2017E-13
(RNAi- Lb) - (RNAi+ Lb)	-0.29737	0.12924	Inf	-2.3009	0.1935293

4.4.4 *TK* knockdown does not affect egg laying in gnotobiotic flies

In chapter 3 I showed that *TK* breaks classical life-history tradeoffs in ageing, and that lifespan extension following TK^{RNAi} was not associated with a reduction in reproduction in conventional flies. More, *TK* knockdown also rescued the negative effects of axenia on fecundity. Here, in order to understand whether the egg laying phenotype observed in chapter 3 is attributable to specific bacteria, I tested egg laying in flies that have *TK* knocked down ubiquitously (*DaGS > UAS-TK-RNAi*) when they are mono-colonised with *Ap* or *Lb (*Figure 4.5). In those results, the only significant effect that we can observe is an increase in axenic RNAi+ compared to axenic RNAi- (p value = 0.01, table 4.5)), which recapitulates the previous results (chapter 3). Hence, *TK* knockdown increases the number of eggs in axenic flies, but not in flies colonised with *Ap* or *Lb*. However, given that axenic flies had significantly lower fecundity compared to conventional flies (chapter 3), result consistent with previously published literature, it was unexpected that mono-colonisation with *A. pomorum* or *L. brevis* did not increase the number of eggs. Overall, this indicates that egg laying responds to full unaltered microbiota, or co-colonisation with *A. pomorum* and *L. brevis*, implying that egg-laying might require synergetic interactions of microbes.

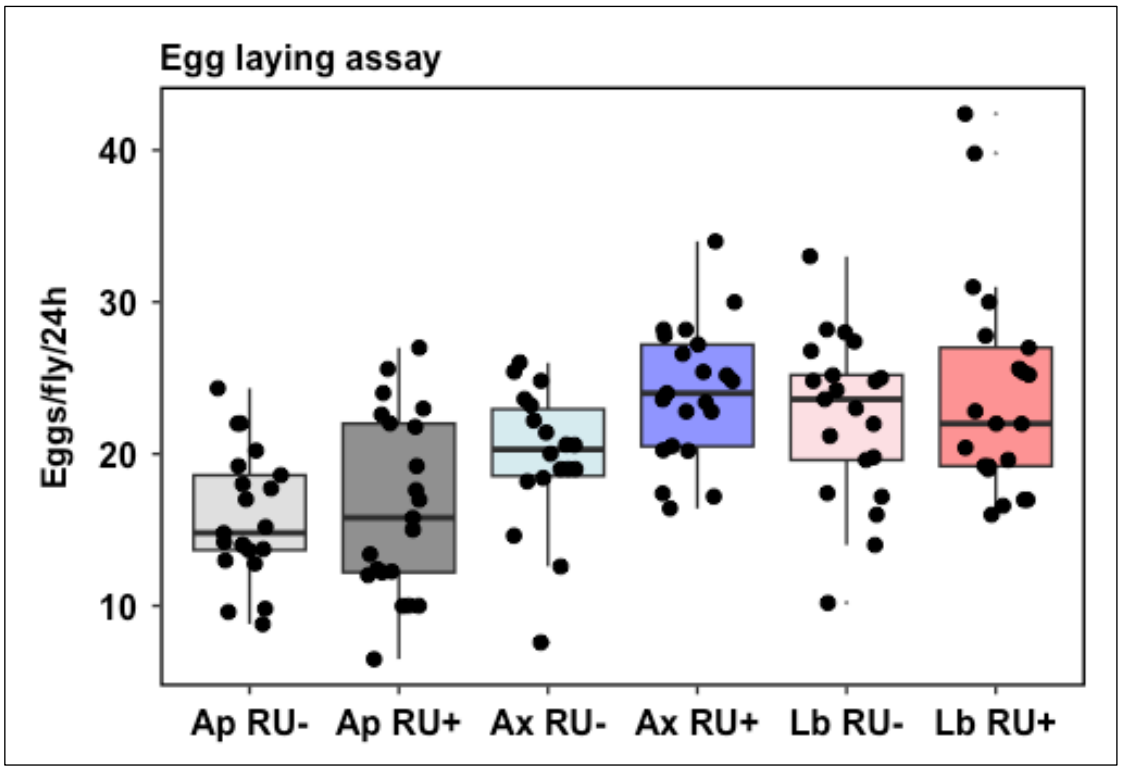

Figure 4.5 Egg-laying is not influenced by mono-colonisation with *A. pomorum* or *L. brevis*.

Number of eggs per fly in *TK* knock-down flies *DaGS* > *UAS-TK-RNAi* V330743 (+) compared to control flies (-) when they are axenic (blue) or gnotobiotic – colonised with *A. pomorum* (grey) or *L. brevis* (red). Statistical significance was determined by two-way ANOVA (Microbes: p value 3.24e-08 ***, RNAi: p value 0.0281 *, Microbes*RNAi: p value = 0.3213). This was followed post-hoc joint tests (Table 4.5). Box plots show median values, first and third quartiles, and 5th and 95th percentiles. Each dot is one sample, with sample groups given on the x-axis and egg numbers on the y-axis. (n=24 samples/condition, each sample containing 5 flies). *** p < 0.0005, *p<0.05.

Table 4.4 Post-hoc joint test on the estimated marginal means to determine the effect of *TK*-knockdown by microbes (Ap, Ax, Lb) on egg laying (Figure 4.5).

model term	*Microbiome*	*df1*	*df2*	*F.ratio*	*p.value*
RNAi+/-	Ap	1	117	0.224	0.63664608
RNAi+/-	Ax	1	117	6.102	0.01494574
RNAi+/-	Lb	1	117	0.914	0.3411467

4.4.5 Feeding behaviour is not influenced by *A. pomorum* or *L. brevis*

In chapter 3 I tested whether the longevity effect was caused by decreased nutrient intake and I showed that *TK* knockdown does not change feeding in conventional flies, but it rescued the reduced feeding phenotype of germ-free flies. Here, to ascertain whether these effects could be attributed to particular commensals, I tested feeding in flies that have *TK* knocked down ubiquitously (DaGS > *UAS-TK*-RNAi) and are mono-colonised with *Ap* or *Lb* (Figure 4.6). The findings illustrate that there is a significant RNAi effect in all microbial condition, showing that knocking down *TK* significantly increases feeding in gnotobiotic as well as in axenic flies. However, there is not a significant microbial effect, suggesting that standardised sets of microbes are not sufficient to induce an effect on feeding. Overall, this experiment suggests that the regulation of feeding may necessitate the presence of a conventional complete microbiota or colonisation with both *A. pomorum* and *L. brevis*. Flies mono-colonised with specific bacteria do not elicit a discernible response in this regard.

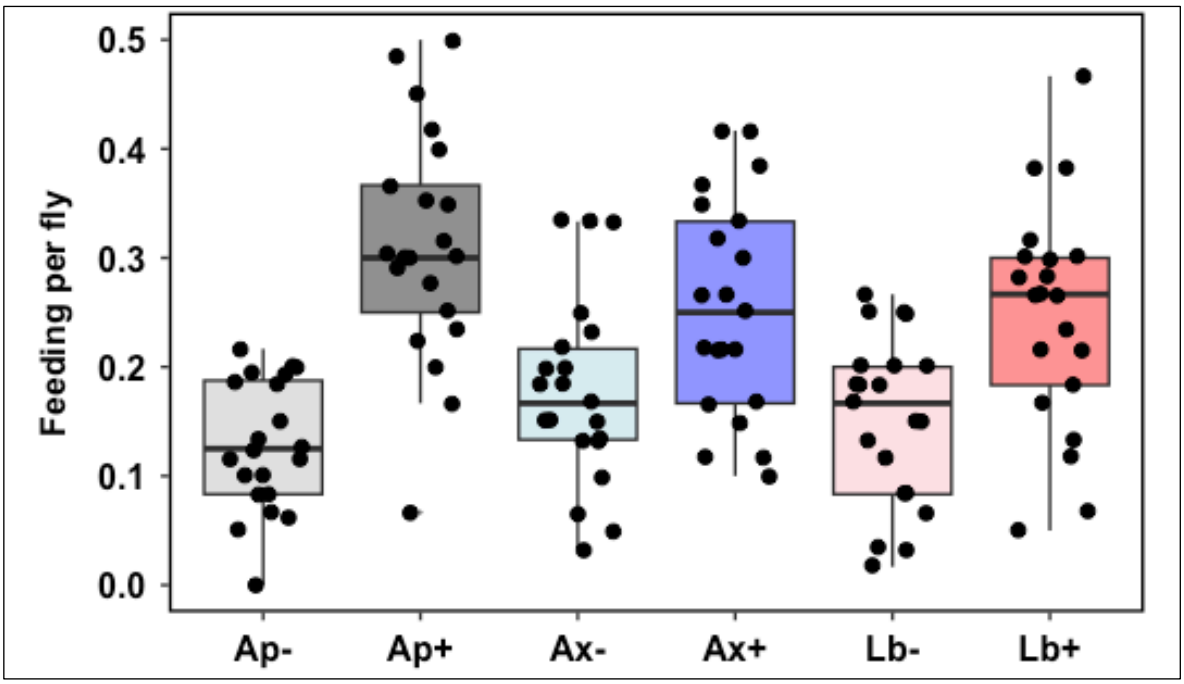

Figure 4.6 Individual gut symbionts do not influence feeding behaviour.

(A) PER assay to measure feeding behaviour in *TK* knock-down flies *DaGS > UAS-TK-RNAi* V330743 (+) compared to RU- control flies (-) when they are axenic (microbiota removed, blue) or gnotobiotic – colonised with *A. pomorum* (grey) or *L. brevis* (red). Statistical significance was determined by two-way ANOVA (Microbes: p value = 0.5574, RNAi: p value = 1.97e-11 ***, Microbes*RNAi: p value = 0.0165). This was followed by post-hoc joint test (Table 4.4). Box plots show

median values, first and third quartiles, and 5th and 95th percentiles. Each dot is one sample, with sample groups given on the x-axis and feeding levels on the y-axis. (n=24 samples/condition, each sample containing 5 flies)*** $p < 0.0005$, *$p < 0.05$.

Table 4.5 Post-hoc joint on the estimated marginal means to determine the effect of *TK*-knockdown by microbes (Ap, Ax, Lb) on feeding behaviour (Figure 4.4).

model term	*Microbes*	*df1*	*df2*	*F.ratio*	*p.value*
RNAi+/-	**Ap**	**1**	**120**	**43.898**	**1.03E-09**
RNAi+/-	**Ax**	**1**	**120**	**7.69**	**0.00643886**
RNAi+/-	**Lb**	**1**	**120**	**11.77**	**0.00082621**

4.4.6 Transcriptome analysis of ubiquitous *TK* knockdown gnotobiotic flies

4.4.6.1 Normalised expression

Taken together, my results so far demonstrate a vast array of interacting effects between *TK* and commensal microbes. Specifically, both *A. pomorum* and *L. brevis* communicate with *TK* and this interplay regulates several phenotypes such as lifespan, lipid metabolism, fecundity, feeding and stress resistance. However, it is unclear whether *Ap* and *Lb* regulate *TK* via similar or distinct mechanisms. Moreover, the phenotypic outcomes were not always correlated, suggesting that each phenotype might be regulated through distinct mechanisms. To gain a systemic view of how different microbes interact with *TK* to modulate host physiology, and to identify candidate downstream mechanisms that mediate this interaction, I decided to perform an RNA-seq experiment where I ubiquitously knocked down *TK* using the same genetic system that has been employed in all experiments so far (*DaGS > UAS-TK-RNAi*) in axenic flies and flies colonised with either *A. pomorum* or *L. brevis*.

First of all, I have analysed the quality of my samples. Figure 4.7 shows the distribution of expression values for each sample. Generally, these are expected to look highly similar across all samples regardless of sample group, and thus are

useful for assessing the quality of the experiment technically. Outlier samples with atypical distributions of expression values can be indicative of technical issues with that sample – such as insufficient quantities of RNA during library preparation. In this case, all samples look highly similar, proving that they are good quality.

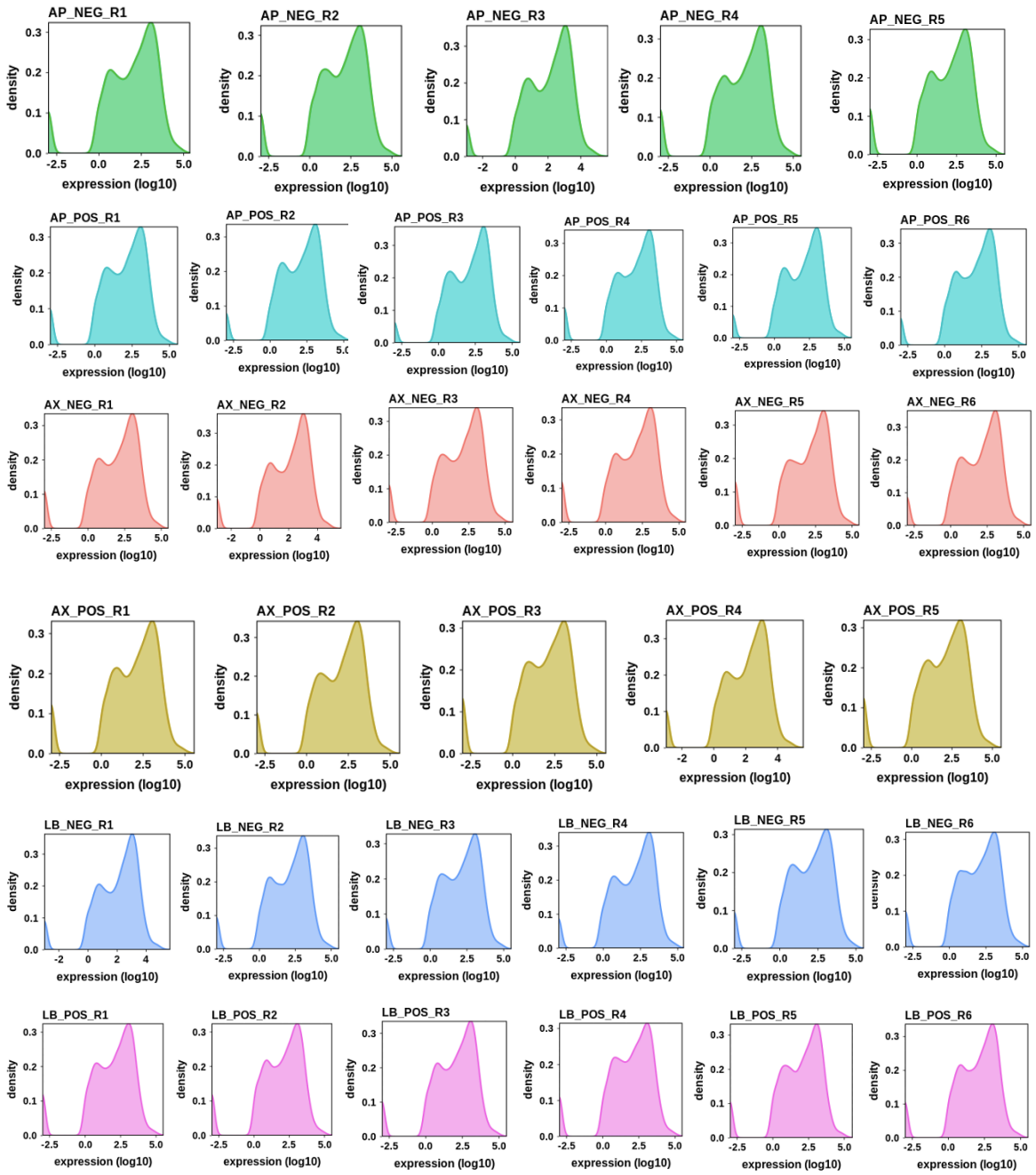

Figure 4.7 Density plots showing the overall distribution of expression values for each sample.

Expression values are given on x-axis and are on a log 10 scale. The gene density is given on the y-axis. Samples are extracted from *TK* knock-down flies *DaGS* > *Uas-Tk-RNAi V330743* (pos) compared to control flies (neg) when they are axenic

(AX) or gnotobiotic – colonised with *Acetobacter pomorum* (AP) or *Lactobacillus brevis* (LB).

Next, I have performed principal component analysis (PCA) using all expression values to find underlying variables (known as principal components) that best differentiate my samples. Principal components are dimensions along which data points are most spread out. Each component will describe a proportion of the total underlying variation between genes and samples. Components are ordered by the % of the underlying variation that they describe, with PC1 explaining the most variation. In figure 4.8 each sample is plotted based on its PC1 vs PC2 values (left) and its PC3 vs PC4 values (right). The important comparisons here are the knockdowns within each microbial condition (neg vs pos). This provides an understanding of the impact of *TK* knockdown in axenic, *Ap* and *Lb* flies. The plots show that sample groups that separate the most are axenic RNAi- vs axenic RNAi+, thus suggesting a bigger difference in their transcriptome. The groups with the least separation are *Lb* RNAi- vs *Lb* RNAi+.

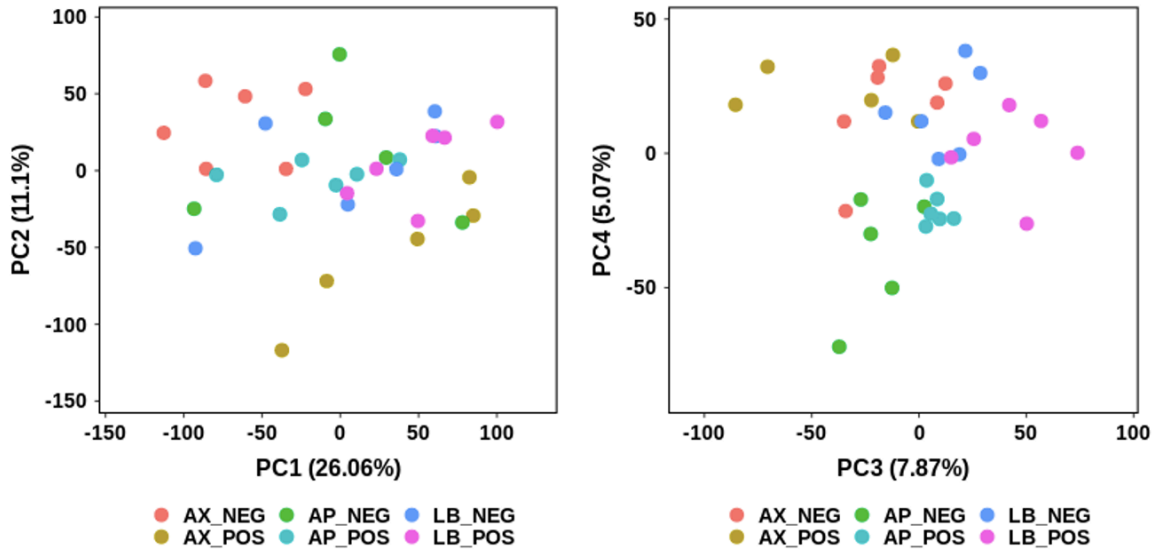

Figure 4.8 Gene expression data - PCA.

The scatterplots show PC1 vs PC2 (left) and PC3 vs PC4 (right). Individual samples are represented by dots. The percentage of total variation explained by each component is given in the x and y-axis as appropriate. To control over representation of very highly expressed genes, all gene expression values were scaled on a gene-by-gene basis using the z-score transformation, prior to the PCA.

Furthermore, I performed a sample-by-sample correlation analysis heatmap to highlight the differences and similarity between samples based on how strongly or weakly they correlate with each other across all gene expression values (Figure 4.9). The heatmap shows all possible combinations of correlations (Spearman Correlation Coefficient) between two samples. The diagonal line, comparing a sample to itself, should always give a correlation of 1. The upper and lower plots are identical, however in the lower plot the samples have been hierarchically clustered, so that more similar samples are grouped together on the x and y axis. The graphs illustrate that sample groups do not always separate, suggesting that different sample groups do not have very different expression patterns and thus exhibit high correlation values. The group that perfectly clustered together is axenic RNAi-, suggesting that it has a highly different profile than the other groups.

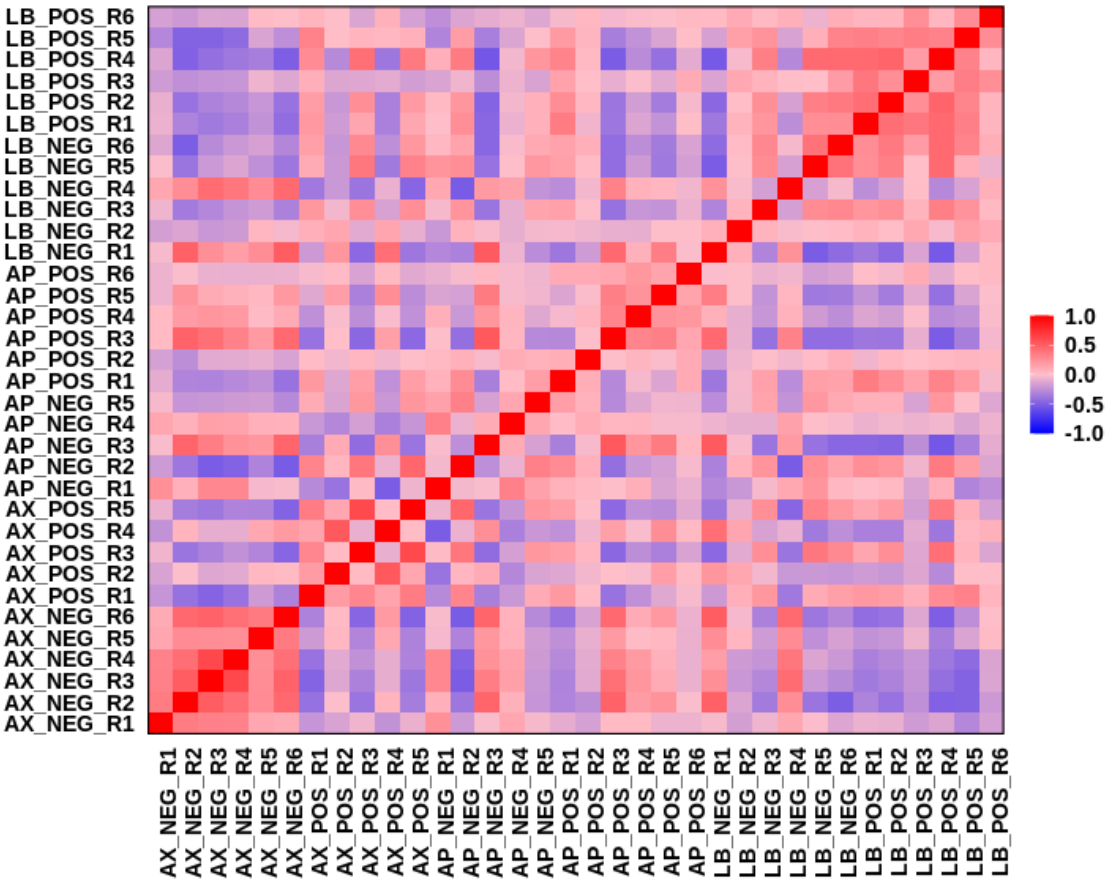
LB_POS_R6
LB_POS_R5
LB_POS_R4
LB_POS_R3
LB_POS_R2
LB_POS_R1
LB_NEG_R6
LB_NEG_R5
LB_NEG_R4
LB_NEG_R3
LB_NEG_R2
LB_NEG_R1
AP_POS_R6
AP_POS_R5
AP_POS_R4
AP_POS_R3
AP_POS_R2
AP_POS_R1
AP_NEG_R5
AP_NEG_R4
AP_NEG_R3
AP_NEG_R2
AP_NEG_R1
AX_POS_R5
AX_POS_R4
AX_POS_R3
AX_POS_R2
AX_POS_R1
AX_NEG_R6
AX_NEG_R5
AX_NEG_R4
AX_NEG_R3
AX_NEG_R2
AX_NEG_R1
AX_NEG_R1 AX_NEG_R2 AX_NEG_R3 AX_NEG_R4 AX_NEG_R5 AX_NEG_R6 AX_POS_R1 AX_POS_R2 AX_POS_R3 AX_POS_R4 AX_POS_R5 AP_NEG_R1 AP_NEG_R2 AP_NEG_R3 AP_NEG_R4 AP_NEG_R5 AP_POS_R1 AP_POS_R2 AP_POS_R3 AP_POS_R4 AP_POS_R5 AP_POS_R6 LB_NEG_R1 LB_NEG_R2 LB_NEG_R3 LB_NEG_R4 LB_NEG_R5 LB_NEG_R6 LB_POS_R1 LB_POS_R2 LB_POS_R3 LB_POS_R4 LB_POS_R5 LB_POS_R6
1.0
0.5
0.0
-0.5
-1.0

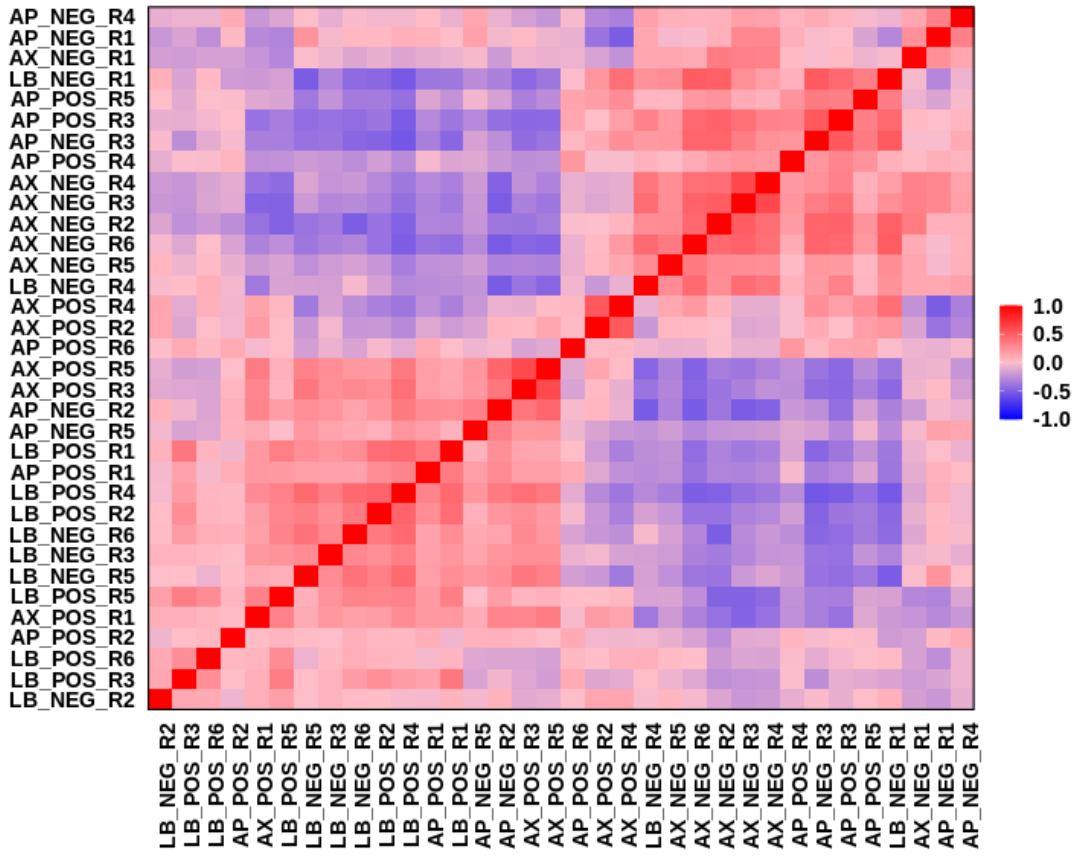
AP_NEG_R4
AP_NEG_R1
AX_NEG_R1
LB_NEG_R1
AP_POS_R5
AP_POS_R3
AP_NEG_R3
AP_POS_R4
AX_NEG_R4
AX_NEG_R3
AX_NEG_R2
AX_NEG_R6
AX_NEG_R5
LB_NEG_R4
AX_POS_R4
AX_POS_R2
AP_POS_R6
AX_POS_R5
AX_POS_R3
AP_NEG_R2
AP_NEG_R5
LB_POS_R1
AP_POS_R1
LB_POS_R4
LB_POS_R2
LB_NEG_R6
LB_NEG_R3
LB_NEG_R5
LB_POS_R5
AX_POS_R1
AP_POS_R2
LB_POS_R6
LB_POS_R3
LB_NEG_R2
LB_NEG_R2 LB_POS_R3 LB_POS_R6 AP_POS_R2 AX_POS_R1 LB_POS_R5 LB_NEG_R3 LB_NEG_R6 LB_POS_R2 LB_POS_R4 AP_POS_R1 LB_POS_R1 AP_NEG_R5 AP_NEG_R2 AX_POS_R3 AX_POS_R5 AP_POS_R6 AX_POS_R2 AX_POS_R4 LB_NEG_R4 AX_NEG_R5 AX_NEG_R6 AX_NEG_R2 AX_NEG_R3 AX_NEG_R4 AP_POS_R4 AP_NEG_R3 AP_POS_R3 AP_POS_R5 LB_NEG_R1 AX_NEG_R1 AP_NEG_R1 AP_NEG_R4
1.0
0.5
0.0
-0.5
-1.0

Figure 4.9 Heatmap of among-sample correlation in gene expression.

Correlations between each pairwise combination of samples is shown. The correlations were calculated using Spearman Correlation based on all gene expression values. The level of correlation (Spearman Correlation Coefficient) is represented by colour intensity, with strong positive correlation in red, no correlation in light pink and strong anti-correlation in blue. The bottom plot has been hierarchically clustered on both axes using, Spearman distances, with UPMGA agglomeration and mean reordering.

As a further quality control check, I looked at the ten most highly expressed genes in each sample group. This can be a useful control for the success of the experiment technically - as many of those genes should be housekeeping genes. Nevertheless, our results show that the most expressed genes are housekeeping genes and they are also consistent between groups (Supplementary figure 1). However, there was one exception- *Chorion protein 15 (Cp15)*. This gene was consistently one of the most highly expressed genes in all sample groups, except in the axenic RNAi- group. Therefore, I decided to plot it for better visualisation. The results indicate that *Cp15* is strongly downregulated in axenic RNAi- samples.

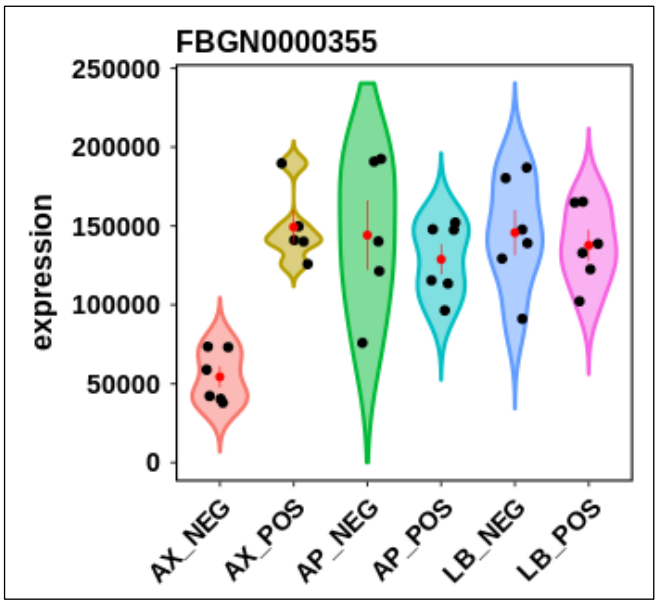

Figure 4.10 Violin and jitter plot showing the expression of *Cp15*.

Each dot is one sample, with sample groups given on the x-axis and gene expression on the y-axis. The mean and standard error for each sample group is given as a red dot and line.

4.4.6.2 Differential expression

4.4.6.2.1 Differential expression in *TK* knockdown flies colonised with *A. pomorum*

I then performed differential expression analysis using the DESeq2 R package to understand the impact of *TK* knockdown in different microbial settings. I expected that *TK* knockdown would block some effects of microbiota, as observed for lifespan. The first comparison was between *TK* knockdown (pos) and control (neg) flies colonised with *Acetobacter pomorum*. Initially, I performed PCA (Figure 4.11) and correlation analysis (Figure 4.12) to envision the global variation in the dataset. Those results indicated that *TK* knockdown separated the samples on the third principal component (explaining 11% of variance), suggesting that the two sample groups exhibited differences in their transcriptomes, but random variation among samples was a bigger source of variance (i.e. on the first and second principal components). Subsequently, after differential expression analysis I visualised the data using a volcano plot to assess the relationship between the fold change and the associated p−value for each gene (Figure 4.13). There is a consistent relationship between the fold change and p−values across all genes. Moreover, the direction of changes between the two conditions seems balanced. Similarly, I have visualised the data using a MA plot where the mean expression of each gene was plotted against its fold change (Figure 4.14). This gave an indication of whether there are lowly expressed genes that might lose statistical power because they have fewer reads. In this case, low expression was not correlated with fewer significant genes.

Furthermore, in figure 4.15A the behaviour of each sample and sample group at each of the differentially expressed genes is analysed using a heatmap. The bar chart of the number of significantly upregulated and downregulated genes shows that there is a similar directionality of the differentially expressed genes.

Moreover, considering that there are only 81 upregulated genes and 86 downregulated, I decided that the stringency of significance should not be increased.

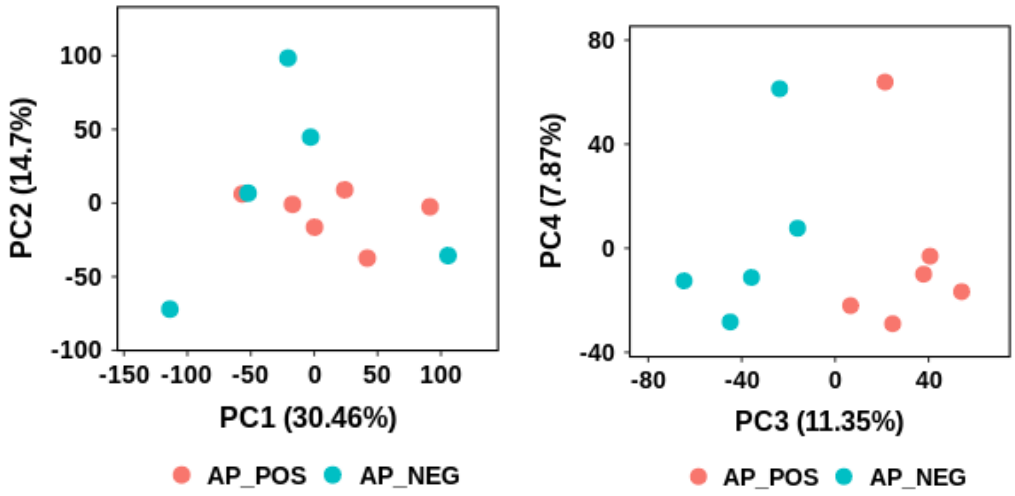

Figure 4.11 Gene expression data - PCA.

The scatterplots show PC1 vs PC2 (left) and PC3 vs PC4 (right). Individual samples are represented by dots. The percentage of total variation explained by each component is given in the x and y-axis as appropriate. To control over representation of very highly expressed genes, all gene expression values were scaled on a gene by gene basis using the z-score transformation, prior to the PCA.

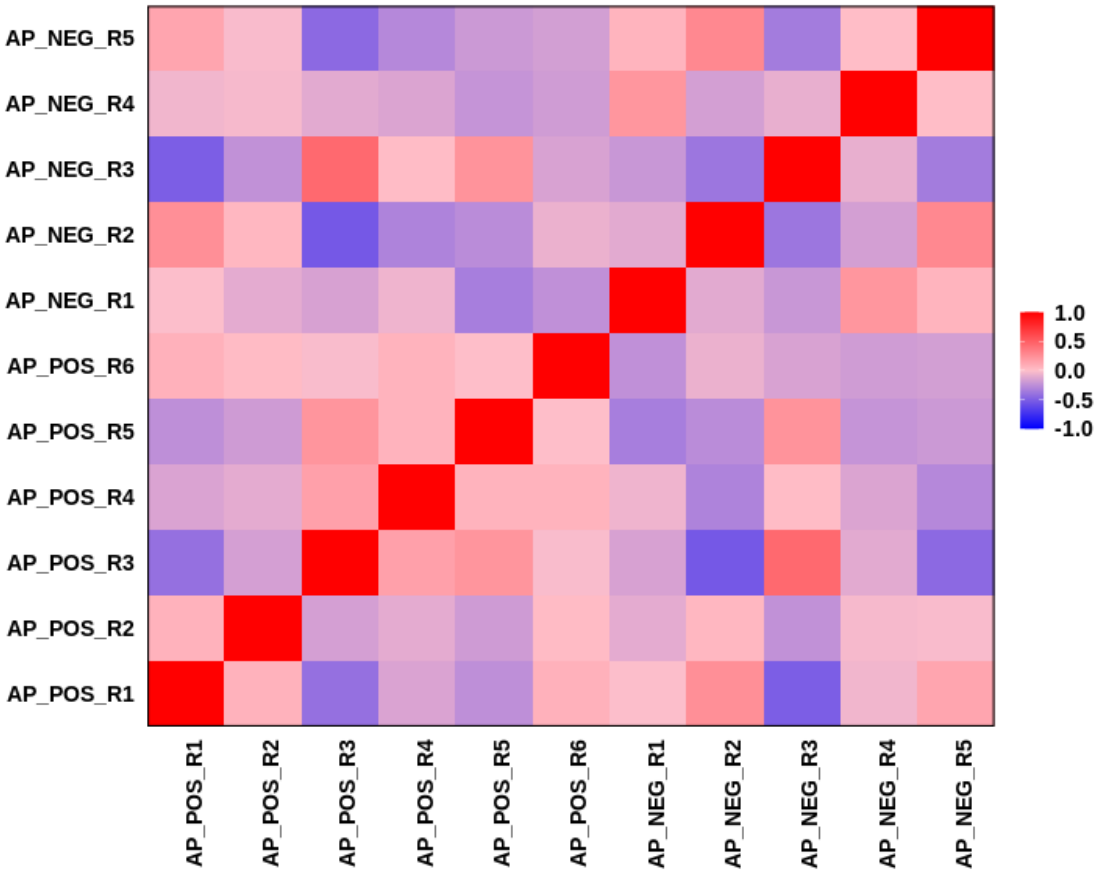
AP_NEG_R5
AP_NEG_R4
AP_NEG_R3
AP_NEG_R2
AP_NEG_R1
AP_POS_R6
AP_POS_R5
AP_POS_R4
AP_POS_R3
AP_POS_R2
AP_POS_R1
AP_POS_R1
AP_POS_R2
AP_POS_R3
AP_POS_R4
AP_POS_R5
AP_POS_R6
AP_NEG_R1
AP_NEG_R2
AP_NEG_R3
AP_NEG_R4
AP_NEG_R5
1.0
0.5
0.0
-0.5
-1.0

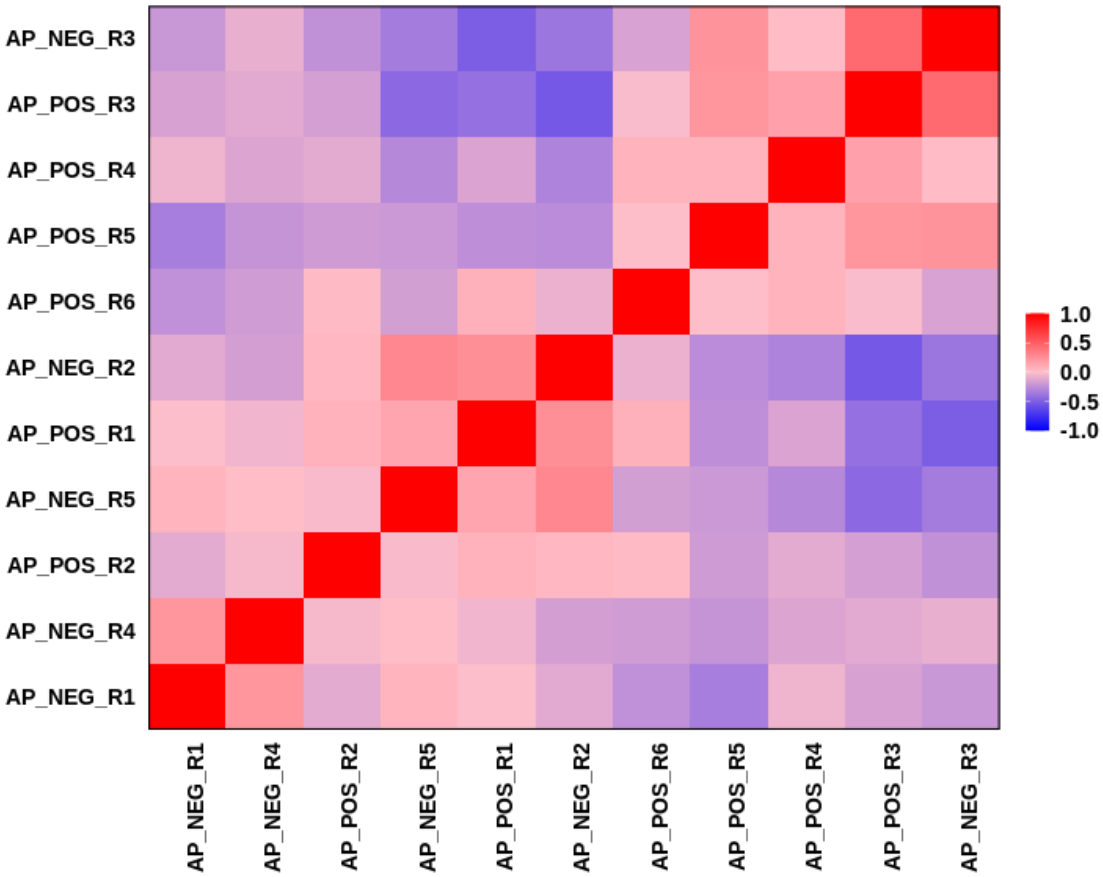
AP_NEG_R3
AP_POS_R3
AP_POS_R4
AP_POS_R5
AP_POS_R6
AP_NEG_R2
AP_POS_R1
AP_NEG_R5
AP_POS_R2
AP_NEG_R4
AP_NEG_R1
AP_NEG_R1
AP_NEG_R4
AP_POS_R2
AP_NEG_R5
AP_POS_R1
AP_NEG_R2
AP_POS_R6
AP_POS_R5
AP_POS_R4
AP_POS_R3
AP_NEG_R3
1.0
0.5
0.0
-0.5
-1.0

Figure 4.12 Heatmap of sample correlation.

Correlations between each pairwise combination of samples is shown. The correlations were calculated using Spearman Correlation based on all gene expression values. The level of correlation (Spearman Correlation Coefficient) is represented by colour intensity, with strong positive correlation in red, no correlation in light pink and strong anti-correlation in blue. The bottom plot has been hierarchically clustered on both axis using, Spearman distances, with UPMGA agglomeration and mean reordering.

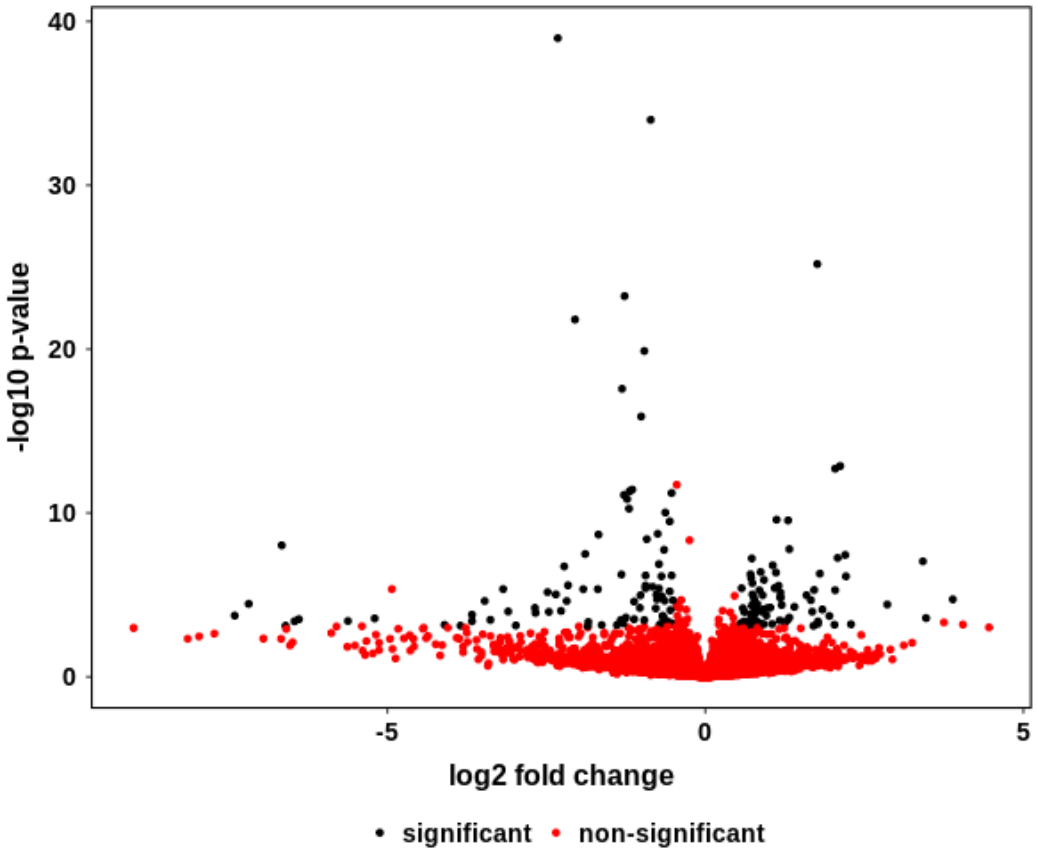

Figure 4.13 Volcano plot comparing the effect of *TK* knockdown in *A. pomorum* mono-colonised flies.

Significantly differential genes (p.adj < 0.05, absolute log2 fold > 0.5) are shown in red and non−significant genes in black. A positive fold change indicates higher expression in ap neg than in ap pos.

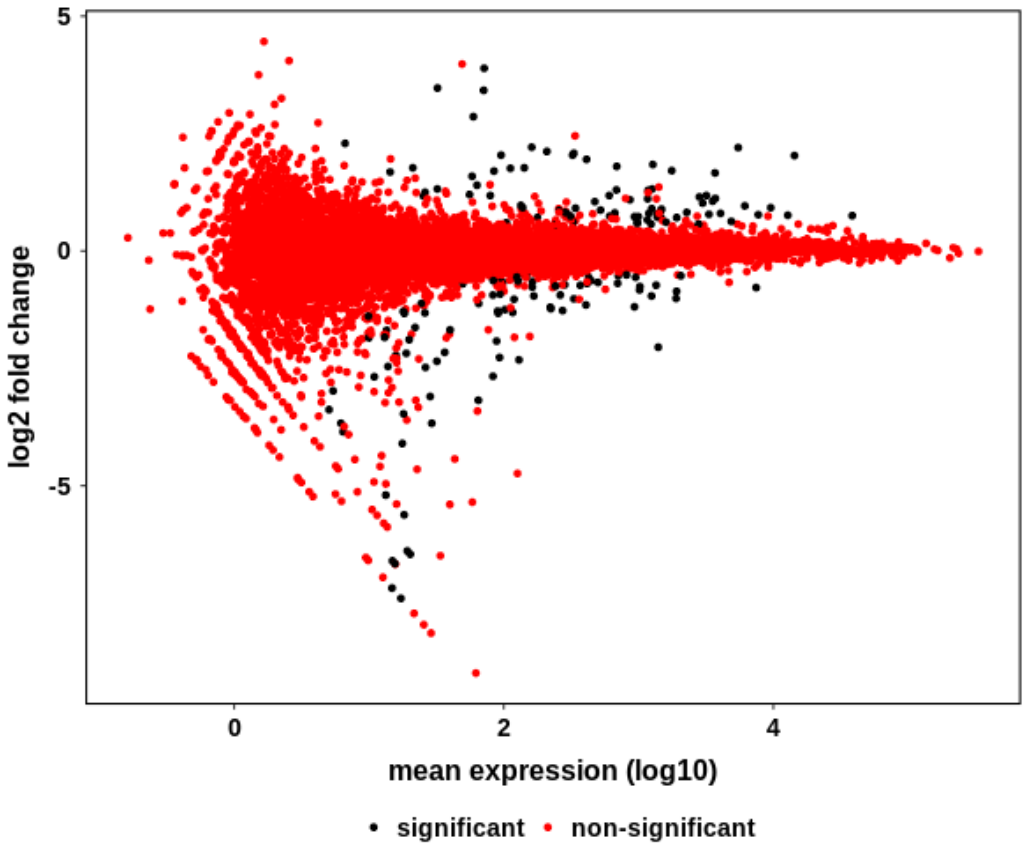

Figure 4.14 MA plot comparing the effect of *TK* knockdown in *A. pomorum* mono-colonised flies.

Significantly differential genes (p.adj < 0.05, absolute log2 fold-change > 0.5) are shown in red and non−significant genes in black. A positive fold change indicates higher expression in ap neg than in ap pos.

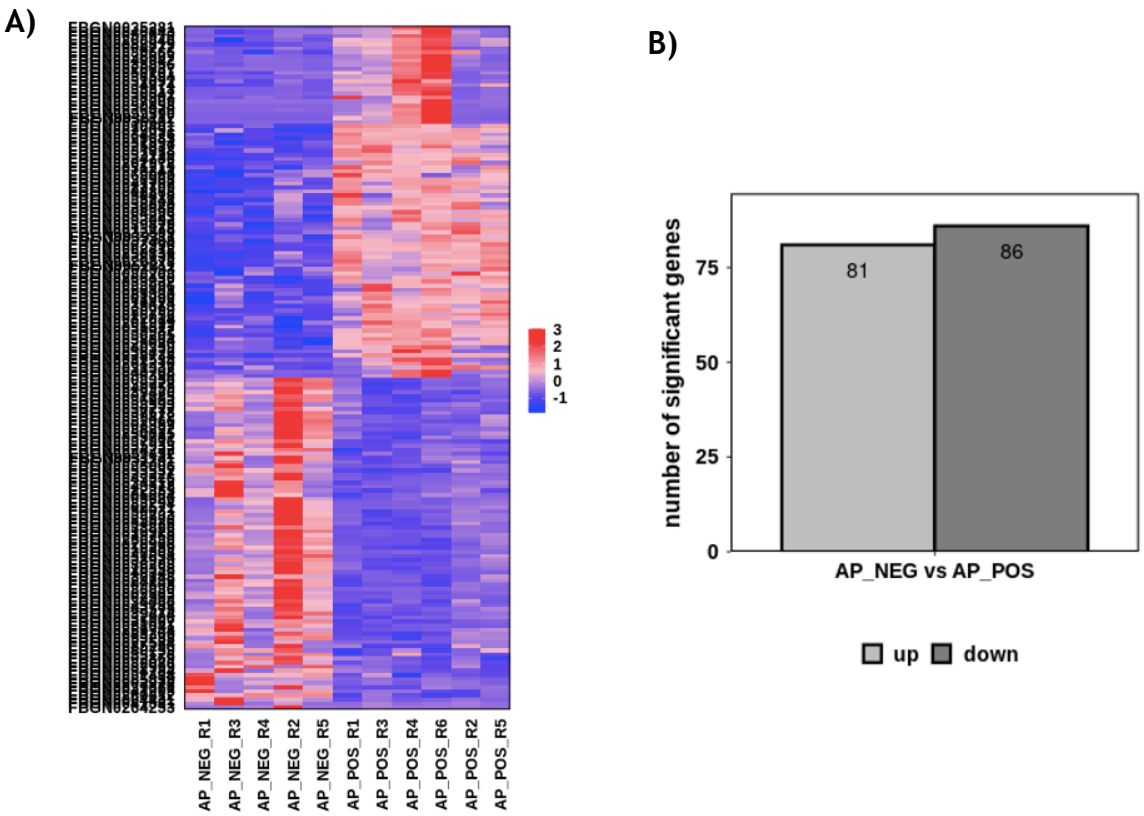

Figure 4.15 Differential gene expression upon *TK* knockdown, in whole flies associated with *A. pomorum*.

A) Hierarchically clustered heatmap of the significantly differentially expressed genes (p.adj < 0.05, absolute log2 fold > 0.5) between Ap neg and Ap pos. Samples are on the x axis and genes on the y axis. Colour intensity represents expression level (row Z-scores), with blue representing low expression, and red representing high expression. Expression levels have been row scaled into z−scores. The y-axis (both plots) and x-axis (right plot) have been hierarchically clustered using, Spearman distances, with UPMGA agglomeration and mean reordering. B) Bar chart showing the number of significantly differentially expressed genes (p.adj < 0.05, absolute log2 fold > 0.5), between ap neg and ap pos.

I further performed gene ontology enrichment by biological process (Figure 4.16A), molecular function (Figure 4.16B) and KEGG pathway enrichment (Figure 4.16C) in the same transcriptomes of *A. pomorum* flies $TK^{RNAi+/-}$, based on differentially expressed genes. The results indicate that those genes are involved in processes related to immune system regulation and defence responses to bacteria, but also sugar and lipid metabolism (Figure 4.16A). Moreover, the functions of those genes are predominantly in peptidoglycan

binding and biosynthesis or catabolising enzymatic activities (Figure 4.16B). Lastly, the KEGG pathway enrichment demonstrates that the gene products of this dataset are involved in Toll and Imd signalling, neuroactive ligand-receptor interaction and galactose metabolism (Figure 4.16C).

A)

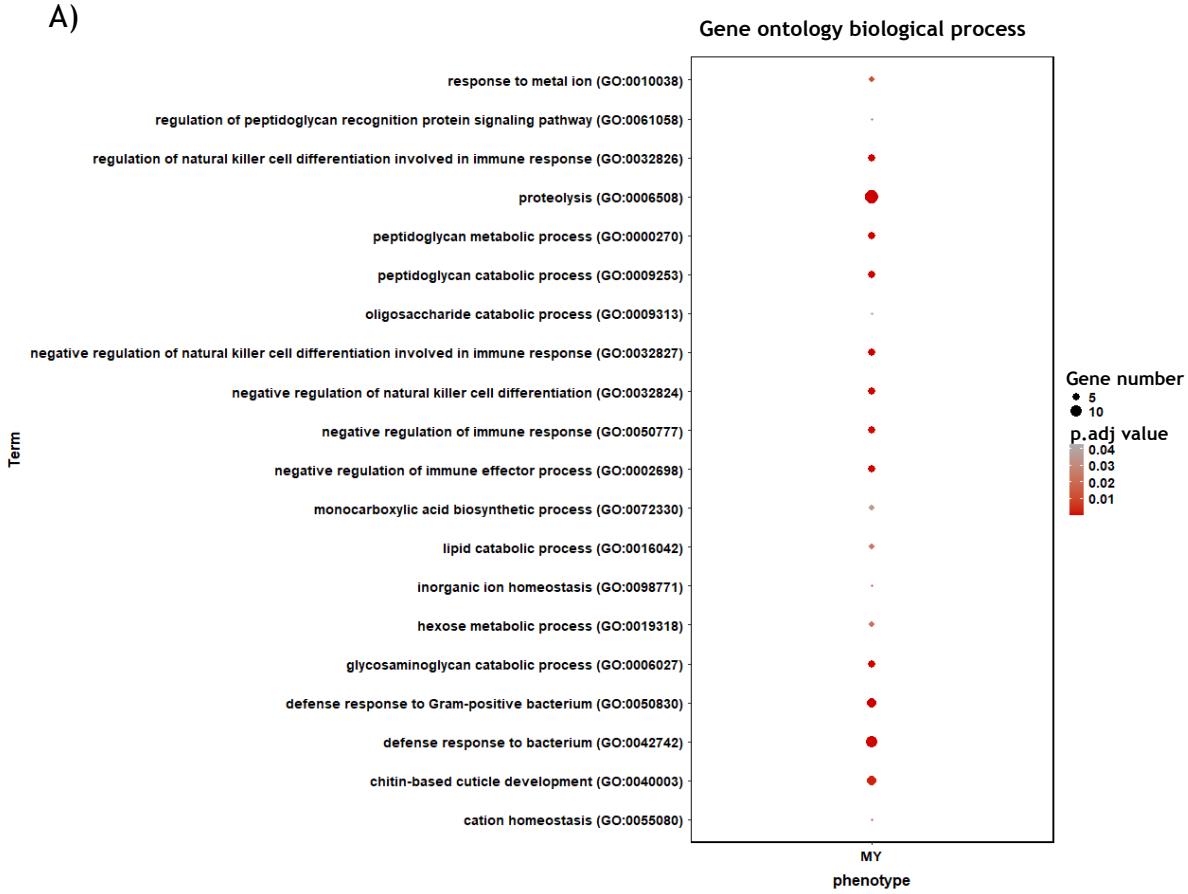

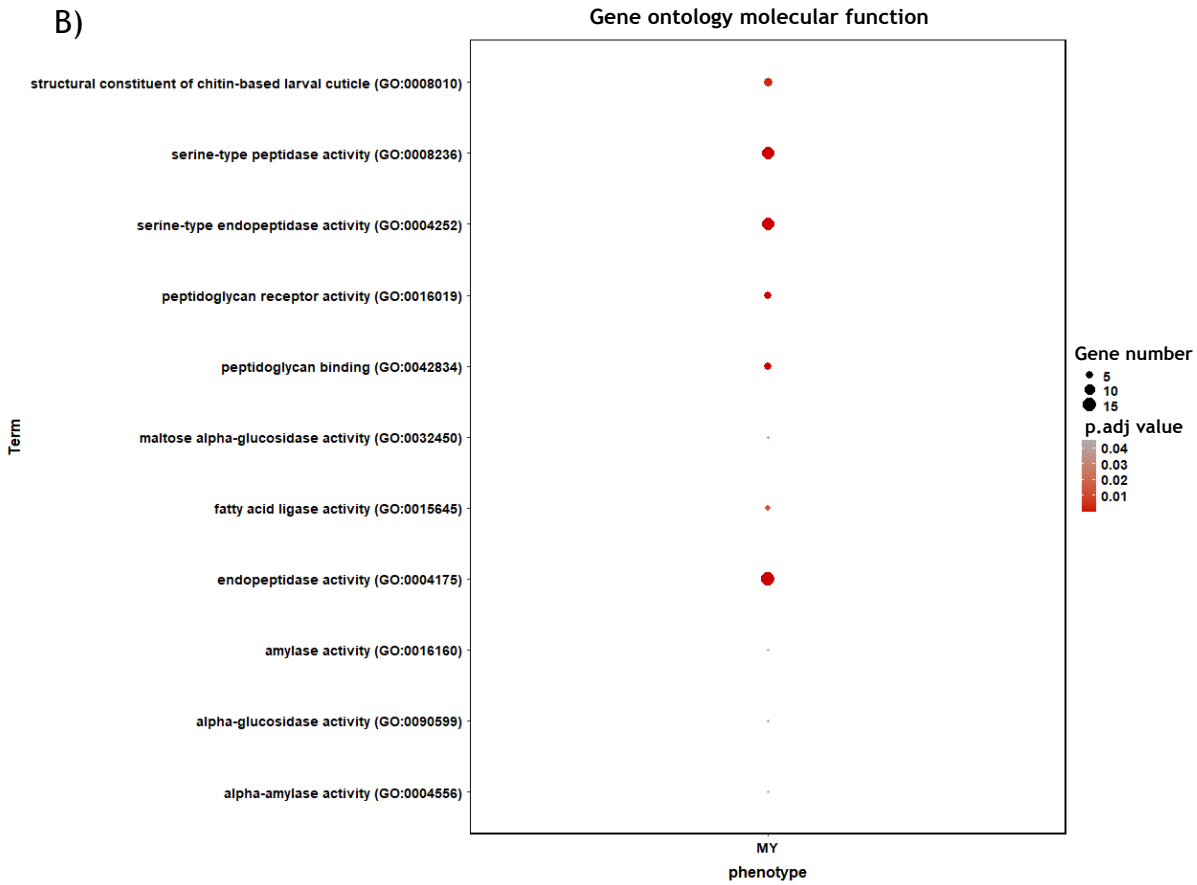

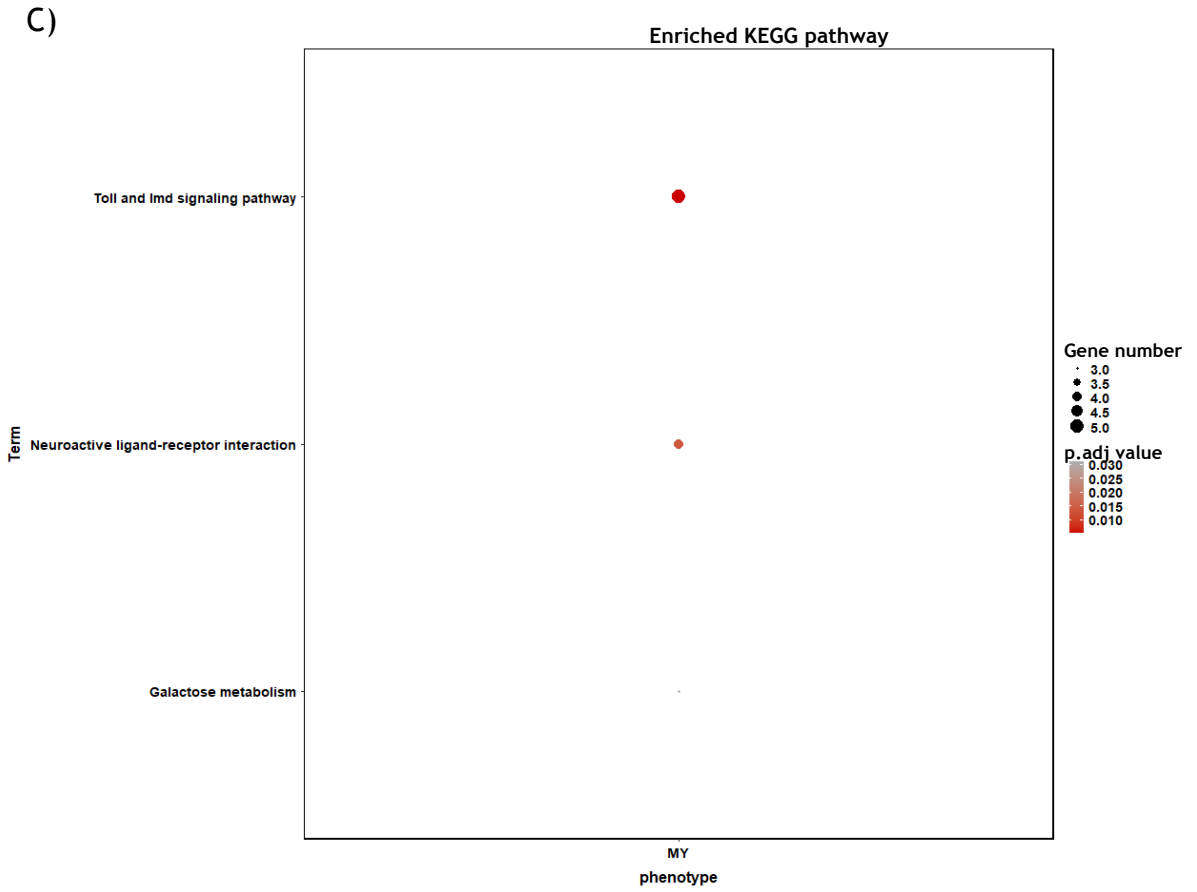

Figure 4.16 Enrichment analysis comparing the effect of *TK* knockdown in *A. pomorum* mono-colonised flies.

A) Gene ontology enrichment by biological process, B) gene ontology enrichment by molecular function and C) KEGG pathway enrichment in the transcriptomes of gnotobiotic female flies colonised with *Acetobacter pomorum* comparing control vs *TK* knockdown flies, based on differentially expressed genes with p.adj < 0.05, absolute log2 fold > 0.5.

Considering that one of the biggest findings in the enrichment analysis was Imd pathway and responses to bacteria and that Imd signalling was previously shown to be activated in *TK*+ EE cells by acetate, I decided to look at the differentially expressed genes involved in bacterial immune response (Figure 4.17). The results indicate that different components of the Imd signalling pathway, from antimicrobial peptides (attacin b, listericin, lysozyme x) to PGRP receptors, become downregulated when *TK* is knocked down in *Ap* colonised flies. Overall, this suggests that in the presence of *Ap*, *TK* upregulates the Imd signalling pathway.

Due to the fact ligand receptor signalling appeared in the KEGG analysis, I investigated whether other endocrine factors could compensate for the lack of *TK* in the knockdown (Figure 4.18). I identified a few candidate endocrine factors that were upregulated when *TK* was knocked down*: SIFamide receptor,* which is known to reduce reproductive behaviours and extend lifespan (Paik et al., 2012; Park et al., 2014); *7B2*, which acts as a molecular chaperone for the neuroendocrine convertase amon (Hwang et al., 2000); *Juvenile hormone binding protein*, which is involved in egg maturation and reproduction (Bilen et al., 2013); and *NPF receptor,* which responds to the neuropeptide *NPF,* which I showed to be downregulated by the presence of microbiota in chapter 3. Moreover, it is well established that that ageing is associated with increased proteotoxicity. Heat shock proteins were shown to counteract this proteotoxic effect and thus promote longevity (Murshid et al., 2013; Tower, 2011). My results show that heat shock proteins are upregulated in *TK* knockdown flies compared to control flies, which could explain the increased lifespan phenotype (Figure 4.19).

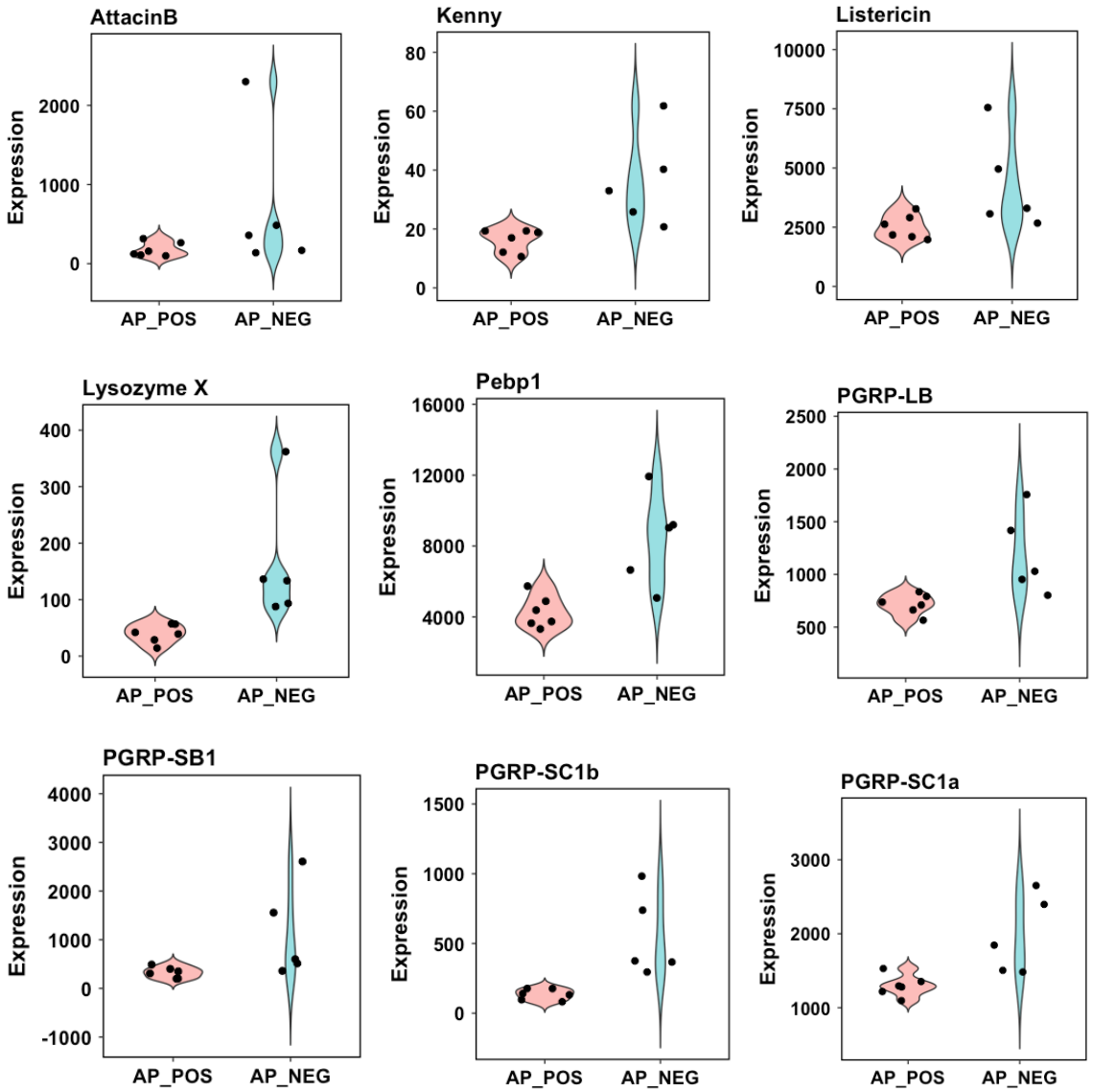

Figure 4.17 *TK* knockdown decreases the expression of genes involved in bacterial immune response in *A. pomorum*-colonised flies.

Violin and jitter plot of the differentially expressed genes involved in bacterial immune response (p.adj < 0.05, absolute log2 fold > 0.5) between control (AP_NEG) vs *TK* knockdown flies (AP_POS) colonised with *Acetobacter pomorum*. Each dot is one sample, with sample groups given on the x-axis and gene expression on the y-axis.

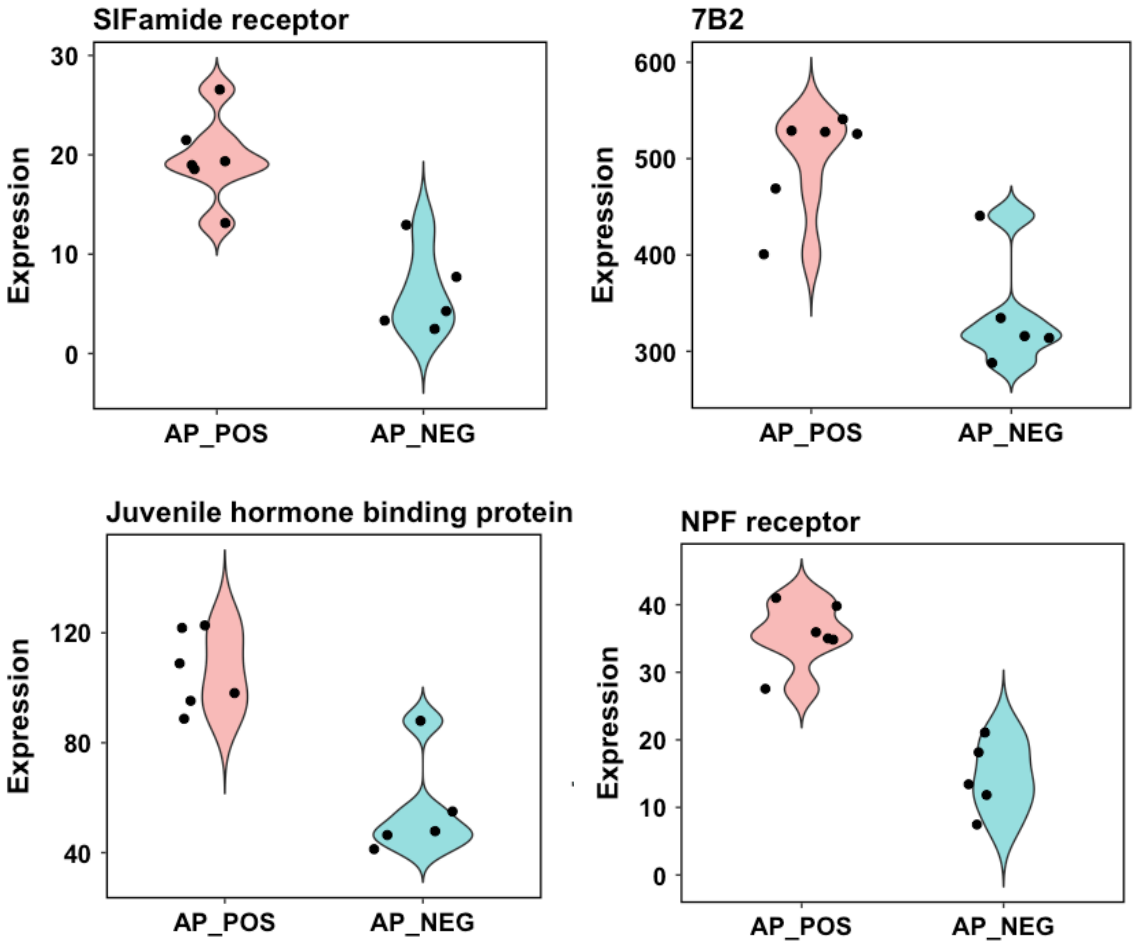

Figure 4.18 *TK* knockdown in *A. pomorum*-colonised flies increases the expression of genes involved in endocrine signalling.

Violin and jitter plot of the differentially expressed genes encoding endocrine factors (p.adj < 0.05, absolute log2 fold > 0.5) between control (AP_NEG) vs *TK* knockdown flies (AP_POS) colonised with *Acetobacter pomorum*. Each dot is one sample, with sample groups given on the x-axis and gene expression on the y-axis.

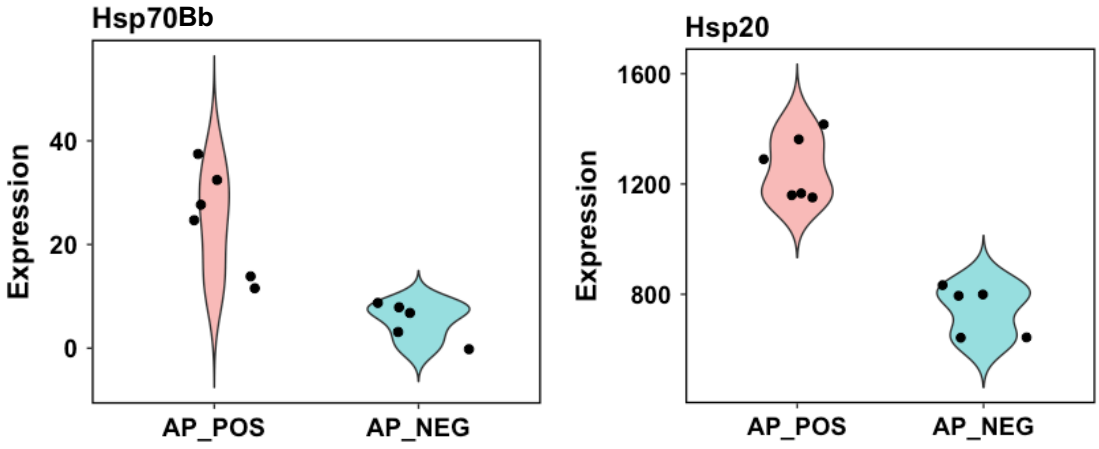

Figure 4.19 *TK* knockdown in *A. pomorum*-colonised flies increases the expression of genes encoding heat shock proteins.

Violin and jitter plot of the differentially expressed genes encoding heat shock proteins (p.adj < 0.05, absolute log2 fold > 0.5) between control (AP_NEG) vs *TK* knockdown flies (AP_POS) colonised with *A. pomorum*. Each dot is one sample, with sample groups given on the x-axis and gene expression on the y-axis.

4.4.6.2.2 Differential expression in *TK* knockdown flies colonised with *L. brevis*

The next comparison is between *TK* knockdown (pos) and control (neg) flies colonised with *Lactobacillus brevis*. I performed the same sequence of analysis as presented above. The PCA (Figure 4.20) and correlation analysis (Figure 4.20) show that there is little difference in the expression pattern of the two sample groups. Furthermore, the volcano plot shows that there are more genes that have a negative log2 fold change, meaning more genes significantly upregulated when *TK* is knocked down. This can also be clearly observed in figure 4.23B showing that in the control group (Lb neg) there are only 14 genes upregulated and 54 downregulated. Furthermore, the heatmap in figure 4.15A demonstrates the consistency of differentially expressed genes in each sample.

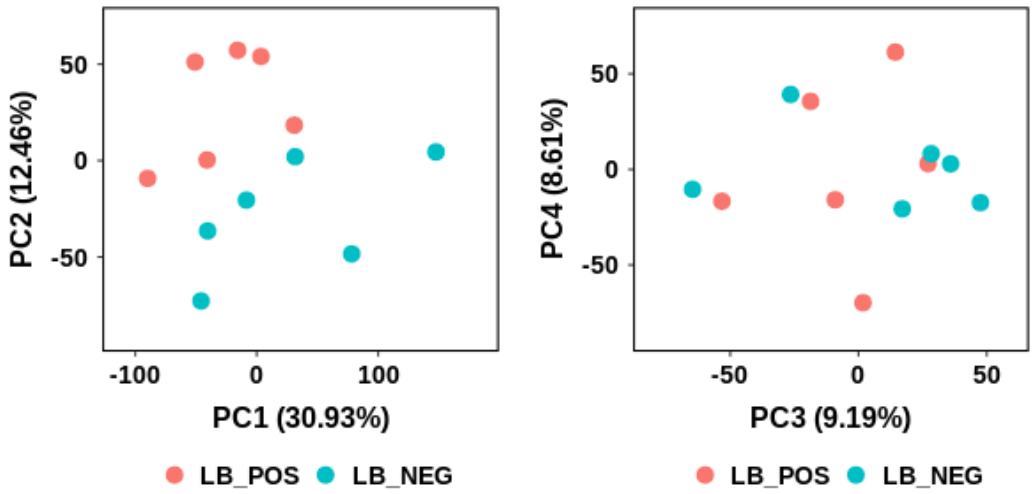

Figure 4.20 Principal Component Analysis (PCA).

Scatterplots show PC1 vs PC2 (left) and PC3 vs PC4 (right). Individual samples are represented by dots. The percentage of total variation explained by each component is given in the x and y-axis as appropriate. To control over representation of very highly expressed genes, all gene expression values were scaled on a gene by gene basis using the z-score transformation, prior to the PCA.

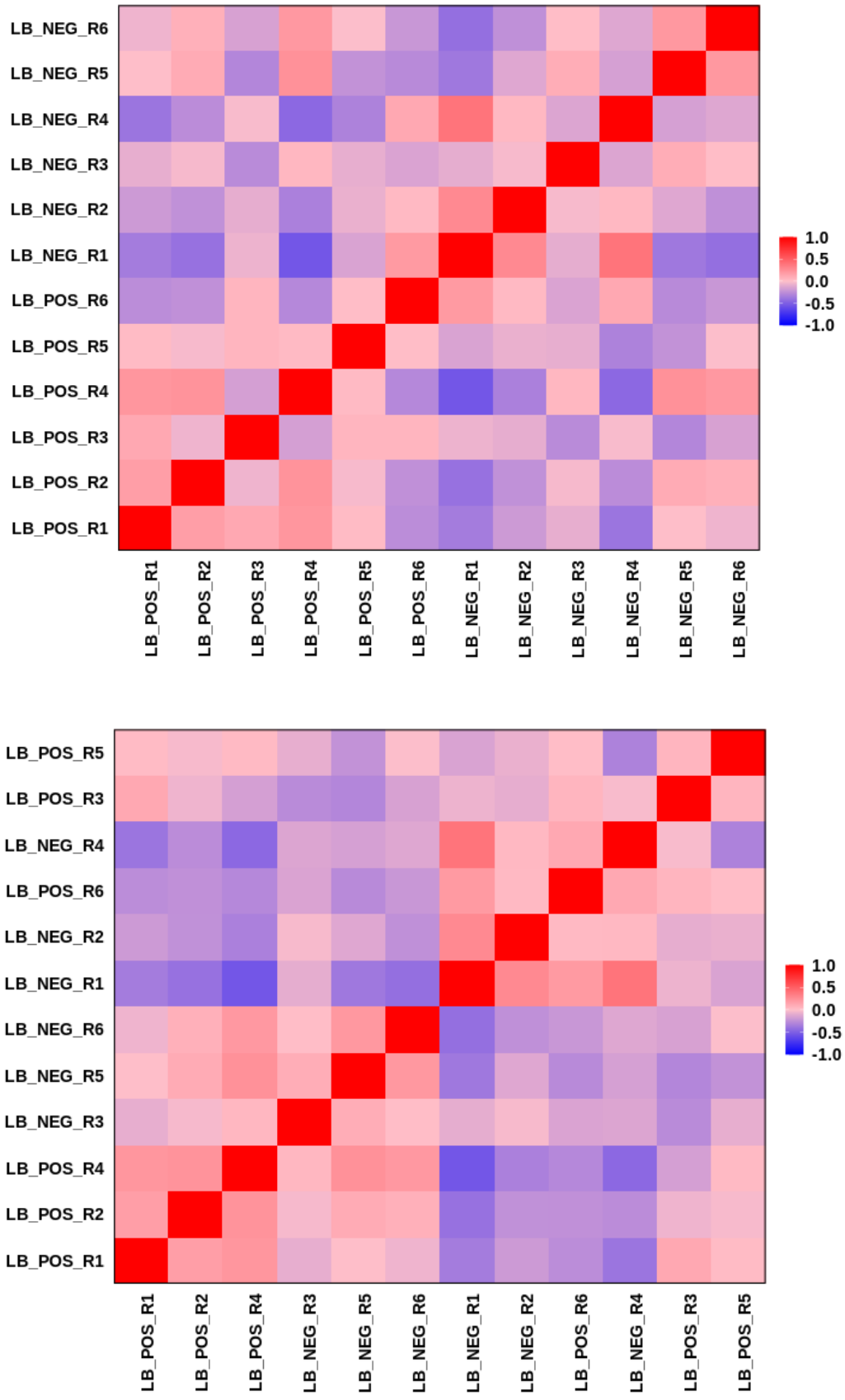

Figure 4.21 Heatmap of sample correlation.

Correlations between each pairwise combination of samples is shown. The correlations were calculated using Spearman Correlation based on all gene expression values. The level of correlation (Spearman Correlation Coefficient) is represented by colour intensity, with strong positive correlation in red, no correlation in light pink and strong anti-correlation in blue. The right had plot has been hierarchically clustered on both axis using, Spearman distances, with UPMGA agglomeration and mean reordering.

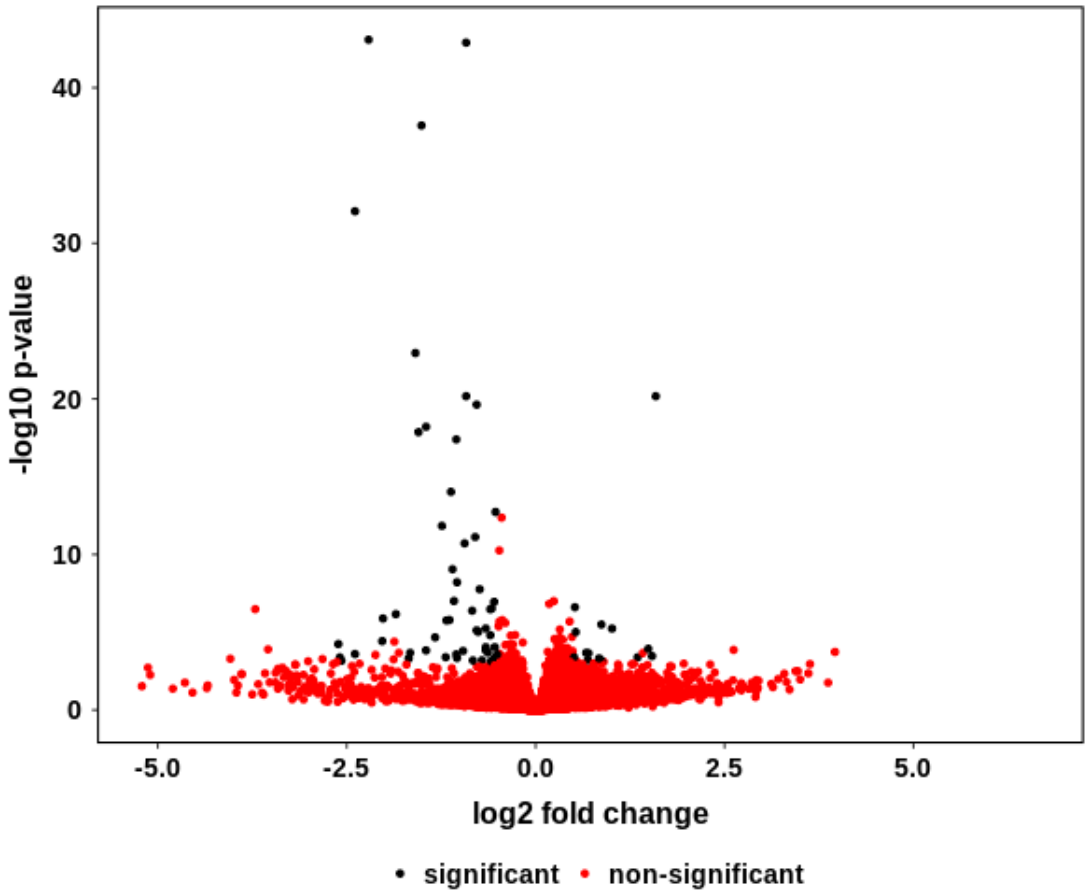

Figure 4.22 Volcano plot comparing the effect of *TK* knockdown in *L. brevis* mono-colonised flies.

Significantly differentially expressed genes (p.adj < 0.05, absolute log2 fold > 0.5) are shown in red and non−significant genes in black. A positive fold change indicates higher expression in lb neg than in lb pos.

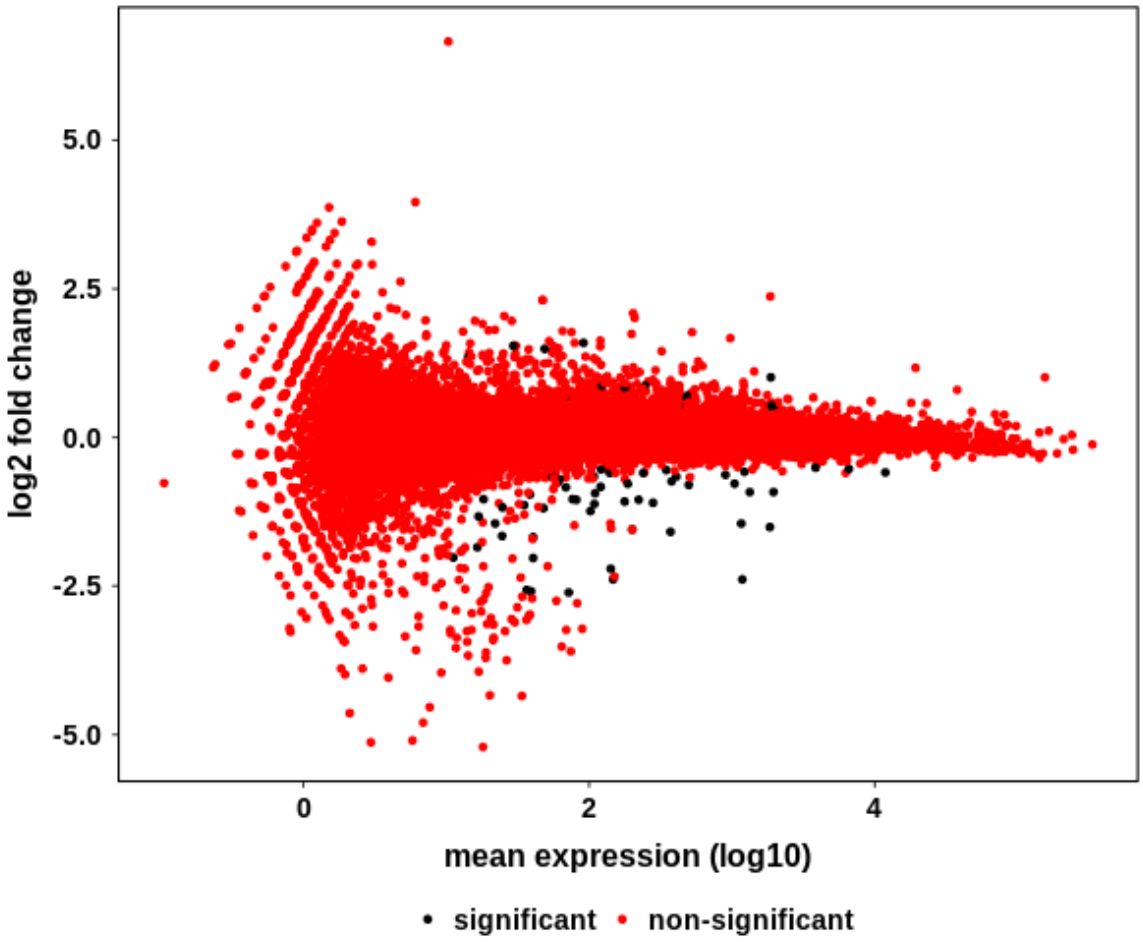

Figure 4.23 MA plot comparing the effect of *TK* knockdown in *L. brevis* mono-colonised flies.

Significantly differential genes (p.adj < 0.05, absolute log2 fold > 0.5) are shown in red and non−significant genes in black. A positive fold change indicates higher expression in lb neg than in lb pos.

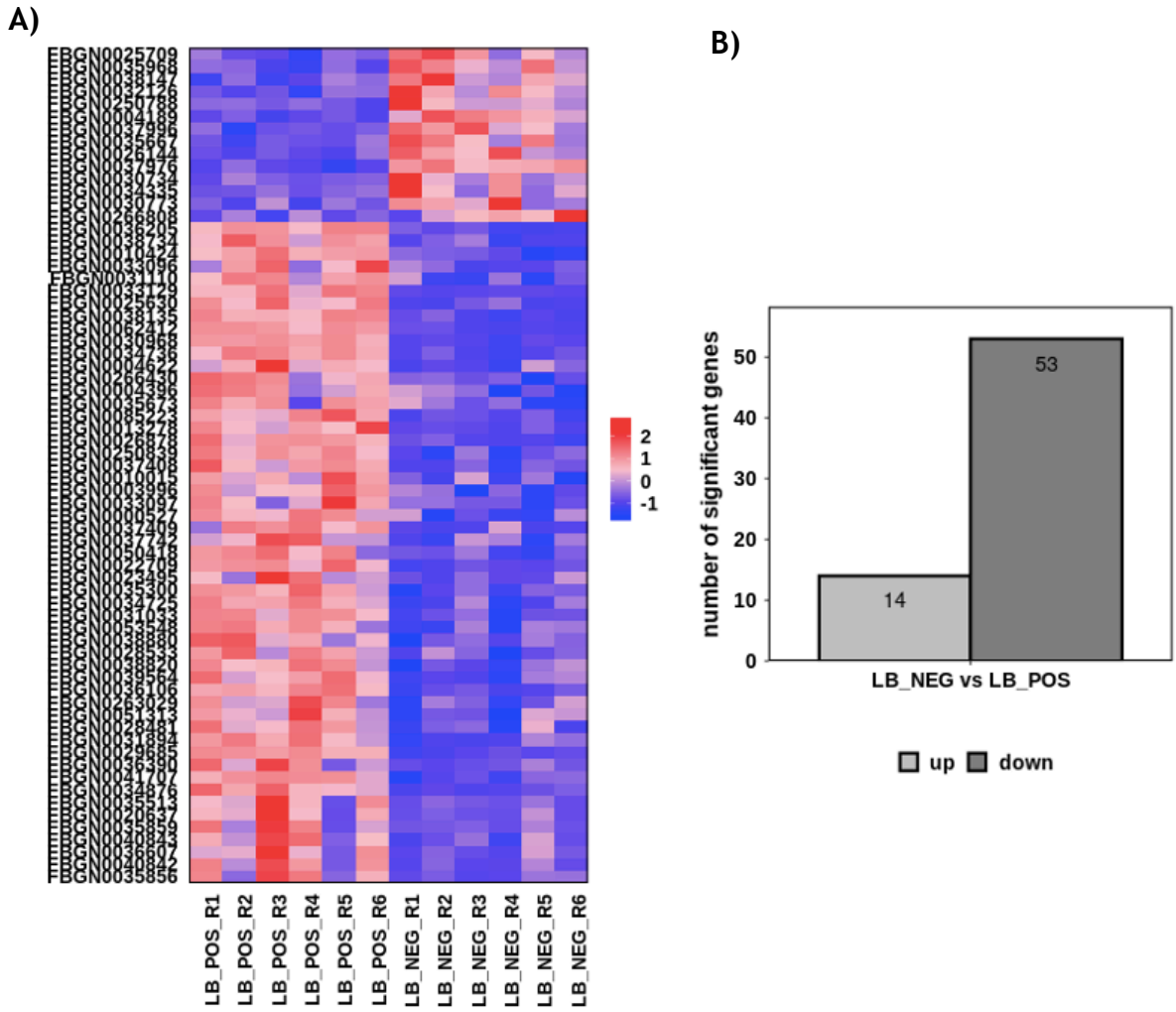

Figure 4.24 Genes that are differentially expressed following *TK* suppression in flies that are colonised with *L. brevis*.

A) Hierarchically clustered heatmap of the significantly differentially expressed genes (p.adj < 0.05, absolute log2 fold > 0.5) between lb neg and lb pos. Samples are on the x axis and genes on the y axis. Colour intensity represents expression level, with blue representing low expression, and red representing high expression. Expression levels have been row scaled into z−scores. The y-axis (both plots) and x-axis (right plot) have been hierarchically clustered using, Spearman distances, with UPMGA agglomeration and mean reordering. B) Bar chart showing the number of significantly differentially expressed genes (p.adj < 0.05, absolute log2 fold > 0.5), between lb neg and lb pos. Upregulated genes are higher in lb neg than in lb pos.

Gene ontology enrichment by biological process (Figure 4.24A) and molecular function (Figure 4.24B) was then performed on genes that were differentially expressed in *L. brevis*-associated flies in presence or absence of TK^{RNAi}. The findings revealed that those genes were involved in processes related to

neuropeptide signalling and lipid and fatty acid metabolism (Figure 4.24A). Accordingly, these genes primarily play roles in neuropeptide receptor and GPCR activity, as well as in fatty acid synthesis (Figure 4.24B). Given that one of the most significant discoveries in the enrichment analysis is neuropeptide signalling, I looked at the differentially expressed genes encoding endocrine factors (Figure 4.25). Similar to the results from gnotobiotic flies colonised with *A. pomorum*, in the presence of *L. brevis*, when *TK* is knocked down *NPF receptor*, *Juvenile hormone binding protein*, *SIFamide receptor* and *7B2* were upregulated. Additionally, one of the *TK* receptors, *TKR99D*, was upregulated when *TK* was depleted, suggesting that compensatory mechanisms to counteract the knockdown effect. Another interesting finding was that the expression of the peptide *CCHamide-2* was downregulated when *TK* levels were reduced. *CCHamide*-2 is an orexigenic neuropeptide that induces appetite and stimulates food intake, controlling growth by directly regulating the production and release of insulin-like peptides(Ren et al., 2015). Furthermore, the heat shock protein *Hsp70Bb* was again upregulated in *TK* knockdown flies colonised with *Lb*, similar to the *Ap* results.

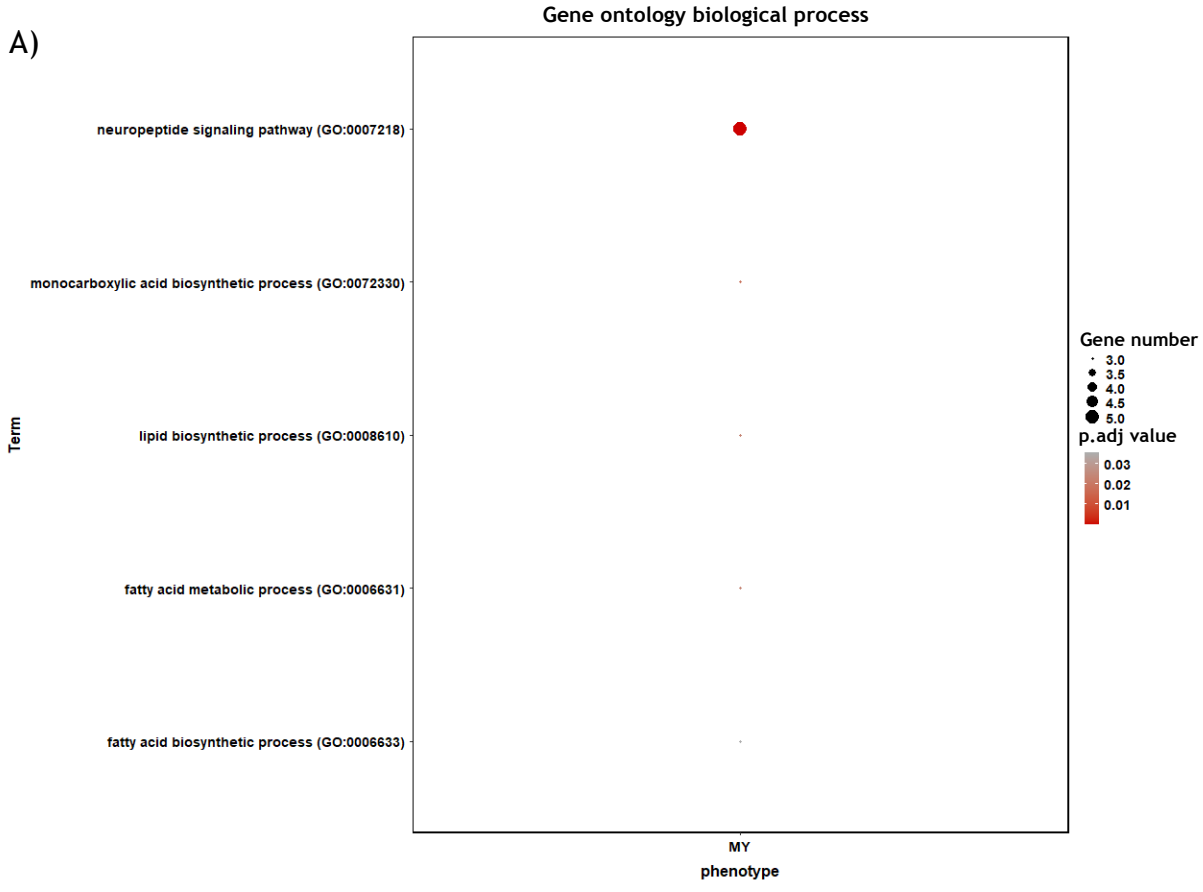

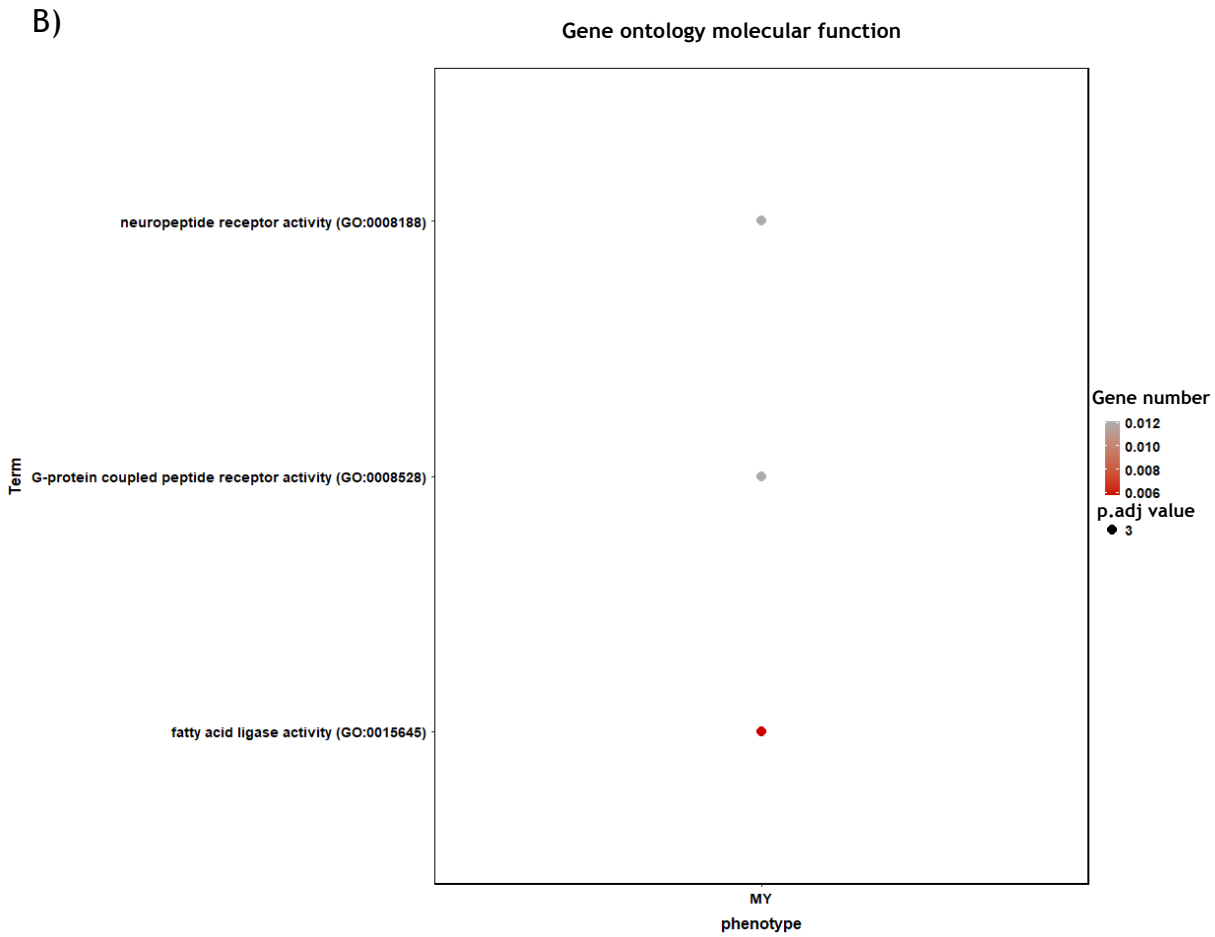

Figure 4.25 Enrichment analysis of RNA-seq.

Analysis reveals genes involved in processes related to neuropeptide signalling and lipid and fatty acid metabolism primarily playing roles in neuropeptide receptor and fatty acid synthesis. Gene ontology enrichment by A) biological process and B) molecular function in the transcriptomes of gnotobiotic female flies colonised with *Lactobacillus brevis* comparing control vs *TK* knockdown flies, based on differentially expressed genes with p.adj < 0.05, absolute log2 fold > 0.5.

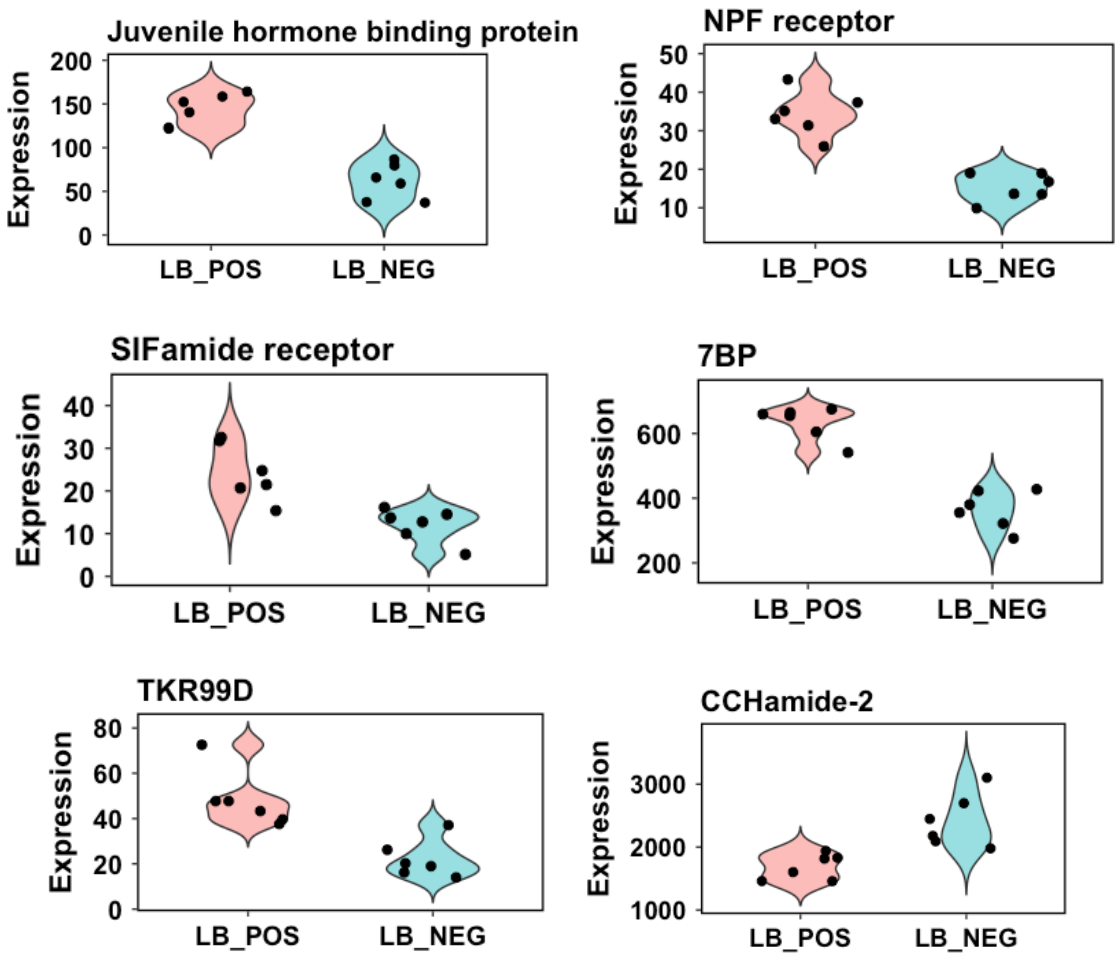

Figure 4.26 *TK* knockdown in *L. brevis*-colonised flies alters the expression of genes involved in endocrine signalling.

Differential expression (p.adj < 0.05, absolute log2 fold > 0.5) between control (LB_NEG) vs *TK* knockdown flies (LB_POS). Each dot is one sample, with sample groups given on the x-axis and gene expression on the y-axis.

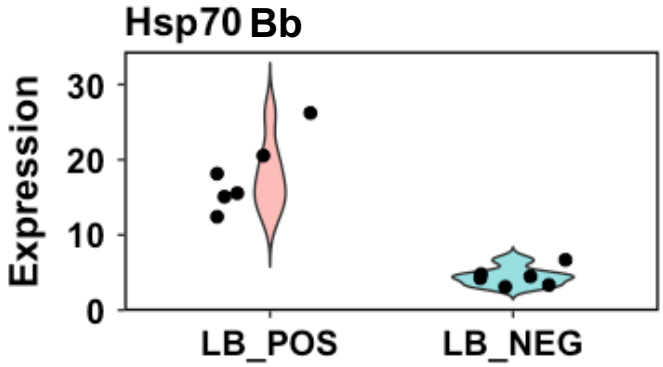

Figure 4.27 *TK* knockdown in *L. brevis*-colonised flies increases the expression of heat shock protein 70 bb (Hsp70 Bb).

Differential expression (p.adj < 0.05, absolute log2 fold > 0.5) between control (LB_NEG) vs *TK* knockdown flies (LB_POS). Each dot is one sample, with sample groups given on the x-axis and gene expression on the y-axis.

4.4.6.2.3 Differential expression in *TK* knockdown axenic flies

Lastly, the third comparison involves flies with *TK* knockdown (designated as "pos") and control flies (referred to as "neg"), in axenic conditions. The PCA analysis illustrates that sample groups separate, demonstrating high global variation in the dataset (Figure 4.28). Accordingly, the correlation heatmaps in figure 4.29 shows that samples within each sample group strongly correlate with each other, indicating different expression patterns between axenic RNAi+ and axenic RNAi-. Following differential expression analysis, the volcano plot (Figure 4.30) showed that the most significant differently expressed genes are upregulated when *TK* is knocked down (Ax pos). An MA plot then confirmed that low expression was not correlated with fewer significant genes (Figure 4.31). Finally, the bar chart of the number of significantly up and downregulated genes clearly demonstrates that there are substantially more differentially expressed genes in the axenic group, compared to Ap or Lb samples, with 1125 upregulated and 1210 downregulated genes when *TK* is depleted.

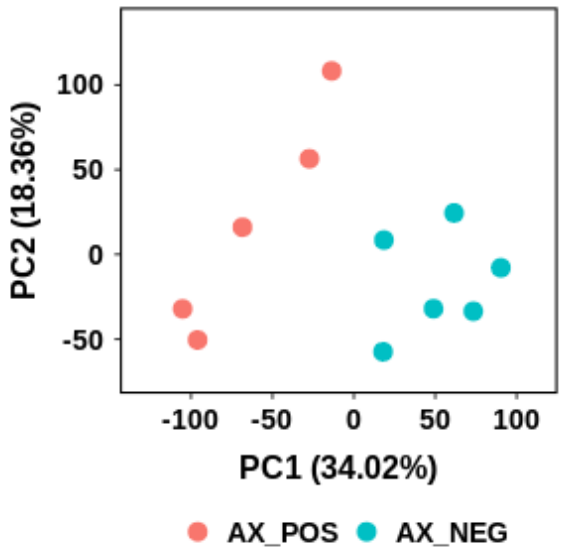

Figure 4.28 Gene expression data Principal Component Analysis (PCA). Scatterplot shows PC1 vs PC2. Individual samples are represented by dots. The percentage of total variation explained by each component is given in the x and

y-axis as appropriate. To control over representation of very highly expressed genes, all gene expression values were scaled on a gene by gene basis using the z-score transformation, prior to the PCA.

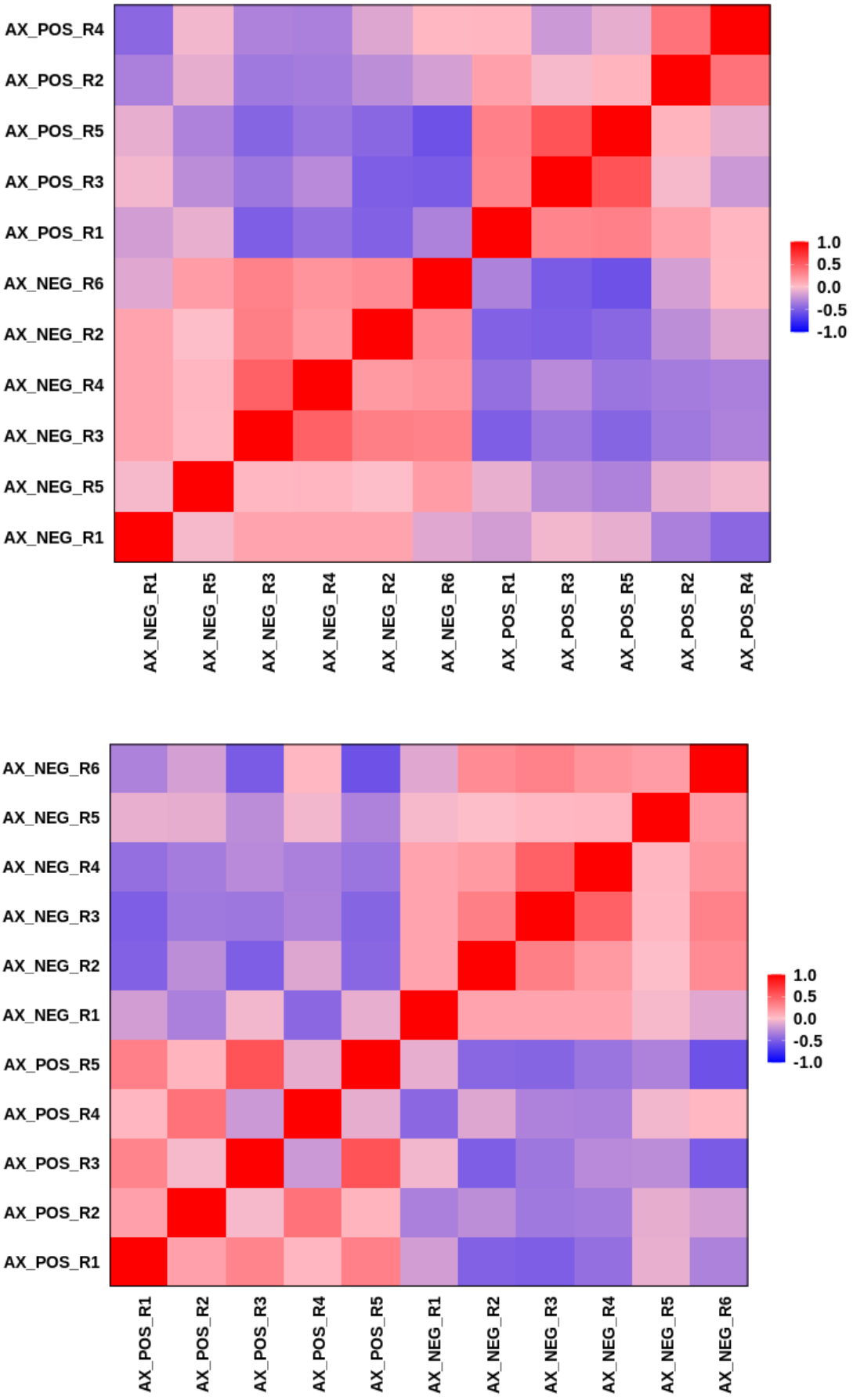

Figure 4.29 Heatmap of sample correlation.

Correlations between each pairwise combination of samples is shown. The correlations were calculated using Spearman Correlation based on all gene expression values. The level of correlation (Spearman Correlation Coefficient) is represented by colour intensity, with strong positive correlation in red, no correlation in light pink and strong anti-correlation in blue. The right had plot has been hierarchically clustered on both axes using, Spearman distances, with UPMGA agglomeration and mean reordering.

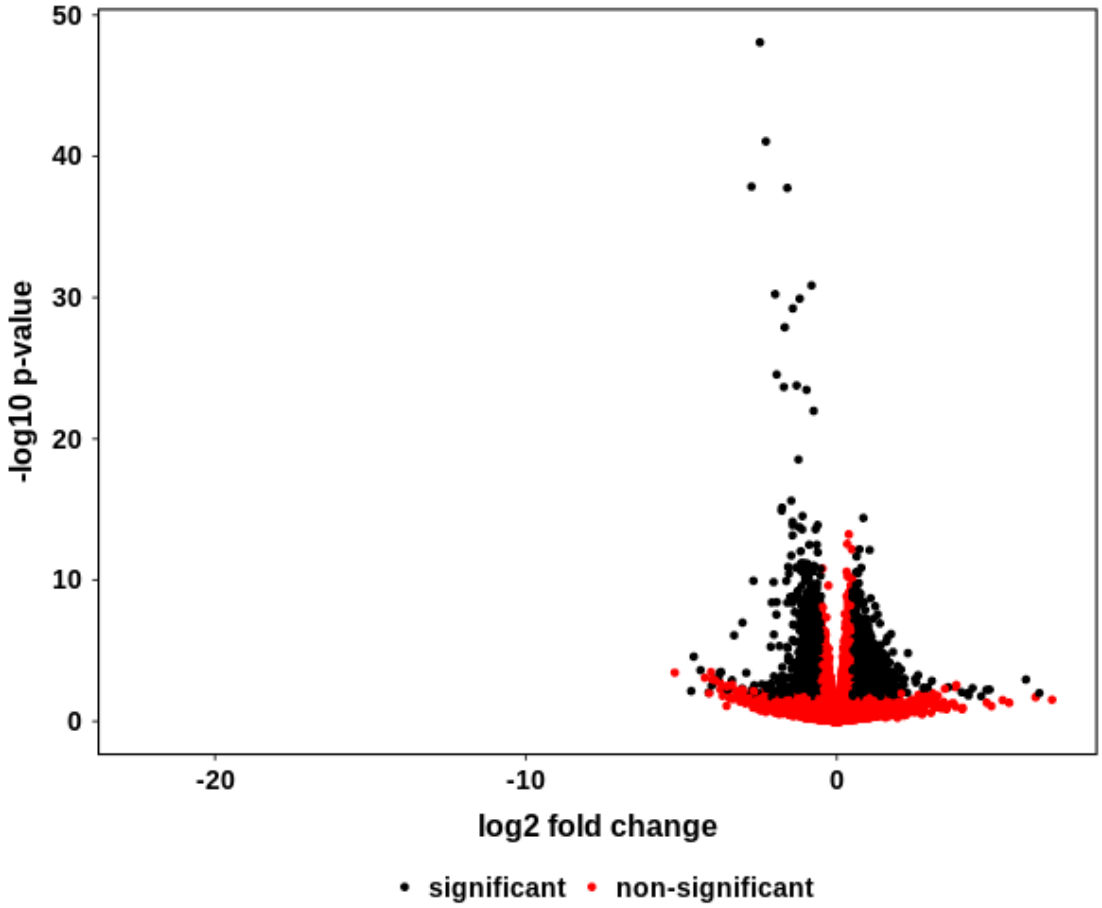

Figure 4.30 Volcano plot comparing the effect of *TK* knockdown in axenic flies.

Significantly differential genes (p.adj < 0.05, absolute log2 fold > 0.5) are shown in black and non−significant genes in red. A positive fold change indicates higher expression in ax neg than in ax pos.

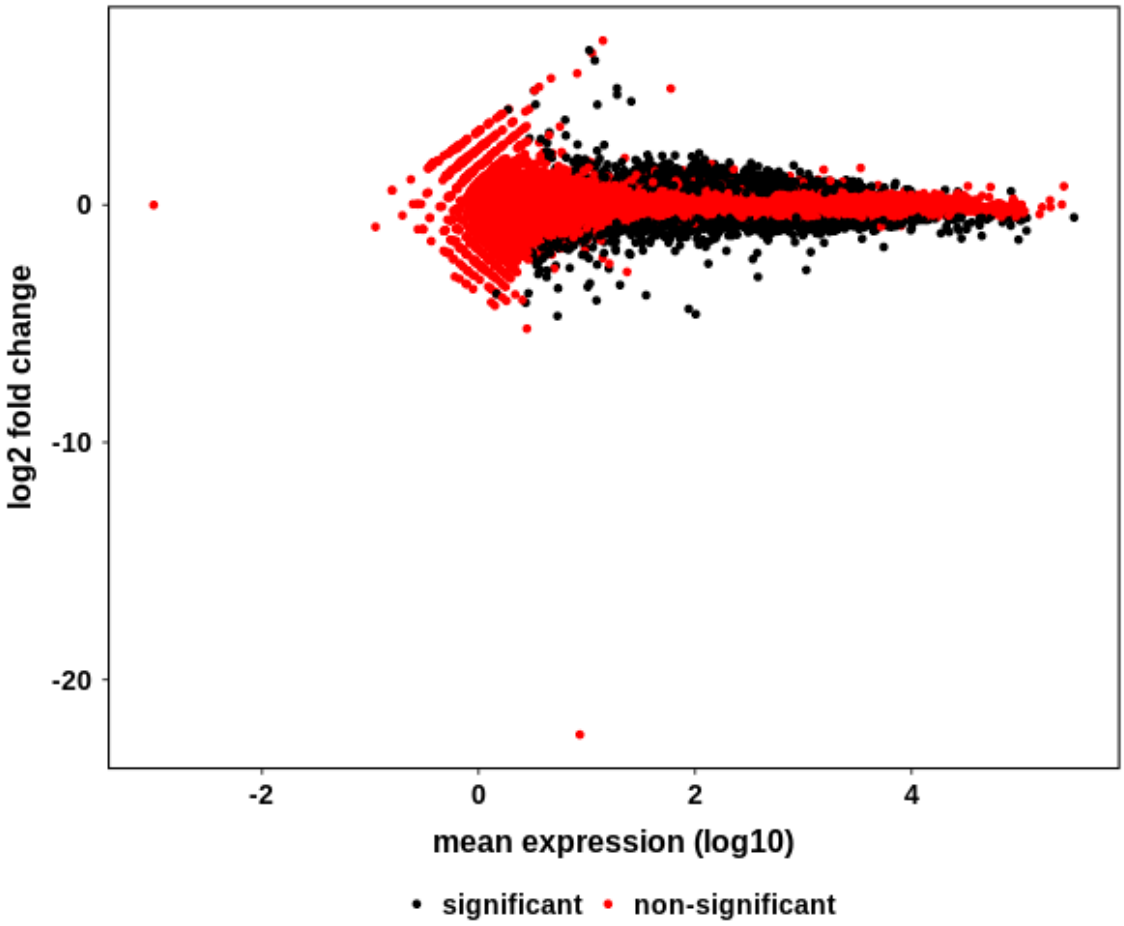

Figure 4.31 MA plot comparing the effect of *TK* knockdown in axenic flies.

Significantly differential genes (p.adj < 0.05, absolute log2 fold > 0.5) are shown in black and non-significant genes in red. A positive fold change indicates higher expression in ax neg than in ax pos.

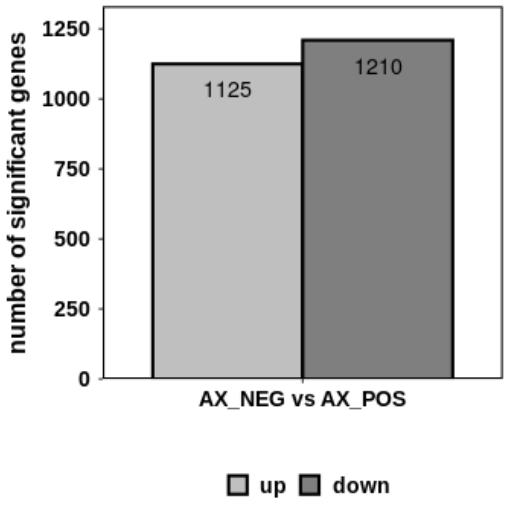

Figure 4.32 The number of significantly differentially expressed genes when *TK* is knocked down in axenic flies.

Upregulated genes are higher in ax neg than in ax pos (p.adj < 0.05, absolute log2 fold > 0.5).

I proceeded to conduct gene ontology enrichment analysis based on biological process (Figure 4.33A), molecular function (Figure 4.33B), cellular composition (Figure 4.33C) and KEGG pathway enrichment (Figure 4.33D) using genes that were differentially expressed after inducing TK^{RNAi} in axenic flies. From the biological process enrichment analysis, it can be observed that the most enriched terms are involved in proteolysis, glucose metabolism, RNA transcription and ATPase activity. In addition, the main functions of those genes are involved in transcription regulation, DNA replication, mitosis, meiosis, telomere maintenance, protein breakdown, processing and maturation, eggshell formation, fat body development and cholesterol transport. As expected, considering that DNA replication and transcription were the biggest findings, the most enriched terms for the cellular components are in the nucleus, chromatin and microtubules. Other cellular enriched parts are the vitelline plasma membrane. Finally, the KEGG pathway enrichment reveals that the gene products of this dataset are mostly involved in neuroactive-ligand interaction, DNA replication and homologous recombination, fat metabolism, lysine degradation and longevity regulating pathways.

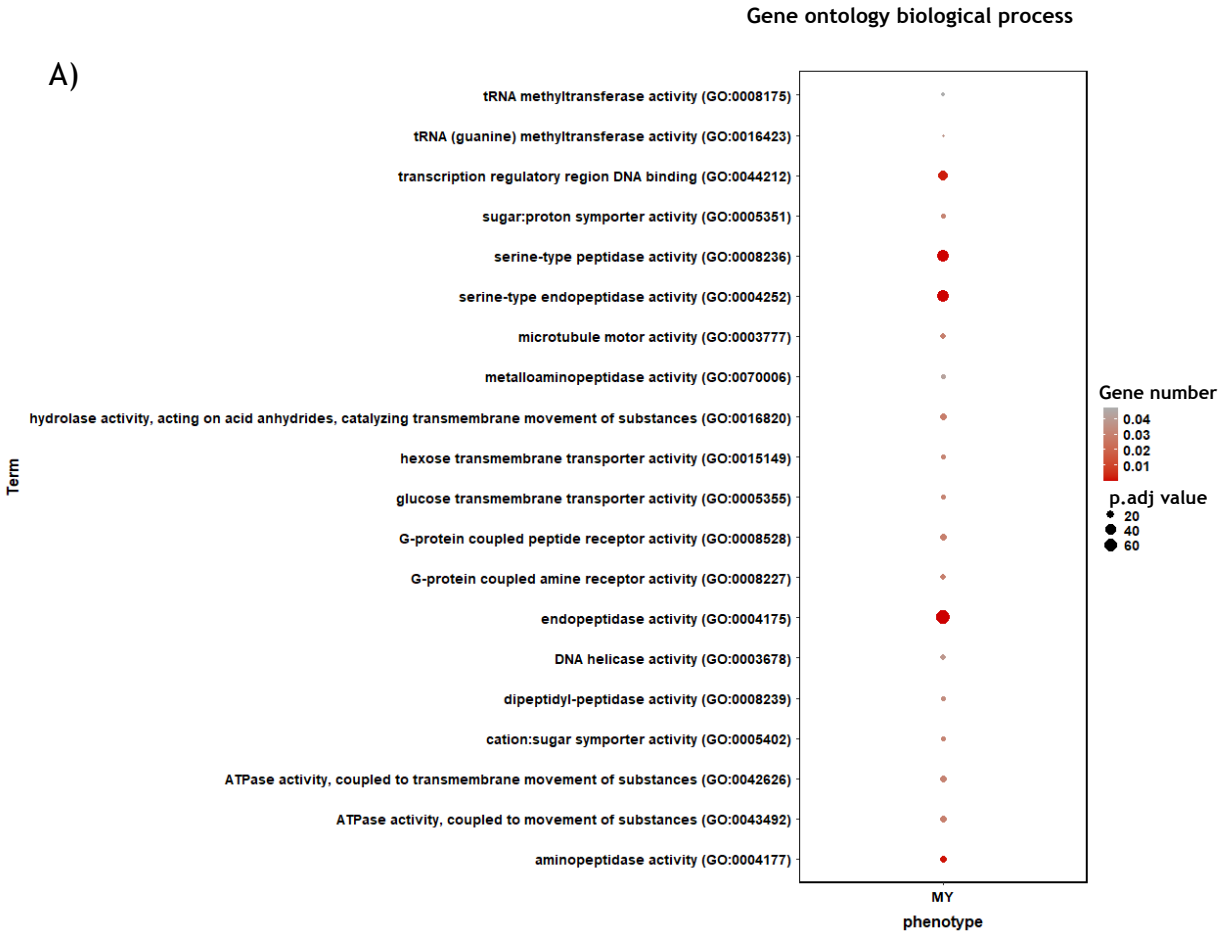
Gene ontology biological process
A)
tRNA methyltransferase activity (GO:0008175)
tRNA (guanine) methyltransferase activity (GO:0016423)
transcription regulatory region DNA binding (GO:0044212)
sugar:proton symporter activity (GO:0005351)
serine-type peptidase activity (GO:0008236)
serine-type endopeptidase activity (GO:0004252)
microtubule motor activity (GO:0003777)
metalloaminopeptidase activity (GO:0070006)
hydrolase activity, acting on acid anhydrides, catalyzing transmembrane movement of substances (GO:0016820)
hexose transmembrane transporter activity (GO:0015149)
glucose transmembrane transporter activity (GO:0005355)
G-protein coupled peptide receptor activity (GO:0008528)
G-protein coupled amine receptor activity (GO:0008227)
endopeptidase activity (GO:0004175)
DNA helicase activity (GO:0003678)
dipeptidyl-peptidase activity (GO:0008239)
cation:sugar symporter activity (GO:0005402)
ATPase activity, coupled to transmembrane movement of substances (GO:0042626)
ATPase activity, coupled to movement of substances (GO:0043492)
aminopeptidase activity (GO:0004177)
Term
MY
phenotype
Gene number
0.04
0.03
0.02
0.01
p.adj value
20
40
60

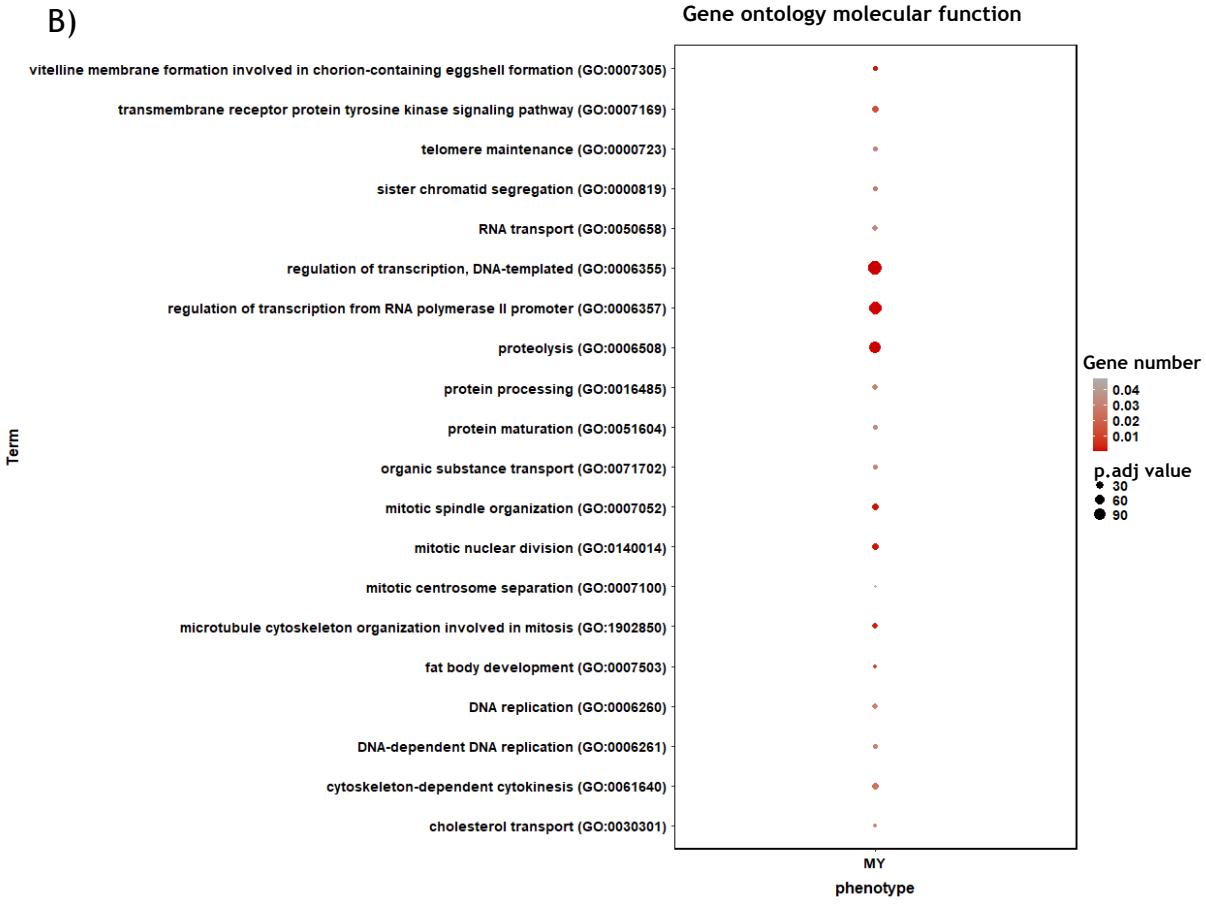
B)
Gene ontology molecular function
vitelline membrane formation involved in chorion-containing eggshell formation (GO:0007305)
transmembrane receptor protein tyrosine kinase signaling pathway (GO:0007169)
telomere maintenance (GO:0000723)
sister chromatid segregation (GO:0000819)
RNA transport (GO:0050658)
regulation of transcription, DNA-templated (GO:0006355)
regulation of transcription from RNA polymerase II promoter (GO:0006357)
proteolysis (GO:0006508)
protein processing (GO:0016485)
protein maturation (GO:0051604)
organic substance transport (GO:0071702)
mitotic spindle organization (GO:0007052)
mitotic nuclear division (GO:0140014)
mitotic centrosome separation (GO:0007100)
microtubule cytoskeleton organization involved in mitosis (GO:1902850)
fat body development (GO:0007503)
DNA replication (GO:0006260)
DNA-dependent DNA replication (GO:0006261)
cytoskeleton-dependent cytokinesis (GO:0061640)
cholesterol transport (GO:0030301)
Term
MY
phenotype
Gene number
0.04
0.03
0.02
0.01
p.adj value
30
60
90

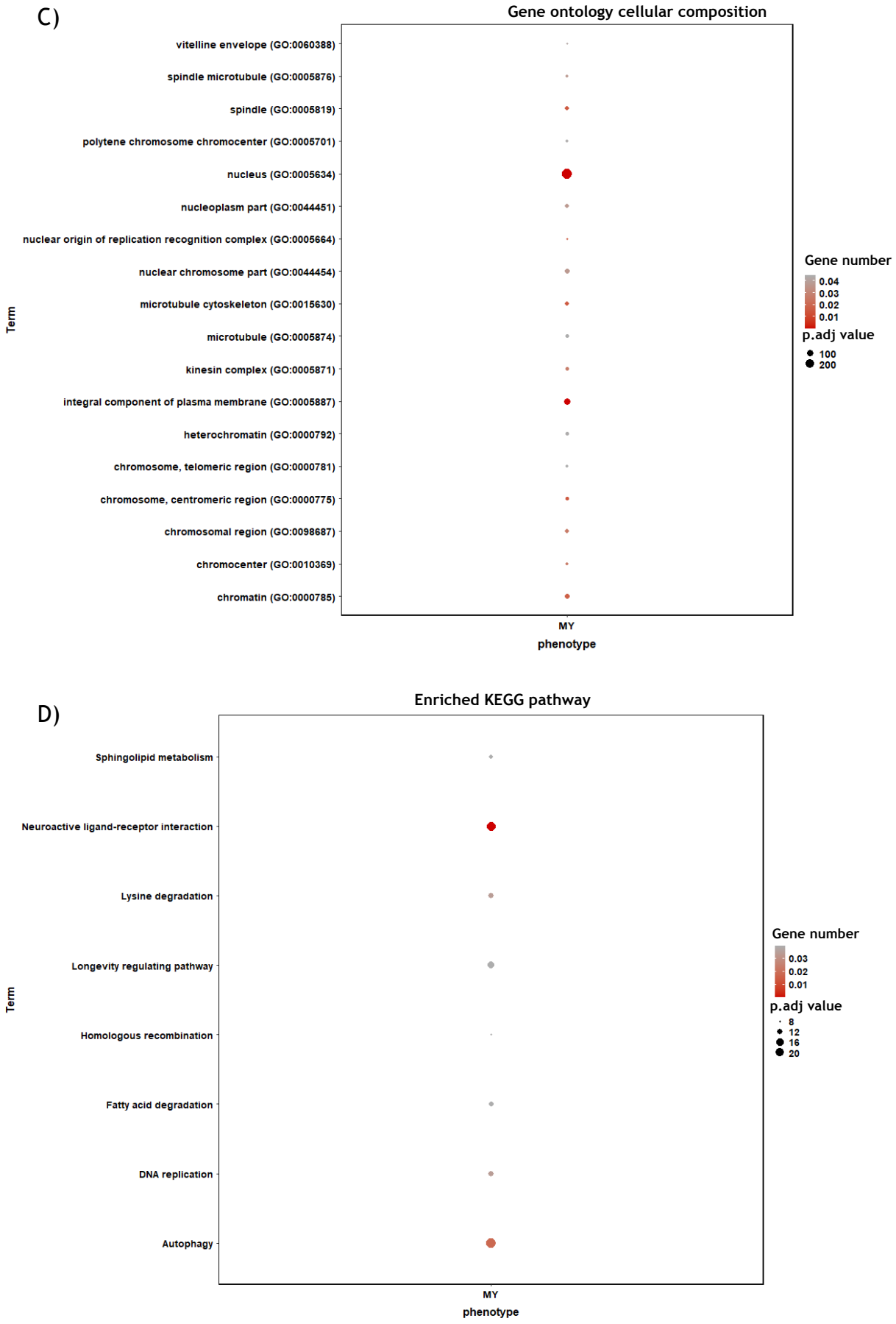

Figure 4.33 Enrichment analysis of RNA-seq data.

A) Gene ontology enrichment by biological process, B) gene ontology enrichment by molecular function, C) gene ontology enrichment by cellular composition and D) KEGG pathway enrichment in the transcriptomes of axenic female flies comparing control vs *TK* knockdown flies, based on differentially expressed genes with p.adj < 0.05, absolute log2 fold > 0.5.

First of all, I looked at which endocrine factors were differentially expressed in *TK* knockdown axenic flies compared to control axenic flies. Interestingly, several neuropeptides and their receptors increased in expression in response to TK^{RNAi+}, including *AstA, AstaA receptor, Burs, Itp, NPF, sNPF, NPF receptor, DH31 receptor, TKR99D, CCHa-1, Capa, Nplp4, SIFamide receptor* and *7B2* (Figure 4.34). Overall, this suggests that *TK* interacts with other signalling molecules and when *TK* is absent other signalling molecules might compensate. Moreover, considering that most of those neuropeptides were not differentially expressed in the presence of *A. pomorum* or *L. brevis*, commensal microbes might affect the compensatory mechanisms. Secondly, when looking at the expression of heat shock proteins, it appeared that *Hsp70Bb* was upregulated again when *TK* is knocked down, consistent with *Ap* and *Lb* results. However, *Hsp70Aa* was downregulated in the presence of TK^{RNAi} (Figure 4.35).

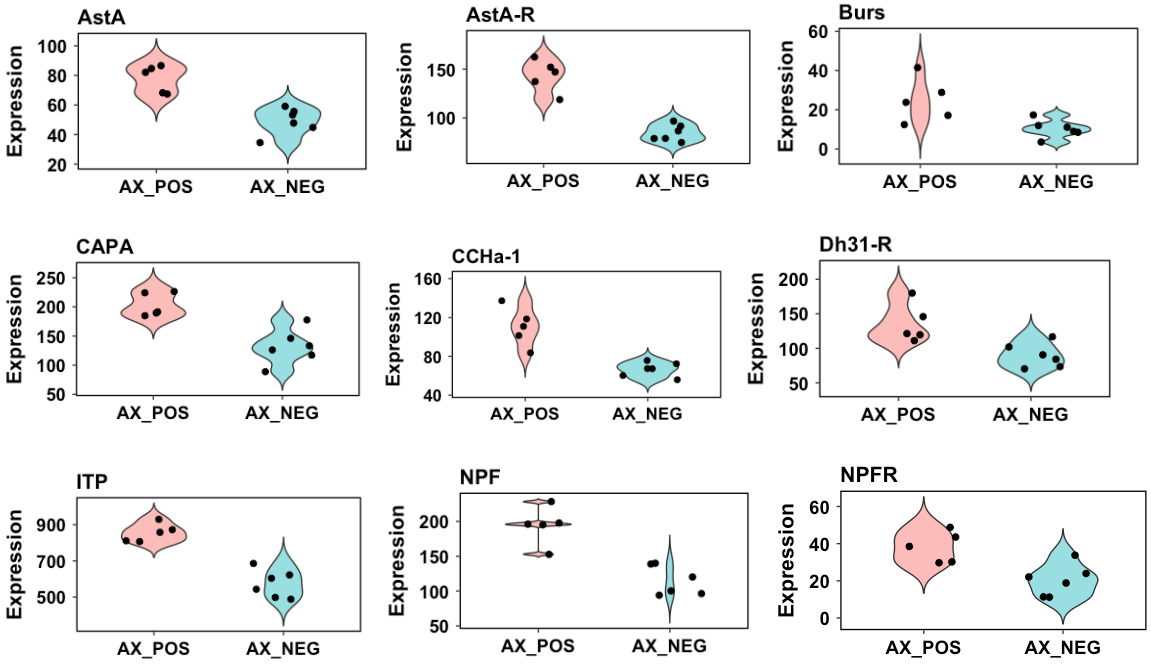

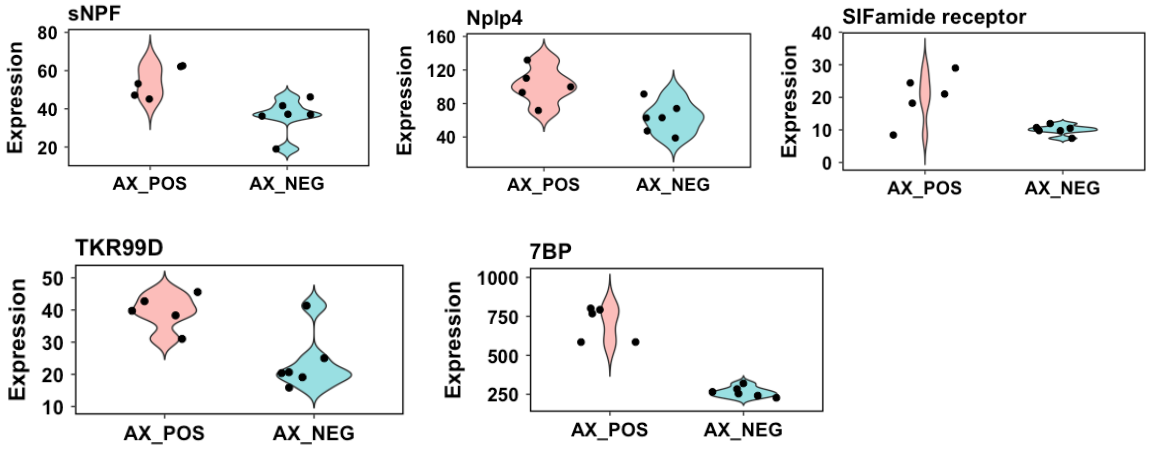

Figure 4.34 *TK* knockdown in axenic flies increases the expression of genes encoding endocrine factors

Differential expression (p.adj < 0.05, absolute log2 fold > 0.5) between control (AX_NEG) vs *TK* knockdown flies (AX_POS). Each dot is one sample, with sample groups given on the x-axis and gene expression on the y-axis.

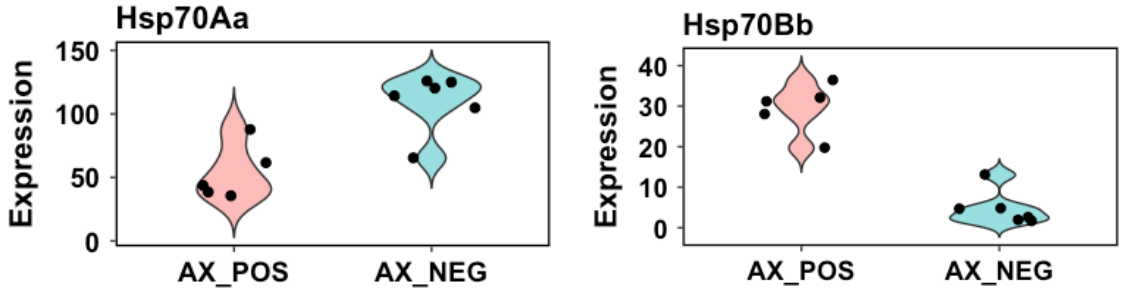

Figure 4.35 *TK* knockdown in axenic flies alters the expression of genes encoding heat shock proteins.

Differential expression (p.adj < 0.05, absolute log2 fold > 0.5) between control (AX_NEG) vs *TK* knockdown flies (AX_POS). Each dot is one sample, with sample groups given on the x-axis and gene expression on the y-axis.

In previous chapters, I showed that the TAG phenotype exhibited a huge metabolic shift in axenic *TK* knockdown flies, specifically with the impact of *TK* knockdown reversed in the absence of microbiota and, *vice versa*, *TK* knockdown reversing the impact of microbiota on TAG. I decided to explore the genes that might contribute to this effect. To address this, I plotted the differentially expressed genes from the enriched KEGG pathways cholesterol transport (Figure 4.36) and fat body development (Figure 4.37). The results reveal that *Neural Lazarillo* is strongly upregulated in the absence of *TK*. *Neuronal Lazarillo (NLaz)* was previously shown to act downstream of JNK to maintain metabolic

homeostasis, by controlling lipid biogenesis and circulating carbohydrate levels (Pasco and Léopold, 2012). Moreover, *NLaz* is known to negatively regulate IIS pathway, whereas *NLaz* mutants present elevated IIS (Hull-Thompson et al., 2009). Other cholesterol related upregulated genes are *Npc1b*, involved in midgut sterol absorption (Voght et al., 2007), and *Npc2e,* known to bind LPS and thus link lipid metabolism with immunity in *Drosophila (Voght et al., 2007).* Conversely, *Scap,* required for the activation of sterol regulatory element binding proteins (SREBPs) (Matthews et al., 2010) and *Start1,* known to regulate ecdysone synthesis (Roth et al., 2004) were downregulated in response to *TK* depletion. Additionally, several genes involved in fat body development, such as *mmp1*, *mmp2*, *six4*, *sparc* and *srp* were upregulated in TK^{RNAi+} axenic flies (Figure 4.36).

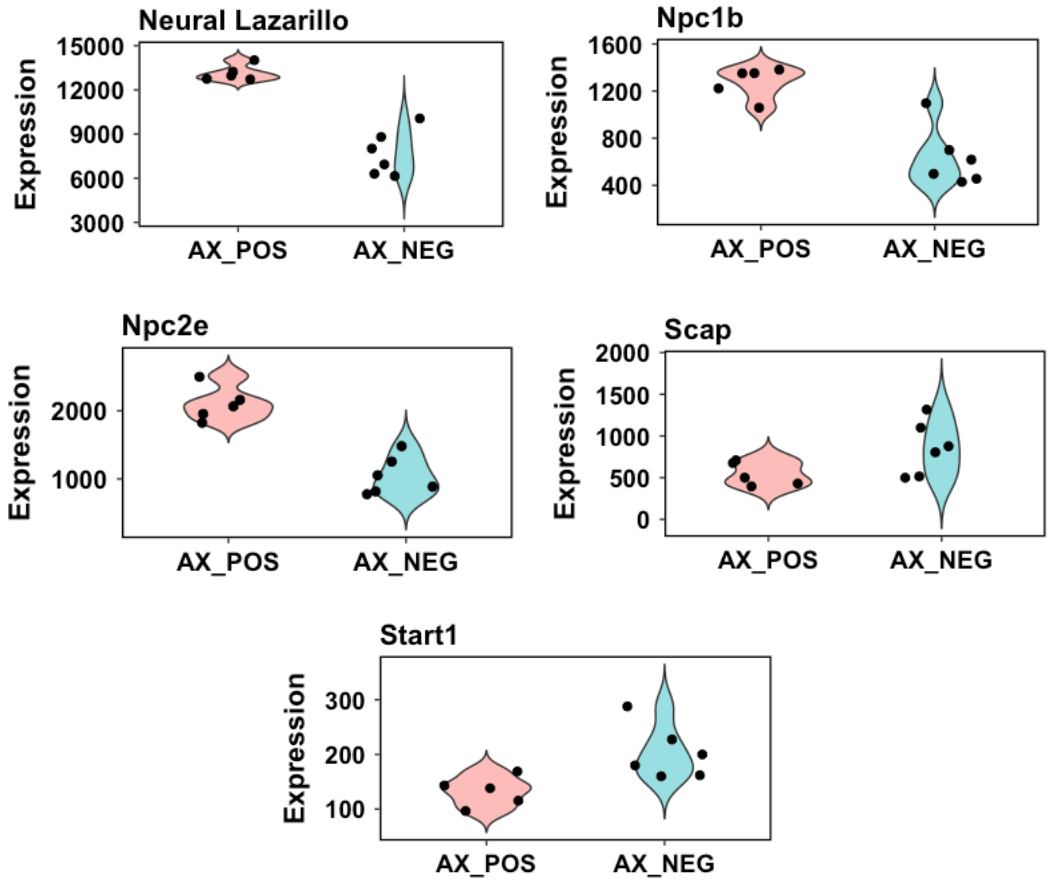

Figure 4.36 Changes in expression of genes involved in cholesterol transport and metabolism upon *TK* knockdown in axenic flies.

Differential expression (p.adj < 0.05, absolute log2 fold > 0.5) between control (AX_NEG) vs *TK* knockdown flies (AX_POS). Each dot is one sample, with sample groups given on the x-axis and gene expression on the y-axis.

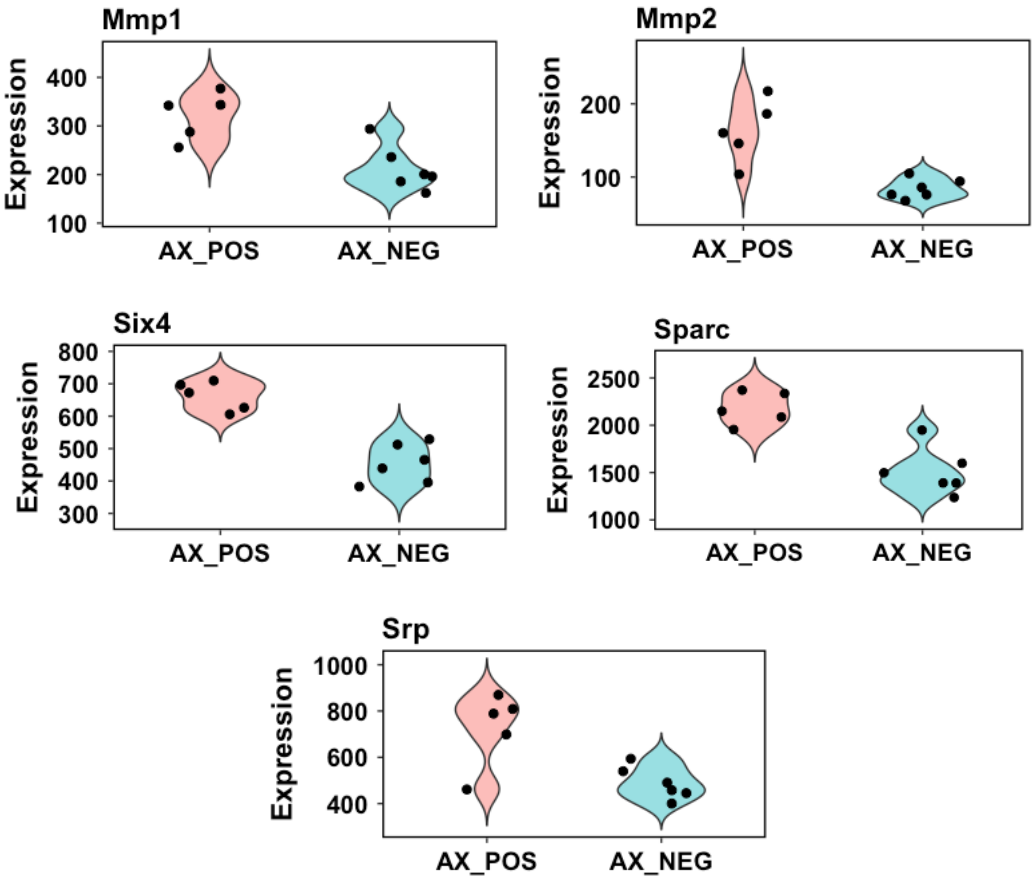

Figure 4.37 *TK* knockdown in axenic flies increases the expression of genes involved in fat body development.

Differential expression (p.adj < 0.05, absolute log2 fold > 0.5) between control (AX_NEG) vs *TK* knockdown flies (AX_POS) in axenic female flies. Each dot is one sample, with sample groups given on the x-axis and gene expression on the y-axis.

Another surprising finding was that autophagy-related genes, including the central regulator of autophagy *TOR*, had reduced expression in *TK* knockdown flies when they are axenic (Figure 4.38). It is well established that *mTOR* is a key component of cellular metabolism and a central regulator of ageing in many organisms (Papadopoli et al., 2019). Not only *mTOR*, but also other genes involved in longevity regulating pathways were differentially expressed in axenic flies when *TK* was knocked down (Figure 4.38). Notably, *PKA-C2*, *CrebA* and *Meng* are upregulated in axenic TK^{RNAi+} which are all members of the (cAMP)/protein kinase A pathway known to regulate stress responses, longevity and memory (Horiuchi et al., 2008; Tong et al., 2007). However, the tumour suppressor *p53* recognised to promote longevity by reducing somatic mutations is downregulated in *TK* knockdown samples (Rodier et al., 2007). In conclusion, *TK*

impacts several regulators of ageing in axenic flies. However, the longevity experiments showed no lifespan extension in axenic flies following *TK* knockdown. Moreover, considering the pattern of differential expression, it is unclear wheatear lack of *TK* negatively or positively impacts longevity regulating pathways. Overall, it appears that there is a balance of both negative and positive effects.

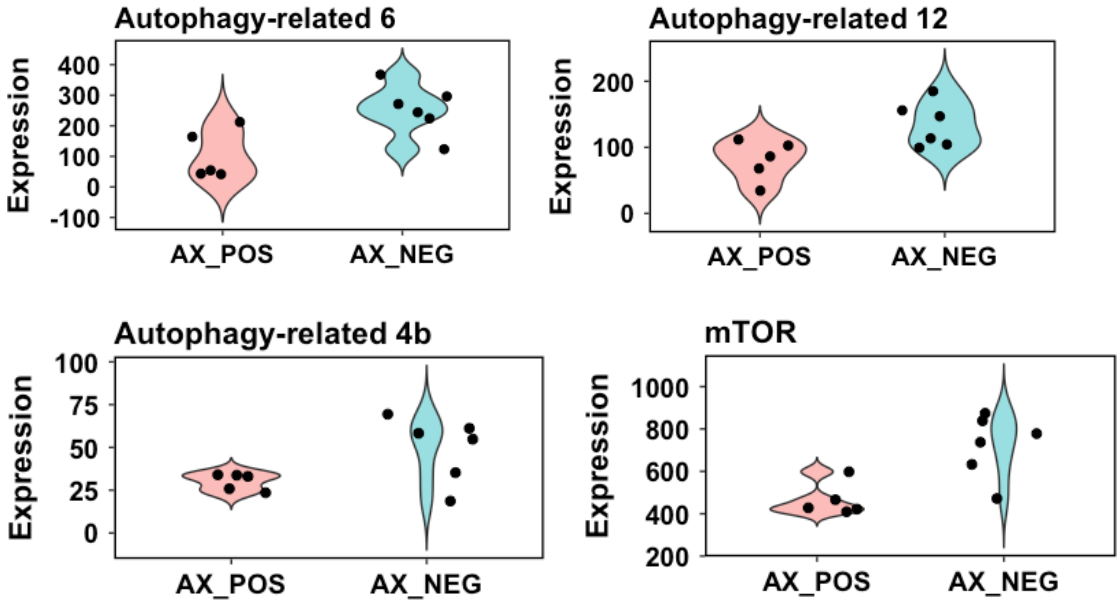

Figure 4.38 *TK* knockdown in axenic flies downregulates autophagy-related genes.

Differential expression (p.adj < 0.05, absolute log2 fold > 0.5) between control (AX_NEG) vs *TK* knockdown flies (AX_POS). Each dot is one sample, with sample groups given on the x-axis and gene expression on the y-axis.

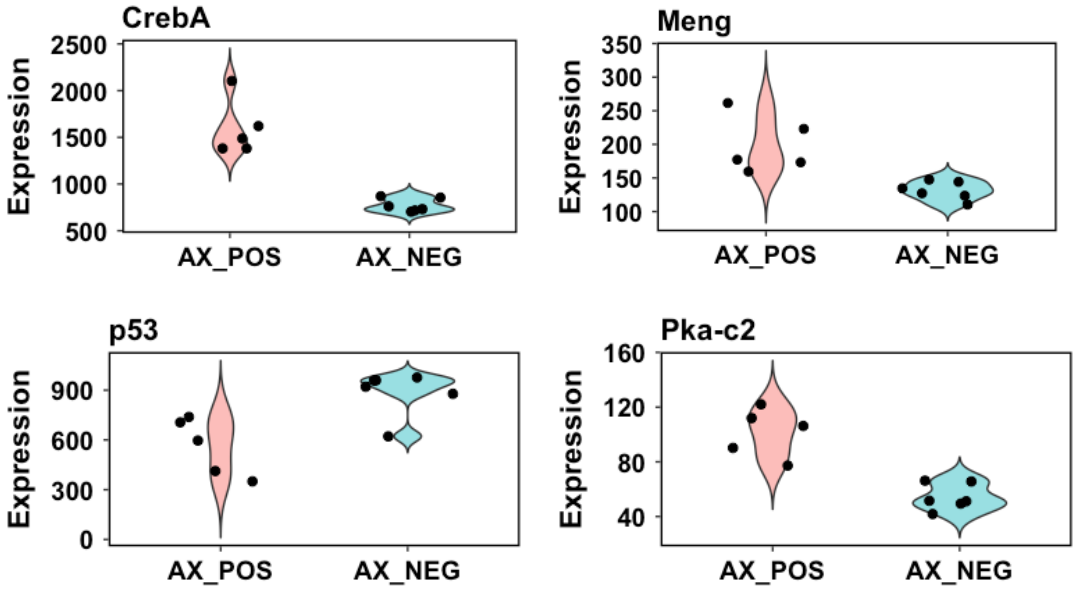

Figure 4.39 *TK* knockdown in axenic flies alters the expression of genes involved in longevity regulating pathways.

Differential expression (p.adj < 0.05, absolute log2 fold > 0.5) between control (AX_NEG) vs *TK* knockdown flies (AX_POS). Each dot is one sample, with sample groups given on the x-axis and gene expression on the y-axis.

4.4.6.2.4 *TK* knockdown affects IIS pathway in axenic flies

Another finding from the differential expression analysis between axenic *TK* RNAi+/- was that many genes encoding components of the IIS pathway were significant. Those genes were only differentially expressed in the axenic dataset. However, considering that IIS is a central regulator of lifespan and metabolism, and thus could play a key role in controlling the many phenotypes observed in my experiments, I decided to plot the expression of those genes in all three microbial conditions: gnotobiotic flies colonised with *A. pomorum* or *L. brevis* and axenic flies (Figure 4. 40). The findings illustrated that insulin like peptides (Ilps) expressed in the brain (*Ilp2, Ilp3, Ilp4, Ilp5*) were upregulated when *TK* is knocked down. However, *Ilp6* and *Ilp8* expressed in the fat body and ovary respectively, were downregulated in response to the lack of *TK* (Figure 4.39*)*. Moreover, *Hnf4,* which is required for glucose-stimulated Ilp2 secretion, is downregulated in *TK* mutants (Barry and Thummel, 2016). The single *Drosophila* insulin receptor, *InR*, transduces the signal from the *Ilps* to the lipid *PI 3-kinase*, through the single *Drosophila* insulin receptor substrate, *CHICO* (Giannakou and Partridge, 2007). All of those components, *InR*, *PI 3-kinase* and *CHICO* were downregulated in *TK* knockdown axenic flies compared to control axenic flies. Looking at the pattern of expression of those genes, we can see that Axenic TK^{RNAi+} samples are more similar to *Ap* TK^{RNAi}+ samples, while Axenic TK^{RNAi-} resemble *Ap* TK^{RNAi+}. Overall, this would mirror the metabolic shift observed in the TAG phenotype. Interestingly, the negative regulator of *PI 3-kinase, Pten,* in axenic TK^{RNAi+} samples. *PDK1* and *Akt* kinases required to phosphorylate the TF *FOXO*, leading to its inactivation and translocation to the cytoplasm *CHICO* (Giannakou and Partridge, 2007), is also downregulated when *TK* is knocked down in axenic flies. However, while this should subsequently lead to increased *FOXO* levels in those samples, the results indicate the opposite, suggesting that something else is regulating *FOXO* expression. Ultimately, *Sirt1*, activated by

autophagy and known to increase *FOXO* signalling (Maiese, 2020) is downregulated in axenic *TK* knockdown samples.

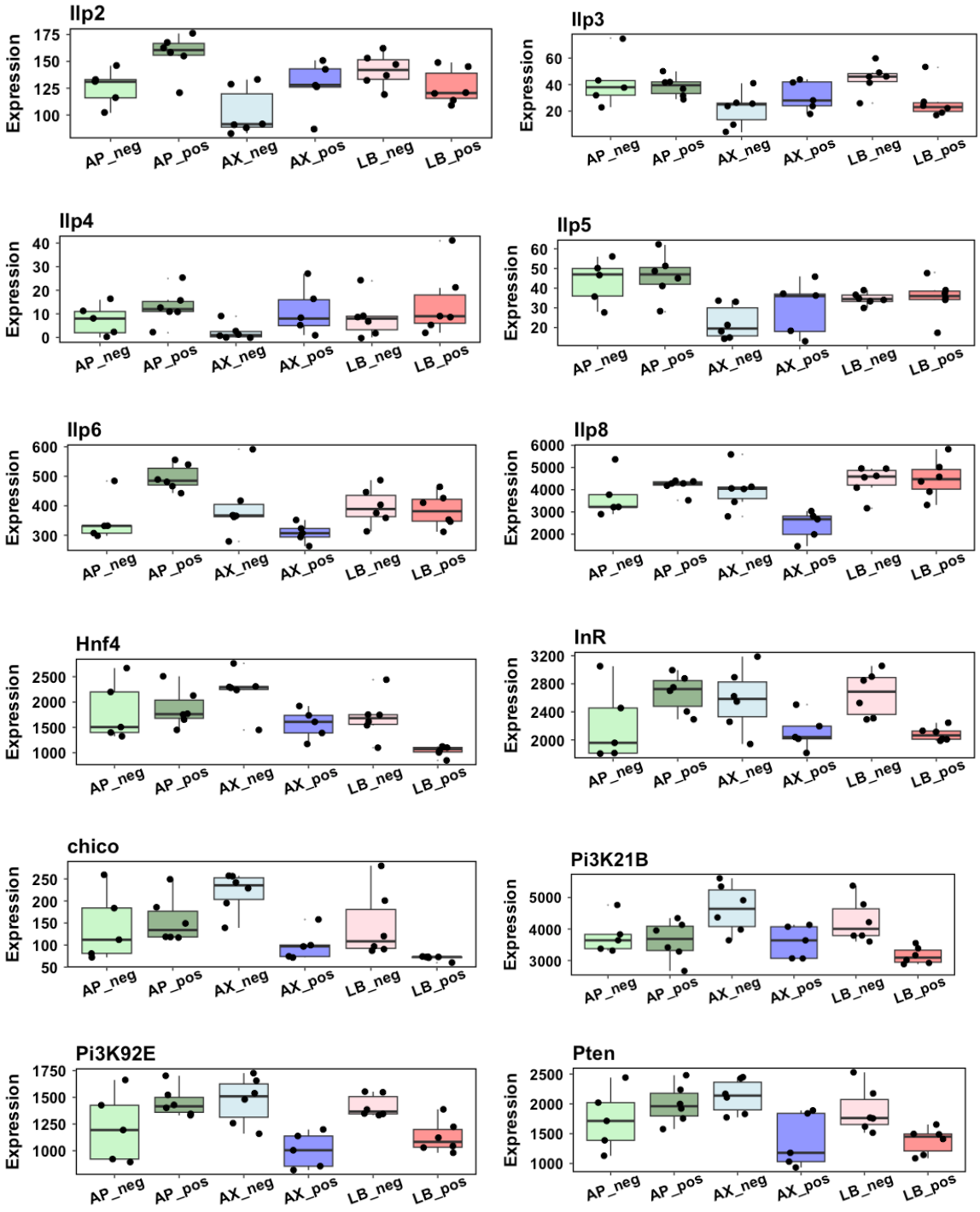

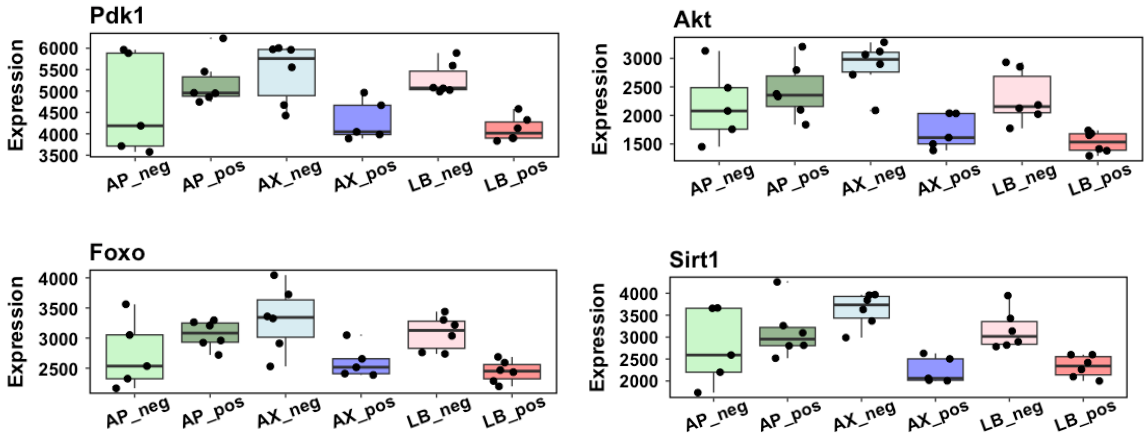

Figure 4.40 Expression of genes encoding insulin pathway components is modulated by *TK*.

Box plots of the differentially expressed genes encoding IIS pathway components (p.adj < 0.05, absolute log2 fold > 0.5) between control (AX_NEG) vs *TK* knockdown flies (AX_POS) in axenic female flies. Each dot is one sample, with sample groups given on the x-axis and gene expression on the y-axis.

4.4.6.2.5 Uncovering the overlap between lifespan extension following *TK* knockdown or microbiota depletion

To better understand the interplay between *TK*, microbiota and longevity, the following questions need to be addressed: Why does *TK* knockdown only extend lifespan in conventional or gnotobiotic flies, but not in germ free flies? What are the potential mechanisms that extend lifespan when microbiota is depleted vs those involved in *TK* knockdown induced longevity? Is there commonality between the two? To delve into those questions, I analysed the intersection of differentially expressed genes between *Ap* RNAi- vs *Ap* RNAi+ and *Ap* RNAi- vs Ax RNAi-. The results indicate that there are 73 commonly differentially expressed genes. Notably, in this dataset genes encoding components of the Imd pathway were predominant, being downregulated in *TK* knockdown samples in the *Ap* RNAi- vs *Ap* RNAi+ comparison and also in *Ap* control samples in the *Ap* RNAi- vs Ax RNAi- comparison. Overall, this suggests that downregulation of the Imd pathway plays a role in lifespan extension following *TK* knockdown or microbiota depletion. Moreover, this analysis also pointed to genes involved in proteolysis and lipid/fatty acids metabolism. Similarly, I performed the equivalent comparisons for flies colonised with *Lb*. Here, there were only 11 commonly

differentially expressed genes. Among those, the appetite and insulin regulator *CCHamide-2* was downregulated when Lb was knocked down (Lb- vs Lb+) and also in Lb- when compared to Ax-. Other genes were mostly involved in amino acid binding and transport, proteolysis and neuronal development.

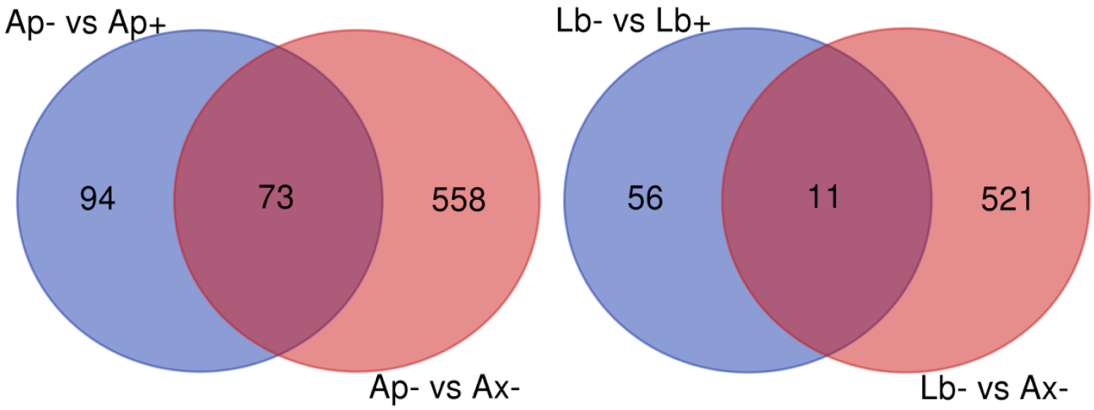

Figure 4.41 The overlap between differentially expressed genes following *TK* knockdown or microbiota depletion in gnotobiotic flies.

Venn diagrams were drawn based on the RNA-seq data sets. Left: Blue circle indicates the number of genes that are differentially expressed in the *A. pomorum* RNAi+/- group; red circle represents the number of genes that are differentially expressed in the *A. pomorum* RNAi-/ axenic RNAi- group. Right: Blue circle indicates the number of genes that are differentially expressed in the *L. brevis* RNAi+/- group; red circle represents the number of genes that are differentially expressed in the *L. brevis* RNAi-/ axenic RNAi- group.

4.5. Discussion and conclusions

4.5.1 *TK* responds differently to mono-association with *A. pomorum* vs *L. brevis*

A. pomorum and *L. brevis* are the most predominant microbiota species in *Drosophila*. *A. pomorum* has been recognised as a crucial regulator of host nutritional and lifespan indices as flies associated with *A. pomorum* have lower TAG levels and are shorter lived compared to axenic flies (Newell and Douglas, 2014). Thus, *A. pomorum* has been shown to recapitulate conventional phenotypes. On the other hand, *L. brevis,* was shown to have lifespan and TAG phenotypes more similar to axenic flies (Newell and Douglas, 2014). The findings presented here are consistent with this, *A. pomorum* following conventional phenotypes, while *L. brevis* being more similar to axenic features.

Overall, in my results *TK* was shown to interact with both *A. pomorum* and *L. brevis*. Although, *TK* expression is upregulated by *A. pomorum*, as well as by *L. brevis*, *A. pomorum* has a stronger effect. Accordingly, in terms of lifespan, here I demonstrate that *TK* knockdown increases lifespan in a bacterial specific manner. *TK* knockdown extends lifespan in flies mono-associated with *A. pomorum* or with L. brevis, but not in axenic flies. Importantly, the longevity effect is stronger in the presence of *Ap* compared to *Lb*. Furthermore, in terms of lipid metabolism *A. pomorum* recapitulates the conventional phenotype, while *L. brevis* does not have a significant effect. This indicates that *A. pomorum* communicate with *TK* to induce systemic metabolic effects on host.

Previous studies demonstrated that *TK* responds to microbial by-products, such as acetate or LPS. *Acetobacter* are Gram-negative bacteria within the class of alpha-proteobacteria that produce acetic acid by aerobic fermentation (Schönborn et al., 2021). Moreover, there is strong evidence that the main metabolic by-product produced by *Acetobacter, acetate,* is essential for normal *Drosophila* development and metabolic homeostasis (Hang et al., 2014; Shin et al., 2011). On the other hand, *Lactobacilli* are Gram-positive lactic acid-producing bacteria from the Firmicutes phylum, which promote the systemic growth of fly larvae under nutrient-limiting conditions (Storelli et al., 2011). While the main metabolic by-product of *L. brevis* fermentation is lactate, it can also produce acetate (Guo et al., 2017). Furthermore, lactate can be converted to acetate through aerobic metabolism. Importantly, considering its biosynthetic capabilities *A. pomorum* is recognised as more metabolically capable than *L. brevis* (Newell et al., 2014)(Chaston et al., 2014). Furthermore, being a Gram-negative bacterium *A. pomorum contains LPS,* while *L. bacillus* is Gram-positive and thus lacks LPS. Taking everything into consideration, a possible explanation for the phenotypic differences resulted from mono-association with *A. pomorum* vs *L. brevis* could be that *TK* is sensing more microbial cues from *A. pomorum* compared to *L. brevis*.

Table 4.6. Summary of the phenotypic effects of *TK* knockdown when flies are axenic vs mono-colonised with *A. pomorum* or *L. brevis.*

Phenotype	*A. pomorum*	*L. Brevis*	Axenic

Lifespan	Strongly increases lifespan	Slightly increases lifespan	No significant effect
TAG	Increases TAG	No significant effect	Decreases TAG
Egg laying	No significant effect	No significant effect	Increases egg laying
Feeding	Increases feeding behaviour	Increases feeding behaviour	Increases feeding behaviour
Starvation	Decreases starvation resistance	No significant effect	Increases starvation resistance

4.5.2 Disentangling the potential mechanisms responsible for the microbial* *TK* regulation of lifespan

The fact that *TK* knockdown extends lifespan in the presence of commensal microbes, but not in germ-free flies, implying that it could mediate the effects of microbes on host longevity, is one of the most striking result in this study. However, there are several questions that need to be answered in order to better understand the lifespan regulating effects of *TK*. For example, it is unclear whether lifespan extension following *TK* knockdown employs similar or distinct mechanisms in *A. pomorum* vs *L. brevis* mono-colonised flies as well as what happens in axenic *TK* knockdown flies where lifespan extension is masked.

One similarity in the differential expression analysis of *TK* knockdown flies mono-associated with *Ap* or *Lb* and germ-free is the upregulation of several endocrine factors. For example, *SIFR is a* GPCR expressed in the intestines, brain and thoracicoabdominal ganglion of adult flies (Jørgensen et al., 2006; Veenstra et al., 2008). Its ligand, *SIFamide* is produced in *pars intercerebralis* (PI) of the brain. Reduced levels of SIFamide causes hyperactive courtship behaviours in both sexes (Terhzaz et al., 2007). Consequently, it has been proposed that increased *SIFR* may reduce reproductive behaviours and consequently extend lifespan. Moreover, *7B2* was also upregulated in TK^{RNAi+} samples. *7B2* is required for the activation and secretion of the prohormone convertase *amontillado*

(amon) necessary for the production of bioactive neuropeptide hormones. Another key function of *amon* is to enable the production of the glucose regulatory hormone *AKH* in the corpora cardiaca endocrine cells (Rhea et al., 2010). Moreover, *amon* knock-out mice have been shown to be hypoglycemic, slow-growing and defective in processing proglucagon, prosomatostatin-14, and proinsulin (Furuta et al., 1997, 1998). A human patient deficient in amon, with extreme childhood obesity and low insulin levels, has also been identified (Jackson et al., 1997). Consequently, this suggests that *TK* knockdown induces critical changes in hormone and neuropeptide production. *Jhbp2* is a juvenile hormone responsive protein. Previous studies suggest that reduced juvenile hormone is sufficient to extend fly lifespan and it also limits reproduction by inhibiting the production of yolked eggs. However, juvenile hormone control of longevity was not attributed to the reduced physiological costs of egg production, suggesting that different mechanisms are employed by *JH* in regulating lifespan or reproduction. I conclude that *TK* might act in similar ways and that upregulation of *Jhbp2* could explain the egg laying phenotype, but not the lifespan phenotype. *NPFR* is another endocrine factor that is upregulated when *TK* is depleted. *NPF-NPFR* signalling mediates food signalling and is required for satiety, being a key factor in the internal state of hunger in the brain. Moreover, *NPF* was shown to always be co-expressed with *TK* in EECs, indicating that upregulated *NPF* signalling might try to compensate for downregulated *TK* signalling.

An interesting difference is that the *TK* receptor *TK*R99D becomes upregulated in response to *TK* knockdown in Lb and Ax flies, but not in Ap flies. This could suggest that Ap might diminish *TK*-dependent compensatory mechanisms. Similarly, CCHamide-2 is also upregulated in Lb and Ax flies *TK* RNAi+, but not in Ap flies. As previously, mentioned CCHamide-2 increases food intake and insulin production. However, the feeding experiment showed that *TK* knockdown increases feeding behaviour in Ap, Lb and Ax flies. While, increased CCHamide-2 could explain the increased food intake in Lb and Ax flies, Ap flies might use different mechanisms. Another striking difference is that in axenic flies only, *TK* knockdown leads to increased expression of several other neuropeptides. This could indicate, that in the absence of microbes, feedback mechanisms compensate for the lack of *TK* and that this compensatory feedback is stopped

by the presence of microbes. Overall, a plausible explanation for the differences observed in lifespan duration between Ap, Lb and Ax flies is that *TK* interaction with microbes naturally has a pro-ageing effect, this effect is stopped by microbiota or *TK* depletion and in the case of both microbiota and *TK* depletion, compensatory mechanisms may stop further lifespan extension.

The Venn diagrams help clarify these differences, by showing which genes genes are associated with the increased lifespan of axenic flies and those of *TK* knockdown. The results indicate that in *A. pomorum* mono-associated flies the main mechanism seems to be downregulation of the Imd pathway, while in Lb flies upregulated *CCHamide-2* and proteolysis. Finally, *TK* knockdown leads to upregulation of the heat shock proteins *HspBb* and *Hsp20* in Ap flies and only of the *HspBb* in Lb flies. However, in axenic flies *TK* knockdown leads to both upregulation and downregulation of heat shock protein. Considering that heat shock proteins counteract proteotoxicity and promote longevity (Murshid et al., 2013; Tower, 2011), this could further explain why the strongest lifespan effect is in the presence of Ap.

4.5.3 Unrevealing the means through which *TK* interacts with microbes to trigger a metabolic shift

Overall, my results establish *TK* as a key mediator of the microbe-host crosstalk in terms of lipid metabolism. *TK* was previously shown to suppress the synthesis of triacylglycerides in enterocytes (Song et al., 2014). Other studies demonstrated that disruption of the IMD pathway signalling in *TK*+ EE cells results in reduced expression of *TK* and AMPs, leading to the accumulation of lipid droplets in enterocytes, depletion of lipid droplets in the fat body, and hyperglycaemia (Kamareddine et al., 2018). Moreover, nutrient deprivation was shown to enhance the production of *TK* in the midgut and *TK* loss was shown to increase lipid production and storage (Song et al., 2014). Consistent with previous research, our results in chapter 3 show that *TK* knockdown leads to increased TAG levels in conventional flies. However, when flies were made axenic, the effect of *TK* knockdown was masked. *A. pomorum* recapitulates the conventional phenotype, while *L. brevis* does not have a significant effect. This

indicates that *A. pomorum* communicate with *TK* to induce systemic metabolic effects on host. Moreover, the differential expression analysis in *A. pomorum* mono-associated flies shows that *TK* knockdown leads to a decrease in genes encoding Imd pathway components. Overall, those findings conform with the previous studies that Imd pathway inhibition leads to decreased *TK* and increased lipid levels, suggesting that the immune-endocrine relationship between *TK* and Imd pathway is bidirectional.

Furthermore, increased adiposity is a conserved phenotype in axenic animals (Bäckhed et al. 2007, Dobson et al., 2015, Vijay-Kumar et al., 2010), thus explaining the TK^{RNAi-} axenic phenotype. However, it is unclear why TK^{RNAi+} axenic samples have decreased TAG levels. Endocrine control of insulin/IGF signaling (IIS) activity plays a pivotal role in regulating metabolic homeostasis. Stress and inflammatory signaling pathways, such as Jun-N-terminal Kinase (JNK) signaling suppress IIS, thereby limiting anabolic processes to enhance stress tolerance and prolong lifespan (Hull-Thompson et al., 2009). This intricate interplay represents an adaptive response that effectively manages energy resources during challenging conditions. However, excessive JNK activity in the adipose tissue of vertebrates has been identified as a contributor to insulin resistance, a key factor in the development of type II diabetes. Therefore, maintaining a delicate balance in the interaction between JNK and IIS is essential to ensure the appropriate metabolic adaptation to environmental stresses.

Previous research has unveiled that JNK signaling is indispensable for metabolic homeostasis in flies and that this function is mediated by *NLaz*, a homolog of vertebrate Apolipoprotein D (ApoD) and Retinol Binding Protein 4 (RBP4). Moreover, *NLaz* has been shown to be overexpressed in response to stress, which subsequently restrains growth and extends lifespan—phenotypes that align with reduced IIS activity. *NLaz* has also been demonstrated to repress IIS activity in adult flies (Pasco and Léopold, 2012). My results indicate that *TK* knockdown leads to *Nlaz* over-expression in axenic flies. This could suggest that *TK* knockdown induces metabolic stress and thus *Nlaz* levels increase. Accordingly, the RNAseq data also indicates that IIS signaling upstream *FOXO* is downregulated when *TK* is depleted in axenic flies. However, unexpectedly

FOXO levels are also downregulated, suggesting that other signaling pathways are governing *FOXO* expression. My data further shows that *mTOR* is downregulated when in *TK* loss-of-function axenic flies. Moreover, the tumour suppressor *p53* which is controlled by JNK signalling is downregulated in axenic *TK* RNAi+ samples. To put everything together, my hypothesis is that microbiota depletion or *TK* knockdown produces a low level of stress, inducing a hormetic response that subsequently leads to increased fat levels and lifespan. The concomitant depletion of both microbiota and *TK* might generate a stronger stress response, disrupting the homeostasis between JNK, IIS and mTOR signalling and leading to decreased adiposity and stalling lifespan extension. This hypothesis is also supported by the starvation resistance phenotype, where axenic TK^{RNAi+} flies are the least resistance to stress.

Chapter 5
5.1 Summary

The intricate interplay between the gut, its resident microbiota, and the central nervous system is a promising area of research with profound implications for human health. This chapter delves into the gut specific role of the neuropeptide hormone tachykinin. The results provide strong evidence that supressing *TK* specifically in the EE cells lining the gut is sufficient to significantly increase lifespan in the presence of *A. pomorum*. Strikingly, gut-specific *TK* knockdown improves the resistance to nutritional deficit, implying that the previously observed trade-off for starvation stress is related to brain-derived *TK*. Moreover, the role of gut *TK* in lipid metabolism is also explored. However, further studies are needed in order to better understand the complex interactions within the microbiota-*TK*-gut-brain axis and its significance in shaping lipid metabolism. Lastly, this chapter demonstrates that suppression of gut *TK* recapitulates the global knockdown feeding phenotype, but not the egg laying phenotype. Overall, this chapter explores the tissue specific effects of the neuropeptide hormone *TK*. The outcomes of this chapter hold promise for the development of targeted interventions aimed at restoring balance within this axis, offering new avenues for therapeutic strategies.

5.2 Introduction

5.2.1 Neuropeptides and the microbiota-gut-brain axis

While commensal bacteria maintains a symbiotic relationship with the host, the local innate immune system eliminates opportunistic or virulent bacteria from the gut (Artis, 2008). Growing evidence suggests that a well-balanced gut microbiota not only significantly contributes to the immune system but also profoundly influences brain function (Foster and McVey Neufeld, 2013; Petra et al., 2015; Sherman et al., 2015). During the invasion of pathogens, microbial componetns, such as LPS can directly impact the function of enteric neurons, spinal sensory neurons, and the vagus nerve. This occurs through the activation of Toll-like receptors or the translocation and release of neuropeptides and hormones (Yang et al., 1998).

The gut, housing nearly 100 million neurons, serves as the largest immune-competent organ in the human body (Buhner et al., 2017; Rajvanshi and Box, 2011). The majority of these neurons belong to the enteric nervous system (ENS), autonomously regulating gut functions. The remaining extrinsic nerves connect the central nervous system (CNS) to the gut, forming either the afferent gut-brain or efferent brain-gut axis (Carabotti et al., 2015; Rhee et al., 2009) The long-recognized bidirectional communication between the brain and the gut (Petra et al., 2015; Sherman et al., 2015) relies on the interaction between the central and peripheral nervous systems and the immune system. Notably, neuropeptides produced during immune responses or in the presence of infectious agents or malignant cells exhibit neuroendocrine-like activity that influences both brain and gut functions.

Neuropeptides can regulate a vast array of biological activities. Serving as neurotransmitters, they form components of the autonomic nervous system, acting locally at peripheral sites. As neuromodulators, neuropeptides can impact central regulatory centres, while their roles as neurohormones and hormones allow them to reach the immune system, peripheral vessels, organs, and glands through the circulatory system (Lotti et al., 2014). Close and intricate interactions between the neuropeptidergic and immunological systems are

reported to contribute significantly to host immune homeostasis. Neuropeptides, such as substance P (SP) manifest a variety of proinflammatory or anti-inflammatory effects crucial for modulating innate and adaptive immune responses (Lai et al., 2017; Sabatino et al., 2017)

5.2.2 Different physiological roles of *TK* produced from the brain vs gut-derived *TK*

SP, the archetypal mammalian tachykinin, was the first neuropeptide ever to be isolated from brain tissue as early as 1931 by Von Euler and Gaddum. From the very beginning, it was acknowledged that SP is synthesized in both the brain and the intestine (Von Euler and Gaddum, 1931; Hökfelt et al., 2001). Moreover, it is now clear that tachykinins are mostly present in neurons in the CNS and neurons and EE cells linked to the intestine (Otsuka and Yoshioka, 1993; Nässel, 1999; Hökfelt et al., 2001; Satake et al., 2013; Steinhoff et al., 2014), as well as in various other mammalian cell types, including hematopoietic cells (Zhang et al., 2000; Morteau et al., 2001), endothelial cells, Leydig cells, and immune cells (Almeida et al., 2004). As a result, they exhibit widespread and pleiotropic distribution, being produced by diverse cell types and thus functioning not only as neuropeptides but also as gut hormones.

Disentangling the tissue specific functions of SP in the brain and gut provides insights into its role in orchestrating complex physiological processes. In the brain, SP was shown to be involved in the perception and modulation of pain (Mantyh, 2002). Moreover, brain-derived SP was implicated in emotional regulation and the stress response, modulating the activity of brain regions associated with emotional processing and the HPA axis (Ebner and Singewald, 2006). Furthermore, previous studies demonstrated that brain-derived SP plays a role in neurogenic inflammation, by provoking mast cells to release pro-inflammatory molecules within the brain, as well as influencing the activity of microglia and mast cells (Skaper et al., 2017). On the other hand, gut-derived SP modulates gut motility and peristalsis (Holzer, 1988), regulates glandular secretion of fluids and electrolytes (Van Gils et al., 2012) and induces local inflammation correlated with irritable bowel syndrome (Barbara et al., 2004).

In invertebrates, tachykinin is similarly produced by neurons of the CNS and by EE cells of the intestine, but the presence of invertebrate *TK* in other cell types has not been reported (Nässel et al., 2019). Functional analysis has revealed that invertebrate *TK* is also pleiotropic. In the CNS, tachykinin often acts as a neuromodulator, influencing synaptic transmission and modulating neuronal activity (Nässel and Winther, 2010). It also plays a role in regulating reproductive behaviours, including aspects of courtship and mating (Jiang et al., 2013). Lastly, invertebrate brain-derived tachykinins were shown to play a role in stress response and nociception, influencing how organisms respond to environmental stressors and perceive pain-like stimuli (Im et al., 2015). Furthermore, tachykinins produced in the gut were implicated in gut motility (Nässel and Winther, 2010), lipid metabolism (Song et al., 2014) and regulation of neuroendocrine signalling pathways (Nässel et al., 1995b; Birse et al., 2011; Meschi et al., 2019). Overall, there is evidence showing that *TK* derived from either the brain or gut exhibit distinct functions: *TK* derived from gut largely controls processes related to intestinal homeostasis, metabolism and digestion, whereas *TK* derived from brain controls behaviour.

5.2.3 The *GAL4/UAS* system

The ability to perform precise genetic manipulations is essential to the investigation of biological phenomena and is the hallmark of modern genetics. Drosophila genetics offers a unique advantage in its diverse toolkit for precisely manipulating gene expression in specific tissues. The *GAL4l4/UAS* is a binary transgenic system derived from yeast, comprising of *GAL4*, a transcriptional activator protein that recognizes and binds an upstream activating sequence (*UAS*) (Barwell et al., 2017). When the *GAL4* gene is inserted downstream a genomic enhancer, it will be expressed in the cell types in which the enhancer is active. In order to induce the expression of a transgene, the *GAL4* binds to the *UAS* sequence cloned upstream of a transgene of interest leading to transgene expression only in the cell types where *GAL4* is expressed.

Since its introduction, the *GAL4/UAS* system has been upgraded and expanded into more complex systems enabling finer control over transgene expression. *GAL80*, another protein from yeast, is a repressor of *GAL4*. When *GAL80* is

inserted downstream of a regulatory region it can repress *GAL4* activity in the same cells. This tool provides great advantage to restrict the expression of *GAL4s* that are broadly expressed.

5.3 Aims

The primary aim of this chapter is to investigate the role of gut-derived *TK* in modulating host lifespan, lipid metabolism as measured by TAG levels, feeding behaviour, egg deposition, and starvation resistance. To address this, two *GAL4* lines were used, that are mostly expressed in the gut, but have some residual expression in the brain, to drive the expression of *UAS-TK-RNAi*. Those lines were combined with neuronal specific *GAL80s* to repress *GAL4* expression specifically in the brain.

Using these gut-specific genetic systems, I tested whether gut-derived *TK* is sufficient to have an effect on the following biological traits:

1) Lifespan
2) Lipid metabolism
3) Feeding behaviour
4) Egg laying
5) Starvation resistance

5.4 Results

5.5.1 Impact of microbiota members on *TK* transcript and peptide levels

In order to understand which specific microbiota members regulate the expression of *TK* in the gut, I performed RT-qPCR in axenic versus flies mono-cololonised with either *A. pomorum* or *L. brevis* (Figure 5.1). Considering that *TK* is not only produced by EECs, but also by neurons, I checked its expression in the gut (figure 5.1A) vs head (figure 5.1B). Congruent with expression patterns detected in chapter 4, *TK* expression in the gut is upregulated by the presence of *A. pomorum* (p value = 0.021), but not by *L. Brevis* (p value = 0.997). However, the head qPCR data shows that *TK* head expression is not regulated by

microbes. Overall, those findings indicate that *TK* expression is upregulated by *A. pomorum* in the gut only.

To test whether transcriptional modulation of *TK* by microbes in the gut is also apparent at the peptide level, I performed immunostaining of dissected *Drosophila* guts from flies that were either axenic or colonised with *A. pomorum* or *L. brevis* and stained them with anti-*TK* (Figure 5.2). The results indicate that *TK* is expressed in a region-specific manner, more exactly enriched in R1 and R2 (anterior midgut); R3 (gastric region) and R5 (posterior midgut), consistent with previous publications (Hung et al., 2020; Veenstra and Ida, 2014). The flies were starved for 4h before dissection to enable visualization, since yeast particles from fly media can be auto-fluorescent. Unexpectedly, the quantification of *TK* peptide using fluorescence intensity measurements of the immunostained gut regions, indicates that the presence of both *A. pomorum* and *L. brevis* induces upregulation of *TK* peptide in the gut (Figure 5.2A). At the gene level, *TK* expression increases in the presence of *A. pomorum* but not with *L. brevis*, indicating a specific transcriptional response to *A. pomorum*. However, at the peptide level, an increase is observed with both *A. pomorum* and *L. brevis*. This suggests that while *A. pomorum* enhances *TK* synthesis, *L. brevis* may affect post-transcriptional processes such as peptide stability or degradation pathways, leading to an apparent increase in TK peptide retention in the gut. Future experiments could test this by measuring levels of circulating *TK* in the haemolymph. Additionally, the levels of enzymes involved in *TK* secretion can be measured to further confirm whether *A. pomorum* and *L. brevis* employ distinct mechanism in regulating *TK*.

A)

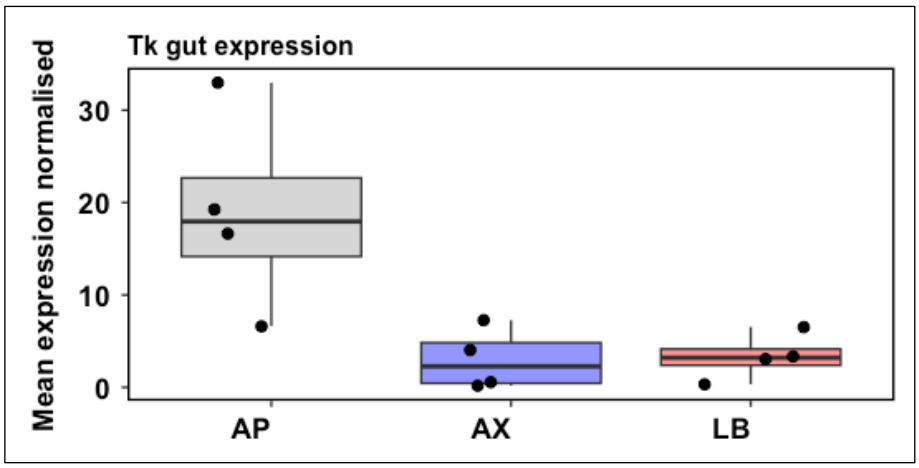

B)

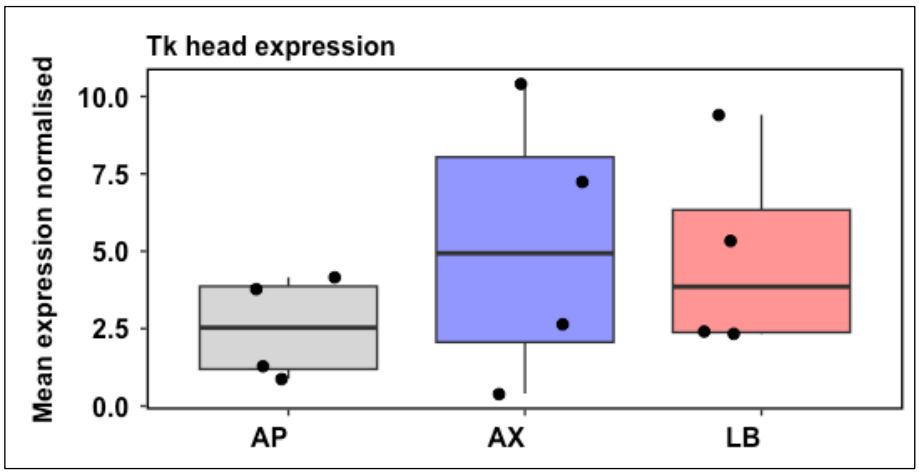

Figure 5.1 Gene expression of the peptide *TK* is regulated by *Acetobacter pomorum* in the gut, but not in the brain.

(B) Relative *TK* gut gene expression in axenic flies versus flies colonised with *Acetobacter pomorum* or *Lactobacillus brevis*. Statistical significance determined by one-way ANOVA (p value = 0.0131 *) with Tukey post-hoc test (AX vs AP: p value = 0.021293; LB vs AP: p value = 0.023606, LB vs AX = 0.997545; n=4 for AX, n=4 for AP, n=4 for LB, each sample containing 10 dissected guts). **(C)** Relative *TK* head gene expression in axenic flies versus flies colonised with *Acetobacter pomorum* or *Lactobacillus brevis*. Statistical significance determined by one-way ANOVA (p value = 0.508; n=4 for AX, n=4 for AP, n=4 for LB, each sample containing 10 dissected brains). Relative expression values were normalised to *ADH*. Box plots show median values, first and third quartiles, and 5th and 95th percentiles. Jitter plots show individual data points. AX: Axenic (blue), Ap: *Acetobacter pomorum (grey)*, Lb:*Lactobacillus brevis (red)*.

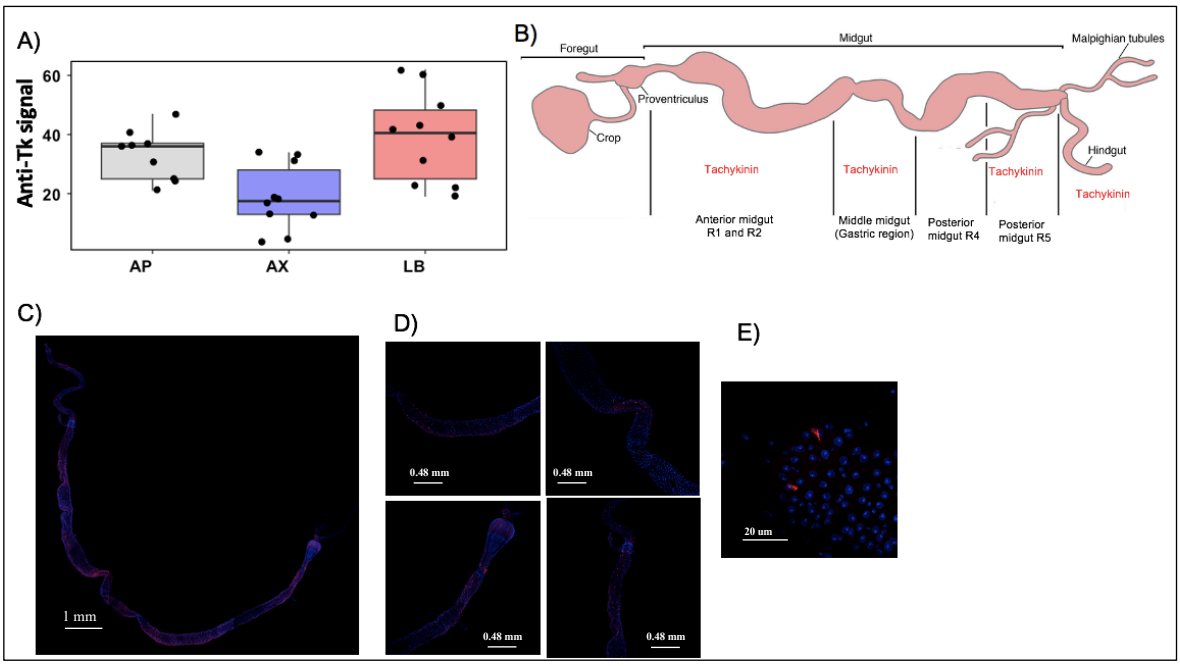

Figure 5.2 Impact of microbiota members on TK gut peptide.

(A) Immunostaining for the *TK* peptide in guts of axenic versus gnotobiotic flies colonised with either *A. pomorum* or *L. brevis*. Statistical significance one-way ANOVA (p value = 0.0026 **) with Tukey post-hoc test (AX vs AP: p value = 0.03868; LB vs AP: p value = 0.5335084; LB vs AX: p value = 0.002272 n=10/Ax, n=10/Ap, n=10/Lb). Box plots show median values, first and third quartiles, and 5th and 95th percentiles. Jitter plots show individual data points. **(B)** In the midgut enteroendocrine cells (EECs) produce peptide hormones in a region-specific manner. Four midgut regions are shown here [based on (Veenstra and Ida, 2014)]. *TK* enriched in R1 and R2 (anterior midgut); R3 (gastric region); and R5 (posterior midgut). **C), D), E)** Confocal images showing fluorescent immunohistochemistry on representative midgut of 3 days old wild-type fly with antiserum to *TK* (*TK* = red, DAPI = blue). Tiled gut in 10x magnification (C), regions of *TK* expression in 20x magnification (D), 63x oil magnification E).

5.5.2 Lifespan extension through *TK* is gut specific

5.5.2.1 Gut specific *TK* knockdown using *Voila-GAL4* in combination with *ChAT-GAL80*

Although the qPCR results suggest that microbial regulation of *TK* is gut specific, it is also known that neuropeptides are mediators of the microbiota-gut-brain axis. Thus, to disentangle the tissue specific effects, I used here *Voila-GAL4* to

drive the expression of *UAS-TK-RNAi* in EE cells. *Voila-GAL4* has a *GAL4* encoding P element transposon inserted within the *prospero* locus. *Prospero* is a transcription factor required for EE cell differentiation and thus an EE cell marker. However, *Voila-GAL4* exhibits residual neuronal expression (Fig 5.4C). To overcome this, I used the *GAL4* repressor *GAL80*, expressed under control of a neuron-specific promoter (Choline acetyl transferase, *ChAT*), to silence the effect of *GAL4* and therefore *UAS-TK-RNAi,* in the brain. First, I tested the efficiency and specificity of combining *Voila-GAL4* with *ChAT-GAL80* expression to block *GAL4* expression from the from the brain without affecting the gut by using a transgenic *Voila-GAL4* line tagged with GFP. The results prove that *ChAT-GAL80* does not affect Voila-positive cells in the gut (Figure 5.3), but it blocks the GFP-*Voila* signal in the brain and ventral nerve cord (Figure 5.4).

Secondly, I checked *TK* knockdown in Voila-positive cells with vs without *ChAT-GAL80* in the gut (figure 5.5A) and head (figure 5.5B) via RT-qPCR. Using the *Voila-GAL4>TK*-RNAi genetic system effectively knocks down *TK* in the gut and the presence of *ChAT-GAL80* does not have a significant influence on this. In the head, the expected pattern where *TK* is depleted in the *TK*-RNAi; *Voila-GAL4* group and the effect is counteracted by the presence of *ChAT-GAL80* can be observed. However, those events did not reach statistical significance. This could be attributed to the fact that *TK* seems to intrinsically have a lower expression in the head as observed in the control groups. Hence, the magnitude of differences between control and knockdown groups would naturally be lower. Moreover, an experimental limitation could be the fact that *TK* expression has been measured in the whole head, rather than the brain where *TK* is known to be highly expressed. Nevertheless, the GFP expression patterns confirm that using *Voila-GAL4* in combination with *ChAT-GAL80* is a specific and efficient tool to deplete *TK* specifically in the gut, without affecting the brain. The qPCR data is complementary, even if non-significant when measuring *TK* head expression. Future studies should increase sample size and measure *TK* expression specifically in the brain rather than head.

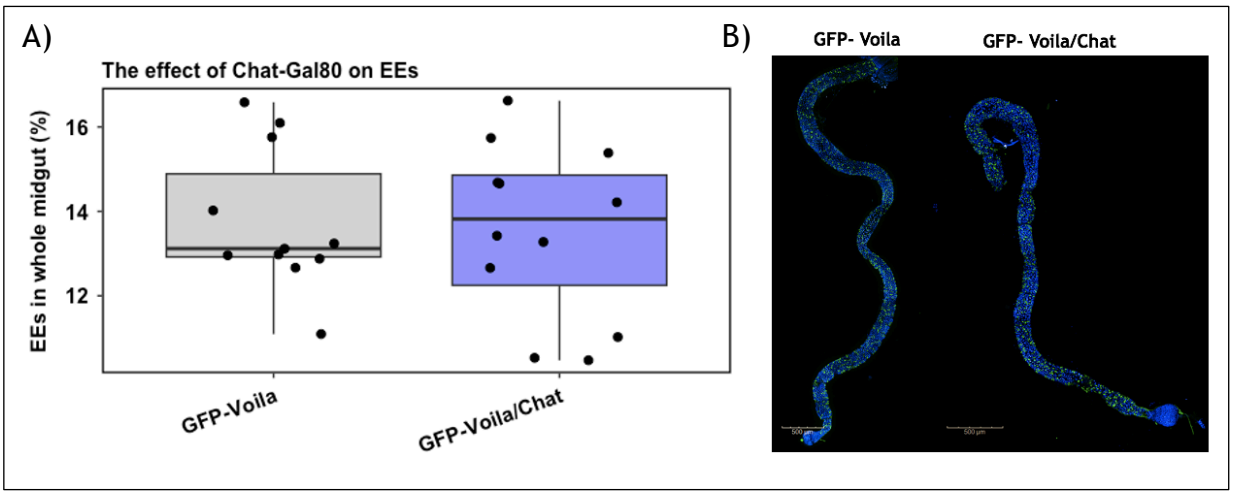

Figure 5.3 The effect of *ChAT-GAL80* in the gut.

A) Quantification of the GFP-positive cells in control (GFP-Voila) versus experimental (GFP-Voila/Chat) samples. Statistical significance was determined by unpaired two-sample t-test (p-value = 0.7939, n=11/GFP-Voila, n=11/GFP-Voila/Chat). Box plots show median values, first and third quartiles, and 5th and 95th percentiles. Jitter plots show individual data points. B) Confocal representative images showing GFP reporter labelling on midguts of 3 days old transgenic flies (*Uas-MCD8::GFP; Voila-GAL4*) with targeted GFP expression to EE cells (GFP = green, DAPI = blue) vs midguts of transgenic *Uas-MCD8::GFP*; *Voila-GAL4* flies recombined with the neuronal repressor *ChAT-GAL80*.

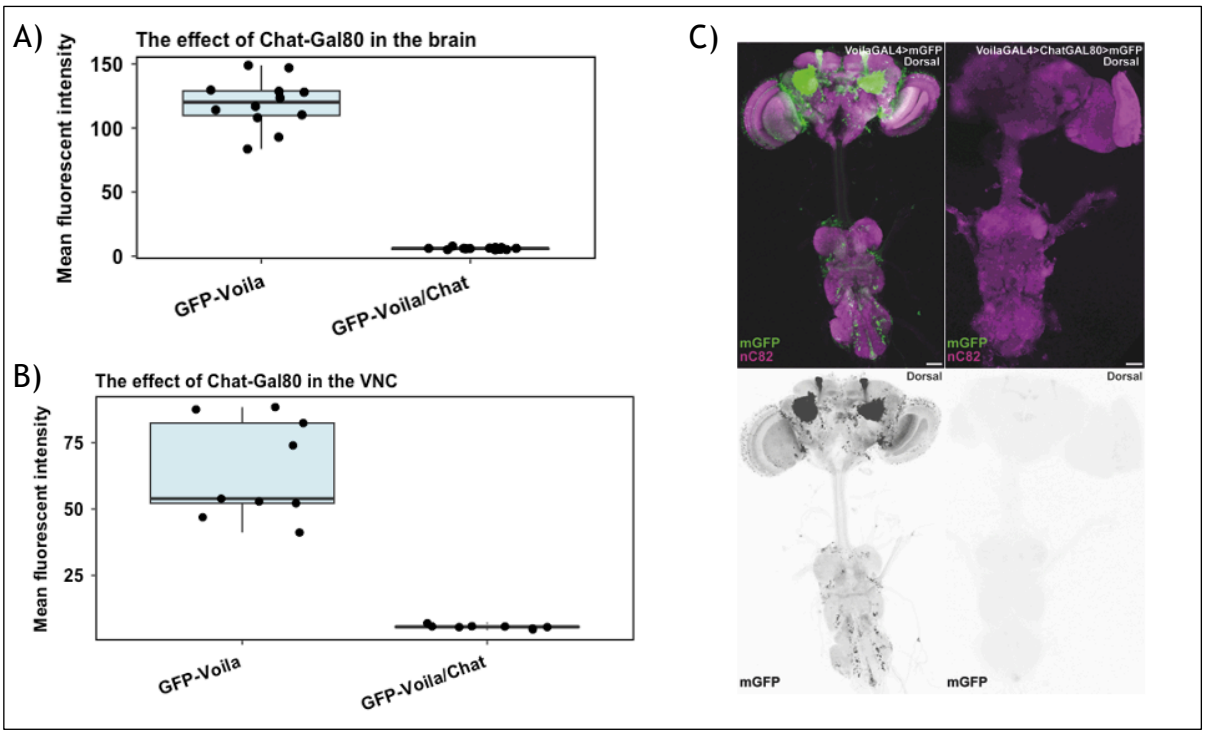

Figure 5.4 The effect of *ChAT-GAL80* in the brain and ventral nerve cord (VNC).

A) Quantification of the GFP in brains of control (GFP-Voila) versus experimental (GFP-Voila/Chat) samples. Statistical significance was determined by unpaired two-sample t-test (p-value = 4.566e-10, n=12/GFP-Voila, n=14/GFP-Voila/Chat). Box plots show median values, first and third quartiles, and 5th and 95th percentiles. Jitter plots show individual data points. B) Quantification of the GFP in VNC of control (GFP-Voila) versus experimental (GFP-Voila/Chat) samples. Statistical significance was determined by unpaired two-sample t-test (p-value = 1.245e-05, n=10/GFP-Voila, n=9/GFP-Voila/Chat). Box plots show median values, first and third quartiles, and 5th and 95th percentiles. Jitter plots show individual data points.C) Confocal representative images showing GFP reporter labelling on brains and VNC of 3 days old transgenic flies (*Uas-MCD8::GFP*; *Voila-GAL4*) with targeted GFP expression to *prospero*-positive cells (GFP = green, DAPI = blue) as controls or recombined with the neuronal repressor *ChAT-GAL80*. This experiment was performed by Dr. Anthony Dornan.

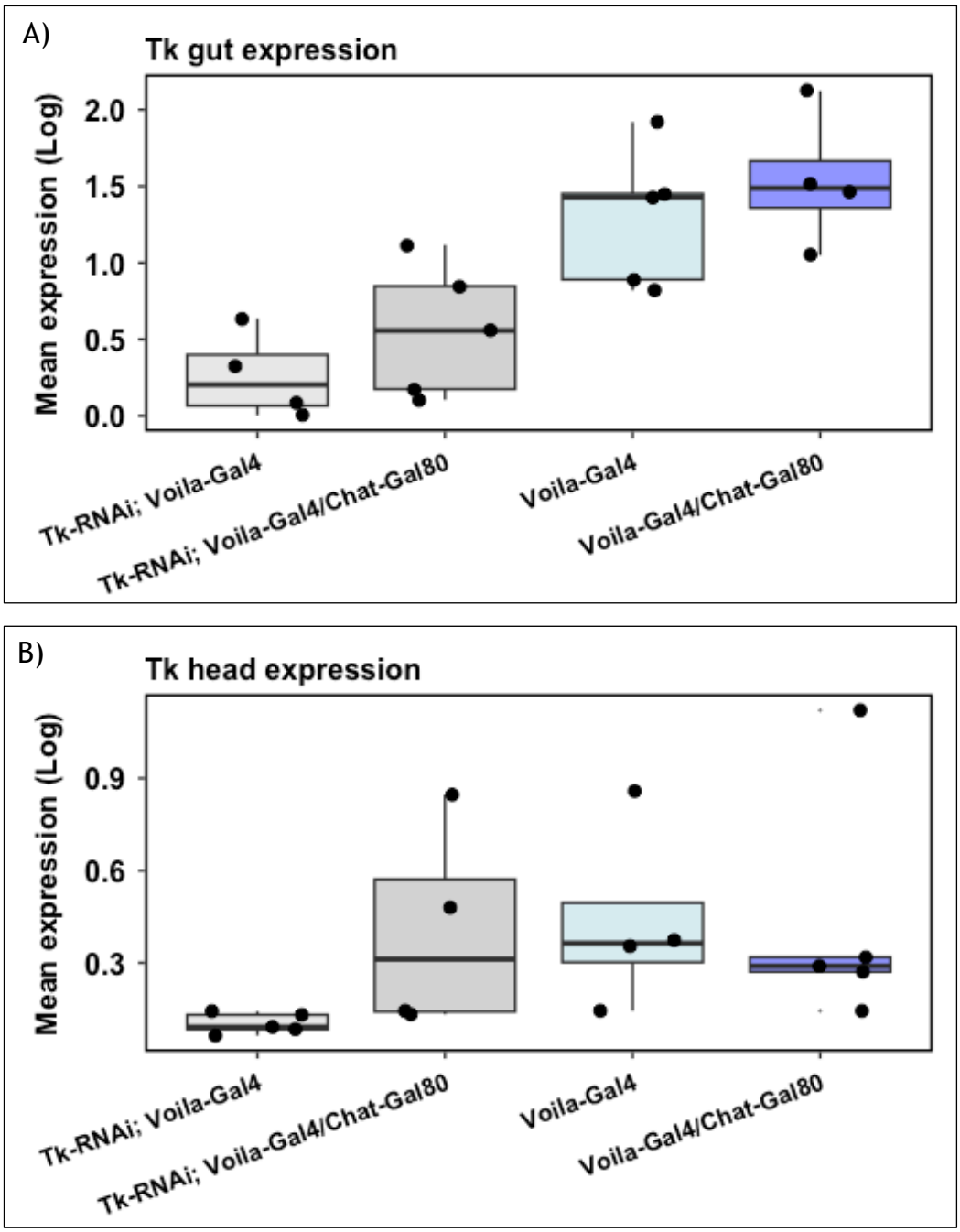

Figure 5.5 *Voila-GAL4* in combination with *ChAT-GAL80* is gut specific.

A) Relative gene expression of *TK* in the gut. *TK*-RNAi *Voila-GAL4* knocks down *TK* in *Voila*-positive cells; *TK*-RNAi;*Voila-GAL4/ChAT-GAL80* knocks down *TK* in *Voila*-positive cells in the gut only; *Voila-GAL4* and *Voila-GAL4/ChAT-GAL80* are used as controls to check the baseline *TK* expression in the presence of the genetic drivers. Statistical significance was determined by two-way ANOVA to test the relative *TK* expression by genotype (P value = 0.001417 **) followed by Tukey post-hoc test (Table 5.1). Relative expression values were normalised to the housekeeping gene *Tubulin*. Box plots show median values, first and third quartiles, and 5th and 95th percentiles. Jitter plots show individual data points. **B)** Relative gene expression of *TK* in the head. *TK*-RNAi;*Voila-GAL4* knocks down

TK in *Voila*-positive cells; *TK*-RNAi;*Voila-GAL4/ChAT-GAL80* knocks down *TK* in *Voila*-positive cells in the gut only; *Voila-GAL4* and *Voila-GAL4/ChAT-GAL80* are used as controls to check the baseline *TK* expression in the presence of the genetic drivers. Statistical significance was determined by two-way ANOVA (P value = 0.2867) followed by Tukey post-hoc test (Table 5.2). Relative expression values were normalised to the housekeeping gene *Tubulin*. Box plots show median values, first and third quartiles, and 5th and 95th percentiles. Jitter plots show individual data points.

Table 5.1 Tukey post hoc testing multiple comparisons of means for *TK-RNAi* driven by *Voila-GAL4* in combination with *ChAT-GAL80* qPCR gut data (Figure 5.4A).

The contrast column represents the groups to be compared; the values of 'diff' column are the mean difference between two groups; 'lwr' shows the lower end point of the interval; 'upr' shows the upper end point; 'p adj' represents the p-value after adjustment for the multiple comparisons.

contrast	*diff*	*lwr*	*uppr*	*p adj*
TK-RNAi; Voila-GAL4/ChAT-GAL80 vs TK-RNAi; Voila-GAL4	0.298671	-0.508753	1.106096	0.7096002
Voila-GAL4 vs TK-RNAi; Voila-GAL4	1.040703	0.2332782	1.848128	0.0103195
Voila-GAL4/ChAT-GAL80 vs TK-RNAi; Voila-GAL4	1.275543	0.4244429	2.126644	0.0032542
Voila-GAL4 vs TK-RNAi; Voila-GAL4/ChAT-GAL80	0.742032	-0.019215	1.50328	0.0571661
Voila-GAL4/ChAT-GAL80 vs TK-RNAi; Voila-GAL4/ChAT-GAL80	0.976872	0.1694474	1.784298	0.0159651
Voila-GAL4/ChAT-GAL80 vs Voila-GAL4	0.234840	-0.572584	1.042265	0.8320763

Table 5.2 Tukey post hoc testing multiple comparisons of means for *TK*-RNAi driven by *Voila-GAL4* in combination with *ChAT-GAL80* qPCR head data (Figure 5.4B).

The contrast column represents the groups to be compared; the values of 'diff' column are the mean difference between two groups; 'lwr' shows the lower end point of the interval; 'upr' shows the upper end point; 'p adj' represents the p-value after adjustment for the multiple comparisons.

contrast	*diff*	*lwr*	*uppr*	*p adj*
TK-RNAi; Voila-GAL4/ChAT-GAL80 vs TK-RNAi; Voila-GAL4	0.29812	-0.28189	0.878133	0.466608
Voila-GAL4 vs TK-RNAi; Voila-GAL4	0.330007	-0.250006	0.91002	0.382501
Voila-GAL4/ChAT-GAL80 vs TK-RNAi; Voila-GAL4	0.326055	-0.22078	0.872897	0.344178
Voila-GAL4 vs TK-RNAi; Voila-GAL4/ChAT-GAL80	0.0318873	-0.5795	0.643275	0.998697
Voila-GAL4/ChAT-GAL80 vs TK-RNAi; Voila-GAL4/ChAT-GAL80	0.027936	-0.55207	0.607949	0.998972
Voila-GAL4/ChAT-GAL80 vs Voila-GAL4	-0.003951	-0.583965	0.576062	0.999997

The same genetic system was employed to examine the tissue specific effects on lifespan. Considering that *TK* responds to *A. pomorum* and *L. brevis* via distinct mechanisms and the interaction between *TK* and each of those microbes seems to have different downstream effects (as observed in the RNA-seq data), I decided to investigate the tissue specific effects for *A. pomorum* colonised flies only, as *A. pomorum* showed a stronger and more consistent response. The lifespan data indicate that knocking-down *TK* specifically in the gut (*TK-RNAi;Voila-GAL4/ChAT-GAL80*) induced significant lifespan extension in the presence of *Acetobacter pomorum*, but not in axenic flies (figure 5.6). This recapitulates my previous results where *TK* was ubiquitously knocked down using a generic driver (*DaGS>Uas-TK-RNAi*), suggesting that knocking down *TK* in the gut is sufficient to extend lifespan in *A. pomorum* mono-colonised flies. Moreover, as expected, and consistent with my previous findings as well as previously published studies, axenic flies are longer lived compared to flies mono-colonised with *A. pomorum*. In other words, *A. pomorum* consistently shortened lifespan in all genotypes except for *TK-RNAi;Voila-GAL4/ChAT-GAL80,* when *TK* was knocked down specifically in the gut.

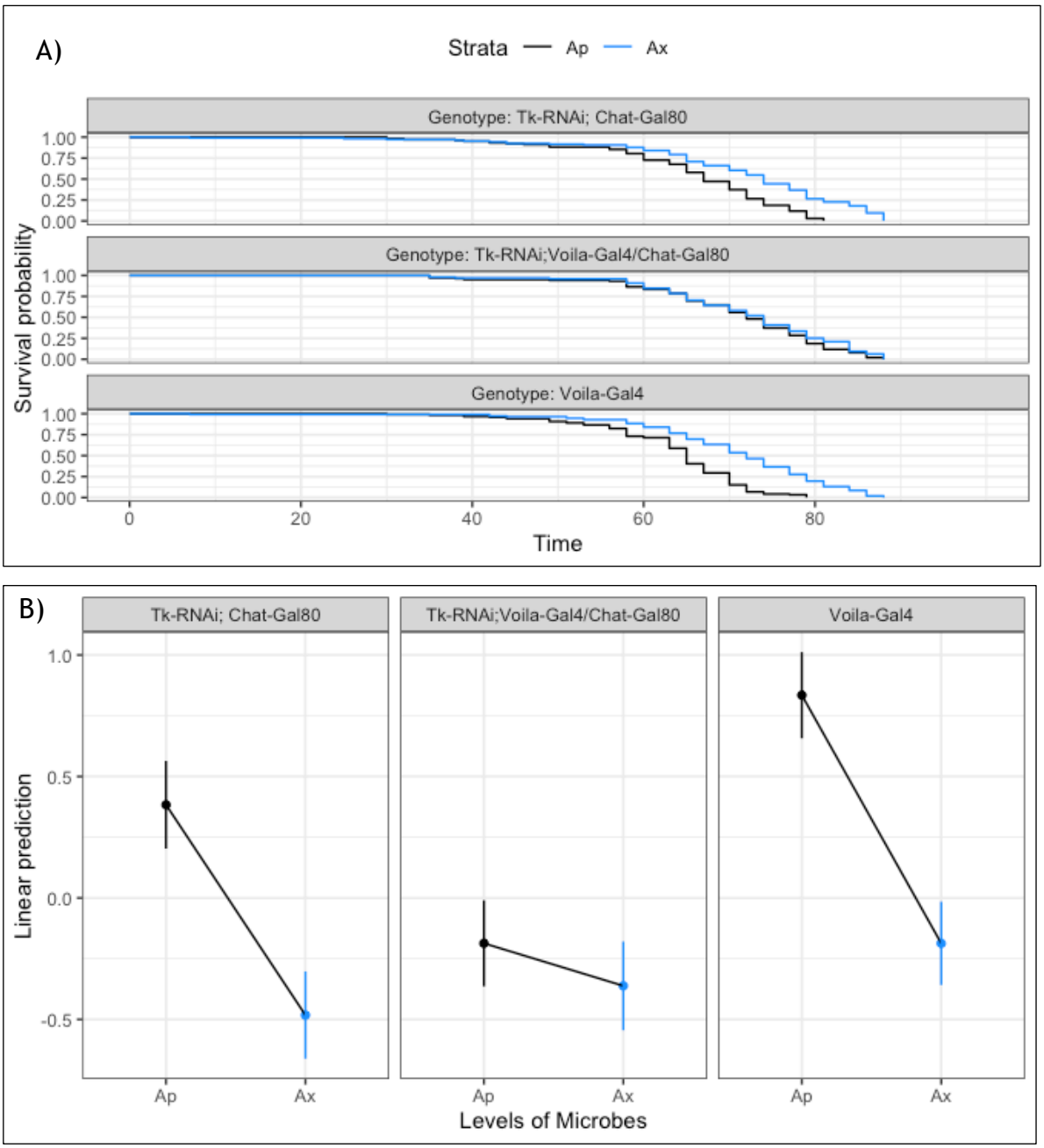

Figure 5.6 Knockdown of *TK* specifically in the blocks the lifespan-shortening effect of *A.pomorum*.

A) Kaplan-Meier survival curves in gut specific tachykinin knock-down flies (*TK*-RNAi;*Voila-GAL4/ChAT-GAL80*) versus control flies (*TK*-RNAi; *ChAT-GAL80* and *Voila-GAL4*) when they are mono-colonised with *Acetobacter pomorum (Ap)* (black) or germ-free flies (Ax) (blue). Statistical significance determined by cox proportional-hazards analysis with Type III test of interactions: Microbes: p value 1.394e-12 ***, Genotype: p value 7.580e-09 ***, Microbes:Genotype: p value 4.099e-05 ***.. Post hoc tests were used to assess the genotype-specific effect of *A pomorum*: *TK-RNAi*; *ChAT-GAL80*: p value <0001, F ratio = 35.731; *TK*-RNAi;*Voila-GAL4/ChAT-GAL80*: p value = 0.2188, F ratio = 1.512; *Voila-GAL4*: p

value <.0001, F ratio = 55.071. Sample size (females): n=120. **B)** Interaction plot for estimated marginal means.

5.5.2.2 Gut specific *TK* knockdown using *TK-GAL4* in combination with *R57C10-GAL80*

In addition to the *Voila-GAL4/ChAT-GAL80* system that I used, I also tested whether a second *GAL4/GAL80* system, using a different *GAL80* and a more specific *GAL4*, also reported to deliver EE-restricted *GAL4* activity, blocked the effect of *A. pomorum* on lifespan. This system, generated by the lab of Kim Rewitz (University of Copenhagen) relies on the pan-neuronal *R57C10-GAL80*, which uses an 872-base-pair enhancer fragment from nSyb to drive codon-optimised *GAL80* with an expression-boosting 3′ UTR in all mature, functional neurons, thus suppressing neuronal *GAL4* and subsequently to restricting activity of the *TK-GAL4* driver to the gut (Kubrak et al., 2022). The expression-boosting 3′ UTR refers to the addition of a sequence to the 3′ end of the *GAL80* mRNA, which can enhance the stability and lifespan of the mRNA, lead to more efficient translation and improve mRNA export from the nucleus, thereby increasing the overall expression levels of the GAL80 protein in neurons. This *GAL80* construct is recombined with *GAL4* knocked into the *TK* locus (not in an exons).

I tested the specificity of this system by qRT-PCR, as previously. *TK-GAL4* was used to drive *TK-RNAi* expression in *TK*-positive cells both in the gut (figure 5.7A) and head (figure 5.7B). Unexpectedly, the addition of *R57C10-GAL80* diminishes the knockdown efficiency in the gut, suggesting that *R57C10* might have residual intestinal expression (Table 5.3). On the other hand, combining *TK-GAL4* with *R57C10-Gal80* significantly supresses neuronal *GAL4* expression in the brain (Table 5.4). Unexpectedly, the RNAi does not significantly reduce gut *TK* expression when recombined with *R57C10-GAL80*. Moreover, the RNAi slightly decreases head *TK* expression even when *R57C10-GAL80* is present. Overall, this result questions the specificity of *R57C10*-Gal80. This could be due to a low sample size and thus low statistical power. Nevertheless, *R57C10-GAL80* was previously thoroughly characterised in combination with an *AstC-GAL4* driver, demonstrating that system can be used specifically target the expression of *AstC* in the *AstC*-expressing EECs (Kubrak et al., 2022).

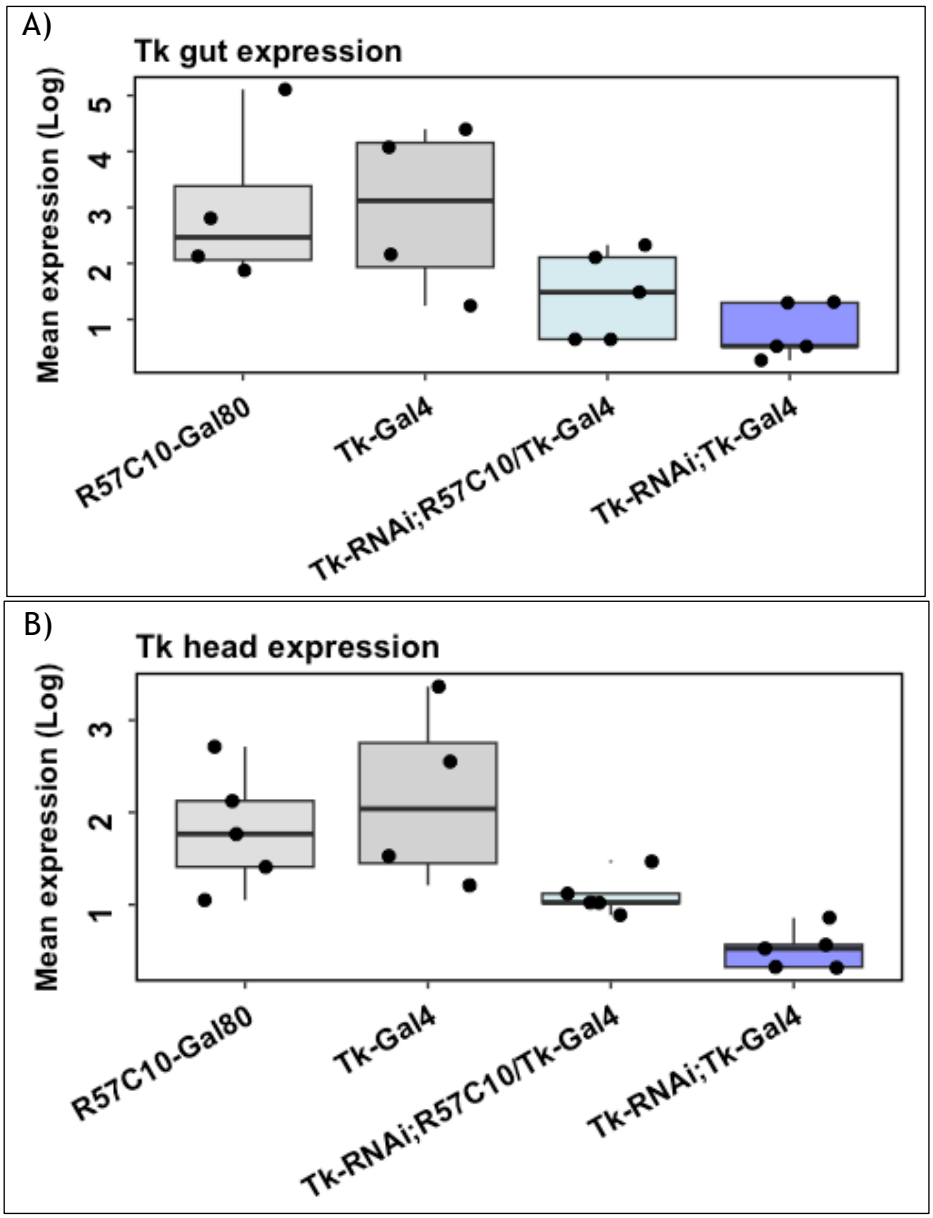

Figure 5.7 *TK-GAL4* in combination with *R57C10*-Gal80 supresses neuronal *GAL4* expression.

A) Relative gene expression of *TK* in the gut. *TK-RNAi;TK-GAL4* knocks down *TK* in *TK*-positive cells; *TK-RNAi;R57C10-GAL80/TK-GAL4* knocks down *TK* in *TK*-positive cells from the gut only; *TK-GAL4* and *R57C10-GAL80* are used as controls to check the baseline *TK* expression in the presence of the genetic constructs *GAL4* and Gal80. Statistical significance was determined by two-way ANOVA to test the relative *TK* expression by genotype (P value = 0.01984 *). Relative expression values were normalised to the housekeeping gene *Tubulin*. Box plots show median values, first and third quartiles, and 5th and 95th percentiles. Jitter plots show individual data points. **B)** Relative gene expression of *TK* in the gut. *TK-RNAi;TK-GAL4* knocks down *TK* in *TK*-positive cells; *TK-RNAi;R57C10/TK-GAL4* knocks down *TK* in *TK*-positive cells from the gut only; *TK-GAL4* and *R57C10-GAL80* are used as controls to check the baseline *TK* expression in the

presence of the genetic drivers. Statistical significance was determined by two-way ANOVA (P value = 0.002629). Relative expression values were normalised to the housekeeping gene *Tubulin*. Box plots show median values, first and third quartiles, and 5th and 95th percentiles. Jitter plots show individual data points.

Table 5.3 Tukey post hoc testing multiple comparisons of means for *TK-RNAi* driven by *TK-GAL4* in combination with *R57C10-GAL80* qPCR - gut data (Figure 5.6A).

The contrast column represents the groups to be compared; the values of 'diff' column are the mean difference between two groups; 'lwr' shows the lower end point of the interval; 'upr' shows the upper end point; 'p adj' represents the p-value after adjustment for the multiple comparisons.

contrast	*diff*	*lwr*	*uppr*	*p adj*
TK-GAL4 vs R57C10-GAL80	-0.00854	-2.26514	2.24805	0.99995
TK-RNAi;R57C10/TK-GAL4 vs R57C10-GAL80	-1.53596	-3.67676	0.60483	0.20529
TK-RNAi;TK-GAL4 vs R57C10-GAL80	-2.19573	-4.33653	-0.0549	0.04359
TK-RNAi;R57C10/TK-GAL4 vs TK-GAL4	-1.52741	-3.66822	0.61338	0.20904
TK-RNAi;TK-GAL4 vs TK-GAL4	-2.18719	-4.32799	-0.0463	0.04453
TK-RNAi;TK-GAL4 vs TK-RNAi;R57C10/TK-GAL4	-0.6597	-2.67813	1.35859	0.77892

Table 5.4 Tukey post hoc testing multiple comparisons of means for *TK-RNAi* driven by *TK-GAL4* in combination with *R57C10-GAL80* qPCR - head data (Figure 5.6B).

The contrast column represents the groups to be compared; the values of 'diff' column are the mean difference between two groups; 'lwr' shows the lower end point of the interval; 'upr' shows the upper end point; 'p adj' represents the p-value after adjustment for the multiple comparisons.

contrast	*diff*	*lwr*	*uppr*	*p adj*
TK-GAL4 vs R57C10-GAL80	0.35108	-0.76024	1.4624	0.79961
TK-RNAi;R57C10/TK-GAL4 vs R57C10-GAL80	-0.70864	-1.7564	0.33912	0.25001
TK-RNAi;TK-GAL4 vs R57C10-GAL80	-1.29458	-2.34234	-0.2468	0.01349
TK-RNAi;R57C10/TK-GAL4 vs TK-GAL4	-1.0597	-2.17104	0.0516	0.06414
TK-RNAi;TK-GAL4 vs TK-GAL4	-1.64566	-2.75698	-0.5343	0.00336
TK-RNAi;TK-GAL4 vs TK-RNAi;R57C10/TK-GAL4	-0.58593	-1.6337	0.4618	0.40179

Gut-specific knockdown of *TK* using this *R57C10-GAL80; TK-GAL4* driver led to significantly increased lifespan in *A. pomorum* mono-colonised flies, but not in germ-free flies (figure 5.8). This recapitulates the previous results, where *TK* was specifically manipulated in the gut using *Voila-GAL4* in combination with *ChAT-GAL80*. Overall, the ubiquitous *TK* knockdown (*DaGS > Uas-TK-RNAi*) lifespan phenotype can be replicated through manipulation of *TK* in EE cells only using two different gut-specific genetic systems. Altogether, this indicates that intestinal *TK* expression is required for *A. pomorum* to modulate lifespan and thus the knockdown stops the microbes from affecting lifespan.

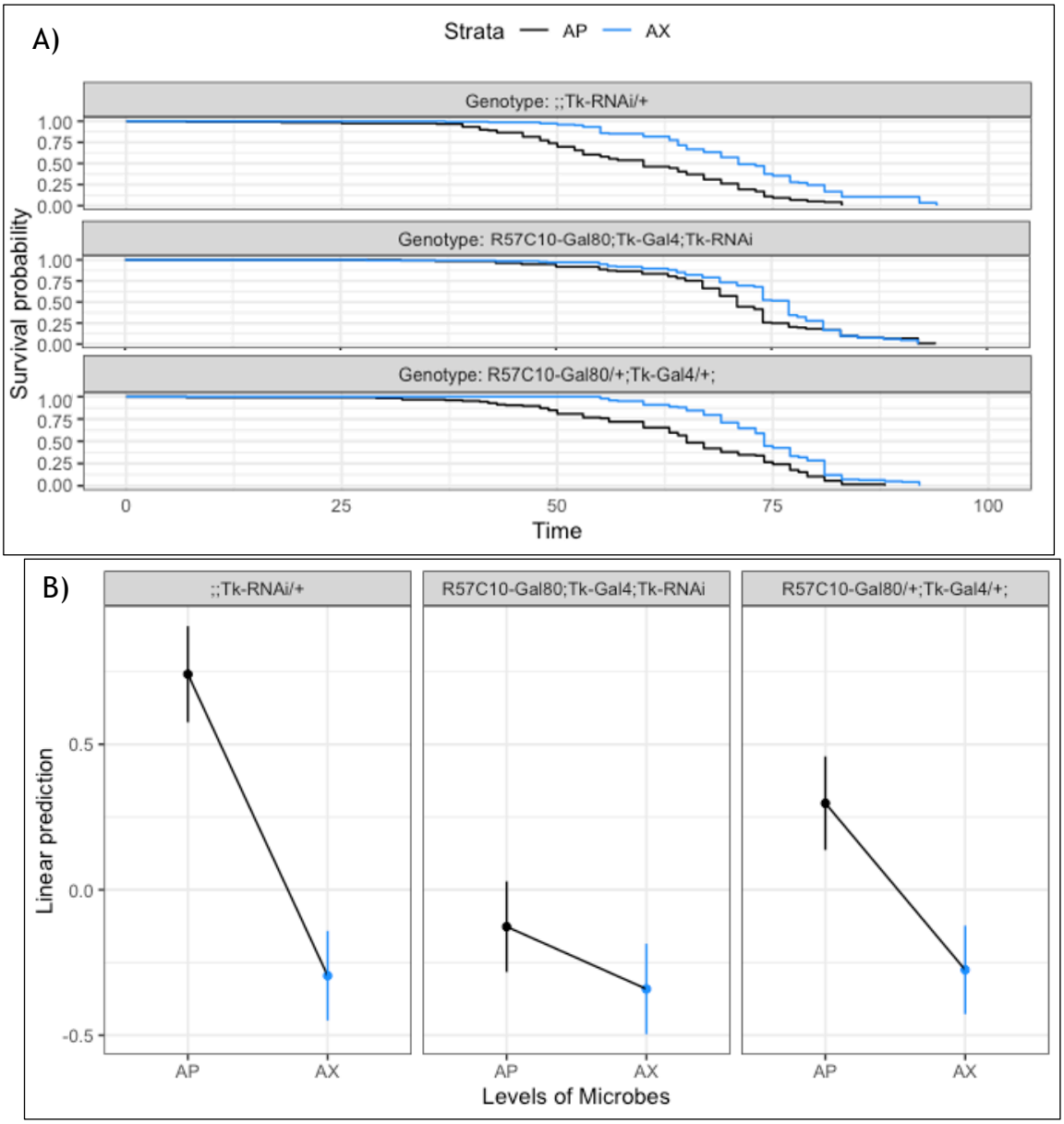

Figure 5.8 Knockdown of *TK* specifically in the gut blocks the lifespan-shortening effect of *A. pomorum*.

A) Kaplan-Meier survival curves in gut specific tachykinin knock-down flies (*R57C10-GAL80; TK-GAL4; TK-RNAi*) versus control flies (*R57C10-GAL80/+; TK-RNAi/+; and ;;TK-RNAi/+*) when they are mono-colonised with *Acetobacter*

pomorum (Ap) (black) or germ-free flies (Ax) (blue). Statistical significance determined by cox proportional-hazards analysis: Microbes: p value 1.394e-12 ***, Genotype: p value 7.580e-09 ***, Microbes:Genotype: p value 4.099e-05 ***. This was followed by post-hoc joint test on the estimated marginal means to test the interaction between gut specific *TK*-knockdown and microbes by genotype: *;;TK-RNAi*/+ F ratio = 66.015, p-value = 4.48E-16; *R57C10-GAL80;TK-GAL4;TK-RNAi*: F ratio = 3.038, p-value = 0.0813; R57C10-Gal80/+;*TK-GAL4*/+;: F ratio = 21.47, p-value = 3.59E-06. Sample size (females): n=105. **B)** Interaction plot for estimated marginal means.

5.5.2.3 The *TK-A. pomorum* interaction is mediated mostly by the gut

In my first lifespan experiment using a gut-specific manipulation of *TK*, I utilised flies where *ChAT-GAL80* was recombined with *UAS-TK-RNAi*. Consequently, when the flies were crossed to *Voila-GAL4*, *TK-RNAi* was expressed in the gut, but the two control genotypes (i.e. *TK-GAL4* alone, and *ChAT-GAL80; UAS-TK-RNAi*) differed in that *GAL80* was expressed in one line but not the other, creating a potentially confounding effect. I therefore designed an experiment to exclude the possibility that differential expression of *GAL80* and *GAL4* among tissues did not block *A. pomorum*'s effect on survival. Furthermore, by deploying a fully factorial design where transgenes where all possible combinations of transgenes were included or excluded, I included conditions where *TK* was knocked down either both in the gut and brain, or in just the gut, allowing me to compare the effect of each knockdown. I conducted this experiment both in axenic vs *A. pomorum* gnotobiotic flies (Figure 5.9).

As expected, in all the control groups axenic flies are substantially longer lived compared to flies mono-colonised with *A. pomorum*. However, when *TK* is knocked down, *A. pomorum* no longer shortens lifespan, because the flies are already long-lived. Knockdown of *TK* in *Voila*-positive cells (*TK-RNAi; Voila-GAL4*) led to a huge increase in lifespan in *A. pomorum* flies, their survival curve becoming identical with that of axenic flies (Table 5.5 – Genotype: *TK-RNAi; Voila-GAL4*, F ratio: 0.002, p value = 0.96224633). Analogously, restricting the knockdown to voila-positive cells from the gut only (*TK-RNAi; Voila-GAL4/ChAT-*

GAL80) significantly increased the lifespan of *A. pomorum* mono-colonised flies. However, the lifespan extending effect was less powerful in the gut-only genotype, with *A. pomorum* mono-colonised flies still exhibiting a slightly shorter lifespan compared to axenic flies (Table 5.5 – Genotype: *TK-RNAi; Voila-GAL4/ ChAT-GAL80*, F ratio = 8.413, p value = 0.00372545). In conclusion, while depleting *TK* in the gut is sufficient to attenuate the effect of *A pomorum* on lifespan, brain-derived *TK* may play an additional but small role.

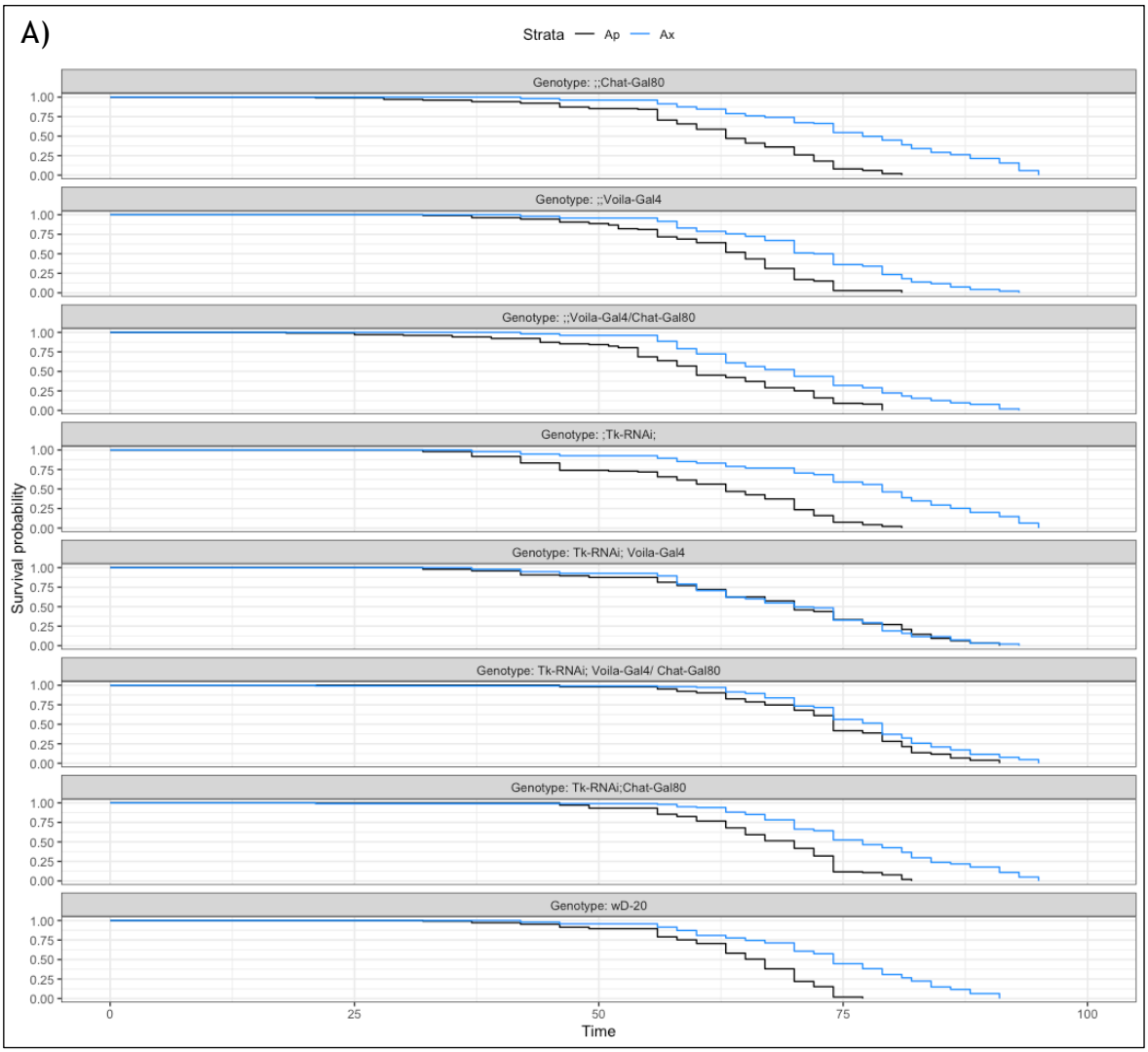

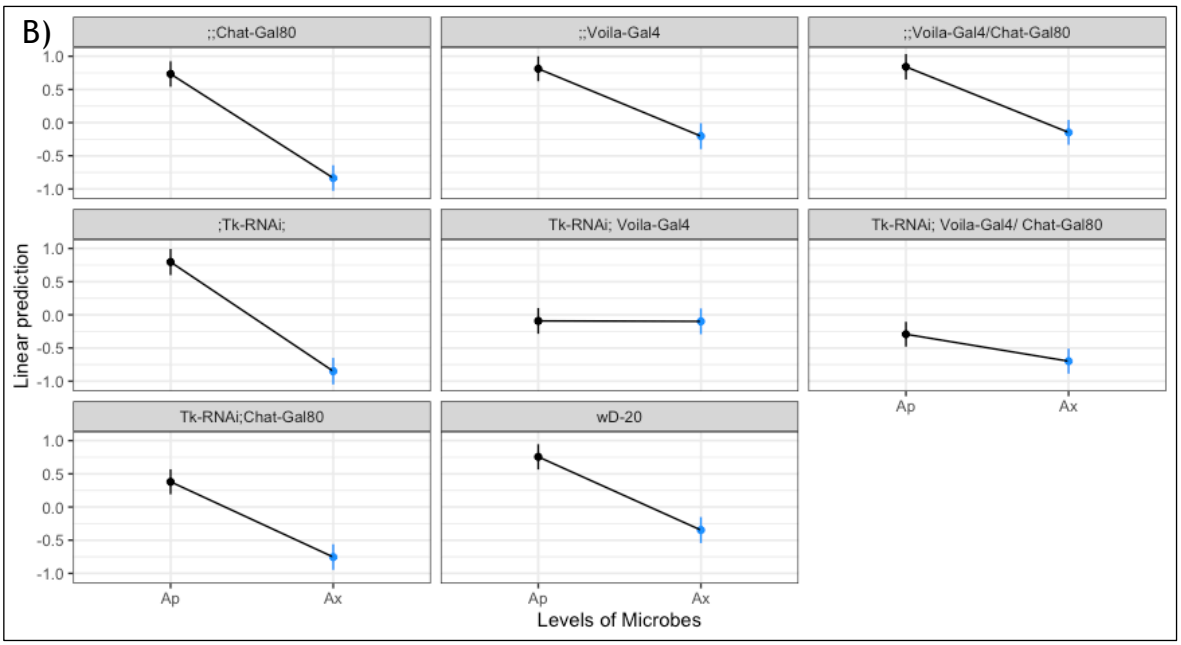

Figure 5.9 Confirming the sufficiency of intestinal *TK* knockdown to attenuate survival effects of *A. pomorum,* relative to fully-factorial controls.

A) Kaplan-Meier survival curves in *TK* knock-down flies (*TK-RNAi; Voila-GAL4*) and gut specific *TK* knockdown flies (*TK*-RNAi; *Voila-GAL4/ChAT-GAL80*) versus control flies (*;;ChAT-GAL80, ;;Voila-GAL4, ;;Voila-GAL4;ChAT-GAL80*, ;*TK*-RNAi;, ;*TK*-RNAi;*ChAT-GAL80*, wD^{-20}) when they are mono-colonised with *Acetobacter pomorum (Ap)* (black) or germ-free flies (Ax) (blue). Statistical significance determined by cox proportional-hazards analysis: Microbes: p value 2.2e-16 ***, Genotype: p value 2.2e-16 ***, Microbes:Genotype: p value 2.2e-16 ***. This was followed post-hoc joint test on the estimated marginal means to test the interaction between *TK*-knockdown and microbes by genotype (Table 5.5). Sample size (females): n=105. **B)** Interaction plot for estimated marginal means.

Table 5.5 Post-hoc joint test on the estimated marginal means testing the interaction between *TK*-knockdown and microbes by genotype for the lifespan data in figure 5.8.

The 'model term' column represents the microbial groups to be compared (Axenic (AX) vs *A. pomorum* (AP)); the 'genotype' column represents the genotype by which the comparisons are made; 'df1' shows the numerator degrees of freedom; 'df2' shows the denominator degrees of freedom. 'F ratio' represents the test statistic used to compute the p-value.

model term	*Genotype*	*df1*	*df2*	*F.ratio*	*p.value*
Microbes	*;;ChAT-GAL80*	1	Inf	115.6	5.81E-27
Microbes	*;;Voila-GAL4*	1	Inf	49.825	1.68E-12

Microbes	;;*Voila-GAL4/ChAT-GAL80*	1	Inf	48.564	3.20E-12
Microbes	;*TK*-RNAi;	1	Inf	119.117	9.87E-28
Microbes	*TK*-RNAi; *Voila-GAL4*	1	Inf	0.002	0.96224633
Microbes	*TK*-RNAi; *Voila-GAL4/ ChAT-GAL80*	1	Inf	8.413	0.00372545
Microbes	*TK*-RNAi;*ChAT-GAL80*	1	Inf	61.907	3.60E-15
Microbes	wD-20	1	Inf	57.737	3.00E-14

5.2.2 Tissue specific effects of *TK* on lipid metabolism

TAG levels in *Drosophila* are controlled by the microbiota, and *TK* may play a role in this. Previously, I demonstrated that ubiquitous *TK* knockdown increase TAG levels in conventional and *A. pomorum* mono-colonised flies. As the gut is the interface between microbiota and host, I looked at the effect of gut-specific knockdown of *TK* using the *Voila-GAL4/ChAT-GAL80* recombinant on the TAG phenotype (Figure 5.10). My previous findings revealed that ubiquitous *TK* knockdown increased TAG levels in conventional and *A. pomorum* mono-colonised flies. The same phenotype of increased adiposity was observed in axenic control flies when compared to either conventional or *A. pomorum* colonised flies. However, when both *TK* and microbiota were depleted, the effect was reversed, flies exhibiting low fat levels.

When *TK* knockdown was restricted to the gut, the increased lipid levels phenotype following microbiota depletion was conserved in the *Voila-GAL4* control group (table 5.6 – p value = 0.045197), but not in the *TK-RNAi; ChAT-GAL80* control group (table 5.6 – p value = 0.888554). This implies a genotype effect, where the genetic construct (*TK-RNAi; ChAT-GAL80*) alone impacts TAG phenotype. Inconsistent with my previous findings, the gut-specific *TK* knockdown does not lead to an increase in lipid levels in *A. pomorum* colonised flies. Although the gut specific *TK* knockdown (*TK-RNAi;Voila-GAL4/ChAT-GAL80*) recapitulates the metabolic shift observed following ubiquitous *TK* knockdown, where TAG levels between axenic and *Ap* flies are no longer significantly different (table 5.6 - p value = 0.168283), it is difficult to conclude whether this is due to a gut specific or a genetic construct effect.

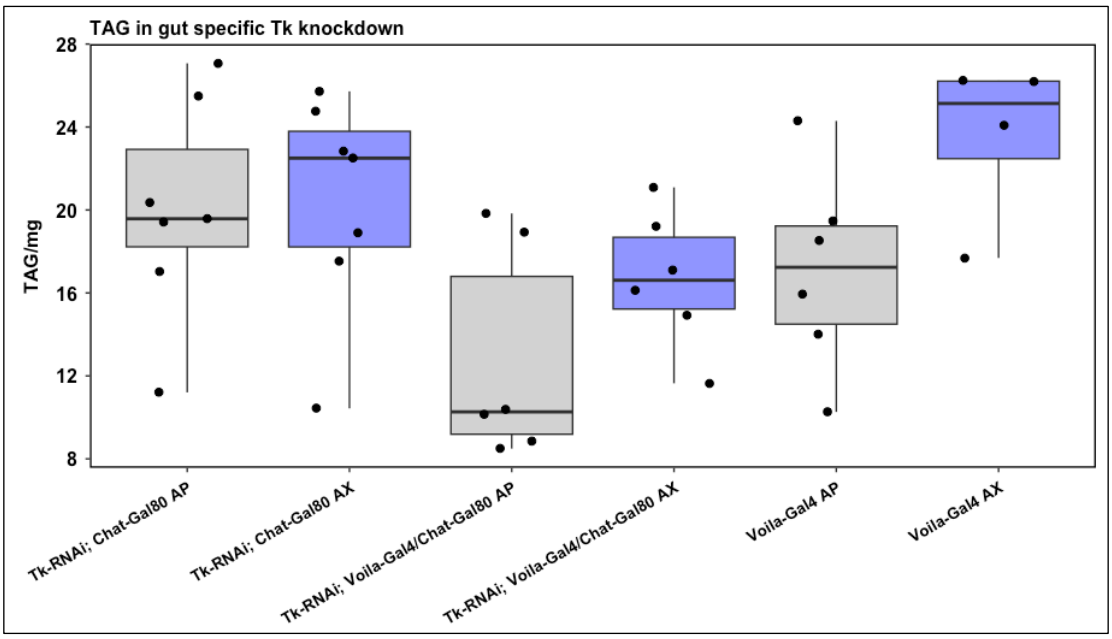

Figure 5.10 The impact of gut specific *TK*^{RNAi} on mediating *A. pomorum* effects on lipid levels.

TAG levels in gut specific *TK* knock-down flies (*TK-RNAi;Voila-GAL4/ChAT-GAL80*) compared to control flies (*TK-RNAi; ChAT-GAL80* and *Voila-GAL4*) when they are axenic (microbiota removed) or mono-colonised with *A. pomorum*. Statistical significance was determined by two-way ANOVA with interaction between microbes and genotype (Genotype: F value = 4.838, p value = 0.0151*, Microbes: F value = 3.975, p value = 0.0554, Genotype:Microbes: F value = 1.203, p value = 0.3143) with post-hoc joint test (table 5.9). Box plots show median values, first and third quartiles, and 5th and 95th percentiles. Jitter plots show individual data points. (n=7/ *TK*-RNAi; *ChAT-GAL80* AP, n=7/ *TK*-RNAi; *ChAT-GAL80* AP, n=6/ *TK*-RNAi;*Voila-GAL4/ChAT-GAL80* AX, n=6/ *TK*-RNAi;*Voila-GAL4/ChAT-GAL80* AP; n=6/ *TK*-RNAi;*Voila-GAL4/ChAT-GAL80* AX; n=6/*Voila-GAL4* AP; n=4/*Voila-GAL4* AX, each sample containing 5 flies). * p < 0.05).

Table 5.6 Post-hoc joint test for estimated marginal means testing the interaction between *TK*-RNAi and microbiota by genotype for TAG data (Figure 5.9).

The 'model term' column represents the microbial groups to be compared; the 'genotype' column represents the genotype by which the comparisons are made; the values of 'estimate' represent the difference between the two emmeans; 'SE' represents standard error; 'df' shows the degrees of freedom; 't ratio' represents the test statistic used to compute the p-value.

Model term	*Genotype*	*estimate*	*SE*	*df*	*t.ratio*	*p.value*
Ap - Ax	*TK*-RNAi; *ChAT-GAL80*	-0.36202	2.561539	30	-0.14132	0.88855
Ap - Ax	*TK*-RNAi; *Voila-GAL4/ChAT-GAL80*	-3.90627	2.766778	30	-1.41184	0.16828
Ap - Ax	*Voila-GAL4*	-6.46503	3.093352	30	-2.08997	0.04519

5.2.3 Gut specific *TK* knockdown fully recapitulates the ubiquitous knockdown feeding phenotype, but not the egg laying phenotype

In the previous chapters, it was determined that flies with a ubiquitous *TK* knockdown did not exhibit classical life-history age associated trade-offs exhibited in wild type flies. Lifespan extension in conventional flies did not correspond with reduction in reproduction, nor was it associated with decreased nutrient intake caused by altered feeding patterns. Axenics no longer had reduced reproductive capacity and had increased feeding rates. However, experiments with gnotobiotes showed that these findings were not attributable to a single bacterial species. To determine if these effects can be attributable to a single tissue, I decided to test the effects of gut specific *TK*-knockdown (*R5-GAL80/TK-RNAi; TK-GAL4*) on feeding (Figure 5.11) and egg laying (Figure 5.12) when microbiota is conventional vs axenic. The feeding results reveal that in control flies (*R5-GAL80; TK-GAL4* and *TK-RNAi*), microbiota depletion leads to reduced feeding (Table 5.7). However, in the experimental condition (*R5-GAL80/TK-RNAi; TK-GAL4*) the reduced feeding of axenic flies is rescued. In conclusion, gut-derived *TK* knockdown recapitulates the ubiquitous knockdown phenotype, suggesting that the feeding response regulates the microbial dependent feeding response and recapitulates the ubiquitous *TK* knockdown phenotype.

Furthermore, I tested egg laying using the same gut specific *TK* knockdown system. In the control groups (*R5-GAL80; TK-GAL4* and *TK-RNAi*) axenia consistently leads to highly reduced egg numbers. Nevertheless, in the experimental condition (*R5-GAL80/TK-RNAi; TK-GAL4*) knocking down *TK* in the

gut significantly increases egg laying in conventional flies (Table 5.8). However, gut targeted *TK* knockdown does not rescue the reduced egg laying attributed to microbiota depletion as observed in my previous results. Overall, the gut specific *TK* knockdown does not fully recapitulate the ubiquitous knockdown egg laying phenotype, suggesting *TK* in the brain plays a role in regulating the effects of microbes on fecundity.

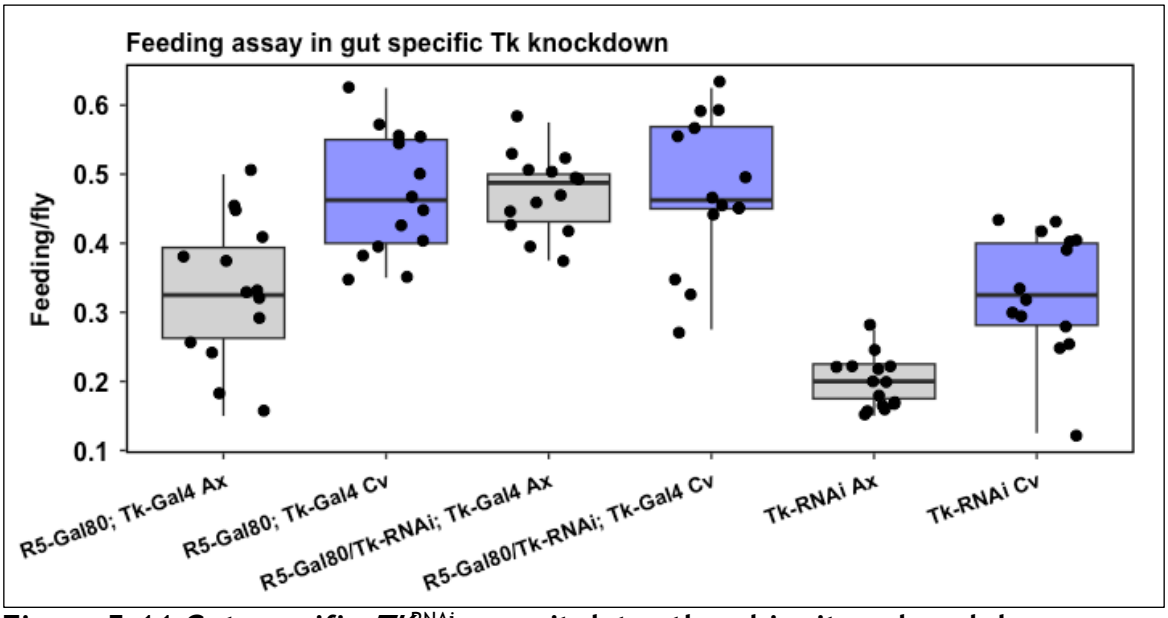

Figure 5.11 Gut specific *TK*^{RNAi} recapitulates the ubiquitous knockdown feeding phenotype.

PER assay to measure behavioural feeding in gut-specific *TK* knock-down flies (*R5-GAL80/TK-RNAi; TK-GAL4*) compared to *UAS (TK-RNAi*) and *GAL80-GAL4* recombinant (*R5-GAL80; TK-GAL4*) control flies when they are axenic (microbiota removed) or conventional (microbiota unaltered). Box plots show median values, first and third quartiles, and 5th and 95th percentiles. Jitter plots show individual data points. Statistical significance determined using orthogonal regression model and ANOVA Type III (Microbes: p value = 1.166e-05 ***, Genotype: p value 1.490e-15 ***, Microbes:Genotype p value = 0.0002064 *** followed by post-hoc joint test (Table 5.7). *** p < 0.0005,. **p <0.005.

Table 5.7 Post-hoc joint test for estimated marginal means testing the interaction between *TK-RNAi* and microbiota for feeding data (Figure 5.10).

The 'contrast' column represents the microbial groups to be compared; the 'genotype' column represents the genotype by which the comparisons are made; the values of 'estimate' represent the difference between the two emmeans;

'SE' represents standard error; 'df' shows the degrees of freedom; 't ratio' represents the test statistic used to compute the p-value.

contrast	*estimate*	*SE*	*df*	*t.ratio*	*p.value*
(Ax R5-GAL80; TK-GAL4) - (Cv R5-GAL80; TK-GAL4)	-0.614506	0.14591	79	-4.21130	0.00091
(Ax R5-GAL80; TK-GAL4) - (Ax R5-GAL80/TK-RNAi; TK-GAL4)	-0.630786	0.14591	79	-4.32287	0.00061
(Ax R5-GAL80; TK-GAL4) - (Cv R5-GAL80/TK-RNAi; TK-GAL4)	-0.639532	0.14591	79	-4.38281	0.00049
(Ax R5-GAL80; TK-GAL4) - (Ax TK-RNAi)	0.673577	0.14346	79	4.69504	0.00015
(Ax R5-GAL80; TK-GAL4) - (Cv TK-RNAi)	0.002950	0.14591	79	0.02021	1
(Cv R5-GAL80; TK-GAL4) - (Ax R5-GAL80/TK-RNAi; TK-GAL4)	-0.01628	0.14591	79	-0.11157	0.99999
(Cv R5-GAL80; TK-GAL4) - (Cv R5-GAL80/TK-RNAi; TK-GAL4)	-0.02502	0.14591	79	-0.17150	0.9999786
(Cv R5-GAL80; TK-GAL4) - (Ax TK-RNAi)	1.288083	0.14346	79	8.97834	0
(Cv R5-GAL80; TK-GAL4) - (Cv TK-RNAi)	0.617456	0.14591	79	4.23152	0.00085
(Ax R5-GAL80/TK-RNAi; TK-GAL4) - (Cv R5-GAL80/TK-RNAi; TK-GAL4)	-0.008746	0.14591	79	-0.05993	0.99999
(Ax R5-GAL80/TK-RNAi; TK-GAL4) - (Ax TK-RNAi)	1.304363	0.14346	79	9.09182	0
(Ax R5-GAL80/TK-RNAi; TK-GAL4) - (Cv TK-RNAi)	0.633736	0.14591	79	4.34309	0.00057
(Cv R5-GAL80/TK-RNAi; TK-GAL4) - (Ax TK-RNAi)	1.313109	0.14346	79	9.15278	0
(Cv R5-GAL80/TK-RNAi; TK-GAL4) - (Cv TK-RNAi)	0.642482	0.14591	79	4.40303	0.00046
(Ax TK-RNAi) - (Cv TK-RNAi)	-0.67062	0.14346	79	-4.67447	0.00016

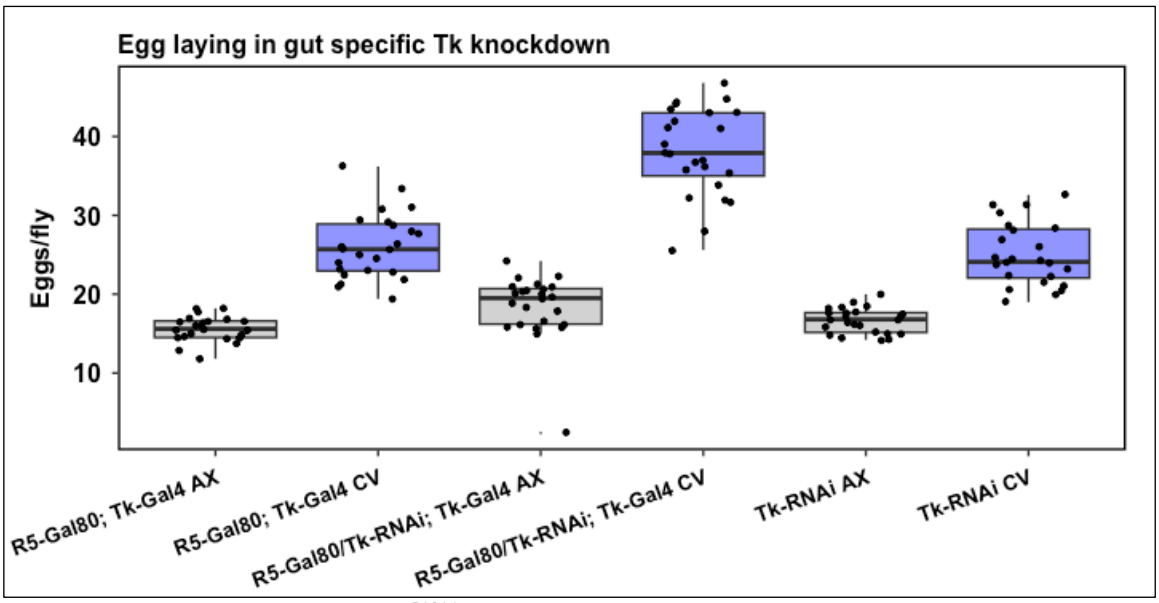

Figure 5.12 Gut specific *TK*^{RNAi} does not recapitulate the ubiquitous knockdown egg laying phenotype.

Number of eggs per fly in gut-specific *TK* knock-down flies (*R5-GAL80/TK-RNAi; TK-GAL4*) compared to *UAS* (*TK-RNAi*) and *GAL80-GAL4* recombinant (*R5-GAL80; TK-GAL4*) control flies when they are axenic (microbiota removed) or conventional (microbiota unaltered). Box plots show median values, first and third quartiles, and 5th and 95th percentiles. Jitter plots show individual data points. Statistical significance was determined by two-way ANOVA (Microbes: p value 2e-16 ***, Genotype: <2e-16 ***, Microbes*Genotype: 1.94e-11 ***) with post-hoc joint test (table 5.8) (n=24 samples/condition, each sample containing 5 flies). *** p < 0.0005.

Table 5.8 Post-hoc joint test for estimated marginal means testing the interaction between *TK*-RNAi and microbiota for egg-laying data (Figure 5.11).

The 'contrast' column represents the microbial groups to be compared; the 'genotype' column represents the genotype by which the comparisons are made; the values of 'estimate' represent the difference between the two emmeans; 'SE' represents standard error; 'df' shows the degrees of freedom; 't ratio' represents the test statistic used to compute the p-value.

contrast	*estimate*	*SE*	*df*	*t.ratio*	*p.value*
(Ax R5-GAL80; TK-GAL4) - (Cv R5-GAL80; TK-GAL4)	-10.5257	1.115134	137	-9.438977	6.91E-14
(Ax R5-GAL80; TK-GAL4) - (Ax R5-GAL80/TK-RNAi; TK-GAL4)	-2.78405	1.115134	137	-2.496612	0.132316
(Ax R5-GAL80; TK-GAL4) - (Cv R5-GAL80/TK-RNAi; TK-GAL4)	-22.4590	1.115134	137	-20.14023	1.01E-14
(Ax R5-GAL80; TK-GAL4) - (Ax TK-RNAi)	-1.06739	1.115134	137	-0.957186	0.930462
(Ax R5-GAL80; TK-GAL4) - (Cv TK-RNAi)	-9.40072	1.115134	137	-8.430129	7.08E-13
(Cv R5-GAL80; TK-GAL4) - (Ax R5-GAL80/TK-RNAi; TK-GAL4)	7.741666	1.103207	137	7.0174191	1.42E-09
(Cv R5-GAL80; TK-GAL4) - (Cv R5-GAL80/TK-RNAi; TK-GAL4)	-11.9333	1.103207	137	-10.81694	5.05E-14
(Cv R5-GAL80; TK-GAL4) - (Ax TK-RNAi)	9.458333	1.103207	137	8.5734883	3.52E-13
(Cv R5-GAL80; TK-GAL4) - (Cv TK-RNAi)	1.125	1.103207	137	1.0197541	0.910633
(Ax R5-GAL80/TK-RNAi; TK-GAL4) - (Cv R5-GAL80/TK-RNAi; TK-GAL4)	-19.675	1.103207	137	-17.83436	1.01E-14
(Ax R5-GAL80/TK-RNAi; TK-GAL4) - (Ax TK-RNAi)	1.716666	1.103207	137	1.5560692	0.62870083
(Ax R5-GAL80/TK-RNAi; TK-GAL4) - (Cv TK-RNAi)	-6.61666	1.103207	137	-5.997665	2.51E-07
(Cv R5-GAL80/TK-RNAi; TK-GAL4) - (Ax TK-RNAi)	21.39166	1.103207	137	19.390435	1.01E-14
(Cv R5-GAL80/TK-RNAi; TK-GAL4) - (Cv TK-RNAi)	13.05833	1.103207	137	11.836701	2.03E-14
(Ax TK-RNAi) - (Cv TK-RNAi)	-8.33333	1.103207	137	-7.553734	8.11E-11

5.2.4 Gut specific *TK* knockdown increases starvation resistance

As discussed in the previous chapters, increased lifespan following *TK* knockdown in conventional and *Ap* flies is associated with a trade-off for starvation resistance. My data demonstrated that, global *TK* knockdown had a detrimental effect on starvation resistance increased lifespan in conventional, *Ap* flies and axenic flies.

Surprisingly, when *TK* was knocked down specifically in the gut in conventional flies (Figure 5.13) the flies became significantly less sensitive to starvation than control conventional flies (Table 5.8). Moreover, in the axenic group gut targeted *TK* depletion did not have a significant effect on starvation resistance. This is again unexpected compared to the ubiquitous knockdown which had a huge detrimental effect. Overall, this suggests that the negative effects of ubiquitous *TK* knockdown are rescued and also improved by restoring *TK* expression in the brain, implying that knocking down *TK* specifically in the gut improves both lifespan and healthspan.

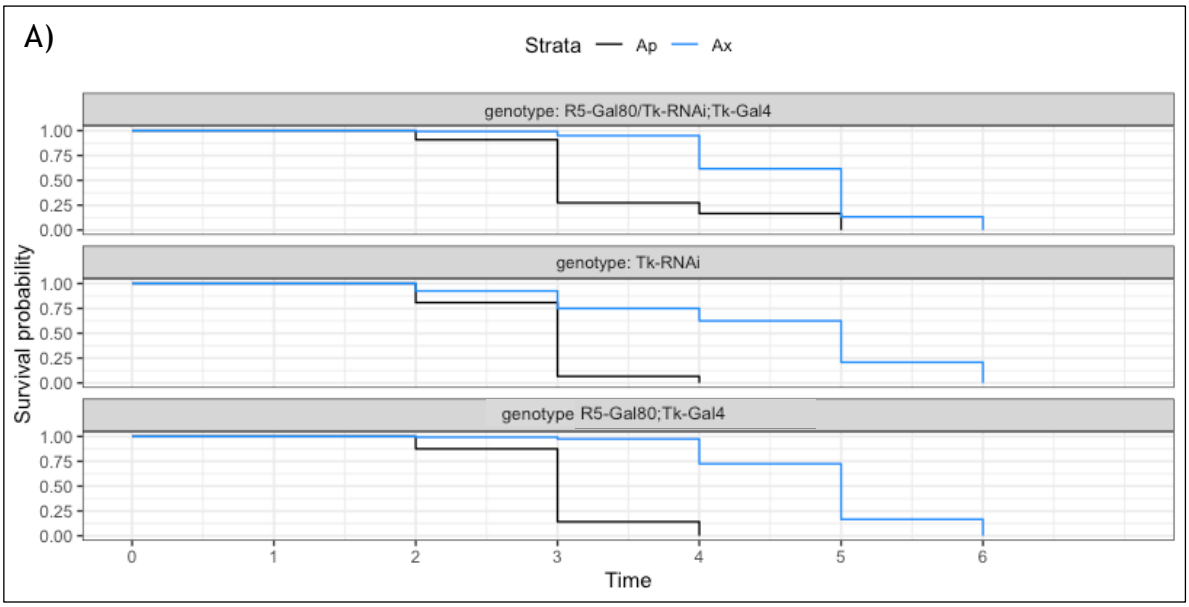

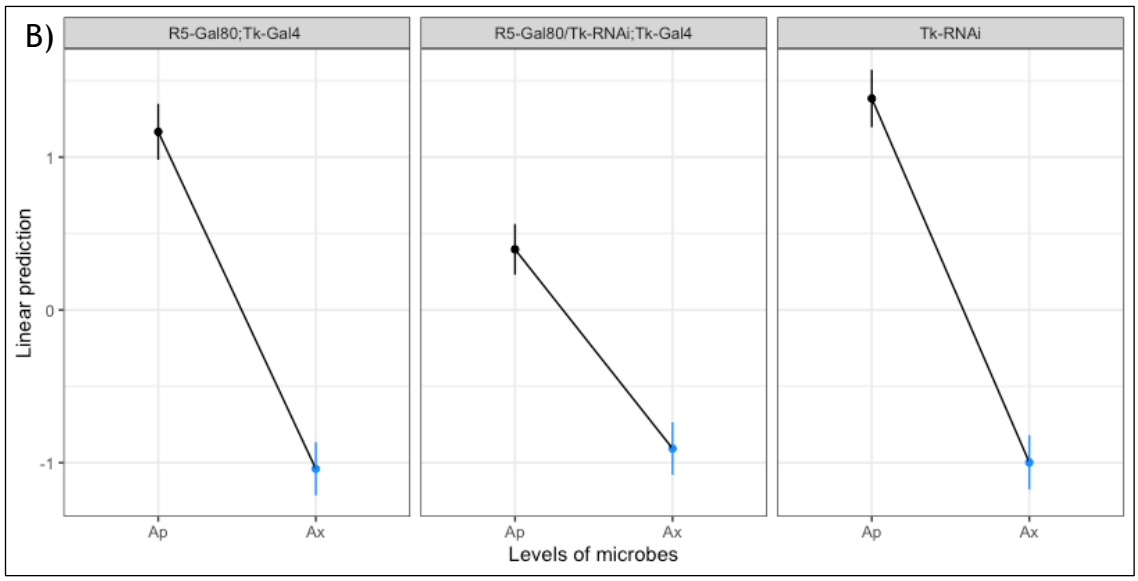

Figure 5.13 Gut specific *TK*^{RNAi} increases starvation resistance.

Starvation resistance in gut specific *TK* knockdown flies (*R5-GAL80/TK-RNAi;TK-GAL4*) compared to *UAS* (*TK-RNAi*) and *GAL80-GAL4* (*R5-GAL80; TK-GAL4*) control flies when they are axenic (black) vs colonised with *A. pomorum* (blue) **(A)** Kaplan-Meier survival curves. Statistical significance determined by analysis of deviance (type III tests) for cox proportional-hazards analysis: Microbes: df = 1, p value 2.2e-16 ***, Genotype: df = 2, p value 9.080e-06 ***, Microbes:Genotype: df = 2, p value 1.239e-08 ***. This was followed by post-hoc joint test (table 5.8). Sample size (females): n=120. **(B)** Interaction plot for estimated marginal means.

Table 5.9 Post-hoc joint test for estimated marginal means testing the interaction between *TK-RNAi* and microbiota for starvation resistance data (Figure 5.12).

contrast	*estimate*	*SE*	*df*	*z.ratio*	*p.value*
(Ap R5-GAL80;TK-GAL4) - (Ax R5-GAL80;TK-GAL4)	2.2060876	0.148243	Inf	14.88147	4.35E-50
(Ap R5-GAL80;TK-GAL4) - (Ap R5-GAL80/TK-RNAi;TK-GAL4)	0.7696327	0.136045	Inf	5.657192	1.54E-08
(Ap R5-GAL80;TK-GAL4) - (Ax R5-GAL80/TK-RNAi;TK-GAL4)	2.0733532	0.146749	Inf	14.12849	2.54E-45
(Ap R5-GAL80;TK-GAL4) - (Ap TK-RNAi)	-0.217828	0.129439	Inf	-1.68286	0.092401
(Ap R5-GAL80;TK-GAL4) - (Ax TK-RNAi)	2.1640409	0.150447	Inf	14.38405	6.52E-47
(Ax R5-GAL80;TK-GAL4) - (Ap R5-GAL80/TK-RNAi;TK-GAL4)	-1.436454	0.134108	Inf	-10.7111	9.03E-27
(Ax R5-GAL80;TK-GAL4) - (Ax R5-GAL80/TK-RNAi;TK-GAL4)	-0.132734	0.129149	Inf	-1.02776	0.304062
(Ax R5-GAL80;TK-GAL4) - (Ap TK-RNAi)	-2.423916	0.150850	Inf	-16.0683	4.25E-58

(Ax R5-GAL80;TK-GAL4) - (Ax TK-RNAi)	-0.042046	0.129367	Inf	-0.32501	0.7451674
(Ap R5-GAL80/TK-RNAi;TK-GAL4) - (Ax R5-GAL80/TK-RNAi;TK-GAL4)	1.3037204	0.133254	Inf	9.783724	1.32E-22
(Ap R5-GAL80/TK-RNAi;TK-GAL4) - (Ap TK-RNAi)	-0.987461	0.137933	Inf	-7.15897	8.13E-13
(Ap R5-GAL80/TK-RNAi;TK-GAL4) - (Ax TK-RNAi)	1.3944081	0.136141	Inf	10.2423	1.28E-24
(Ax R5-GAL80/TK-RNAi;TK-GAL4) - (Ap TK-RNAi)	-2.291182	0.149365	Inf	-15.3394	4.17E-53
(Ax R5-GAL80/TK-RNAi;TK-GAL4) - (Ax TK-RNAi)	0.0906877	0.129600	Inf	0.69974	0.484083
(Ap TK-RNAi) - (Ax TK-RNAi)	2.3818697	0.15295	Inf	15.57231	1.12E-54

5.5 Discussion and conclusions

5.5.1 Suppression of gut *TK* increases both lifespan and starvation resistance

My previous experiments used a more holistic approach via ubiquitous *TK* knockdown. To examine if we could pinpoint these effects to specific tissues, particularly the gut, as it is the interface between microbiota and host, I used a gut specific *TK* knockdown system. The results provide strong evidence that removing *TK* specifically in the EE cells lining the intestine is sufficient to recapitulate the ubiquitous *TK* knockdown phenotype, i.e., to substantially increase lifespan in the presence of *A. pomorum*. This is expected considering the close proximity of commensal microbes with EE cells and the fact that gut peptides were shown to be secreted from those cells in response to microbial by-products. Moreover, this further supports the initial hypothesis that EE cells may act as a relay between microbiota and distal host tissues, modifying release of hormones into circulation in response to by-products of gut microbiota. Nevertheless, considering that tachykinin receptors are expressed both in the gut and CNS, it remains to be explored whether *TK* acts locally or systemically through the gut-brain axis to induce its pro-ageing effect in response to microbes. This will be investigated in chapter 6.

Furthermore, one of the most striking findings in this chapter is that gut-targeted *TK* knockdown does not have a detrimental impact on axenic flies and it even increases the resistance to food shortage in *A. pomorum* mono-colonised

flies. This is contrary to the global *TK* knockdown results which led to a significant decrease in starvation resistance in axenic, conventional and *A. pomorum* colonised flies. *A. pomorum* gnotobiotes are still more sensitive to starvation compared to axenic flies, which could be attributed to the fact that axenic flies have increased fat reserves. Although, gut TK^{RNAi} does not fully rescue the decreased starvation resistance of *A. pomorum* mono-colonised flies it nevertheless has a highly significant positive impact on their ability to respond to acute nutritional stress. Overall, this suggests that gut specific *TK* knockdown not only increases lifespan duration, but also potentially improves lifespan content (healthspan). However, besides starvation resistance, other healthspan indicators, such as, sleep, gut permeability, metabolic rate or telomere length should be investigated to better understand the health status of those long-lived specimens.

5.5.2 Gut microbes impact lipid metabolism through the *TK*-gut-brain system

In terms of lipid metabolism, the results indicate that gut-targeted *TK* knockdown in *A. pomorum* mono-colonised flies does not recapitulate the increased adiposity phenotype following global knockdown, suggesting that brain-derived *TK* plays a role in lipid metabolism. This is inconsistent with a previous study published by Song et al., 2014 showing that gut *TK* controls lipid production locally in the gut, without signalling to the brain via circulation. However, their study explores the interplay between *TK* and intestinal lipid homeostasis in flies that harbour a full, unaltered microbiota, while my approach focuses on the interaction between *TK* and microbes (here specifically *A. pomorum*), and the impact of this interplay on biological processes such as lipid metabolism. Furthermore, it is known that gut microbial community impacts both lipid metabolism and neuropeptide function (Holzer and Farzi, 2014). Thus, a possible explanation could be that in the presence of *A. pomorum* only gut-derived *TK* is not sufficient to regulate lipid metabolism.

On the other hand, the TAG phenotype in axenic flies is consistent between gut targeted and ubiquitous *TK* knockdown. This implies that the metabolic shift observed related to axenia relies on gut-derived *TK*. In conclusion, gut microbes

seem to play a central role in controlling the lipid metabolism through the *TK*-gut-brain system. However, considering that we do notice a genotype effect in the control groups, this experiment should be repeated in order to make more plausible conclusions. Furthermore, to better understand the complex interaction between *TK* and the microbiota-gut-brain axis, lipid levels should be measured in both gut and brain specific *TK* knockdown in conventional, *A. pomorum* gnotobiotic and axenic flies.

5.5.3 Suppression of gut *TK* recapitulates the global knockdown feeding phenotype, but not the egg laying phenotype

Considering that my previous findings in chapter 4 indicated that feeding and egg laying respond to full unaltered microbiota, but not to specific gnotobiotas, I decided to test the effects of gut specific *TK*-knockdown on conventional flies compared to axenic flies. The results revealed that suppression of gut *TK* recapitulates the ubiquitous knockdown phenotype, suggesting that the feeding response is gut specific. Previous studies, exploring different gut peptides such as *NPF* (Malita et al., 2022) or *AstC* (Kubrak et al., 2022) demonstrated that those peptides regulate food intake and preference as well as metabolic homeostasis in a gut specific manner. Moreover, it has been previously shown that tachykinin controls glucose satiety and regulates glucose – fructose preference in response, however relying neuropeptidergic signalling by tachykinin (Musso et al., 2021). Future experiments should further investigate *TK* and microbiota-gut-brain axis effects on food preferences and satiety. Lastly, the gut specific knockdown does not recapitulate the ubiquitous knockdown phenotype, suggesting that *TK* in the brain also controls the reproduction response.

Table 5.10. Summary of the phenotypic effects of gut specific *TK* knockdown.

Phenotype	*A. pomorum*	*Conventional*	*Axenic*	*Recapitulates ubiquitous TK^{RNAi}?*
Lifespan	Strongly increases lifespan	N/A	Not significant	YES
TAG	Inconclusive	N/A	Inconclusive	Inconclusive

Egg laying	N/A	Increases egg laying	Decreases egg laying	NO
Feeding	N/A	Increases feeding behaviour	Decreases feeding behaviour	YES
Starvation	Increases starvation resistance	N/A	Not significant	NO

Chapter 6
6.1 Summary

Despite the complexity of ageing, simple genetic manipulations can increase lifespan and improve healthspan in model organisms. My findings established specific Tachykinin knockdown as a novel genetic intervention that leads to lifespan extension downstream of the microbiota. The upstream regulation of this system is dependent on the intestinal commensal microbes. In this chapter, I demonstrate that in order to achieve lifespan modulation, the bacterium *A. pomorum* regulates *TK* expression, which then targets its receptor *TKR99D* in the brain. Characterization of IIS signalling, such as *4E-BP* expression and Akt phosphorylation, suggests an interplay between microbes, tachykinin and insulin signalling. Ablation of insulin producing cells phenocopies the tachykinin knockdown lifespan phenotype. Regulation of lifespan by reduced insulin signalling is largely dependent on the Forkhead box-O transcription factor, *dFOXO*. However, knockdown of tachykinin in null-*dFOXO* mutants showed that, while *dFOXO* is required for *TK* to modulate lifespan, it is not required for microbial lifespan regulation. Overall, this suggests that other interacting mechanisms are likely to be involved. I have then tested the role of AKH, the fly ortholog of mammalian glucagon, because of the interaction I have previously characterised between fly metabolism, *TK*, and microbiota, but the results did not support a role between this second signalling axis and longevity. Overall, these findings contribute to the understanding of the intricate relationship between *TK* signalling and microbiota and provide avenues for future research in unravelling the underlying biological mechanisms involved.

6.2 Introduction

6.2.1 Tachykinin receptors: cross-reactivity between mammals and flies?

In humans, there are three tachykinin receptors (NK1R, NK2R and NK3R). NK1R is the main receptor, with substance P as the cognate ligand. Substance P has been indicated as having a wide variety of functions and has been implicated in several disease states such as depression, migraine, IBS, asthma and pain disorders (Harrison, 2001). Notably, NK1R antagonists have been developed and are utilised as antiemetics for managing nausea and vomiting associated with chemotherapy treatment (Chen et al., 2019). The overexpression of NK1R and excessive signalling through Substance P and NK1R have been correlated with poor prognosis in cancer patients, prompting research into the potential use of antagonists for anticancer applications (Majkowska-Pilip et al., 2019).

In the realm of human tachykinin receptors, there is demonstrated cross-reactivity in substrate binding across all receptors, albeit with varying affinities (Page, 2005). Numerous efforts have been made to comprehend the binding mechanism and domains of NK1R and substance P, leading to the identification of several key structures (Boyd et al., 1996, Lequin et al., 2002, Alves et al., 2006, Chen et al., 2019). While the binding domains of the NKRs are not entirely characterized, Ehrenmann et al. (2021) identified crucial residues involved in this cross-reactivity. Interestingly, similarities exist between these residues and their counterparts in fly and mouse receptor sequences (Figure 6.1). Furthermore, it has been established that certain NKR1 receptor antagonists exhibit cross-reactivity in humans, rats, guinea pigs, rabbits, and hamsters (Advenier et al., 1992).

Figure 6.1 Aligned peptide sequences of the human and mouse *NKR1-3*, and the *Drosophila NKD* and *DTKR*.

Highlighted residues were found to form the C terminus binding pocket in human NK1R. Residues highlighted in pink form a hydrophobic subpocket. Residues highlighted in blue are involved in hydrophobic interactions with Phenylalanine and Leucine of Substance P C terminus. Residues highlighted in yellow interact with Leucine in C terminus of substance P. Residues highlighted in green form stabilising hydrogen bonds with substance P (Figure produced by Miriam Wood).

6.2.3 *Drosophila* tachykinin receptors

The *Drosophila* genome encodes two cognate tachykinin receptors: *TKR99D* (*DTKR*) and *TKR86C* (*NKD*) (Birse et al., 2006). The Drosophila tachykinin (*dTK*) gene encodes a prepro-Tachykinin that is processed into six mature tachykinin peptides (D*TK*s) (Siviter et al., 2000). All six D*TK*s can activate *TK*R99D, increasing cytoplasmic Ca2+ and cAMP levels (Birse et al., 2006). In Drosophila, D*TK*s regulates gut contractions (Siviter et al., 2000), enteroendocrine homeostasis (Amcheslavsky et al., 2014; Song et al., 2014), stress resistance (Kahsai et al., 2010a; Soderberg et al., 2011), olfaction (Ignell et al., 2009), locomotion (Kahsai et al., 2010b), aggressive behaviours (Asahina et al., 2014), pheromone detection in gustatory neurons (Shankar et al., 2015), nociception

(Im et al., 2015), fructose preference (Musso et al., 2021), satiety, feeding behaviour and regulation of energy homeostasis (Qi et al., 2021). Of the 6 peptides encoded by the *TK* locus *TK*-6 is the only one known to activate NKD (Poels et al., 2009). The functions of NKD are less studied and understood, being mostly associated with developmental processes (Birse et.,al 2006) and complex behaviours such as aggression (Wohl et al., 2023). *NKD* is expressed in the CNS and ventral nerve cord (thoracico-abdominal ganglions), while *DTKR* is mostly expressed in the CNS, also exhibiting lower expression in the crop and heart (Figure 6.2). In conclusion, the intricate roles of D*TK*s and its receptors, highlight their diverse functions in various physiological and behavioural processes.

Importantly, previous research revealed that *DTKR* is expressed in insulin producing cells (IPCs) in the brain, and targeted knockdown of the receptor in those cells leads to increased insulin signalling, thus suggesting that *DTKR* inhibits insulin signalling in the brain IPCs (Birse et al., 2011). Moreover, the ablation of IPCs was shown to extend median and maximal lifespan and increase resistance to oxidative stress and starvation (Broughton et al., 2005). However, this was also associated with altered metabolism, such as increased fasting glucose levels and increased storage of lipids and carbohydrates (Broughton et al., 2005). Therefore, understanding the role of *DTKR* in inhibiting insulin signalling in brain IPCs could provide valuable insights into the molecular mechanisms that may influence ageing. Further exploration of the interactions between *DTKR*, insulin signalling, and the ageing process could contribute to the development of strategies for modulating ageing and age-related diseases.

	Adult Male		Adult Female	
Tissue	FPKM	Enrichment	FPKM	Enrichment
Head	1.3	N.A.	1.5	N.A.
Eye	0.2	N.A.	0.3	N.A.
Brain / CNS	3.8	1.9	3.9	1.9
Thoracicoabdominal ganglion	2.6	1.3	3.2	1.6
Crop	0.0	N.A.	0.0	N.A.
Midgut	0.0	N.A.	0.0	N.A.
Hindgut	0.0	N.A.	0.0	N.A.
Malpighian Tubules	0.2	N.A.	0.7	N.A.
Fat body	0.0	N.A.	0.0	N.A.
Salivary gland	0.0	N.A.	0.0	N.A.
Heart	0.0	N.A.	0.0	N.A.
Trachea				
Ovary			0.0	N.A.
Virgin Spermatheca			0.0	N.A.
Mated Spermatheca			0.0	N.A.
Testis	0.6	N.A.		
Accessory glands	0.0	N.A.		
Carcass	0.1	N.A.	0.1	N.A.
Rectal pad	0.0	N.A.	0.0	N.A.
Garland cells				

	Adult Male		Adult Female	
Tissue	FPKM	Enrichment	FPKM	Enrichment
Head	1.8	N.A.	1.5	N.A.
Eye	0.5	N.A.	0.5	N.A.
Brain / CNS	4.5	2.2	4.0	2.0
Thoracicoabdominal ganglion	1.8	N.A.	1.8	N.A.
Crop	2.2	1.1	1.4	N.A.
Midgut	1.9	N.A.	0.2	N.A.
Hindgut	0.8	N.A.	0.6	N.A.
Malpighian Tubules	0.7	N.A.	0.7	N.A.
Fat body	0.7	N.A.	0.2	N.A.
Salivary gland	0.8	N.A.	0.2	N.A.
Heart	2.6	1.3	1.8	N.A.
Trachea				
Ovary			0.0	N.A.
Virgin Spermatheca			0.0	N.A.
Mated Spermatheca			0.0	N.A.
Testis	0.5	N.A.		
Accessory glands	0.0	N.A.		
Carcass	0.3	N.A.	0.2	N.A.
Rectal pad	1.0	N.A.	1.0	N.A.
Garland cells				

Figure 6.2 Tissue expression of the cognate tachykinin receptors *NKD* (left) and *DTKR* (right).

Data generated with FlyAtlas2.

6.2.2 IIS signalling in *Drosophila*

The IIS signalling network has demonstrated a conserved role in ageing, spanning from yeast to mammals, and seemingly encompassing humans (Flachsbart et al., 2009; Giannakou and Partridge, 2007). In *Drosophila*, manipulating the activity of various components of this network has been shown to positively influence lifespan and enhance locomotor and cardiac functions during the ageing process (Partridge et al., 2011). The determination of lifespan in *Drosophila* involves intricate interactions between the brain, fat body (equivalent to the mammalian liver and white adipose tissue), and the germ line, showcasing substantial communication between different tissues (Piper and Partridge, 2018). Processes such as cellular detoxification pathways, increased autophagy, and modified protein synthesis have all been implicated in the extension of lifespan resulting from reduced IIS activity (Gems and Partrige, 2012; Fontana et al., 2010; Hwangbo et al., 2004; Rubinsztein et al., 2011). The reduction in insulin signalling can exert an acute effect in lowering the mortality rate, suggesting that it may mitigate the consequences of age-related damage rather than preventing its occurrence outright (Tatar et al., 2003).

The *Drosophila* IIS pathway includes seven insulin-like molecules (DILP1–DILP7) (Grönke et al., 2010). DILPs are predicted structurally to be similar to human insulin and are thus considered to be insulin orthologues. There is a single Drosophila insulin receptor, dINR, which transduces the signal from the DILPs to the PI3-kinase, through the single Drosophila insulin receptor substrate, CHICO (Oldham and Hafen, 2003). Dp110 is the catalytic subunit and Dp60 is the regulatory subunit of PI 3-kinase, which converts phosphatidylinositol (4,5)-bisphosphate [PtdIns(4,5)P2] to phosphatidylinositol (1,4,5)-trisphosphate [PtdIns(1,4,5)P3]. The action of PI 3-kinase is antagonised by dPTEN, which dephosphorylates PtdIns(4,5)P2 to PtdIns(1,4,5)P3 (PIP3). The intracellular second messenger PIP3 plays a pivotal role in the signal transduction by binding to specific kinases and bringing them close to their substrates, facilitating the

phosphorylation and activation of downstream signalling molecules, including PKB (Akt) which ultimately phosphorylates the transcription factor *dFOXO* (Partridge et al., 2011; Puig et al., 2003), leading to its inactivation and translocation to the cytoplasm. As a transcription factor, *dFOXO* regulates the expression of multiple genes, including the translation initiation factor 4E (eIF4E)-binding protein (4E-BP) which maintains proteostasis, decreases feeding, and reduces insulin secretion, thereby altering systemic metabolism and extending lifespan (Chatterjee and Perrimon, 2021).

6.3 Aims

Why should *TK* knockdown extend lifespan? As an endocrine signal, *TK* presumably mediates a relay between the gut and other tissues. The tachykinin receptor *DTKR* was shown to be expressed in IPCs in the brain (Birse et al., 2011). This was noteworthy because downregulating IIS signalling has a conserved effect of extending lifespan in flies, mice and nematodes (Broughton et al., 2005, Selman et al., 2008, Kenyon et al., 1993). Therefore, the main aims of this chapter are to investigate: 1) the tachykinin receptors and target tissues controlling lifespan via microbiota and 2) the downstream consequences of tachykinin signalling on systemic IIS signalling and 3) the link between tachykinin, microbiota and IIS.

6.4. Results

6.4.1 Brain *DTKR*-RNAi extends lifespan in the presence of *A. pomorum*

In *Drosophila* there are two main receptors for tachykinin: *TKR99D* (*DTKR*) and *TKR86C* (*NKD*) (Birse et al., 2006). Considering the vast physiological roles of *DTKR* in regulating metabolism and insulin signalling I hypothesised that tachykinin signals through *DTKR* in the brain to regulate lifespan downstream of the microbiota. Therefore, I tested the effect of *DTKR* knockdown in the brain using a brain specific driver (*ElavGS*) (Figure 6.3). The results indicate that knocking down *DTKR* in the brain significantly extends lifespan in flies colonised with *A. pomorum*, but not axenic flies. This recapitulates our *TK* knockdown

results, thus confirming our hypothesis. Moreover, I tested the effect of the *NKD* receptor knockdown in the brain (Figure 6.4). In those flies the knockdown does not induce lifespan extension in the presence of microbes, suggesting that *NKD* is not required for microbial regulation of lifespan. However, unexpectedly, the results also indicate that *NKD* suppression in the brain blocks the longevity effect of axenia. More exactly, axenic *NKD* RNAi+ flies exhibit shorter lifespan, similar to *A. pomorum* colonised flies. This confirms that *TK* is required for the microbiota to modulate lifespan, suggesting potential compensatory mechanisms between the two receptors. In conclusion, the observed significant lifespan extension upon *DTKR* knockdown underscores the pivotal role of this receptor in mediating the impact of *TK* signalling on longevity.

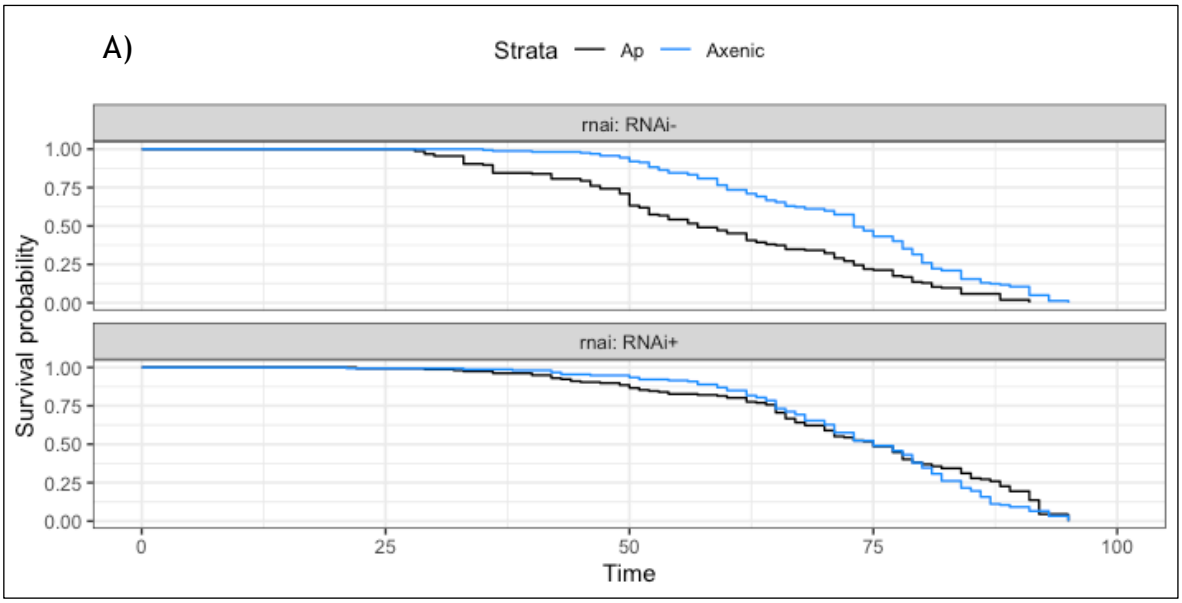

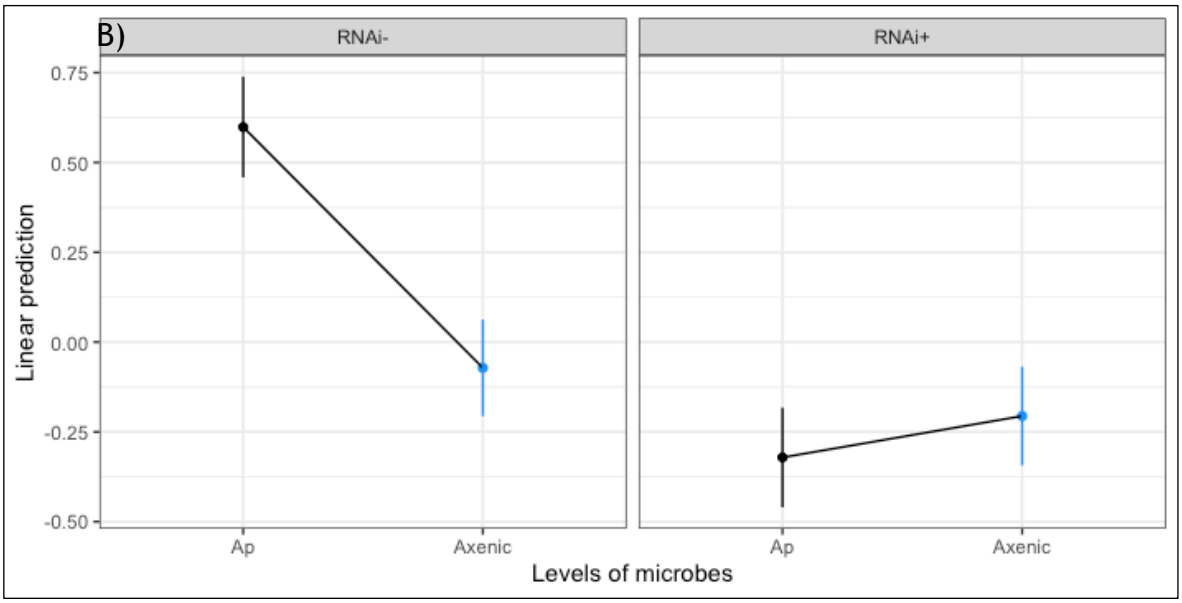

Figure 6.3 Knockdown of *DTKR* in the brain extends lifespan in the presence of *A. pomorum*.

A) Kaplan-Meier survival curves in brain specific *ElavGS>Uas-DTKR-RNAi* knock-down flies (RNAi+) versus control flies (RNAi-) in gnotobiotic flies colonised with Acetobacter pomorum (Ap) or germ-free (Axenic) flies. Statistical significance determined by cox proportional-hazards analysis: Microbes: p value 0.0005639 ***, RNAi: p value 1.326e-10 ***, Microbes:RNAi: p value 1.361e-06 ***. Sample size (females): n=150. This was followed by pairwise comparisons for estimated marginal means between *TK* knockdown and microbial condition (values shown in table 6.1). (B) Interaction plot for estimated marginal means.

Table 6.1 Pairwise comparisons for estimated marginal means testing the interaction between *TK-RNAi* and microbiota for *ElavGS>Uas-DTKR-RNAi* lifespan data (Figure 6.1).

Control samples are labelled with (RNAi-) and knockdown samples labelled with (RNAi+). Microbial conditions are: *A.pomorum* gnotobiotic flies (Ap) and Axenic flies.

contrast	*estimate*	*SE*	*df*	*z.ratio*	*p.value*
(Ap RNAi-) - (Axenic RNAi-)	0.670437	0.113646	Inf	5.89933193	3.65E-09
(Ap RNAi-) - (Ap RNAi+)	0.919739	0.117266	Inf	7.84314969	4.39E-15
(Ap RNAi-) - (Axenic RNAi+)	0.804418	0.115965	Inf	6.93668589	4.01E-12
(Axenic RNAi-) - (Ap RNAi+)	0.249301	0.113293	Inf	2.20049041	0.027772
(Axenic RNAi-) - (Axenic RNAi+)	0.133980	0.112963	Inf	1.18605192	0.235601
(Ap RNAi+) - (Axenic RNAi+)	-0.11532	0.1145936	Inf	-1.0063441	0.3142500

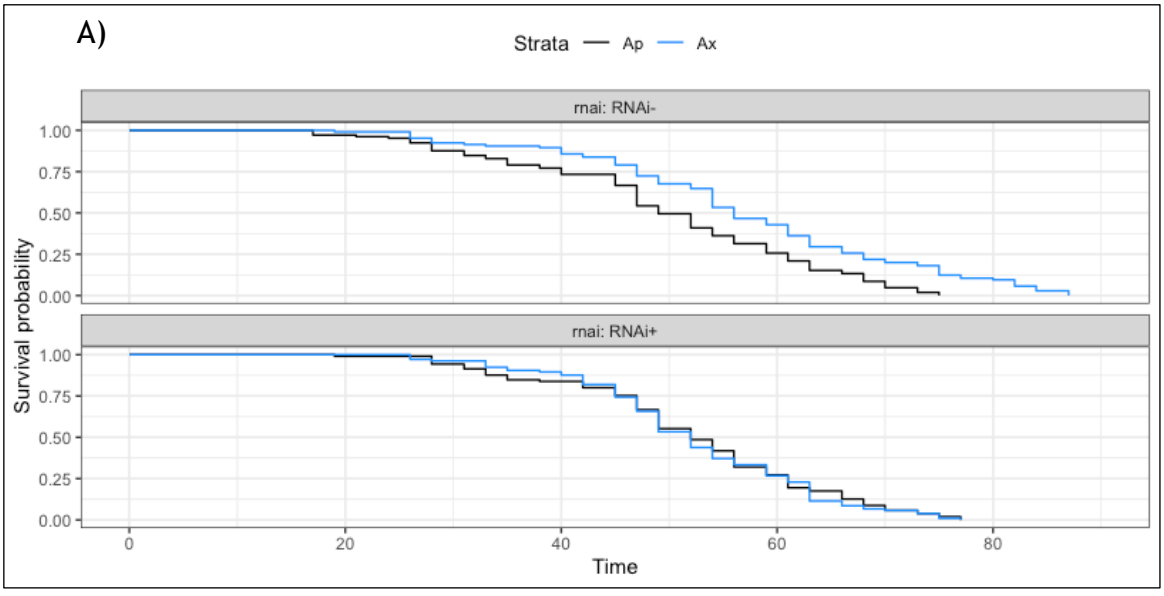

B)

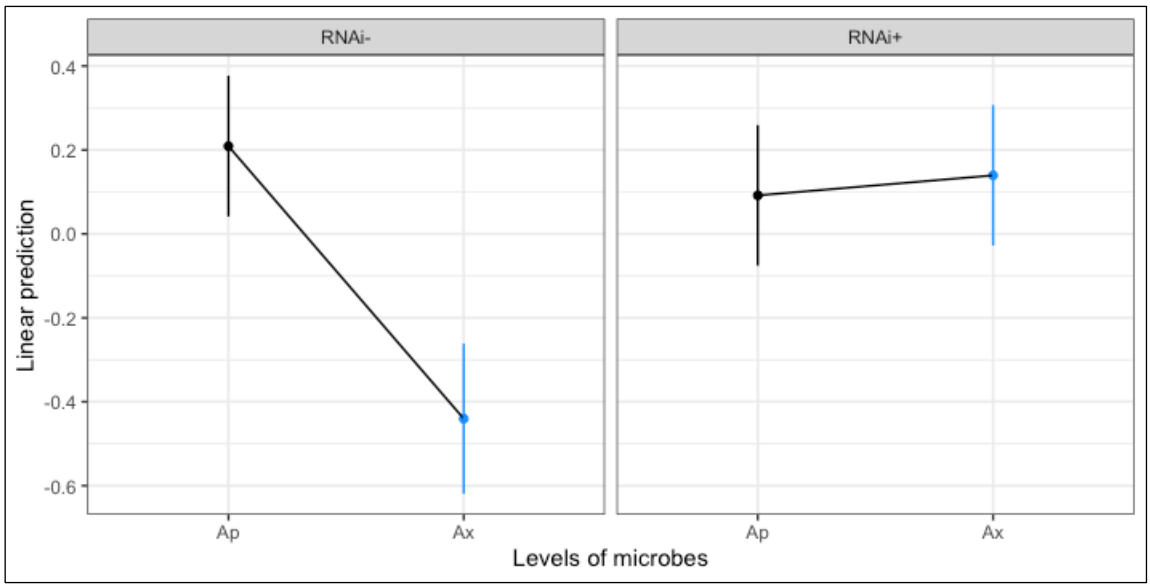

Figure 6.4 Knockdown of *NKD* in the brain does not extend lifespan in the presence of microbes, but it blocks lifespan extension in axenic flies.

A) Kaplan-Meier survival curves in brain specific *ElavGS>Uas-NKD-RNAi* knockdown flies (RNAi+) versus control flies (RNAi-) in gnotobiotic flies colonised with Acetobacter pomorum (Ap) or germ-free (Axenic) flies. Statistical significance determined by cox proportional-hazards analysis: Microbes: p value 0.0027212 **, RNAi: p value 0.0209593 *, Microbes:RNAi: p value 0.0005408 ***. Sample size (females): n=105.This was followed by pairwise comparisons for estimated marginal means between *TK* knockdown and microbial condition (values shown in table 6.2). (B) Interaction plot for estimated marginal means.

Table 6.2 Pairwise comparisons for estimated marginal means testing the interaction between *TK-RNAi* and microbiota for *ElavGS>Uas-NKD-RNAi* lifespan data (Figure 6.2).

Control samples are labelled with (RNAi-) and knockdown samples labelled with (RNAi+). Microbial conditions are: *A.pomorum* gnotobiotic flies (Ap) and Axenic flies.

contrast	*estimate*	*SE*	*df*	*z.ratio*	*p.value*
(Ap RNAi-) - (Ax RNAi-)	0.649458	0.145966	Inf	4.44936871	8.61E-06
(Ap RNAi-) - (Ap RNAi+)	0.117333	0.138495	Inf	0.84720325	0.396881
(Ap RNAi-) - (Ax RNAi+)	0.069625	0.138197	Inf	0.50381009	0.614394
(Ax RNAi-) - (Ap RNAi+)	-0.53212	0.145357	Inf	-3.6608028	0.000251
(Ax RNAi-) - (Ax RNAi+)	-0.57983	0.145638	Inf	-3.9813011	6.85E-05
(Ap RNAi+) - (Ax RNAi+)	-0.04770	0.138448	Inf	-0.3445934	0.7304

6.4.2 Ablation of insulin producing neurons phenocopies the *TK* knockdown phenotype

Reduced insulin/IGF1 signalling is known to extends lifespan in mice, worms and flies (Selman et al., 2008, Clancy et al., 2001, Kenyon et al., 1994). In flies, *Drosophila* insulin like peptides (Dilps) activate the insulin receptor (dInR) which relays the signal to Akt kinase. Akt phosphorylates the transcription factor FOXO, thus decreasing its output. FOXO regulates genes involved in metabolism, cellular proliferation, stress resistance, and apoptosis. Downregulation of any components of the pathway upstream FOXO results in lifespan extension (Piper et al 2011). Based on the fact that *TK – DTKR* was shown to regulate insulin producing cells (IPCs) in the brain (Nassel et. al, 2011), I hypothesised that insulin signalling plays a role on the effects of *TK* on lifespan. Insulin producing cells can be ablated by expressing the proapoptotic *Reaper* (*Rpr*) under control of the *Dilp2* promoter, which robustly and repeatably extends lifespan (Broughton et al., 2005; Saud et al., 2015). In figure 6.5 I ablated the IPCs using the *DilpGS* to drive the expression of the pro-apoptotic gene Reaper specifically in IPCs and tested the effect of ablation on lifespan in *A. pomorum* gnotobiotic and axenic flies. The results phenocopy the *TK* knockdown and *DTKR* knockdown models.

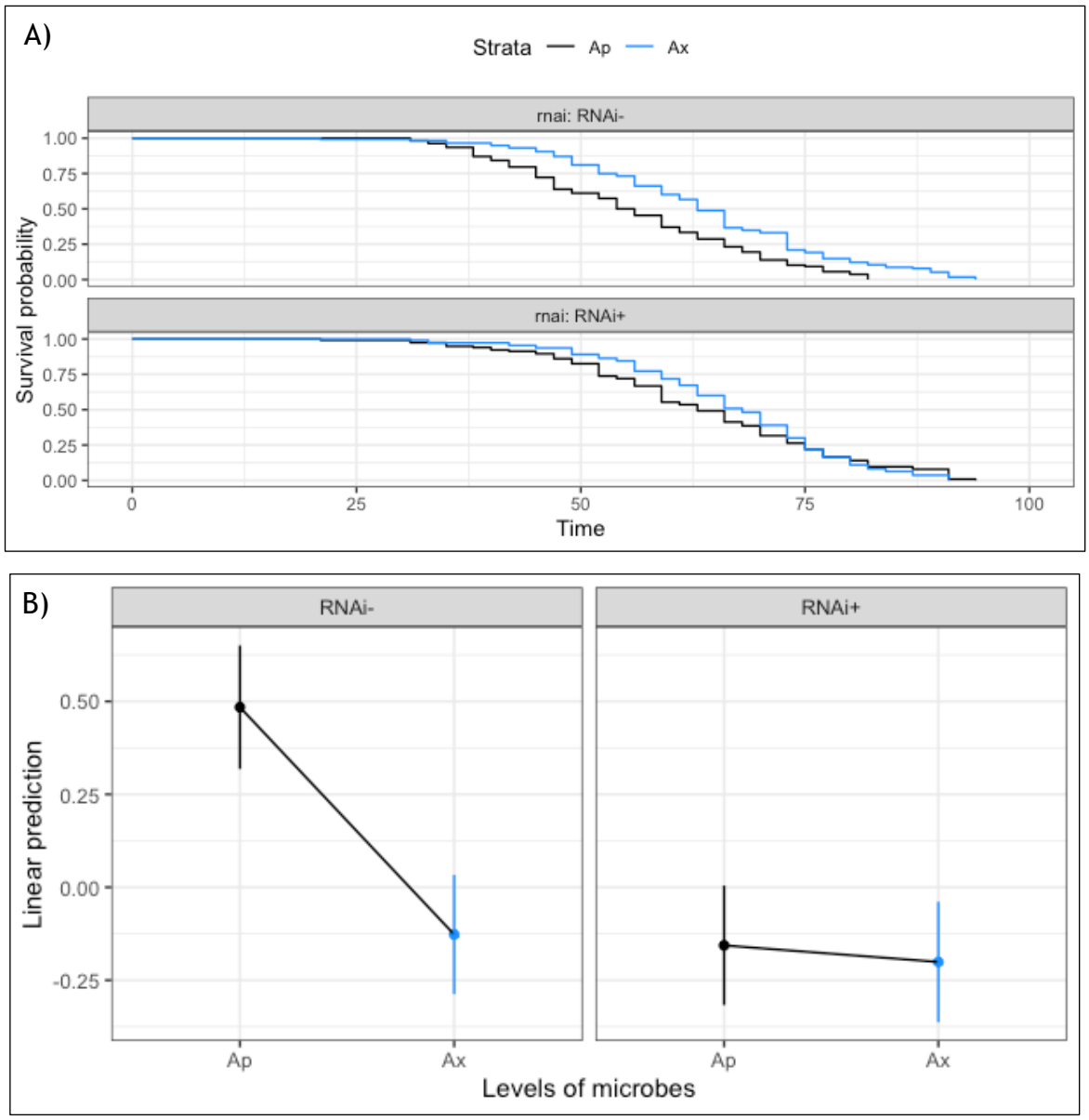

Figure 6.5 Ablation of insulin producing neurons phenocopies the *TK* knockdown phenotype.

A) Kaplan-Meier survival curves in flies that have ablated IPCs using the *DilpGS* to drive the expression of the pro-apoptotic gene *Repear* specifically in IPCs. The graph compares IPCs ablated flies (RNAi+) versus control flies (RNAi-) in gnotobiotic flies colonised with *Acetobacter pomorum* (Ap) or germ-free (Axenic) flies. Statistical significance determined by cox proportional-hazards analysis: Microbes: p value 0.0005782 ***, RNAi: p value 0.0001848 ***, Microbes:RNAi: p value 0.0034035 **. Sample size (females): n=135. This was followed by pairwise comparisons for estimated marginal means between *TK* knockdown and microbial condition (values shown in table 6.3). (B) Interaction plot for estimated marginal means.

Table 6.3 Pairwise comparisons for estimated marginal means testing the interaction between *TK*-RNAi and microbiota for DilpGS>Uas-Reaper lifespan data (Figure 6.3).

Control samples are labelled with (RNAi-) and knockdown samples labelled with (RNAi+). Microbial conditions are: *A.pomorum* gnotobiotic flies (Ap) and Axenic (Ax) flies.

contrast	*estimate*	*SE*	*df*	*z.ratio*	*p.value*
(Ap RNAi-) - (Ax RNAi-)	0.611432	0.1367145	Inf	4.4723260	7.74E-06
(Ap RNAi-) - (Ap RNAi+)	0.640723	0.1371288	Inf	4.6724173	2.98E-06
(Ap RNAi-) - (Ax RNAi+)	0.685262	0.1368104	Inf	5.0088469	5.48E-07
(Ax RNAi-) - (Ap RNAi+)	0.029291	0.1323675	Inf	0.2212869	0.824869
(Ax RNAi-) - (Ax RNAi+)	0.073830	0.1343041	Inf	0.5497265	0.582506
(Ap RNAi+) - (Ax RNAi+)	0.044539	0.1343840	Inf	0.3314331	0.740317

6.4.3 Potential mechanisms – Insulin/IGF1 (IIS) signalling H

I further tested the expression of *Thor* (*4E-BP*) (Figure 6.6) in *TK* knockdown flies colonised with Ap vs axenic flies. Thor functions as a metabolic brake used under stress conditions and is activated by *FOXO*. The results indicate that microbial condition does not have a significant effect on Thor expression levels (p value = 0.88408). However, *TK* knockdown has a significant impact (p value = 0.01235). More exactly, when *TK* is supressed, Thor levels increase in Ap flies, but not in Ax flies. This suggests that knocking down *TK* in the presence of Ap downregulates IIS, which results in increased *FOXO* levels and thus increased Thor expression.

This is further confirmed by analysing the protein levels of phosphorylated Akt (active form of Akt) (Figure 6.7). In Ap colonised flies, *TK* knockdown decreases phospho-Akt levels, this would indicate higher FOXO and longer lifespan, which fits our observed phenotypes. Similarly, axenic RNAi- flies have lower phospho-Akt and increased lifespan. However, knocking down *TK* in axenic flies resulted in higher Akt levels, which does not explain their long lifespan. Nevertheless, the results indicate that the interaction between *TK* and *A. pomorum* plays a significant role in regulating P-Akt protein levels (p value = 0.000398). Overall, our results indicate that IIS likely play a role in regulating the lifespan effects of *TK*, but other mechanisms might also be involved.

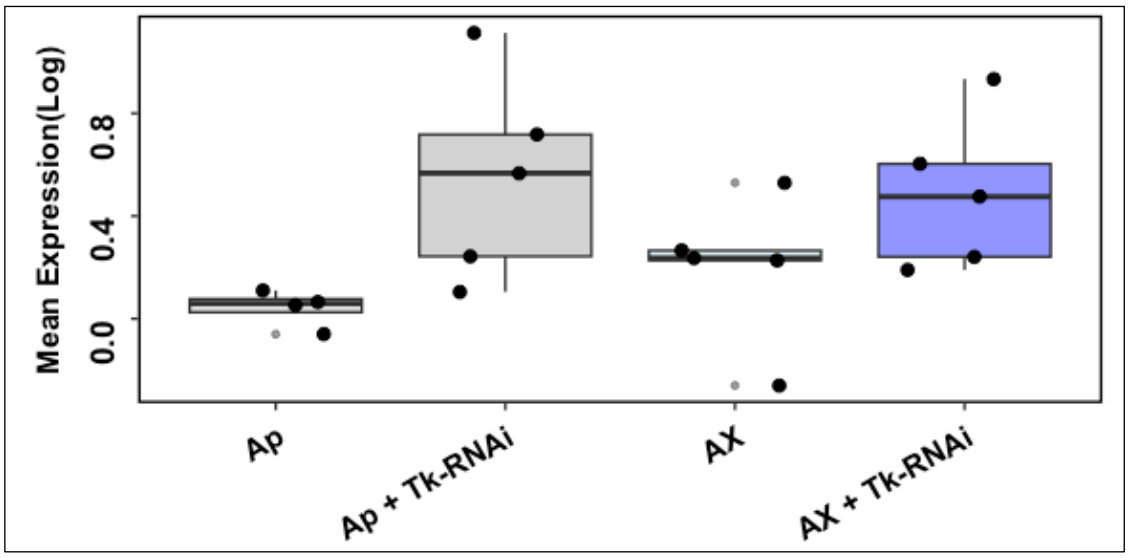

Figure 6.6 Gene expression of the translational repressor *Thor* (*4E-BP*) is regulated by *A. pomorum*.

Mean fold change in whole-fly gene expression of *Thor* in ubiquitous *TK* knockdown flies (*TK-RNAi*) when their microbiota is axenic versus mono-colonised with *A. pomorum*. Statistical significance determined by two-way ANOVA testing the interaction between microbes and RNAi (Microbes: p value = 0.88408, RNAi: p value = 0.01235 *, Microbes:RNAi: p value = 0.44210. (n=4 AP RNAi-, n=5 AP RNAi+, n=5 AX RNAi-, N=5 AX RNAi+; each sample containing 15 flies). Box plots show median values, first and third quartiles, and 5th and 95th percentiles. Jitter plots show individual data points. Genotype: *DaGS>Uas-TK-RNAi*.

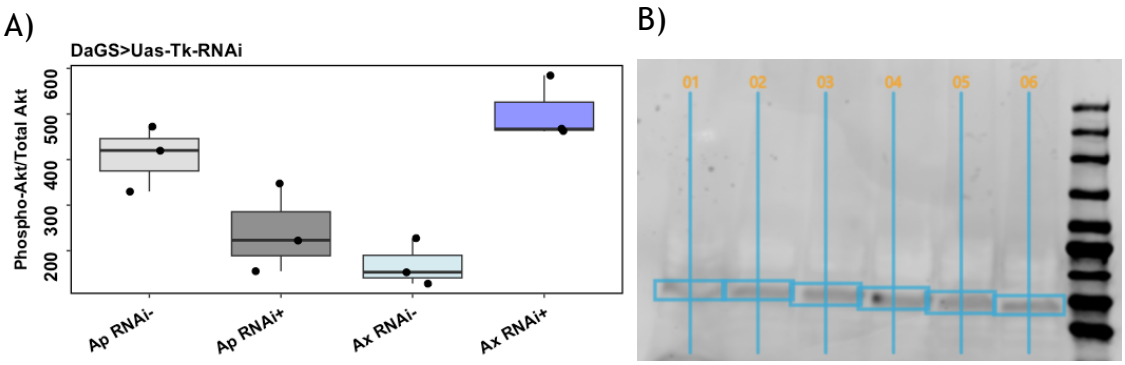

Figure 6.7 The interaction between *TK* and *A. pomorum* impacts phospho-Akt protein levels.

A) Protein levels of phosphorylated Akt normalised to total Akt in *TK*-knockdown flies (RNAi+) compared to control flies (RNAi-) when they are axenic (blue) or colonised with *A. pomorum*. Statistical significance determined by two-way ANOVA testing the interaction between microbes and RNAi: (Microbes: p value =

0.88408, RNAi: p value = 0.01235 *, Microbes: p value 0.781790, RNAi: p value = 0.083773, Microbes:RNAi: p value 0.000398 *** (n=3 samples/condition). Box plots show median values, first and third quartiles, and 5th and 95th percentiles. Jitter plots show individual data points. Genotype: *DaGS>Uas-TK-RNAi*. B) Representative western blot image of Phospho-Akt

6.4.4 FOXO is required for *TK* to modulate lifespan, but not required for microbiota to modulate lifespan

To better understand the mechanistic basis of lifespan extension following *TK* knockdown and the role of IIS, I looked at the effect of ubiquitous *TK* knockdown on lifespan in mutants harbouring a null allele of *dFOXO* (*Dags/TK-RNAi;FOXOdelta* - Figure 6.8). Previous studies showed that mutation of *dFOXO* almost completely blocks IIS-dependent lifespan extension interventions (Slack et al., 2011). However, null *dFOXO* mutants did not recapitulate other IIS-mediated phenotypes such as: developmental delay, small body size, reduced egg laying or resistance to oxidative stress, suggesting that additional factors besides *dFOXO* mediate the full IIS response have evolved in *Drosophila* (Slack et al., 2011).

Considering the premises that 1) *TK* mediates the effect of microbiota on lifespan and 2) the interaction between microbiota and *TK* requires IIS and thus *dFOXO* to regulate lifespan, the expected results were that *TK* knockdown, as well as microbiota depletion, will not lead to extended lifespan in a null-*dFOXO* mutant background (Slack et al., 2011). However, the results indicate that *dFOXO* is required for *TK* to modulate lifespan and lifespan extension following *TK* knockdown in *A. pomorum* flies is blocked in null-*dFOXO* mutants (contrast: AP *Dags/TK-RNAi; FOXOdelta* RNAi- vs AP *DaGS/TK-RNAi; FOXOdelta RNAi+*: p value = 0.9999996 – Table 6.4). Unexpectedly, *dFOXO* axenic flies are significantly longer lived than *A. pomorum* mono-colonised flies (contrast: AP *DaGS/TK-RNAi; FOXOdelta RNAi-* vs AX *DaGS/TK-RNAi; FOXOdelta RNAi-*: p value = 1.70E-05), suggesting that *dFOXO* is not required for microbiota to regulate lifespan. Overall, this indicates that while *dFOXO* is required for *TK* to modulate lifespan, the effect of microbiota does not rely on *dFOXO*. In conclusion, other

interacting mechanisms are likely to be involved since this cannot fully explain our phenotypes.

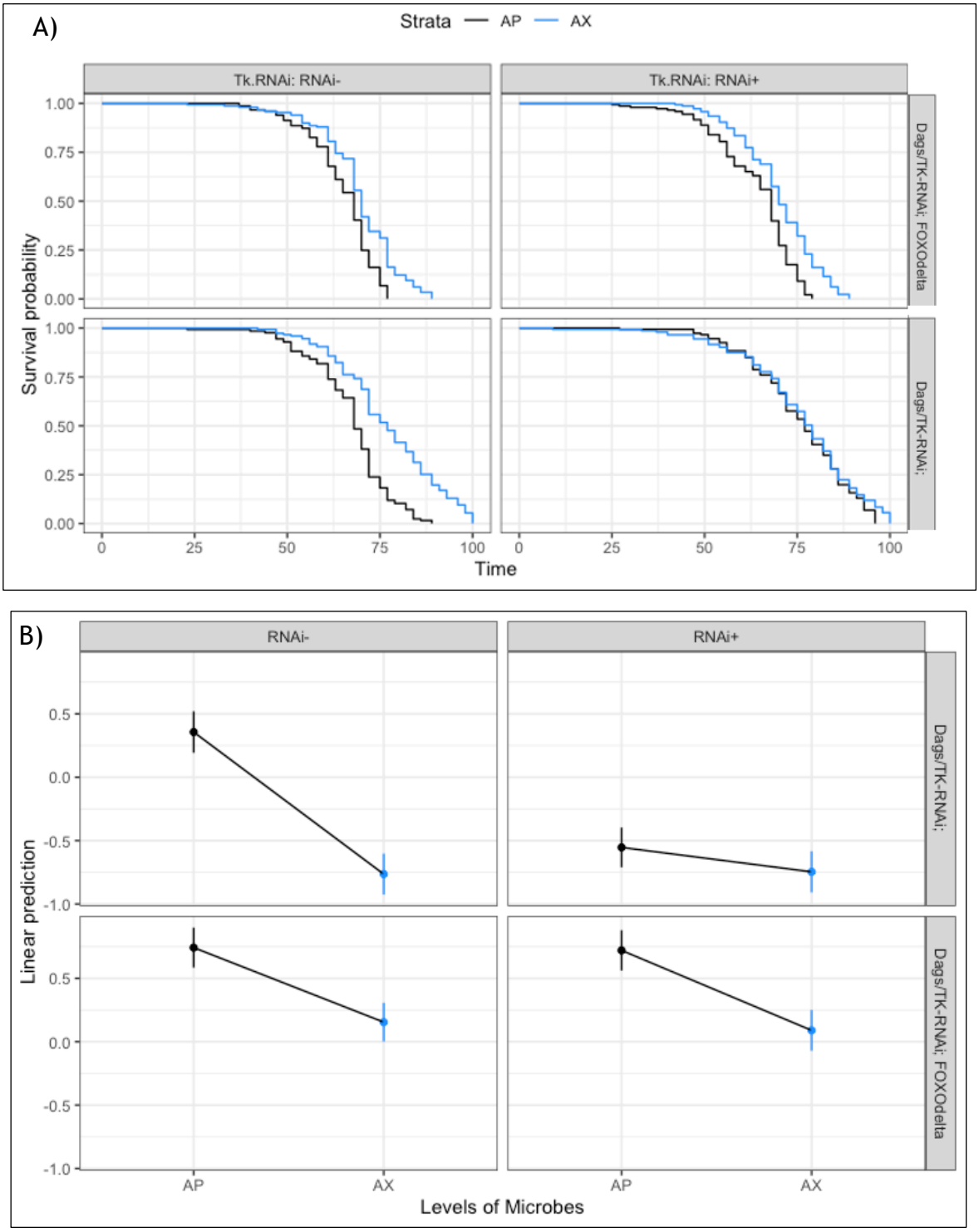

Figure 6.8 The lifespan effect of *A. pomorum* depends on *TK* expression, and the effect of *TK* expression depends on *dFOXO*, but the effect of *A pomorum* is *dFOXO*-independent.

Kaplan-Meier survival curves in ubiquitous tachykinin knockdown in *dFOXO*-null mutants (*Dags/TK-RNAi; FOXOdelta*) compared to control flies (*Dags/TK-RNAi*) when microbiota is depleted (AX) vs mono-colonised with *A. pomorum* (AP).

Statistical significance determined by cox proportional-hazards analysis: Microbes: p value < 2.2e-16 ***, RNAi: p value = 4.672e-05 ***, Genotype: p value < < 2.2e-16 ***, Microbes*RNAi: p value = 0.0002368 ***, Microbes*Genotype: p value = 0.6991107, Genotype*RNAi: p value = 0.0007913 ***, Microbes*Genotype**TK.RNAi*: 5.384e-05 ***. Sample size (females): n=135. This was followed by pairwise comparisons for estimated marginal means between Microbes**TK*-RNAi*Genotype (values shown in table 6.4). (B) Interaction plot for estimated marginal means.

Table 6.4 Pairwise comparisons for estimated marginal means testing the interaction between *TK*-knockdown and microbiota and mutant genotype for *dFOXO*-null mutants lifespan data (Figure 6.6).

TK-knockdown: RNAi- (*TK* unaltered), RNAi+ (*TK* knocked-down); Microbiota: germ-free flies (AX), flies mono-colonised with *A. pomorum* (AP). Genotypes: Control (Wild-type FOXO) = *DaGS/ TK-RNAi*, Mutant (FOXO-null) = *DaGS/TK-RNAi; FOXOdelta*.

contrast	*estimate*	*SE*	*df*	*z.ratio*	*p.value*
(AP Dags/TK-RNAi; RNAi-) - (AX Dags/TK-RNAi; RNAi-)	1.12045378	0.1279744	Inf	8.75529	6.38E-14
(AP Dags/TK-RNAi; RNAi-) - (AP Dags/TK-RNAi; FOXOdelta RNAi-)	-0.3860106	0.1220890	Inf	-3.16171	0.0336958
(AP Dags/TK-RNAi; RNAi-) - (AX Dags/TK-RNAi; FOXOdelta RNAi-)	0.20176451	0.1213502	Inf	1.662662	0.7115381
(AP Dags/TK-RNAi; RNAi-) - (AP Dags/TK-RNAi; RNAi+)	0.90986655	0.1251267	Inf	7.271561	1.00E-11
(AP Dags/TK-RNAi; RNAi-) - (AX Dags/TK-RNAi; RNAi+)	1.10246559	0.1282181	Inf	8.598355	7.16E-14
(AP Dags/TK-RNAi; RNAi-) - (AP Dags/TK-RNAi; FOXOdelta RNAi+)	-0.36422809	0.1229645	Inf	-2.96205	0.0609808
(AP Dags/TK-RNAi; RNAi-) - (AX Dags/TK-RNAi; FOXOdelta RNAi+)	0.26665504	0.1250043	Inf	2.133166	0.3933269
(AX Dags/TK-RNAi; RNAi-) - (AP Dags/TK-RNAi; FOXOdelta RNAi-)	-1.50646442	0.1269158	Inf	-11.8697	0
(AX Dags/TK-RNAi; RNAi-) - (AX Dags/TK-RNAi; FOXOdelta RNAi-)	-0.91868926	0.1223846	Inf	-7.50657	1.75E-12
(AX Dags/TK-RNAi; RNAi-) - (AP Dags/TK-RNAi; RNAi+)	-0.21058723	0.1188731	Inf	-1.77152	0.63954117
(AX Dags/TK-RNAi; RNAi-) - (AX Dags/TK-RNAi; RNAi+)	-0.01798818	0.1174922	Inf	-0.15310	0.9999999

(AX Dags/TK-RNAi; RNAi-) - (AP Dags/TK-RNAi; FOXOdelta RNAi+)	-1.48468187	0.1274415	Inf	-11.6499	0
(AX Dags/TK-RNAi; RNAi-) - (AX Dags/TK-RNAi; FOXOdelta RNAi+)	-0.85379873	0.1258019	Inf	-6.78684	3.21E-10
(AP Dags/TK-RNAi; FOXOdelta RNAi-) - (AX Dags/TK-RNAi; FOXOdelta RNAi-)	0.58777515	0.1178890	Inf	4.985835	1.70E-05
(AP Dags/TK-RNAi; FOXOdelta RNAi-) - (AP Dags/TK-RNAi; RNAi+)	1.29587719	0.1239727	Inf	10.45291	7.78E-14
(AP Dags/TK-RNAi; FOXOdelta RNAi-) - (AX Dags/TK-RNAi; RNAi+)	1.48847624	0.1271865	Inf	11.70309	0
(AP Dags/TK-RNAi; FOXOdelta RNAi-) - (AP Dags/TK-RNAi; FOXOdelta RNAi+)	0.02178255	0.1171148	Inf	0.185993	0.9999996
(AP Dags/TK-RNAi; FOXOdelta RNAi-) - (AX Dags/TK-RNAi; FOXOdelta RNAi+)	0.65266569	0.1219804	Inf	5.350575	2.43E-06
(AX Dags/TK-RNAi; FOXOdelta RNAi-) - (AP Dags/TK-RNAi; RNAi+)	0.70810203	0.1194498	Inf	5.928026	8.56E-08
(AX Dags/TK-RNAi; FOXOdelta RNAi-) - (AX Dags/TK-RNAi; RNAi+)	0.900701083	0.1226514	Inf	7.343581	5.87E-12
(AX Dags/TK-RNAi; FOXOdelta RNAi-) - (AP Dags/TK-RNAi; FOXOdelta RNAi+)	-0.5659926	0.1186913	Inf	-4.76861	5.07E-05
(AX Dags/TK-RNAi; FOXOdelta RNAi-) - (AX Dags/TK-RNAi; FOXOdelta RNAi+)	0.064890533	0.120013	Inf	0.540691	0.99943703
(AP Dags/TK-RNAi; RNAi+) - (AX Dags/TK-RNAi; RNAi+)	0.192599045	0.119533	Inf	1.611254	0.74370666
(AP Dags/TK-RNAi; RNAi+) - (AP Dags/TK-RNAi; FOXOdelta RNAi+)	-1.27409464	0.124504	Inf	-10.2333	6.75E-14
(AP Dags/TK-RNAi; RNAi+) - (AX Dags/TK-RNAi; FOXOdelta RNAi+)	-0.6432115	0.1229218	Inf	-5.23268	4.63E-06
(AX Dags/TK-RNAi; RNAi+) - (AP Dags/TK-RNAi; FOXOdelta RNAi+)	-1.4666936	0.1276914	Inf	-11.4862	0
(AX Dags/TK-RNAi; RNAi+) - (AX Dags/TK-RNAi; FOXOdelta RNAi+)	-0.83581055	0.1260313	Inf	-6.63176	9.28E-10

(AP Dags/TK-RNAi; FOXOdelta RNAi+) - (AX Dags/TK-RNAi; FOXOdelta RNAi+)	0.63088313	0.122693	Inf	5.141964	7.52E-06

6.4.5 Suppression of *AKHR* in the fat body does not recapitulate the *TK* knockdown phenotype

Having established that the microbiota's impact on lifespan is not dependent on *dFOXO*, the investigation shifted towards unravelling an alternative mechanistic pathway through which the microbiota exerts its influence on the regulation of lifespan. This exploration led to an examination of *adipokinetic hormone (AKH)* and its receptor *(AKHR)* signalling as a potential alternative pathway in the context of microbiota-*TK* interaction. Previous research in locusts, demonstrated that, *TK* neurons in the lateral neurosecretory cell group send axons to the corpora cardiaca where they contact cells producing adipokinetic hormone (AKH), the fly analogue of mammalian glucagon (Nässel et al., 1995b). More, it was also shown that *TK*s induce AKH release in vitro (Nässel et al., 1995b). Thus, I tested whether regulation of lifespan via microbiota – *TK* requires *AKH* – *AKHR* signalling. To address this, I knocked down *AKHR* in the fat body (*S106-GS* > *AKHR-RNAi*) and examined the lifespan when the microbiota of those flies is either depleted (Ax) or colonised with *A. pomorum* (Ap) (Figure 6.9). However, the results indicate that suppression of *AKHR* does not influence lifespan.

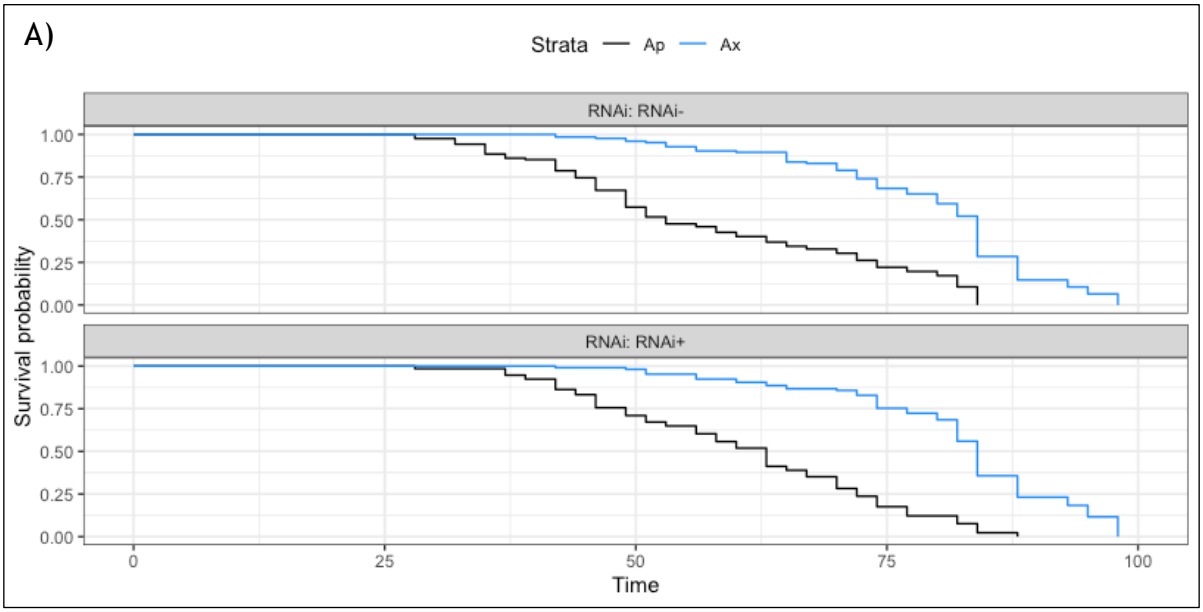

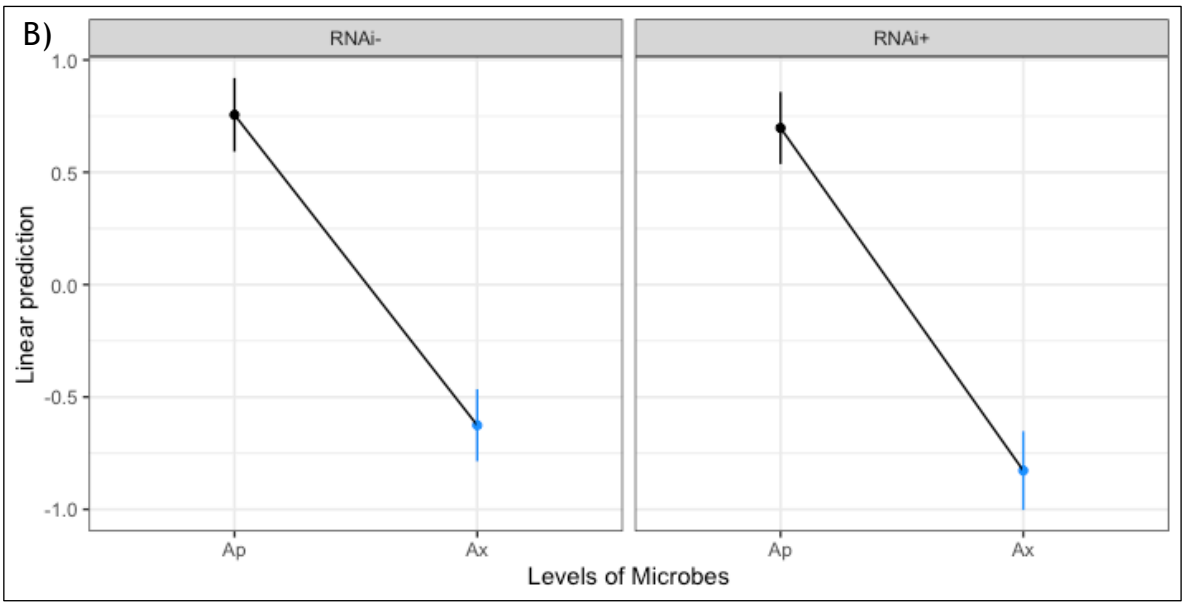

Figure 6.9 Knock-down of *AKHR* in the fat body does not have an effect on lifespan in axenic or *A. pomorum* mono-colonised flies.

A) Kaplan-Meier survival curves in corpora cardiaca *AKHR* knock-down flies (RNAi+) versus control flies (RNAi-) in flies mono-colonised with *Acetobacter pomorum* (Ap) or germ-free (Axenic) flies. Statistical significance determined by cox proportional-hazards analysis: Microbes: p value <2e-16 ***, RNAi: p value = 0.1577, Microbes:RNAi: p value = 0.4362. Sample size (females): n=135.This was followed by pairwise comparisons for estimated marginal means between *TK* knockdown and microbial condition (values shown in table 6.2). (B) Interaction plot for estimated marginal means.

Table 6.5 Pairwise comparisons for estimated marginal means testing the interaction between *TK-RNAi* and microbiota for *S106GS>UAS-AKHR-RNAi* lifespan data (Figure 6.7).

Control samples are labelled with (RNAi-) and knockdown samples labelled with (RNAi+). Microbial conditions are: *A.pomorum* gnotobiotic flies (Ap) and Axenic (Ax) flies.

contrast	*estimate*	*SE*	*df*	*z.ratio*	*p.value*
(Ap RNAi-) - (Ax RNAi-)	1.381418	0.137455	Inf	10.049924	9.19E-24
(Ap RNAi-) - (Ap RNAi+)	0.058439	0.126311	Inf	0.4626599	0.6436081
(Ap RNAi-) - (Ax RNAi+)	1.582983	0.146759	Inf	10.786245	4.00E-27
(Ax RNAi-) - (Ap RNAi+)	-1.32297	0.135446	Inf	-9.767539	1.55E-22
(Ax RNAi-) - (Ax RNAi+)	0.201565	0.133797	Inf	1.5064935	0.1319405
(Ap RNAi+) - (Ax RNAi+)	1.524544	0.144775	Inf	10.530408	6.26E-26

6.5 Discussion and conclusions

6.5.1 *Drosophila TK Receptor* (*DTKR*) in the brain modulates lifespan in the presence of *A. pomorum*

In this chapter I provide evidence for the importance of the tachykinin receptor *DTKR* in the brain as a key modulator of Drosophila lifespan in the presence of the symbiont *A. pomorum*. This extends our understanding of how the nervous system, particularly the brain, contributes to the regulation of lifespan in response to commensal microbes. The differential effects observed between *DTKR* and *NKD* suggest specific and non-redundant roles for these receptors in the regulation of lifespan. While *DTKR* knockdown recapitulated the lifespan extension phenotype, *NKD* not only failed to reproduce this effect but also interfered with microbial-mediated lifespan regulation. This implies divergent functions and potential antagonistic interactions between these two receptors. The receptor-specific effects could also suggest that different receptors may mediate distinct responses to microbial stimuli, contributing to the complexity of host-microbe interactions.

Previous studies have implicated the tachykinin signalling pathway in various physiological processes, including immune response modulation and stress adaptation (Nässel et al., 2019).The current findings add to this knowledge by highlighting its significance in the regulation of lifespan, particularly in the presence of gut microbes. The role of gut microbiota in host longevity has also been a subject of increasing interest. Several studies have demonstrated a clear connection between the composition of the gut microbiome and the ageing process (Arias-Rojas and Iatsenko, 2022). The findings presented in this thesis contribute a novel perspective to the existing literature by suggesting that tachykinin signalling could play a pivotal role as a key mediator in this complex relationship.

The specific role of *DTKR* in the brain adds nuance to our understanding of how this pathway contributes to microbial-modulated longevity. The gut-brain axis is a complex network of bidirectional communication between the gut and the central nervous system. The current results indicate that tachykinin signalling,

from the gut (chapter 5) to the *DTKR* receptor in the brain, influences the interplay between the host and its commensal microbes, impacting overall lifespan.

6.5.2 A role for Insulin/IGF1 signalling

The investigation into insulin signalling as a potential mechanism sheds light on possible downstream effectors that may mediate the observed lifespan extension response. The premises for this were: (1) *TK* signalling via *DTKR* regulates brain IPCs (Birse et al., 2011). (2) *TK* receptor *DTKR* is expressed in insulin producing cells (IPC) in the brain (Soderberg et al., 2011); (3) in the fed fly levels of ILPs are high, which suppresses expression of *DTKR* (Ko et al., 2015); (4) *TK* acts on the renal tubules to regulate *ILP* signalling in response to stress (Soderberg et al., 2011).

My results indicate that ablation of IPCs phenocopies the ubiquitous and gut-specific tachykinin, as well as the brain-specific *DTKR* knockdown lifespan phenotypes. Previous studies show that ablation of *Drosophila* IPCs in the brain leads to of extension of median and maximal lifespan and increased resistance to oxidative stress and starvation (Broughton et al., 2005; Rulifson et al., 2002). However, it also induces significant metabolic trade-offs such as increased fasting glucose levels in the haemolymph (similar to that found in diabetic mammals), increased storage of lipids and carbohydrates, reduced fecundity, and reduced tolerance of heat and cold (Broughton et al., 2005). Moreover, another study conducted by Saud et al., 2015 reveals that the ablation of the IPCs extends lifespan and delays the age-related decline in neuromuscular health irrespective of the amount of dietary sugar, it cannot rescue the lifespan-shortening effects of excess sugar. On the other hand, ablation of IPCs was shown to prevent adult obesity resulting from excess sugar, independent from the canonical effector of IIS, *dFOXO* (Saud et al., 2015). However, to date, there are no studies who investigate the impact of IPCs in axenic or gnotobiotic flies. Overall, we demonstrate for the first time that IPCs ablation in the brain increases lifespan in *A. pomorum* mono-colonised flies, but not in axenic flies, suggesting that IPCs mediate the effect of microbes on lifespan, thus phenocopying the *TK* lifespan phenotype.

Certainly, TOR and IIS represent evolutionarily conserved pathways that are influenced by commensals in fruit flies (Fan et al., 2018; Bana and Cabreiro, 2019) (Figure 6.10). For instance, pyrroloquinoline quinone-dependent alcohol dehydrogenase (PQQ-ADH) produced by *A. pomorum* was shown to regulate IIS in *Drosophila*, proving essential for enhancing larval growth on a low-yeast diet (Shin et al., 2011). As the suppression of TOR and IIS pathways is recognised to promote longevity (Bana and Cabreiro, 2019), it becomes crucial to investigate whether commensal microbes such as *A. pomorum* might impact ageing negatively by activating the IIS and TOR pathways, respectively. Intriguingly, the chemical inhibition of TOR through rapamycin treatment has been observed to alter microbiome composition and extend lifespan, both in calorie-restricted and axenic flies, thus implying that the lifespan-promoting effect of rapamycin is independent of the microbiota (Schinaman et al., 2019).

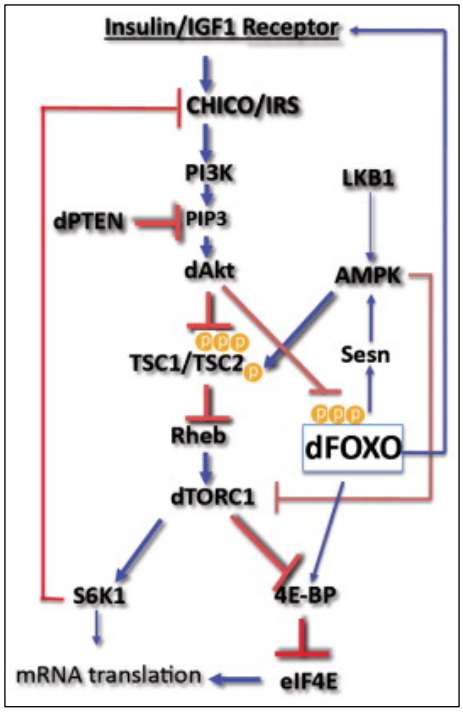

Figure 6.10 The signalling pathway from Insulin/IGF1 receptor through IRS, PI3K, and Akt in flies.

Akt inhibits FOXO through direct phosphorylation, and indirectly activates dTORC1, which in turn stimulates protein synthesis. dTORC1 and its downstream effector, S6K, elicit negative feedback loops to inhibit Akt. When activated FOXO induces the expression of Sesn, which activates AMPK to inhibit dTORC1. In addition, FOXO elevates the expression of 4E-BP downstream of dTORC1, and induces the expression of Insulin/IGF1 receptor to activate Akt. Adapted from (Hay, 2011).

My results show that the expression of *4E-BP* is increased in response to *TK* suppression in *A. pomorum* colonised flies, but not in axenic flies. This suggests that mTOR/IIS is inhibited in *TK* knockdown *A. pomorum* mono-colonised flies, which could explain their increased lifespan. This is further supported by the western blotting data, where in flies colonised with Ap, *TK* knockdown decreases phospho-Akt levels, indicating higher FOXO and thus longer lifespan, which fits our observed phenotypes. Similarly, axenic RNAi- flies have lower phospho-Akt and increased lifespan. However, acknowledging the regulation of 4E-BP activity by phosphorylation, it is critical to note that changes in *4E-BP* mRNA expression do not directly correlate with 4E-BP activity, which is primarily regulated post-translationally through phosphorylation (Pause et al., 1994; Gingras et al., 1999). Therefore, our mRNA expression data should be complemented with analyses of 4E-BP phosphorylation status to fully elucidate its activity and impact on lifespan. Figure 6.11 presents a conceptual model outlining the potential impact of gut microbiota on tachykinin signalling and their subsequent interaction with insulin signalling *Drosophila melanogaster*. The schematic illustrates the hypothesised regulatory loop wherein gut microbes modulate tachykinin signalling, which in turn could influence the activity of the insulin signalling pathway, ultimately affecting the expression of downstream insulin signalling targets.

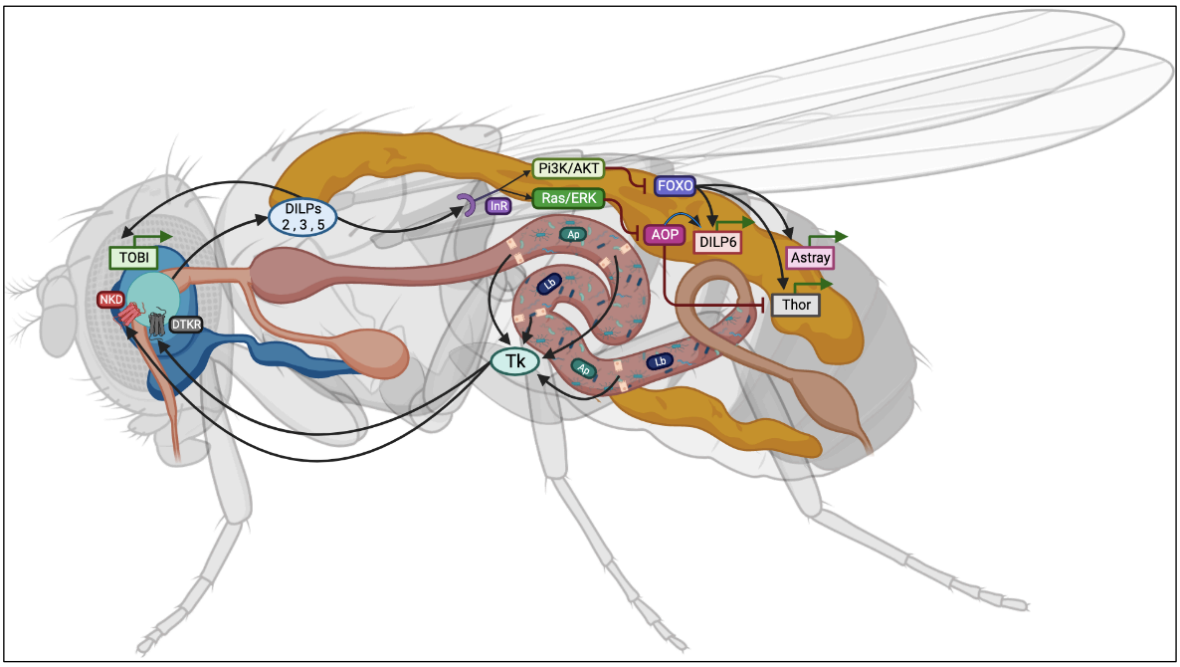

Figure 6.11. Schematic diagram illustrating the proposed interactions among the gut microbiome, tachykinin signalling, and systemic insulin signalling within *Drosophila melanogaster* [Figure produced by Miriam Wood].

Moreover, the null-*dFOXO* lifespan experiment reveals that while *dFOXO* is required for *TK* to modulate lifespan, microbiota does not rely on *dFOXO*. Considering the main hypothesis of this thesis: tachykinin mediates the effect of microbiota on lifespan, the expected result was that in null-*dFOXO* mutants the lifespan extension effect of both *TK* knockdown and microbiota depletion will be blocked, if the downstream effector is *dFOXO*. Alternatively, if lifespan extension is *dFOXO*-independent, lifespan extension would still be present following axenia or *TK* suppression. However, my results indicate a more complex interaction. One explanation for this could be that the presence of the microbiota dictates gene regulation in a subset of the transcriptome, which includes genes involved in growth regulation, metabolism and neurophysiology (Dobson et al., 2016). Therefore, this suggests that the flow of information in *Drosophila* transcriptional networks is microbiota-dependent, and thus axenic animals lacking any microbial influence will have a very distinct overall architecture of the transcriptome. Considering the uniqueness of the transcriptional network subsequent to microbiota depletion, it is plausible to propose that axenic animals may not adhere to conventional signalling pathways. Moreover, another explanation could be that in *Drosophila*, several adult phenotypes are regulated by IIS independently of *dFOXO* (Slack et al., 2011), and the transcriptional response to IIS in flies could involve other transcription factors (Alic et al., 2011), confirming the existence of *dFOXO*-independent pathways responding to IIS.

Chapter 7 General discussion

Overall, using *Drosophila* as a model, I have discovered a novel role for the neuropeptide hormone *tachykinin* in mediating the effects of microbiota on the host. What makes these findings particularly captivating is not just their novelty, but also their potential therapeutic significance. It is noteworthy that the presence of a mammalian homolog adds a layer of translational promise to these discoveries. Overall, unravelling the intricate interplay between *tachykinin*, microbiota, and host health not only enriches our knowledge of fundamental biological processes but also opens new avenues for developing targeted therapies aimed at modulating these interactions to promote longevity and improve overall health. The bridge between basic science and potential clinical

applications established by this research marks a valuable contribution to the field and paves the way for future investigations into the therapeutic potential of *tachykinin*-related interventions.

In this thesis I demonstrated that *TK* expression is regulated by bacteria, and specifically by *A. pomorum* in the gut, but not in the brain. Consistent with previous research, my results show that *TK* knockdown leads to increased lipid levels in conventional flies. However, when flies were made axenic, the effect of tachykinin knockdown was masked. *A. pomorum* recapitulates the conventional phenotype, while *L. brevis* does not have a significant effect. This indicates that *A. pomorum* communicate with *TK* to induce systemic metabolic effects on host. Gut-targeted *TK* knockdown in *A. pomorum* mono-colonised flies did not recapitulate the increased adiposity phenotype following global knockdown, suggesting that brain-derived *TK* plays a role in lipid metabolism.

Moreover, perhaps the most interesting result is that downregulating *TK* expression increases lifespan in a bacterial specific manner. Removing *TK* specifically in the EE cells was sufficient to recapitulate the ubiquitous *TK* knockdown phenotype, i.e., to substantially increase lifespan in the presence of *A. pomorum*. This further supports the initial hypothesis that EE cells may act as a relay between microbiota and distal host tissues, modifying release of hormones into circulation in response to by-products of gut microbiota. Considering that tachykinin receptors are expressed both in the gut and CNS, I then checked whether *TK* acts locally or systemically through the gut-brain axis to induce its pro-ageing effect in response to microbes. The results indicated that tachykinin signalling, from the gut to the DTKR receptor in the brain, influences the interplay between the host and its commensal microbes, impacting overall lifespan. In terms of potential mechanisms mediating the impact of the interaction between *A. pomorum* and *TK* - feeding and egg laying assays suggest that nutrient restriction and reduced reproduction can be excluded. However, impacts on *4E-BP* and Akt expression imply involvement in the IIS/TOR signalling network. Supporting this, the ablation of IPCs replicates the *TK* knockdown lifespan phenotype. Nevertheless, *TK* knockdown in null-*dFOXO* mutants indicates that, while *dFOXO* is essential for *TK*-mediated lifespan

modulation, it is dispensable for microbial lifespan regulation, implying the existence of additional interacting mechanisms.

Furthermore, another important finding that gut-targeted *TK* knockdown does not have a detrimental impact on axenic flies and it even increases the resistance to food shortage in *A. pomorum* mono-colonised flies. This is contrary to the global *TK* knockdown results which led to a significant decrease in starvation resistance in axenic, conventional and *A. pomorum* colonised flies.

While my results provide strong evidence that gut-*TK* is sufficient to mediate the effect of bacteria on host lifespan, future studies should address whether it is also necessary. To investigate this, a *TK* null mutant could be used in combination with UAS/GAL4 line to re-express *TK* and check whether that restores the effect of microbes on lifespan. Another way to check this could be by using genetic flipases, which allows targeted expression of *GAL80* just in one tissue or everywhere else. For example, RNAi could be expressed against *TK* just in the neurons or everywhere other than neurons.

Moreover, assessing healthspan indicators is crucial to determine if the observed increase in lifespan is accompanied by an improvement in overall health and functionality. Thus, healthspan indicators, such as, sleep, gut permeability, physical activity and locomotion, limbic assays, tissue integrity, metabolic rate or telomere length should be investigated to better understand the health status of those long-lived specimens.

Furthermore, a comprehensive understanding of the regulation of metabolism requires an exploration of various metabolic indices beyond lipid metabolism. To gain a more complete picture of how microbiota, *TK*, and metabolism are interlinked, it is essential to extend the investigation to other metabolic parameters, such as measuring glucose, trehalose, glycogen and ATP levels. While I have successfully demonstrated the regulatory influence of both conventional microbiota and the gut symbiont *A. pomorum* on *TK* expression, future studies should focus on elucidating the specific components or metabolites derived from bacteria that mediate the observed regulatory impact on *TK* expression. Metabolomic profiling or functional studies with bacterial

components or metabolites could be used to address this. Lastly, to establish the evolutionary conservation of the observed effects and their potential translational relevance, it is relevant to extend these findings to mammalian models.

References

Ahlman, H., Nilsson, O., 2001. The gut as the largest endocrine organ in the body. Annals of Oncology 12, S63–S68. https://doi.org/10.1093/annonc/12.suppl_2.S63

Ahlman, H. and Nilsson, O., 2001. The gut as the largest endocrine organ in the body. *Annals of Oncology*, 12, pp.S63-S68.

Al Saud, S.N., Summerfield, A.C., Alic, N., 2015. Ablation of insulin-producing cells prevents obesity but not premature mortality caused by a high-sugar diet in Drosophila. Proceedings of the Royal Society B: Biological Sciences 282, 20141720. https://doi.org/10.1098/rspb.2014.1720

Alic, N., Andrews, T.D., Giannakou, M.E., Papatheodorou, I., Slack, C., Hoddinott, M.P., Cochemé, H.M., Schuster, E.F., Thornton, J.M., Partridge, L., 2011. Genome-wide dFOXO targets and topology of the transcriptomic response to stress and insulin signalling. Mol Syst Biol 7, 502. https://doi.org/10.1038/msb.2011.36

Arias-Rojas, A., Iatsenko, I., 2022. The Role of Microbiota in Drosophila melanogaster Aging. Front Aging 3, 909509. https://doi.org/10.3389/fragi.2022.909509

Barbara, G., Stanghellini, V., De Giorgio, R., Cremon, C., Cottrell, G.S., Santini, D., Pasquinelli, G., Morselli-Labate, A.M., Grady, E.F., Bunnett, N.W., Collins, S.M., Corinaldesi, R., 2004. Activated mast cells in proximity to colonic nerves correlate with abdominal pain in irritable bowel syndrome. Gastroenterology 126, 693–702. https://doi.org/10.1053/j.gastro.2003.11.055

Barker, N., van Es, J.H., Kuipers, J., Kujala, P., van den Born, M., Cozijnsen, M., Haegebarth, A., Korving, J., Begthel, H., Peters, P.J., Clevers, H., 2007. Identification of stem cells in small intestine and colon by marker gene Lgr5. Nature 449, 1003–1007. https://doi.org/10.1038/nature06196

Barry, W.E., Thummel, C.S., The Drosophila HNF4 nuclear receptor promotes glucose-stimulated insulin secretion and mitochondrial function in adults. eLife 5, e11183. https://doi.org/10.7554/eLife.11183

Barwell, T., DeVeale, B., Poirier, L., Zheng, J., Seroude, F., Seroude, L., 2017. Regulating the UAS/GAL4 system in adult Drosophila with Tet-off GAL80 transgenes. PeerJ 5, e4167. https://doi.org/10.7717/peerj.4167

Beck, M.L., Freihaut, B., Henry, R., Pierce, S., Bayer, W.L., 1975. A serum haemagglutinating property dependent upon polycarboxyl groups. Br J Haematol 29, 149–156. https://doi.org/10.1111/j.1365-2141.1975.tb01808.x

Benguettat, O., Jneid, R., Soltys, J., Loudhaief, R., Brun-Barale, A., Osman, D., Gallet, A., 2018. The DH31/CGRP enteroendocrine peptide triggers intestinal contractions favoring the elimination of opportunistic bacteria. PLoS Pathog 14, e1007279. https://doi.org/10.1371/journal.ppat.1007279

Bharucha, K.N., Tarr, P., Zipursky, S.L., 2008. A glucagon-like endocrine pathway in Drosophila modulates both lipid and carbohydrate homeostasis. J Exp Biol 211, 3103–3110. https://doi.org/10.1242/jeb.016451

Biagi, E., Franceschi, C., Rampelli, S., Severgnini, M., Ostan, R., Turroni, S., Consolandi, C., Quercia, S., Scurti, M., Monti, D., Capri, M., Brigidi, P. and Candela, M., 2016. Gut Microbiota and Extreme Longevity. *Current Biology*, 26(11), pp.1480-1485.

Biagi, E., Nylund, L., Candela, M., Ostan, R., Bucci, L., Pini, E., Nikkïla, J., Monti, D., Satokari, R., Franceschi, C., Brigidi, P. and De Vos, W., 2010. Correction: Through Ageing, and Beyond: Gut Microbiota and Inflammatory Status in Seniors and Centenarians. *PLoS ONE*, 5(6).

Biagi, E., Rampelli, S., Turroni, S., Quercia, S., Candela, M. and Brigidi, P., 2017. The gut microbiota of centenarians: Signatures of longevity in the gut microbiota profile. *Mechanisms of Ageing and Development*, 165, pp.180-184.

Bilen, J., Atallah, J., Azanchi, R., Levine, J.D., Riddiford, L.M., 2013. Regulation of onset of female mating and sex pheromone production by juvenile hormone in Drosophila melanogaster. Proceedings of the National Academy of Sciences 110, 18321–18326. https://doi.org/10.1073/pnas.1318119110

Bingham, P.M., 1980. The Regulation of White Locus Expression: A Dominant Mutant Allele at the White Locus of DROSOPHILA MELANOGASTER. Genetics 95, 341–353. https://doi.org/10.1093/genetics/95.2.341

Birse, R.T., Söderberg, J.A.E., Luo, J., Winther, Å.M.E., Nässel, D.R., 2011. Regulation of insulin-producing cells in the adult Drosophila brain via the tachykinin peptide receptor DTKR. Journal of Experimental Biology 214, 4201–4208. https://doi.org/10.1242/jeb.062091

Biteau B, Karpac J, Supoyo S, DeGennaro M, Lehmann R, Jasper H. 2010. Lifespan extension by preserving proliferative homeostasis in Drosophila. PLOS Genet. 6:e1001159

Bjedov I, Toivonen JM, Kerr F, Slack C, Jacobson J, Foley A, Partridge L. 2010Mechanisms of life span extension by rapamycin in the fruit fly Drosophila melanogaster. Cell Metab. 11, 35-46.

Blum, J.E., Fischer, C.N., Miles, J., Handelsman, J., 2013. Frequent Replenishment Sustains the Beneficial Microbiome of Drosophila melanogaster. mBio 4, 10.1128/mbio.00860-13. https://doi.org/10.1128/mbio.00860-13

Bogunovic, M., Davé, S.H., Tilstra, J.S., Chang, D.T.W., Harpaz, N., Xiong, H., Mayer, L.F., Plevy, S.E., 2007. Enteroendocrine cells express functional Toll-like receptors. Am J Physiol Gastrointest Liver Physiol 292, G1770-1783. https://doi.org/10.1152/ajpgi.00249.2006

Bonfini, A., Liu, X., Buchon, N., 2016. From pathogens to microbiota: How Drosophila intestinal stem cells react to gut microbes. Dev Comp Immunol 64, 22–38. https://doi.org/10.1016/j.dci.2016.02.008

Broderick, N.A., Buchon, N., Lemaitre, B., 2014. Microbiota-Induced Changes in Drosophila melanogaster Host Gene Expression and Gut Morphology. mBio 5. https://doi.org/10.1128/mBio.01117-14

Broderick, N.A., Lemaitre, B., 2012. Gut-associated microbes of Drosophila melanogaster. Gut Microbes 3, 307–321. https://doi.org/10.4161/gmic.19896

Brogiolo, W., Stocker, H., Ikeya, T., Rintelen, F., Fernandez, R., Hafen, E., 2001. An evolutionarily conserved function of the Drosophila insulin receptor and insulin-like peptides in growth control. Current Biology 11, 213–221. https://doi.org/10.1016/S0960-9822(01)00068-9

Brooks L, Viardot A, Tsakmaki A, Stolarczyk E, Howard JK, Cani PD, Everard A, Sleeth ML, Psichas A, Anastasovskaj J, Bell JD, Bell-Anderson K, Mackay CR, Ghatei MA, Bloom SR, Frost G, Bewick GA. Fermentable carbohydrate stimulates FFAR2-dependent colonic PYY cell expansion to increase satiety. Mol Metab. 2016;6(1):48–60.

Broughton, S.J., Piper, M.D.W., Ikeya, T., Bass, T.M., Jacobson, J., Driege, Y., Martinez, P., Hafen, E., Withers, D.J., Leevers, S.J., Partridge, L., 2005a. Longer lifespan, altered metabolism, and stress resistance in Drosophila from ablation of cells making insulin-like ligands. Proceedings of the National Academy of Sciences 102, 3105–3110. https://doi.org/10.1073/pnas.0405775102

Brummel, T., Ching, A., Seroude, L., Simon, A.F., Benzer, S., 2004. Drosophila lifespan enhancement by exogenous bacteria. Proc Natl Acad Sci U S A 101, 12974–12979. https://doi.org/10.1073/pnas.0405207101

Buchon, N., Broderick, N., Chakrabarti, S. and Lemaitre, B., 2009. Invasive and indigenous microbiota impact intestinal stem cell activity through multiple pathways in Drosophila. *Genes & Development*, 23(19), pp.2333-2344.
Buchon, N., Broderick, N.A., Lemaitre, B., 2013. Gut homeostasis in a microbial world: insights from Drosophila melanogaster. Nat Rev Microbiol 11, 615–626. https://doi.org/10.1038/nrmicro3074
Buchon, N., Osman, D., 2015. All for one and one for all: Regionalization of the Drosophila intestine. Insect Biochem Mol Biol 67, 2–8. https://doi.org/10.1016/j.ibmb.2015.05.015
Burnett, C., Valentini, S., Cabreiro, F., Goss, M., Somogyvári, M., Piper, M.D., Hoddinott, M., Sutphin, G.L., Leko, V., McElwee, J.J., Vazquez-Manrique, R.P., Orfila, A.-M., Ackerman, D., Au, C., Vinti, G., Riesen, M., Howard, K., Neri, C., Bedalov, A., Kaeberlein, M., Sőti, C., Partridge, L., Gems, D., 2011. Absence of effects of Sir2 overexpression on lifespan in C. elegans and Drosophila. Nature 477, 482–485. https://doi.org/10.1038/nature10296
Cabreiro, F., Gems, D., 2013. Worms need microbes too: microbiota, health and aging in Caenorhabditis elegans. EMBO Mol Med 5, 1300–1310. https://doi.org/10.1002/emmm.201100972
Caers, J., Verlinden, H., Zels, S., Vandersmissen, H.P., Vuerinckx, K., Schoofs, L., 2012. More than two decades of research on insect neuropeptide GPCRs: an overview. Front Endocrinol (Lausanne) 3, 151. https://doi.org/10.3389/fendo.2012.00151
Capo, F., Wilson, A., Di Cara, F., 2019. The Intestine of Drosophila melanogaster: An Emerging Versatile Model System to Study Intestinal Epithelial Homeostasis and Host-Microbial Interactions in Humans. Microorganisms 7, 336. https://doi.org/10.3390/microorganisms7090336
Chandler, J.A., Lang, J.M., Bhatnagar, S., Eisen, J.A., Kopp, A., 2011. Bacterial Communities of Diverse Drosophila Species: Ecological Context of a Host–Microbe Model System. PLOS Genetics 7, e1002272. https://doi.org/10.1371/journal.pgen.1002272
Chaston, J.M., Newell, P.D., Douglas, A.E., 2014. Metagenome-Wide Association of Microbial Determinants of Host Phenotype in Drosophila melanogaster. mBio 5, e01631-14. https://doi.org/10.1128/mBio.01631-14
Chatterjee, N., Perrimon, N., 2021. What fuels the fly: Energy metabolism in Drosophila and its application to the study of obesity and diabetes. Science Advances 7, eabg4336. https://doi.org/10.1126/sciadv.abg4336
Chen, J., Kim, S.-M., Kwon, J.Y., 2016. A Systematic Analysis of Drosophila Regulatory Peptide Expression in Enteroendocrine Cells. Mol Cells 39, 358–366. https://doi.org/10.14348/molcells.2016.0014
Chen, J., Xu, N., Wang, C., Huang, P., Huang, H., Jin, Z., Yu, Z., Cai, T., Jiao, R., Xi, R., 2018. Transient Scute activation via a self-stimulatory loop directs enteroendocrine cell pair specification from self-renewing intestinal stem cells. Nat Cell Biol 20, 152–161. https://doi.org/10.1038/s41556-017-0020-0
Chen, L., Toke, N.H., Luo, S., Vasoya, R.P., Fullem, R.L., Parthasarathy, A., Perekatt, A.O., Verzi, M.P., 2019. A reinforcing HNF4-SMAD4 feed-forward module stabilizes enterocyte identity. Nat Genet 51, 777–785. https://doi.org/10.1038/s41588-019-0384-0
Chung, B.Y., Ro, J., Hutter, S.A., Miller, K.M., Guduguntla, L.S., Kondo, S., Pletcher, S.D., 2017. Drosophila Neuropeptide F Signaling Independently Regulates Feeding and Sleep-Wake Behavior. Cell Rep 19, 2441–2450. https://doi.org/10.1016/j.celrep.2017.05.085

Clark, R., Salazar, A., Yamada, R., Fitz-Gibbon, S., Morselli, M., Alcaraz, J., Rana, A., Rera, M., Pellegrini, M., Ja, W. and Walker, D., 2015. Distinct Shifts in Microbiota Composition during Drosophila Aging Impair

Clark, R.I., Salazar, A., Yamada, R., Fitz-Gibbon, S., Morselli, M., Alcaraz, J., Rana, A., Rera, M., Pellegrini, M., Ja, W.W., Walker, D.W., 2015a. Distinct shifts in microbiota composition during Drosophila aging impair intestinal function and drive mortality. Cell Rep 12, 1656–1667. https://doi.org/10.1016/j.celrep.2015.08.004

Cole, J.J., Faydaci, B.A., McGuinness, D., Shaw, R., Maciewicz, R.A., Robertson, N.A., Goodyear, C.S., 2021. Searchlight: automated bulk RNA-seq exploration and visualisation using dynamically generated R scripts. BMC Bioinformatics 22, 411. https://doi.org/10.1186/s12859-021-04321-2

Consuegra, J., Grenier, T., Baa-Puyoulet, P., Rahioui, I., Akherraz, H., Gervais, H., Parisot, N., Da Silva, P., Charles, H., Calevro, F., Leulier, F., 2020. Drosophila-associated bacteria differentially shape the nutritional requirements of their host during juvenile growth. PLoS Biol 18, e3000681. https://doi.org/10.1371/journal.pbio.3000681

Cox, C.R., Gilmore, M.S., 2007. Native microbial colonization of Drosophila melanogaster and its use as a model of Enterococcus faecalis pathogenesis. Infect Immun 75, 1565–1576. https://doi.org/10.1128/IAI.01496-06

Cox, L.M., Blaser, M.J., 2015. Antibiotics in early life and obesity. Nat Rev Endocrinol 11, 182–190. https://doi.org/10.1038/nrendo.2014.210

Deshpande, S.A., Carvalho, G.B., Amador, A., Phillips, A.M., Hoxha, S., Lizotte, K.J., Ja, W.W., 2014. Quantifying Drosophila food intake: comparative analysis of current methodology. Nat Methods 11, 535–540. https://doi.org/10.1038/nmeth.2899

Diehl J.M.C., Meunier J. Surrounding pathogens shape maternal egg care but not egg production in the European earwig. *Behav. Ecol.* 2018;29:128–136. doi: 10.1093/beheco/arx140.

Dillin A, Crawford DK, Kenyon C. 2002Timing requirements for insulin/IGF-1 signaling in *C. elegans*. *Science* **298**, 830-834.

Dobin, A., Davis, C.A., Schlesinger, F., Drenkow, J., Zaleski, C., Jha, S., Batut, P., Chaisson, M., Gingeras, T.R., 2013. STAR: ultrafast universal RNA-seq aligner. Bioinformatics 29, 15–21. https://doi.org/10.1093/bioinformatics/bts635

Dobson AJ, Chaston JM, Newell PD, Donahue L, Hermann SL, Sannino DR, Westmiller S, Wong AC, Clark AG, Lazzaro BP, Douglas AE. Host genetic determinants of microbiota-dependent nutrition revealed by genome-wide analysis of Drosophila melanogaster. Nat Commun. 2015 Feb 18;6:6312.

Dobson, A.J., Chaston, J.M., Douglas, A.E., 2016. The Drosophila transcriptional network is structured by microbiota. BMC Genomics 17, 975. https://doi.org/10.1186/s12864-016-3307-9

Douglas, A., 2018. The Drosophila model for microbiome research. *Lab Animal*, 47(6), pp.157-164.

DROUJININE, I. A. & PERRIMON, N. 2016. Interorgan Communication Pathways in Physiology: Focus on Drosophila. Annu Rev Genet, 50, 539-570.

Drucker, D.J., 2016. Evolving Concepts and Translational Relevance of Enteroendocrine Cell Biology. J Clin Endocrinol Metab 101, 778–786. https://doi.org/10.1210/jc.2015-3449

Duca FA, Swartz TD, Sakar Y, Covasa M. (2012) Increased oral detection, but decreased intestinal signaling for fats in mice lacking gut microbiota. PLoS One, 7(6).

Ebner, K., Singewald, N., 2006. The role of substance P in stress and anxiety responses. Amino Acids 31, 251–272. https://doi.org/10.1007/s00726-006-0335-9

Engel, P., Moran, N.A., 2013. The gut microbiota of insects – diversity in structure and function. FEMS Microbiology Reviews 37, 699–735. https://doi.org/10.1111/1574-6976.12025
Fabbri, E., Zoli, M., Gonzalez-Freire, M., Salive, M., Studenski, S. and Ferrucci, L., 2015. Aging and Multimorbidity: New Tasks, Priorities, and Frontiers for Integrated Gerontological and Clinical Research. Journal of the American Medical Directors Association, 16(8), pp.640-647.
Fan, X., Gaur, U., Yang, M., 2018. Intestinal Homeostasis and Longevity: Drosophila Gut Feeling, in: Wang, Z. (Ed.), Aging and Aging-Related Diseases: Mechanisms and Interventions, Advances in Experimental Medicine and Biology. Springer, Singapore, pp. 157–168. https://doi.org/10.1007/978-981-13-1117-8_10
Fast, D., Duggal, A., Foley, E., 2018. Monoassociation with Lactobacillus plantarum Disrupts Intestinal Homeostasis in Adult Drosophila melanogaster. mBio 9, 10.1128/mbio.01114-18. https://doi.org/10.1128/mbio.01114-18
Flachsbart, F., Caliebe, A., Kleindorp, R., Blanché, H., von Eller-Eberstein, H., Nikolaus, S., Schreiber, S., Nebel, A., 2009. Association of FOXO3A variation with human longevity confirmed in German centenarians. Proc Natl Acad Sci U S A 106, 2700–2705. https://doi.org/10.1073/pnas.0809594106
Fontana, L., Partridge, L. and Longo, V.D., 2010. Extending healthy life span—from yeast to humans. *Science*, 328(5976), pp.321-326. DOI: 10.1126/science.1172539.
Flatt T, Partridge L. 2018Horizons in the evolution of aging. *BMC Biol*. **16**, 93
Fransen, F., van Beek, A., Borghuis, T., Aidy, S., Hugenholtz, F., van der Gaast – de Jongh, C., Savelkoul, H., De Jonge, M., Boekschoten, M., Smidt, H., Faas, M. and de Vos, P., 2017. Aged Gut Microbiota Contributes to Systemical Inflammaging after Transfer to Germ-Free Mice. *Frontiers in Immunology*, 8.
Furness, J.B., Rivera, L.R., Cho, H.-J., Bravo, D.M., Callaghan, B., 2013. The gut as a sensory organ. Nat Rev Gastroenterol Hepatol 10, 729–740. https://doi.org/10.1038/nrgastro.2013.180
Gehart, H., van Es, J.H., Hamer, K., Beumer, J., Kretzschmar, K., Dekkers, J.F., Rios, A., Clevers, H., 2019. Identification of Enteroendocrine Regulators by Real-Time Single-Cell Differentiation Mapping. Cell 176, 1158-1173.e16. https://doi.org/10.1016/j.cell.2018.12.029
Gems, D. and Partridge, L., 2013. Genetics of longevity in model organisms: debates and paradigm shifts. *Annual Review of Physiology*, 75, pp.621-644. DOI: 10.1146/annurev-physiol-030212-183712.
Giannakou, M.E., Partridge, L., 2007. Role of insulin-like signalling in Drosophila lifespan. Trends in Biochemical Sciences 32, 180–188. https://doi.org/10.1016/j.tibs.2007.02.007
Gordon, H.A., Bruckner-kardoss, E., Wostmann, B.S., 1966. Aging in Germ-free Mice: Life Tables and Lesions Observed at Natural Death. Journal of Gerontology 21, 380–387. https://doi.org/10.1093/geronj/21.3.380
Gould, A.L., Zhang, V., Lamberti, L., Jones, E.W., Obadia, B., Korasidis, N., Gavryushkin, A., Carlson, J.M., Beerenwinkel, N., Ludington, W.B., 2018. Microbiome interactions shape host fitness. Proc Natl Acad Sci U S A 115, E11951–E11960. https://doi.org/10.1073/pnas.1809349115
Grenier, T., Leulier, F., 2020. How commensal microbes shape the physiology of Drosophila melanogaster. Current Opinion in Insect Science 41, 92–99. https://doi.org/10.1016/j.cois.2020.08.002
Gribble, F.M., Reimann, F., 2019. Function and mechanisms of enteroendocrine cells and gut hormones in metabolism. Nat Rev Endocrinol 15, 226–237. https://doi.org/10.1038/s41574-019-0168-8

Grönke, S., Clarke, D.-F., Broughton, S., Andrews, T.D., Partridge, L., 2010. Molecular Evolution and Functional Characterization of Drosophila Insulin-Like Peptides. PLOS Genetics 6, e1000857. https://doi.org/10.1371/journal.pgen.1000857
Guo, L., Karpac, J., Tran, S.L., Jasper, H., 2014. PGRP-SC2 promotes gut immune homeostasis to limit commensal dysbiosis and extend lifespan. Cell 156, 109–122. https://doi.org/10.1016/j.cell.2013.12.018
Guo, T., Zhang, L., Xin, Y., Xu, Z., He, H., Kong, J., 2017. Oxygen-Inducible Conversion of Lactate to Acetate in Heterofermentative Lactobacillus brevis ATCC 367. Appl Environ Microbiol 83, e01659-17. https://doi.org/10.1128/AEM.01659-17
Guo, X., Lv, J., Xi, R., 2022. The specification and function of enteroendocrine cells in Drosophila and mammals: a comparative review. The FEBS Journal 289, 4773–4796. https://doi.org/10.1111/febs.16067
Guo, X., Yin, C., Yang, F., Zhang, Y., Huang, H., Wang, J., Deng, B., Cai, T., Rao, Y., Xi, R., 2019b. The Cellular Diversity and Transcription Factor Code of Drosophila Enteroendocrine Cells. Cell Rep 29, 4172-4185.e5. https://doi.org/10.1016/j.celrep.2019.11.048
Hang, S., Purdy, A.E., Robins, W.P., Wang, Z., Mandal, M., Chang, S., Mekalanos, J.J., Watnick, P.I., 2014. The Acetate Switch of an Intestinal Pathogen Disrupts Host Insulin Signaling and Lipid Metabolism. Cell Host & Microbe 16, 592–604. https://doi.org/10.1016/j.chom.2014.10.006
Hay, N., 2011. Interplay between FOXO, TOR, and Akt. Biochimica et Biophysica Acta (BBA) - Molecular Cell Research, PI3K-AKT-FoxO axis in Cancer and Aging 1813, 1965–1970. https://doi.org/10.1016/j.bbamcr.2011.03.013
Hayes K.S., Bancroft A.J., Goldrick M., Portsmouth C., Roberts I.S., Grencis R.K. Exploitation of the intestinal microflora by the parasitic nematode *Trichuris muris*. *Science*. 2010;328:1391–1394.
Hazelrigg, T., Levis, R., Rubin, G.M., 1984. Transformation of white locus DNA in Drosophila: Dosage compensation, zeste interaction, and position effects. Cell 36, 469–481. https://doi.org/10.1016/0092-8674(84)90240-X
Heier, C., Kühnlein, R.P., 2018. Triacylglycerol Metabolism in Drosophila melanogaster. Genetics 210, 1163–1184. https://doi.org/10.1534/genetics.118.301583
Henriques, S.F., Dhakan, D.B., Serra, L., Francisco, A.P., Carvalho-Santos, Z., Baltazar, C., Elias, A.P., Anjos, M., Zhang, T., Maddocks, O.D.K., Ribeiro, C., 2020. Metabolic cross-feeding in imbalanced diets allows gut microbes to improve reproduction and alter host behaviour. Nat Commun 11, 4236. https://doi.org/10.1038/s41467-020-18049-9
Hersoug, L.-G., Møller, P. & Loft, S. Gut microbiota-derived lipopolysaccharide uptake and trafficking to adipose tissue: implications for inflammation and obesity. Obes. Rev. 17, 297–312 (2016).
Hintze, K.J., Cox, J.E., Rompato, G., Benninghoff, A.D., Ward, R.E., Broadbent, J., Lefevre, M., 2014. Broad scope method for creating humanized animal models for animal health and disease research through antibiotic treatment and human fecal transfer. Gut Microbes 5, 183–191. https://doi.org/10.4161/gmic.28403
Hoganson, D.A., Stahly, D.P., 1975a. Regulation of dihydrodipicolinate synthase during growth and sporulation of Bacillus cereus. J Bacteriol 124, 1344–1350. https://doi.org/10.1128/jb.124.3.1344-1350.1975
Holzer, P., & Holzer-Petsche, U., 1997. Tachykinins in the gut. Part I. Expression, release and motor function.. *Pharmacology & therapeutics*, 73 3, pp. 173-217 .https://doi.org/10.1016/S0163-7258(96)00195-7.

Holzer, P., 1988. Local effector functions of capsaicin-sensitive sensory nerve endings: involvement of tachykinins, calcitonin gene-related peptide and other neuropeptides. Neuroscience 24, 739–768. https://doi.org/10.1016/0306-4522(88)90064-4
Holzer, P., Farzi, A., 2014. Neuropeptides and the Microbiota-Gut-Brain Axis. Adv Exp Med Biol 817, 195–219. https://doi.org/10.1007/978-1-4939-0897-4_9
Holzer, P., Reichmann, F., Farzi, A., 2012. Neuropeptide Y, peptide YY and pancreatic polypeptide in the gut–brain axis. Neuropeptides 46, 261–274. https://doi.org/10.1016/j.npep.2012.08.005
Horiuchi, J., Yamazaki, D., Naganos, S., Aigaki, T., Saitoe, M., 2008. Protein kinase A inhibits a consolidated form of memory in Drosophila. Proc Natl Acad Sci U S A 105, 20976–20981. https://doi.org/10.1073/pnas.0810119105
Hull-Thompson, J., Muffat, J., Sanchez, D., Walker, D.W., Benzer, S., Ganfornina, M.D., Jasper, H., 2009a. Control of Metabolic Homeostasis by Stress Signaling Is Mediated by the Lipocalin NLaz. PLOS Genetics 5, e1000460. https://doi.org/10.1371/journal.pgen.1000460
Hung, R., Hu, Y., Kirchner, R., Liu, Y., Xu, C., Comjean, A., Tattikota, S., Li, F., Song, W., Sui, S., Perrimon, N. (2020). A cell atlas of the adult Drosophila midgut. Proceedings of the National Academy of Sciences of the United States of America.
Hwang, J.R., Siekhaus, D.E., Fuller, R.S., Taghert, P.H., Lindberg, I., 2000. Interaction of Drosophila melanogaster prohormone convertase 2 and 7B2. Insect cell-specific processing and secretion. J Biol Chem 275, 17886–17893. https://doi.org/10.1074/jbc.M000032200
Hwangbo, D.S., Gersham, B., Tu, M.P., Palmer, M. and Tatar, M., 2004. Drosophila dFOXO controls lifespan and regulates insulin signalling in brain and fat body. *Nature*, 429(6991), pp.562-566. DOI: 10.1038/nature02549.
Iatsenko, I., Boquete, J.-P., Lemaitre, B., 2018. Microbiota-Derived Lactate Activates Production of Reactive Oxygen Species by the Intestinal NADPH Oxidase Nox and Shortens Drosophila Lifespan. Immunity 49, 929-942.e5. https://doi.org/10.1016/j.immuni.2018.09.017
Iatsenko, I., Kondo, S., Mengin-Lecreulx, D., Lemaitre, B., 2016. PGRP-SD, an Extracellular Pattern-Recognition Receptor, Enhances Peptidoglycan-Mediated Activation of the Drosophila Imd Pathway. Immunity 45, 1013–1023. https://doi.org/10.1016/j.immuni.2016.10.029
Im, S.H., Takle, K., Jo, J., Babcock, D.T., Ma, Z., Xiang, Y., Galko, M.J., 2015. Tachykinin acts upstream of autocrine Hedgehog signaling during nociceptive sensitization in Drosophila. eLife 4, e10735. https://doi.org/10.7554/eLife.10735
ingestion of lactic acid bacteria. J. Dairy Sci. 78, 491–497.
Intestinal Function and Drive Mortality. *Cell Reports*, 12(10), pp.1656-1667.
Itskov, P.M., Moreira, J.-M., Vinnik, E., Lopes, G., Safarik, S., Dickinson, M.H., Ribeiro, C., 2014. Automated monitoring and quantitative analysis of feeding behaviour in Drosophila. Nat Commun 5, 4560. https://doi.org/10.1038/ncomms5560
Ja, W. W. et al. Prandiology of *Drosophila* and the CAFE assay. *Proc. Natl Acad. Sci. USA***104**, 8253–8256 (2007).
Jandhyala, S., 2015. Role of the normal gut microbiota. World Journal of Gastroenterology, 21(29), p.8787.
Jennings, B.H., 2011. Drosophila – a versatile model in biology & medicine. Materials Today 14, 190–195. https://doi.org/10.1016/S1369-7021(11)70113-4
Jian, Z., Zeng, L., Xu, T., Sun, S., Yan, S., Zhao, S., Su, Z., Ge, C., Zhang, Y., Jia, J., Dou, T., 2022. The intestinal microbiome associated with lipid metabolism

and obesity in humans and animals. Journal of Applied Microbiology 133, 2915–2930. https://doi.org/10.1111/jam.15740
Jiang, H., Lkhagva, A., Daubnerová, I., Chae, H.-S., Šimo, L., Jung, S.-H., Yoon, Y.-K., Lee, N.-R., Seong, J.Y., Žitňan, D., Park, Y., Kim, Y.-J., 2013. Natalisin, a tachykinin-like signaling system, regulates sexual activity and fecundity in insects. Proceedings of the National Academy of Sciences 110, E3526–E3534. https://doi.org/10.1073/pnas.1310676110
Johnson, K.O., Shannon, O.M., Matu, J. et al. Differences in circulating appetite-related hormone concentrations between younger and older adults: a systematic review and meta-analysis. Aging Clin Exp Res 32, 1233–1244 (2020).
Jones, R.M., Luo, L., Ardita, C.S., Richardson, A.N., Kwon, Y.M., Mercante, J.W., Alam, A., Gates, C.L., Wu, H., Swanson, P.A., Lambeth, J.D., Denning, P.W., Neish, A.S., 2013. Symbiotic lactobacilli stimulate gut epithelial proliferation via Nox-mediated generation of reactive oxygen species. EMBO J 32, 3017–3028. https://doi.org/10.1038/emboj.2013.224
Jørgensen, L.M., Hauser, F., Cazzamali, G., Williamson, M., Grimmelikhuijzen, C.J.P., 2006. Molecular identification of the first SIFamide receptor. Biochemical and Biophysical Research Communications 340, 696–701. https://doi.org/10.1016/j.bbrc.2005.12.062
Jugder, B.-E., Kamareddine, L., Watnick, P.I., 2021. Microbiota-derived acetate activates intestinal innate immunity via the Tip60 histone acetyltransferase complex. Immunity 54, 1683-1697.e3. https://doi.org/10.1016/j.immuni.2021.05.017
Kamareddine, L., Robins, W.P., Berkey, C.D., Mekalanos, J.J., Watnick, P.I., 2018. The Drosophila Immune Deficiency Pathway Modulates Enteroendocrine Function and Host Metabolism. Cell Metabolism 28, 449-462.e5. https://doi.org/10.1016/j.cmet.2018.05.026
Keebaugh, E.S., Yamada, R., Ja, W.W., 2019. The Nutritional Environment Influences the Impact of Microbes on Drosophila melanogaster Life Span. mBio 10, 10.1128/mbio.00885-19. https://doi.org/10.1128/mbio.00885-19
Kim, S. and Jazwinski, S., 2018. The Gut Microbiota and Healthy Aging: A Mini-Review. *Gerontology*, 64(6), pp.513-520.
Kim, S.K., Rulifson, E.J., 2004b. Conserved mechanisms of glucose sensing and regulation by Drosophila corpora cardiaca cells. Nature 431, 316–320. https://doi.org/10.1038/nature02897
Ko, K., Root, C., Lindsay, S., Zaninovich, O., Shepherd, A., Wasserman, S., Kim, S. and Wang, J., 2015. Starvation promotes concerted modulation of appetitive olfactory behavior via parallel neuromodulatory circuits. eLife, 4.
Koenig, J., Spor, A., Scalfone, N., Fricker, A., Stombaugh, J., Knight, R., Angenent, L. and Ley, R., 2010. Succession of microbial consortia in the developing infant gut microbiome. *Proceedings of the National Academy of Sciences*, 108(Supplement_1), pp.4578-4585.
Kopin, A.S., Lee, Y.M., McBride, E.W., Miller, L.J., Lu, M., Lin, H.Y., Kolakowski, L.F., Beinborn, M., 1992. Expression cloning and characterization of the canine parietal cell gastrin receptor. Proc Natl Acad Sci U S A 89, 3605–3609. https://doi.org/10.1073/pnas.89.8.3605
Kubrak, O., Koyama, T., Ahrentløv, N., Jensen, L., Malita, A., Naseem, M.T., Lassen, M., Nagy, S., Texada, M.J., Halberg, K.V., Rewitz, K., 2022. The gut hormone Allatostatin C/Somatostatin regulates food intake and metabolic homeostasis under nutrient stress. Nat Commun 13, 692. https://doi.org/10.1038/s41467-022-28268-x

Kulka, M., Tancowny, B.P., Schleimer, R.P., 2009. Substance P Modulates Toll-like Receptor-Mediated Activation Of Human Mast Cells. Journal of Allergy and Clinical Immunology 123, S195. https://doi.org/10.1016/j.jaci.2008.12.742
Lai, N.Y., Mills, K., Chiu, I.M., 2017. Sensory neuron regulation of gastrointestinal inflammation and bacterial host defence. J Intern Med 282, 5–23. https://doi.org/10.1111/joim.12591
Langille, M., Meehan, C., Koenig, J., Dhanani, A., Rose, R., Howlett, S. and Beiko, R., 2014. Microbial shifts in the aging mouse gut. *Microbiome*, 2(1).
Lebrun, L.J., Lenaerts, K., Kiers, D., Pais De Barros, J.-P., Le Guern, N., Plesnik, J., Thomas, C., Bourgeois, T., Dejong, C.H.C., Kox, M., Hundscheid, I.H.R., Khan, N.A., Mandard, S., Deckert, V., Pickkers, P., Drucker, D.J., Lagrost, L., Grober, J., 2017. Enteroendocrine L Cells Sense LPS after Gut Barrier Injury to Enhance GLP-1 Secretion. Cell Reports 21, 1160–1168. https://doi.org/10.1016/j.celrep.2017.10.008
Lee, G., Park, J.H., 2004. Hemolymph sugar homeostasis and starvation-induced hyperactivity affected by genetic manipulations of the adipokinetic hormone-encoding gene in Drosophila melanogaster. Genetics 167, 311–323. https://doi.org/10.1534/genetics.167.1.311
Lee, H.-Y., Lee, S.-H., Lee, J.-H., Lee, W.-J., Min, K.-J., 2019. The role of commensal microbes in the lifespan of Drosophila melanogaster. Aging (Albany NY) 11, 4611–4640. https://doi.org/10.18632/aging.102073
Lee, Y.-S., Kim, T.-Y., Kim, Y., Lee, S.-H., Kim, S., Kang, S.W., Yang, J.-Y., Baek, I.-J., Sung, Y.H., Park, Y.-Y., Hwang, S.W., O, E., Kim, K.S., Liu, S., Kamada, N., Gao, N., Kweon, M.-N., 2018. Microbiota-Derived Lactate Accelerates Intestinal Stem-Cell-Mediated Epithelial Development. Cell Host & Microbe 24, 833-846.e6. https://doi.org/10.1016/j.chom.2018.11.002
Leitão-Gonçalves, R., Carvalho-Santos, Z., Francisco, A.P., Fioreze, G.T., Anjos, M., Baltazar, C., Elias, A.P., Itskov, P.M., Piper, M.D.W., Ribeiro, C., 2017. Commensal bacteria and essential amino acids control food choice behavior and reproduction. PLoS Biol 15, e2000862. https://doi.org/10.1371/journal.pbio.2000862
Leone, P., Bischoff, V., Kellenberger, C., Hetru, C., Royet, J., Roussel, A., 2008. Crystal structure of Drosophila PGRP-SD suggests binding to DAP-type but not lysine-type peptidoglycan. Mol Immunol 45, 2521–2530. https://doi.org/10.1016/j.molimm.2008.01.015
Li H, Qi Y, Jasper H. 2016. Preventing age-related decline of gut compartmentalization limits microbiota dysbiosis and extends lifespan. Cell Host Microbe 19:240–53
Lotti, T., D'Erme, A.M., Hercogová, J., 2014. The role of neuropeptides in the control of regional immunity. Clin Dermatol 32, 633–645. https://doi.org/10.1016/j.clindermatol.2014.04.011
Love, M.I., Soneson, C., Hickey, P.F., Johnson, L.K., Pierce, N.T., Shepherd, L., Morgan, M., Patro, R., 2020. Tximeta: Reference sequence checksums for provenance identification in RNA-seq. PLOS Computational Biology 16, e1007664. https://doi.org/10.1371/journal.pcbi.1007664
Luckinbill LS, Arking R, Clare MJ, Cirocco WC, Buck SA. 1984Selection for delayed senescence in *Drosophila melanogaster*.*Evolution* **38**, 996-1003.
Maiese, K., 2020. Targeting the core of neurodegeneration: FoxO, mTOR, and SIRT1. Neural Regen Res 16, 448–455. https://doi.org/10.4103/1673-5374.291382
Maklakov, A. and Chapman, T., 2019. Evolution of ageing as a tangle of trade-offs: energy versus function. Proceedings of the Royal Society B: Biological Sciences, 286(1911), p.20191604.

Mariat, D., Firmesse, O., Levenez, F., Guimarães, V., Sokol, H., Doré, J., Corthier, G. and Furet, J., 2009. The Firmicutes/Bacteroidetes ratio of the human microbiota changes with age. *BMC Microbiology*, 9(1), p.123.
Marniemi, J., Parkki, M.G., 1975b. Radiochemical assay of glutathione S-epoxide transferase and its enhancement by phenobarbital in rat liver in vivo. Biochem Pharmacol 24, 1569–1572. https://doi.org/10.1016/0006-2952(75)90080-5
Martin, A.M., Sun, E.W., Rogers, G.B., Keating, D.J., 2019. The Influence of the Gut Microbiome on Host Metabolism Through the Regulation of Gut Hormone Release. Front Physiol 10, 428. https://doi.org/10.3389/fphys.2019.00428
Martino, M.E., Joncour, P., Leenay, R., Gervais, H., Shah, M., Hughes, S., Gillet, B., Beisel, C., Leulier, F., 2018. Bacterial Adaptation to the Host's Diet Is a Key Evolutionary Force Shaping Drosophila-Lactobacillus Symbiosis. Cell Host & Microbe 24, 109-119.e6. https://doi.org/10.1016/j.chom.2018.06.001
Marx, V., 2015. Metabolism: feeding fruit flies. Nat Methods 12, 609–612. https://doi.org/10.1038/nmeth.3443
Mashaghi, A., Marmalidou, A., Tehrani, M., Grace, P.M., Pothoulakis, C., Dana, R., 2016. Neuropeptide Substance P and the Immune Response. Cell Mol Life Sci 73, 4249–4264. https://doi.org/10.1007/s00018-016-2293-z
Mason JS, Wileman T, Chapman T. 2018Lifespan extension without fertility reduction following dietary addition of the autophagy activator Torinl in Drosophila melanogaster. PLoS ONE 13, e0190105.
Masuda, Y., Tanaka, T., Inomata, N., Ohnuma, N., Tanaka, S., Itoh, Z., Hosoda, H., Kojima, M., Kangawa, K., 2000. Ghrelin stimulates gastric acid secretion and motility in rats. Biochem Biophys Res Commun 276, 905–908. https://doi.org/10.1006/bbrc.2000.3568
Matthews, K.A., Ozdemir, C., Rawson, R.B., 2010. Activation of Sterol Regulatory Element Binding Proteins in the Absence of Scap in Drosophila melanogaster. Genetics 185, 189–198. https://doi.org/10.1534/genetics.110.114975
Matthews, K.A., Ozdemir, C., Rawson, R.B., 2010. Activation of Sterol Regulatory Element Binding Proteins in the Absence of Scap in Drosophila melanogaster. Genetics 185, 189–198. https://doi.org/10.1534/genetics.110.114975
McFall-Ngai, M., Hadfield, M., Bosch, T., Carey, H., Domazet-Lošo, T., Douglas, A., Dubilier, N., Eberl, G., Fukami, T., Gilbert, S., Hentschel, U., King, N., Kjelleberg, S., Knoll, A., Kremer, N., Mazmanian, S., Metcalf, J., Nealson, K., Pierce, N., Rawls, J., Reid, A., Ruby, E., Rumpho, M., Sanders, J., Tautz, D. and Wernegreen, J., 2013. Animals in a bacterial world, a new imperative for the life sciences. Proceedings of the National Academy of Sciences, 110(9), pp.3229-3236.
Micchelli CA, Perrimon N. Evidence that stem cells reside in the adult Drosophila midgut epithelium. Nature. 2006 Jan 26;439(7075):475-9. doi: 10.1038/nature04371. Epub 2005 Dec 7. PMID: 16340959.
Micchelli, C.A., Perrimon, N., 2006. Evidence that stem cells reside in the adult Drosophila midgut epithelium. Nature 439, 475–479. https://doi.org/10.1038/nature04371
Miguel-Aliaga, I., Jasper, H., Lemaitre, B., 2018. Anatomy and Physiology of the Digestive Tract of Drosophila melanogaster. Genetics 210, 357–396. https://doi.org/10.1534/genetics.118.300224
Min, K.-J., Tatar, M., 2018. Unraveling the Molecular Mechanism of Immunosenescence in Drosophila. International Journal of Molecular Sciences 19, 2472. https://doi.org/10.3390/ijms19092472
Mirabeau, O., Joly, J.-S., 2013. Molecular evolution of peptidergic signaling systems in bilaterians. Proc Natl Acad Sci U S A 110, E2028-2037. https://doi.org/10.1073/pnas.1219956110

Moore, C.B., Guthrie, E.H., Huang, M.T.-H., Taxman, D.J., 2010. Short Hairpin RNA (shRNA): Design, Delivery, and Assessment of Gene Knockdown. Methods Mol Biol 629, 141–158. https://doi.org/10.1007/978-1-60761-657-3_10
Morgan, T. H., M., T.H., 1910. SEX LIMITED INHERITANCE IN DROSOPHILA. Science 32.
Murshid, A., Eguchi, T., Calderwood, S.K., 2013. Stress Proteins in Aging and Life Span. Int J Hyperthermia 29, 442–447. https://doi.org/10.3109/02656736.2013.798873
Musso, P.-Y., Junca, P., Gordon, M.D., 2021a. A neural circuit linking two sugar sensors regulates satiety-dependent fructose drive in Drosophila. Science Advances. https://doi.org/10.1126/sciadv.abj0186
Myllymäki, H., Valanne, S., Rämet, M., 2014. The Drosophila Imd Signaling Pathway. The Journal of Immunology 192, 3455–3462. https://doi.org/10.4049/jimmunol.1303309
Nässel, D.R., Williams, M.J., 2014. Cholecystokinin-Like Peptide (DSK) in Drosophila, Not Only for Satiety Signaling. Front Endocrinol (Lausanne) 5, 219. https://doi.org/10.3389/fendo.2014.00219
Nässel, D.R., Winther, A.M.E., 2010. Drosophila neuropeptides in regulation of physiology and behavior. Prog Neurobiol 92, 42–104. https://doi.org/10.1016/j.pneurobio.2010.04.010
Nässel D.R. 1999. Tachykinin-related peptides in invertebrates: a review. Peptides, **20**(1): 141–158.
NECKAMEYER, W. S. & ARGUE, K. J. 2013. Comparative approaches to the study of physiology: Drosophila as a physiological tool. American Journal of Physiology-Regulatory, Integrative and Comparative Physiology, 304, R177- R188.
Newell, P., Chaston, J., Wang, Y., Winans, N., Sannino, D., Wong, A., Dobson, A., Kagle, J. and Douglas, A., 2014. In vivo function and comparative genomic analyses of the Drosophila gut microbiota identify candidate symbiosis factors. Frontiers in Microbiology, 5.
Newell, P.D., Chaston, J.M., Wang, Y., Winans, N.J., Sannino, D.R., Wong, A.C.N., Dobson, A.J., Kagle, J., Douglas, A.E., 2014. In vivo function and comparative genomic analyses of the Drosophila gut microbiota identify candidate symbiosis factors. Front. Microbiol. 5. https://doi.org/10.3389/fmicb.2014.00576
Newell, P.D., Douglas, A.E., 2014. Interspecies Interactions Determine the Impact of the Gut Microbiota on Nutrient Allocation in Drosophila melanogaster. Applied and Environmental Microbiology 80, 788–796. https://doi.org/10.1128/AEM.02742-13
Newell, P.D., Douglas, A.E., 2014. Interspecies Interactions Determine the Impact of the Gut Microbiota on Nutrient Allocation in Drosophila melanogaster. Appl Environ Microbiol 80, 788–796. https://doi.org/10.1128/AEM.02742-13
Nguyen, B., Than, A., Dinh, H., Morimoto, J., Ponton, F., 2020. Parental Microbiota Modulates Offspring Development, Body Mass and Fecundity in a Polyphagous Fruit Fly. Microorganisms 8, 1289. https://doi.org/10.3390/microorganisms8091289
Nguyen, B., Than, A., Dinh, H., Morimoto, J., Ponton, F., 2020. Parental Microbiota Modulates Offspring Development, Body Mass and Fecundity in a Polyphagous Fruit Fly. Microorganisms 8, 1289. https://doi.org/10.3390/microorganisms8091289
Nicholson, J., Holmes, E., Kinross, J., Burcelin, R., Gibson, G., Jia, W. and Pettersson, S., 2012. *Host-Gut Microbiota Metabolic Interactions*.
Nicholson, J.K., Holmes, E., Kinross, J., Burcelin, R., Gibson, G., Jia, W., Pettersson, S., 2012. Host-gut microbiota metabolic interactions. Science 336, 1262–1267. https://doi.org/10.1126/science.1223813

Nøhr, M.K., Pedersen, M.H., Gille, A., Egerod, K.L., Engelstoft, M.S., Husted, A.S., Sichlau, R.M., Grunddal, K.V., Poulsen, S.S., Han, S., Jones, R.M., Offermanns, S., Schwartz, T.W., 2013. GPR41/FFAR3 and GPR43/FFAR2 as cosensors for short-chain fatty acids in enteroendocrine cells vs FFAR3 in enteric neurons and FFAR2 in enteric leukocytes. Endocrinology 154, 3552–3564. https://doi.org/10.1210/en.2013-1142

Obadia, B., Güvener, Z.T., Zhang, V., Ceja-Navarro, J.A., Brodie, E.L., Ja, W.W., Ludington, W.B., 2017. Probabilistic Invasion Underlies Natural Gut Microbiome Stability. Current Biology 27, 1999-2006.e8. https://doi.org/10.1016/j.cub.2017.05.034

Obata, F., Fons, C.O., Gould, A.P., 2018. Early-life exposure to low-dose oxidants can increase longevity via microbiome remodelling in Drosophila. Nat Commun 9, 975. https://doi.org/10.1038/s41467-018-03070-w

Odamaki, T., Kato, K., Sugahara, H., Hashikura, N., Takahashi, S., Xiao, J., Abe, F. and Osawa, R., 2016. Age-related changes in gut microbiota composition from newborn to centenarian: a cross-sectional study. *BMC Microbiology*, 16(1).

Ohlstein B, Spradling A. Multipotent Drosophila intestinal stem cells specify daughter cell fates by differential notch signaling. Science. 2007 Feb 16;315(5814):988-92. doi: 10.1126/science.1136606. PMID: 17303754.

Ohlstein, B., Spradling, A., 2006. The adult Drosophila posterior midgut is maintained by pluripotent stem cells. Nature 439, 470–474. https://doi.org/10.1038/nature04333

Oldham, S., Hafen, E., 2003. Insulin/IGF and target of rapamycin signaling: a TOR de force in growth control. Trends in Cell Biology 13, 79–85. https://doi.org/10.1016/S0962-8924(02)00042-9

Overend, G., Luo, Y., Henderson, L., Douglas, A.E., Davies, S.A., Dow, J.A.T., 2016. Molecular mechanism and functional significance of acid generation in the Drosophila midgut. Sci Rep 6, 27242. https://doi.org/10.1038/srep27242

Paik, D., Jang, Y.G., Lee, Y.E., Lee, Y.N., Yamamoto, R., Gee, H.Y., Yoo, S., Bae, E., Min, K., Tatar, M., Park, J.-J., 2012. Misexpression screen delineates novel genes controlling Drosophila lifespan. Mech Ageing Dev 133, 234–245. https://doi.org/10.1016/j.mad.2012.02.001

Palmer, C., Bik, E., DiGiulio, D., Relman, D. and Brown, P., 2007. Development of the Human Infant Intestinal Microbiota. *PLoS Biology*, 5(7), p.e177.

Pandey, U.B., Nichols, C.D., 2011. Human disease models in Drosophila melanogaster and the role of the fly in therapeutic drug discovery. Pharmacol Rev 63, 411–436. https://doi.org/10.1124/pr.110.003293

Papadopoli, D., Boulay, K., Kazak, L., Pollak, M., Mallette, F.A., Topisirovic, I., Hulea, L., 2019. mTOR as a central regulator of lifespan and aging. F1000Res 8, F1000 Faculty Rev-998. https://doi.org/10.12688/f1000research.17196.1

Park, J.-I., Semyonov, J., Chang, C.L., Hsu, S.Y.T., 2005. Conservation of the heterodimeric glycoprotein hormone subunit family proteins and the LGR signaling system from nematodes to humans. Endocrine 26, 267–276. https://doi.org/10.1385/ENDO:26:3:267

Park, S., Sonn, J.Y., Oh, Y., Lim, C., Choe, J., 2014. SIFamide and SIFamide Receptor Define a Novel Neuropeptide Signaling to Promote Sleep in Drosophila. Mol Cells 37, 295–301. https://doi.org/10.14348/molcells.2014.2371

Parnell, J. and Reimer, R., 2009. Weight loss during oligofructose supplementation is associated with decreased ghrelin and increased peptide YY in overweight and obese adults. *The American Journal of Clinical Nutrition*, 89(6), pp.1751-1759.

Partridge, L., Alic, N., Bjedov, I., Piper, M.D.W., 2011. Ageing in Drosophila: The role of the insulin/Igf and TOR signalling network. Exp Gerontol 46, 376–381. https://doi.org/10.1016/j.exger.2010.09.003

Pasco, M.Y., Léopold, P., 2012a. High Sugar-Induced Insulin Resistance in Drosophila Relies on the Lipocalin Neural Lazarillo. PLoS One 7, e36583. https://doi.org/10.1371/journal.pone.0036583
Pearl, R., 1921. The Biology of Death--VI. Experimental Studies on the Duration of Life. The Scientific Monthly 13, 144–164.
Peck, B., Shanahan, M., Singh, A. and Sethupathy, P., 2017. Gut Microbial Influences on the Mammalian Intestinal Stem Cell Niche. *Stem Cells International*, 2017, pp.1-17.
Perez-Lopez, A., Behnsen, J., Nuccio, S.-P., Raffatellu, M., 2016. Mucosal immunity to pathogenic intestinal bacteria. Nat Rev Immunol 16, 135–148. https://doi.org/10.1038/nri.2015.17
Petra, A.I., Panagiotidou, S., Hatziagelaki, E., Stewart, J.M., Conti, P., Theoharides, T.C., 2015. Gut-Microbiota-Brain Axis and Its Effect on Neuropsychiatric Disorders With Suspected Immune Dysregulation. Clin Ther 37, 984–995. https://doi.org/10.1016/j.clinthera.2015.04.002
Piper, M.D.W., Partridge, L., 2018. Drosophila as a model for ageing. Biochimica et Biophysica Acta (BBA) - Molecular Basis of Disease, Model Systems of Aging 1864, 2707–2717. https://doi.org/10.1016/j.bbadis.2017.09.016
Puig, O., Marr, M.T., Ruhf, M.L., Tjian, R., 2003a. Control of cell number by Drosophila FOXO: downstream and feedback regulation of the insulin receptor pathway. Genes Dev 17, 2006–2020. https://doi.org/10.1101/gad.1098703
Qi, W., Wang, G., Wang, L., 2021. A novel satiety sensor detects circulating glucose and suppresses food consumption via insulin-producing cells in Drosophila. Cell Res 31, 580–588. https://doi.org/10.1038/s41422-020-00449-7
Qin Y, Wade PA. 2018. Crosstalk between the microbiome and epigenome: messages from bugs. J. Biochem. 163:105–12
Rajvanshi, A.K., Box, P.O., 2011. The three minds of the body - Brain, heart and gut.
Rampelli, S., Candela, M., Turroni, S., Biagi, E., Collino, S., Franceschi, C., O'Toole, P. and Brigidi, P., 2013. Functional metagenomic profiling of intestinal microbiome in extreme ageing. Aging, 5(12), pp.902-912.
Rastelli, M., Cani, P. and Knauf, C., 2019. The Gut Microbiome Influences Host Endocrine Functions. *Endocrine Reviews*, 40(5), pp.1271-1284.
Regulation of onset of female mating and sex pheromone production by juvenile hormone in Drosophila melanogaster | PNAS [WWW Document], n.d. URL https://www.pnas.org/doi/10.1073/pnas.1318119110 (accessed 10.20.23).
Rehfeld, J.F., 2017. Cholecystokinin-From Local Gut Hormone to Ubiquitous Messenger. Front Endocrinol (Lausanne) 8, 47. https://doi.org/10.3389/fendo.2017.00047
Reiher, W., Shirras, C., Kahnt, J., Baumeister, S., Isaac, R.E., Wegener, C., 2011. Peptidomics and peptide hormone processing in the Drosophila midgut. J Proteome Res 10, 1881–1892. https://doi.org/10.1021/pr101116g
Ren, G.R., Hauser, F., Rewitz, K.F., Kondo, S., Engelbrecht, A.F., Didriksen, A.K., Schjøtt, S.R., Sembach, F.E., Li, S., Søgaard, K.C., Søndergaard, L., Grimmelikhuijzen, C.J.P., 2015. CCHamide-2 Is an Orexigenic Brain-Gut Peptide in Drosophila. PLoS ONE 10. https://doi.org/10.1371/journal.pone.0133017
Rera, M., Clark, R.I., Walker, D.W., 2012. Intestinal barrier dysfunction links metabolic and inflammatory markers of aging to death in Drosophila. Proc Natl Acad Sci U S A 109, 21528–21533. https://doi.org/10.1073/pnas.1215849110
Resnik-Docampo, M., Sauer, V., Schinaman, J.M., Clark, R.I., Walker, D.W., Jones, D.L., 2018. Keeping it tight: The relationship between bacterial dysbiosis, septate junctions, and the intestinal barrier in Drosophila. Fly 12, 34–40. https://doi.org/10.1080/19336934.2018.1441651

Rhea, J.M., Wegener, C., Bender, M., 2010. The Proprotein Convertase Encoded by amontillado (amon) Is Required in Drosophila Corpora Cardiaca Endocrine Cells Producing the Glucose Regulatory Hormone AKH. PLoS Genet 6, e1000967. https://doi.org/10.1371/journal.pgen.1000967
Rhee, S.H., Pothoulakis, C., Mayer, E.A., 2009. Principles and clinical implications of the brain-gut-enteric microbiota axis. Nat Rev Gastroenterol Hepatol 6, 306–314. https://doi.org/10.1038/nrgastro.2009.35
Ridley, E.V., Wong, A.C.-N., Westmiller, S., Douglas, A.E., 2012. Impact of the resident microbiota on the nutritional phenotype of Drosophila melanogaster. PLoS One 7, e36765. https://doi.org/10.1371/journal.pone.0036765
Rodier, F., Campisi, J., Bhaumik, D., 2007. Two faces of p53: aging and tumor suppression. Nucleic Acids Res 35, 7475–7484. https://doi.org/10.1093/nar/gkm744
Rose MR. 1984Laboratory evolution of posponed senescence in *Drosophila melanogaster*. *Evolution* **38**, 1004-1010.
Roth, G.E., Gierl, M.S., Vollborn, L., Meise, M., Lintermann, R., Korge, G., 2004. The Drosophila gene Start1: A putative cholesterol transporter and key regulator of ecdysteroid synthesis. Proc Natl Acad Sci U S A 101, 1601–1606. https://doi.org/10.1073/pnas.0308212100
Rubinsztein, D.C., Marino, G. and Kroemer, G., 2011. Autophagy and aging. *Cell*, 146(5), pp.682-695. DOI: 10.1016/j.cell.2011.07.030.
Rulifson, E.J., Kim, S.K., Nusse, R., 2002. Ablation of insulin-producing neurons in flies: growth and diabetic phenotypes. Science 296, 1118–1120. https://doi.org/10.1126/science.1070058
Sannino, D.R., Dobson, A.J., Edwards, K., Angert, E.R., Buchon, N., 2018. The *Drosophila melanogaster* Gut Microbiota Provisions Thiamine to Its Host. mBio 9, e00155-18. https://doi.org/10.1128/mBio.00155-18
Saud, S.N.A., Summerfield, A.C., Alic, N., 2015. Ablation of insulin-producing cells prevents obesity but not premature mortality caused by a high-sugar diet in Drosophila. Proceedings of the Royal Society B: Biological Sciences 282. https://doi.org/10.1098/rspb.2014.1720
Schiffrin, E.J., Rochat, F., Link-Amster, H., Aeschlimann, J.M., Donnet-Hughes, A., 1995. Immunomodulation of Human Blood Cells Following the Ingestion of Lactic Acid Bacteria. Journal of Dairy Science 78, 491–497. https://doi.org/10.3168/jds.S0022-0302(95)76659-0
Schiffrin, E.J., Rochat, F., Link-Amster, H., Aeschlimann, J.M., and DonnetHughes, A. (1995). Immunomodulation of human blood cells following the
Schönborn, J.W., Stewart, F.A., Enriquez, K.M., Akhtar, I., Droste, A., Waschina, S., Beller, M., 2021. Modeling Drosophila gut microbe interactions reveals metabolic interconnectivity. iScience 24, 103216. https://doi.org/10.1016/j.isci.2021.103216
Schroeder, B. and Bäckhed, F., 2016. Signals from the gut microbiota to distant organs in physiology and disease. *Nature Medicine*, 22(10), pp.1079-1089.
Scopelliti, A., Bauer, C., Yu, Y., Zhang, T., Kruspig, B., Murphy, D.J., Vidal, M., Maddocks, O.D.K., Cordero, J.B., 2019. A Neuronal Relay Mediates a Nutrient Responsive Gut/Fat Body Axis Regulating Energy Homeostasis in Adult Drosophila. Cell Metab 29, 269-284.e10. https://doi.org/10.1016/j.cmet.2018.09.021
Sedighi, M., Razavi, S., Navab-Moghadam, F., Khamseh, M., Alaei-Shahmiri, F., Mehrtash, A. and Amirmozafari, N., 2017. Comparison of gut microbiota in adult patients with type 2 diabetes and healthy individuals. *Microbial Pathogenesis*, 111, pp.362-369.

Shanbhag, S., Tripathi, S., 2009. Epithelial ultrastructure and cellular mechanisms of acid and base transport in the Drosophila midgut. J Exp Biol 212, 1731–1744. https://doi.org/10.1242/jeb.029306
Share, J.B., 1976. Review of drug treatment for Down's syndrome persons. Am J Ment Defic 80, 388–393.
Sherman, M.P., Zaghouani, H., Niklas, V., 2015. Gut microbiota, the immune system, and diet influence the neonatal gut-brain axis. Pediatr Res 77, 127–135. https://doi.org/10.1038/pr.2014.161
Shi, X.-Z., Zhong, X., Yu, X.-Q., 2012. Drosophila melanogaster NPC2 Proteins Bind Bacterial Cell Wall Components and May Function in Immune Signal Pathways. Insect Biochem Mol Biol 42, 545–556. https://doi.org/10.1016/j.ibmb.2012.04.002
Shin, S.C., Kim, S.-H., You, H., Kim, B., Kim, A.C., Lee, K.-A., Yoon, J.-H., Ryu, J.-H., Lee, W.-J., 2011. Drosophila Microbiome Modulates Host Developmental and Metabolic Homeostasis via Insulin Signaling. Science 334, 670–674. https://doi.org/10.1126/science.1212782
Shin, S.C., Kim, S.-H., You, H., Kim, B., Kim, A.C., Lee, K.-A., Yoon, J.-H., Ryu, J.-H., Lee, W.-J., 2011. *Drosophila* Microbiome Modulates Host Developmental and Metabolic Homeostasis via Insulin Signaling. Science 334, 670–674. https://doi.org/10.1126/science.1212782
Shreiner, A., Kao, J. and Young, V., 2015. The gut microbiome in health and in disease. *Current Opinion in Gastroenterology*, 31(1), pp.69-75.
Slack, C., Giannakou, M.E., Foley, A., Goss, M., Partridge, L., 2011b. dFOXO-independent effects of reduced insulin-like signaling in Drosophila. Aging Cell 10, 735–748. https://doi.org/10.1111/j.1474-9726.2011.00707.x
Smith, K., McCoy, K.D., Macpherson, A.J., 2007. Use of axenic animals in studying the adaptation of mammals to their commensal intestinal microbiota. Semin Immunol 19, 59–69. https://doi.org/10.1016/j.smim.2006.10.002
Smith, P., Willemsen, D., Popkes, M., Metge, F., Gandiwa, E., Reichard, M., Valenzano, D.R., 2017. Regulation of life span by the gut microbiota in the short-lived African turquoise killifish. Elife 6, e27014. https://doi.org/10.7554/eLife.27014
Smith, P., Willemsen, D., Popkes, M., Metge, F., Gandiwa, E., Reichard, M. and Valenzano, D., 2017. Regulation of life span by the gut microbiota in the short-lived African turquoise killifish. *eLife*, 6.
Söderberg JA, Birse RT, Nässel DR. Insulin production and signaling in renal tubules of Drosophila is under control of tachykinin-related peptide and regulates stress resistance. PLoS One. 2011 May 10;6(5):e19866. doi: 10.1371/journal.pone.0019866. PMID: 21572965; PMCID: PMC3091884.
Sommer, F., Bäckhed, F., 2016. Know your neighbor: Microbiota and host epithelial cells interact locally to control intestinal function and physiology. Bioessays 38, 455–464. https://doi.org/10.1002/bies.201500151
Song, W., Veenstra, J., Perrimon, N. (2014). Control of Lipid Metabolism by Tachykinin in Drosophila Cell Reports https://dx.doi.org/10.1016/j.celrep.2014.08.060
Storelli, G., Defaye, A., Erkosar, B., Hols, P., Royet, J., Leulier, F., 2011. Lactobacillus plantarum Promotes Drosophila Systemic Growth by Modulating Hormonal Signals through TOR-Dependent Nutrient Sensing. Cell Metabolism 14, 403–414. https://doi.org/10.1016/j.cmet.2011.07.012
Tack, J., Depoortere, I., Bisschops, R., Delporte, C., Coulie, B., Meulemans, A., Janssens, J., Peeters, T., 2006. Influence of ghrelin on interdigestive gastrointestinal motility in humans. Gut 55, 327–333. https://doi.org/10.1136/gut.2004.060426

Tatar, M., Bartke, A., & Antebi, A., 2003. The endocrine regulation of aging by insulin-like signals. *Science*, 299(5611), pp.1346-1351. DOI: 10.1126/science.1081447.
Tap, J., Mondot, S., Levenez, F., Pelletier, E., Caron, C., Furet, J., Ugarte, E., Muñoz-Tamayo, R., Paslier, D., Nalin, R., Dore, J. and Leclerc, M., 2009. Towards the human intestinal microbiota phylogenetic core. *Environmental Microbiology*, 11(10), pp.2574-2584.
Tauc, H., Rodriguez-Fernandez, I., Hackney, J., Pawlak, M., Ronnen Oron, T., Korzelius, J., Moussa, H., Chaudhuri, S., Modrusan, Z., Edgar, B. and Jasper, H., 2021. Age-related changes in polycomb gene regulation disrupt lineage fidelity in intestinal stem cells. eLife, 10.
Terhzaz, S., Rosay, P., Goodwin, S.F., Veenstra, J.A., 2007. The neuropeptide SIFamide modulates sexual behavior in Drosophila. Biochemical and Biophysical Research Communications 352, 305–310. https://doi.org/10.1016/j.bbrc.2006.11.030
Thaiss, C.A., Zmora, N., Levy, M., Elinav, E., 2016. The microbiome and innate immunity. Nature 535, 65–74. https://doi.org/10.1038/nature18847
Thevaranjan, N., Puchta, A., Schulz, C., Naidoo, A., Szamosi, J., Verschoor, C., Loukov, D., Schenck, L., Jury, J., Foley, K., Schertzer, J., Larché, M., Davidson, D., Verdú, E., Surette, M. and Bowdish, D., 2018. Age-Associated Microbial Dysbiosis Promotes Intestinal Permeability, Systemic Inflammation, and Macrophage Dysfunction. Cell Host & Microbe, 23(4), p.570.
Thomas, A.L., Davis, S.M., Dierick, H.A., 2015. Of Fighting Flies, Mice, and Men: Are Some of the Molecular and Neuronal Mechanisms of Aggression Universal in the Animal Kingdom? PLoS Genet 11, e1005416. https://doi.org/10.1371/journal.pgen.1005416
Tong, J.J., Schriner, S.E., McCleary, D., Day, B.J., Wallace, D.C., 2007. Life extension through neurofibromin mitochondrial regulation and antioxidant therapy for neurofibromatosis-1 in Drosophila melanogaster. Nat Genet 39, 476–485. https://doi.org/10.1038/ng2004
Tower, J., 2011. Heat shock proteins and Drosophila aging. Experimental Gerontology, Aging studies in Drosophila melanogaster 46, 355–362. https://doi.org/10.1016/j.exger.2010.09.002
Turnbaugh, P., Bäckhed, F., Fulton, L. and Gordon, J., 2008. Diet-Induced Obesity Is Linked to Marked but Reversible Alterations in the Mouse Distal Gut Microbiome. *Cell Host & Microbe*, 3(4), pp.213-223.
UGUR, B., CHEN, K. & BELLEN, H. J. 2016. Drosophila tools and assays for the study of human diseases. Disease Models & Mechanisms, 9, 235-244.
Veenstra, J. A., and Ida, T. (2014). More Drosophila enteroendocrine peptides: orcokinin B and the CCHamides 1 and 2. Cell Tissue Res. 357, 607–621. doi: 10.1007/s00441-014-1880-2
Veenstra, J.A., 2009. Peptidergic paracrine and endocrine cells in the midgut of the fruit fly maggot. Cell Tissue Res 336, 309–323. https://doi.org/10.1007/s00441-009-0769-y
Veenstra, J.A., Agricola, H.-J., Sellami, A., 2008. Regulatory peptides in fruit fly midgut. Cell Tissue Res 334, 499–516. https://doi.org/10.1007/s00441-008-0708-3
Vijay-Kumar, M., Aitken, J.D., Carvalho, F.A., Cullender, T.C., Mwangi, S., Srinivasan, S., Sitaraman, S.V., Knight, R., Ley, R.E., Gewirtz, A.T., 2010. Metabolic Syndrome and Altered Gut Microbiota in Mice Lacking Toll-Like Receptor 5. Science 328, 228–231. https://doi.org/10.1126/science.1179721

Voght, S.P., Fluegel, M.L., Andrews, L.A., Pallanck, L.J., 2007. Drosophila NPC1b Promotes an Early Step in Sterol Absorption from the Midgut Epithelium. Cell Metabolism 5, 195–205. https://doi.org/10.1016/j.cmet.2007.01.011
Watnick, P.I., Jugder, B.-E., 2020. Microbial control of intestinal homeostasis via enteroendocrine cell innate immune signaling. Trends Microbiol 28, 141–149. https://doi.org/10.1016/j.tim.2019.09.005
Wohl, M.P., Liu, J., Asahina, K., 2023. Drosophila Tachykininergic Neurons Modulate the Activity of Two Groups of Receptor-Expressing Neurons to Regulate Aggressive Tone. J Neurosci 43, 3394–3420. https://doi.org/10.1523/JNEUROSCI.1734-22.2023
Wong, A.C.-N., Chaston, J.M., Douglas, A.E., 2013. The inconstant gut microbiota of Drosophila species revealed by 16S rRNA gene analysis. ISME J 7, 1922–1932. https://doi.org/10.1038/ismej.2013.86
Worthington, J.J., 2015a. The intestinal immunoendocrine axis: novel cross-talk between enteroendocrine cells and the immune system during infection and inflammatory disease. Biochemical Society Transactions 43, 727–733. https://doi.org/10.1042/BST20150090
Yamamoto, R., Bai, H., Dolezal, A.G., Amdam, G., Tatar, M., 2013. Juvenile hormone regulation of Drosophila aging. BMC Biology 11, 85. https://doi.org/10.1186/1741-7007-11-85
Yu, C.D., Xu, Q.J., Chang, R.B., 2020. Vagal sensory neurons and gut-brain signaling. Curr Opin Neurobiol 62, 133–140. https://doi.org/10.1016/j.conb.2020.03.006
Zhang, C., Daubnerova, I., Jang, Y.-H., Kondo, S., Žitňan, D., Kim, Y.-J., 2021. The neuropeptide allatostatin C from clock-associated DN1p neurons generates the circadian rhythm for oogenesis. Proc Natl Acad Sci U S A 118, e2016878118. https://doi.org/10.1073/pnas.2016878118
Zhao, S., Jang, C., Liu, J., Uehara, K., Gilbert, M., Izzo, L., Zeng, X., Trefely, S., Fernandez, S., Carrer, A., Miller, K., Schug, Z., Snyder, N., Gade, T., Titchenell, P., Rabinowitz, J. and Wellen, K., 2020. Dietary fructose feeds hepatic lipogenesis via microbiota-derived acetate. Nature, 579(7800), pp.586-591.
Wells, J.M., and Mercenier, A. (2008). Mucosal delivery of therapeutic and prophylactic molecules using lactic acid bacteria. Nat. Rev. Microbiol. 6, 349–362.